DE GRUYTER

TEXTBOOK

Wieland Alexander Worthoff,
Hans Georg Krojanski, Dieter Suter

MEDICAL PHYSICS

EXERCISES AND EXAMPLES

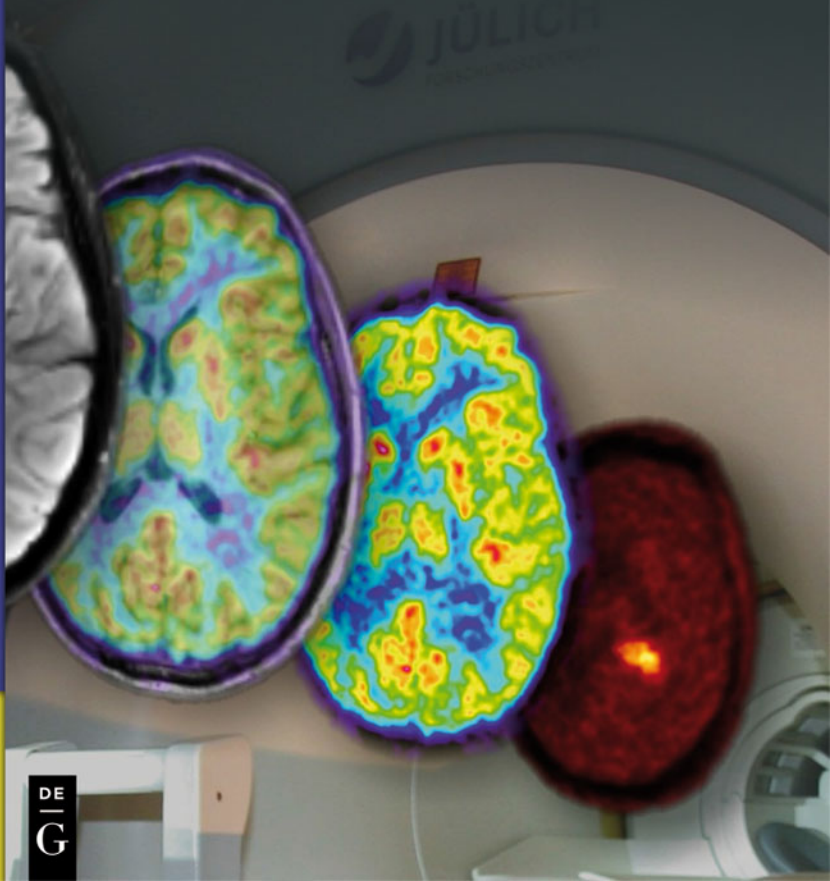

DE G

Wieland Alexander Worthoff, Hans Georg Krojanski, Dieter Suter
Medical Physics
De Gruyter Textbook

Wieland Alexander Worthoff, Hans Georg Krojanski, Dieter Suter

Medical Physics

Exercises and Examples

DE GRUYTER

Physics and Astronomy Classification 2010
87.85.-d, 87.57.-s, 87.59.-e, 87.19.-j, 87.50.-a, 87.53.-j, 87.56.-v, 87.64.-t

Authors
Dr. Wieland Alexander Worthoff
Institute of Neuroscience and Medicine – 4
Medical Imaging Physics
Forschungszentrum Juelich GmbH
52425 Juelich
Germany
w.worthoff@fz-juelich.de

Dr. Hans Georg Krojanski
RRZN – Regionales Rechenzentrum für Niedersachsen
Leibniz Universität Hannover
Schloßwender Straße 5
30159 Hannover
Germany
krojanski@rrzn.uni-hannover.de

Prof. Dr. Dieter Suter
Technische Universität Dortmund
Fakultät Physik
Experimentelle Physik III
Otto-Hahn-Str. 4
44227 Dortmund
Germany
Dieter.Suter@tu-dortmund.de

ISBN 978-3-11-030675-0
e-ISBN 978-3-11-030676-7

Library of Congress Cataloging-in-Publication Data
A CIP catalog record for this book has been applied for at the Library of Congress.

Bibliographic information published by the Deutsche Nationalbibliothek
The Deutsche Nationalbibliothek lists this publication in the Deutsche Nationalbibliografie; detailed bibliographic data are available in the Internet at http://dnb.dnb.de.

Cover image: kindly provided by Prof. Dr. N. J. Shah, Forschungszentrum Juelich GmbH
Typesetting: le-tex publishing services GmbH, Leipzig
Printing and binding: Hubert & Co. GmbH & Co. KG, Göttingen
Translation: Joseph Zabinski
♾Printed on acid-free paper
Printed in Germany

www.degruyter.com

Preface

The methods and techniques of physics are becoming more and more important in medicine. A number of universities have reacted to this trend, and have created different educational opportunities – from enrichment courses to separate majors – to address it. This book is intended primarily for students majoring in the natural sciences or technical fields, who have a solid basic education in physics. The first section is comprised of topics relating to the physics of the body, and the second deals with diagnostic and therapeutic methods. Special attention has been given to choosing exercises and examples that relate to practical applications. The overview presented before each chapter will serve to deepen understanding of the section's content.

January 2012

Wieland Alexander Worthoff
Hans Georg Krojanski
Dieter Suter

Contents

Part I: **Physics of the Body**

1 Breathing and Metabolism

Life processes are based on chemical and biochemical reactions, and require energy. While most plants can generate this energy through photosynthesis and synthesize energy-rich compounds themselves, animals must acquire it by consuming sustenance. The energy contained within compounds consumed, however, must first be liberated by using a sufficient quantity of oxygen. This necessary oxygen is taken in through breathing. In the process, oxygen (O_2) enters the lungs and diffuses into the red blood cells; these then distribute it throughout the entire body. Diffusion is also responsible for the transfer of oxygen from the blood cells through different membranes into the cells of the body, where energy is liberated through biochemical reactions. A measure for the concentration of oxygen is partial pressure. In arterial blood, the partial pressure is roughly 20 kPa and falls along the airway to around 13 kPa. In tissue, it is around ≈ 6 kPa. When breathing, other components of air also enter into the lungs in addition to oxygen; these components are either useless or dangerous to the body. These substances, as well as carbon dioxide (CO_2) exchanged out of the blood, are expelled by the lungs in exhalation.

The process of inhaling and exhaling takes place through a change in the volume of the chest, accomplished by the muscles that surround the chest cavity: the diaphragm, and the intercostal musculature. An adult moves around 0.5 l of air in each breath. Both lungs contain between 300 and 400 million alveoli, with a surface area of up to 100 m^2. On this surface is located a network of capillaries. The exchange of oxygen between the air breathed in and the blood, as well as that of carbon dioxide between the blood and air breathed out, is controlled by diffusion; due to partial pressure gradients of the two substances in the boundary layer between alveoli and capillaries, molecular O_2 and CO_2 flows occur. These flows take place in opposite directions. Beyond the boundary layer, transport generally takes place convectively. The same transfer mechanism takes place at cell walls and boundaries.

Cell boundaries separate the material contained within cells from the exterior, the extracellular space – for example, from air or blood. Generally, the intracellular space is characterized by a negative electric charge; in contrast, the extracellular space is positively charged. The difference is termed the membrane potential. The membrane potential is controlled by the active and passive exchange of ions, above all by sodium ions (Na^+), potassium ions (K^+), and chlorine ions (Cl^-). In analogy to the process of respiration in the lungs, this cellular process is termed cellular respiration. The calculation of material passage through a membrane – the calculation of the amount of material transported per unit time – is very complicated, and assumes knowledge of material transfer on both sides of the membrane. Concentration profiles, material transfer and diffusion coefficients, fluid dynamic and thermodynamic parameters, and anatomic geometry values must be known. These parameters all vary

considerably with the health and age of a person, and calculation is often only possible to an approximation.

Illnesses can significantly disrupt the metabolic functions of certain organs, like the kidneys. If the functional tissue in a kidney is destroyed by up to 70% uremia results. Uremia describes a condition in which toxic substances build up in the blood due to kidney failure. The over-concentration of these toxins in the blood also disrupts or destroys the metabolic processes of other organs of the body. One way to handle the situation is through the use of an artificial kidney. Hemodialysis, a technique of purifying the blood outside the body, has proven effective. In order to maintain a patient's life, a dialysis apparatus must reliably be able to remove urea and other nitrogen-containing products, as well as regulate the electrolyte concentrations of Na^+, K^+, and Cl^- in the blood. While modern dialysis devices can perform these tasks nearly ideally today, they are still not ready to completely take over an additional function of organic kidneys. This function is the production of hormones that contribute to the creation of red blood cells. This deficiency means that dialysis treatment must be accompanied by hormone therapy.

1.1 Breathing

? The average breath stream for inhalation and exhalation in humans is $V^* = 10\,\mathrm{l/min}$.

1. What is the average air velocity in the windpipe (diameter of the windpipe $d_{LR} = 1.5\,\mathrm{cm}$) and (in breathing through the mouth) between the lips, with an open-mouth area of $A_M = 9\,\mathrm{cm}^2$ at 0 °C at sea level?
2. What is the dependency of air pressure and density on elevation z, and what breathing problems can result when climbing mountains? Calculate by considering an approximation of the value by which the flow of breath must increase at an elevation of 8,000 m.

For modeling purposes, assume breathing dynamics in the form of a right-angle oscillation.

[air values: molar mass $M_L = 28.96\,\mathrm{g/mol}$; density at 0 °C at sea level $\rho_{L0} = 1.29\,\mathrm{kg/m^3}$ universal gas constant $R = 8.314\,\mathrm{J/mol\,K}$; air temperature $T = 0\,^\circ\mathrm{C}$]

! Breathing is a periodic process, under non-stationary conditions. However, because we are given and are looking for average values over half the cycle time here, the continuity equation in stationary form $V^* = wA$ can be used. Therefore, average flow velocity is

$$w = \frac{V^*}{A} = \frac{4V^*}{\pi d^2}.$$

1. Therefore, for the windpipe,

$$w_{LR} = \frac{4V_L^*}{\pi d_{LR}} = \frac{4 \cdot 10\,\text{l/min}}{\pi\,(1.5\,\text{cm}^2)} = 0.94\,\text{m/s}$$

and for the mouth,

$$w_M = \frac{V_L^*}{A_M} = \frac{10\,\text{l/min}}{9\,\text{cm}^2} = 0.185\,\text{m/s}.$$

2. When climbing a mountain, pressure p is a function of elevation z. To determine $p\,(z)$, consider an element of volume $dx\,dy\,dz$ of air at elevation dz. In order for this volume element to remain at equilibrium, the weight force must be compensated for exactly by the difference in pressure between the upper and lower surfaces:

$$\left[p\,(z + dz) - p\,(z)\right]\,dx\,dy + \rho_L\,g\,dx\,dy\,dz = 0.$$

With

$$p\,(z + dz) = p\,(z) + \frac{\partial p}{\partial z}\,dz$$

we have

$$\frac{\partial p}{\partial z} + \rho_L g = 0.$$

Considering air as an ideal gas, the ideal gas equation gives

$$\frac{p}{\rho_L} = \frac{p_0}{\rho_{L0}}.$$

The differential equation relating p and z is then

$$\frac{dp}{p} = -\frac{\rho_{L0}}{p_0}\,g\,dz.$$

Integrating, we have

$$\int_{p_0}^{p} \frac{dp}{p} = -\frac{\rho_{L0}}{p_0}\,g \int_0^z dz$$

and therefore

$$p\,(z) = p_0\,e^{-\gamma z} \quad \text{with} \quad \gamma = \left(\frac{\rho_{L0}}{p_0}\right) g.$$

Numerically, $\gamma = \frac{1.29\,\text{kg/m}^3 \cdot 9.81\,\text{m/s}^2}{1 \cdot 10^5\,\text{Pa}} = 1.265 \cdot 10^{-4}\,\text{m}^{-1}$.

The pressure at 8,000 m elevation is

$$\begin{aligned} p_{8{,}000} &= \left(1 \cdot 10^5\,\text{Pa}\right) \exp\left[\left(-1.265 \cdot 10^{-4}\right) \cdot 8{,}000\right] \\ &= 36.349\,\text{Pa} = 0.36\,\text{bar}. \end{aligned}$$

The dependence of density ρ_L follows from the ideal gas equation

$$p\, v_L = \frac{1}{M_L}\, RT.$$

Here, $v_L = \frac{1}{\rho_L}$ is the specific volume of air. Density is then

$$\rho_L(z) = \frac{p(z)\, M_L}{RT} = \frac{p_0 M_L}{RT}\, e^{-\gamma z}.$$

The density at 8,000 m elevation $\rho_{L8,000}$ is therefore

$$\rho_{L8,000} = \frac{p_{8,000}\, M_L}{RT} = \frac{36.349 \cdot 0.02896}{8.314 \cdot 273}\ \mathrm{kg/m^3} = 0.4637\ \mathrm{kg/m^3}.$$

Assuming the volumetric flow in breathing remains roughly constant, the mass flow of air is reduced by

$$\begin{aligned}\Delta m_L^* &= V_L^* (\rho_{L0} - \rho_{L8,000}) \\ &= 10\ \mathrm{l/min}\,(1.29 - 0.4637)\ \mathrm{kg/m^3} = 8.263\ \mathrm{g/min}.\end{aligned}$$

With an oxygen proportion of $\mu_{O_2} = 23.2\%$ (by mass), the intake of oxygen over time is therefore reduced by

$$\Delta m_{O_2}^* = \mu_{O_2} \cdot \Delta m_L^* = 0.232 \cdot 8.263\ \mathrm{g/min} = 1.917\ \mathrm{g/min}.$$

By increasing airflow by

$$V_{L8,000}^* = \frac{\rho_{L0}\, V_L^*}{\rho_{L8,000}} = 27.82\ \mathrm{l/min}.$$

it is possible to compensate. This is nearly three times the flow at sea level. In this calculation, only oxygen compensation through increased airflow is considered. For the transfer of oxygen from the lungs into the blood, the partial pressure difference between these phases is also important. This is ignored within the scope of this approximation.

Methods of increasing oxygen flow:

(a) training the diaphragm musculature to reduce lung pressure
(b) elevating breathing rate
(c) using an oxygen device

1.2 Human Elevation Limits

? If the partial pressure of oxygen in the alveoli falls below the critical value of around $p(O_2, \text{alveoli}) = 50$ mm Hg brain function is disrupted. This value is reached if the partial pressure of oxygen in the air falls to $p(O_2) = 12.9$ kPa. Using the barometric formula

for barometric elevation, determine the corresponding elevation at which this value is reached; consider the composition of the air to be constant (nitrogen and noble gases: 79.1%, oxygen: 20.9%, carbon dioxide: 0.03%). Is the elevation limit calculated realistic? Can people live at even higher elevations? What determines the "ultimate" elevation limit?
[density of air $\rho = 1.29\ \mathrm{kg/m^3}$, air pressure at sea level $p\,(0) = 101.3\ \mathrm{kPa}$]

Barometric formula: !

$$p(h) = p(0)e^{-\frac{\rho_0 gh}{p_0}} \Leftrightarrow h = \frac{p(0)}{\rho_0 g} \cdot \ln\left(\frac{p(0)}{p(h)}\right).$$

The reference pressure of air is 101.3 kPa. Using the oxygen partial pressure $p(\mathrm{O_2})$ given, the air pressure is $p(h)$ is

$$p(h) = \frac{p(\mathrm{O_2})}{20.9\%} = 61.7\ \mathrm{kPa}.$$

The height boundary is therefore around 4,000 m

$$h = \frac{101.3 \cdot 10^3\ \mathrm{Pa\,m^3\,s^2}}{1.29\ \mathrm{kg} \cdot 9.81\ \mathrm{m}} \ln\left(\frac{101.3}{61.7}\right) = 3{,}968.8\ \mathrm{m}.$$

Hyperventilation can raise the partial pressure of oxygen in the blood. By employing it, breathing without technological assistance is possible up to around 7,000 m. In the compensation zone of 3,000 m – 5,300 m, the body can adapt. In the disruption zone (5,300 m – 7,000 m) most people experience a severe reduction in capabilities. Some examples of adaptation to life at high altitudes include the lama cloister of Rongbuk in Tibet (≈ 5,000 m) and the mountain worker settlement of Auncanquilcha in Chile (≈ 5,300 m). At elevations of more than 5,300 m acclimatization is no longer possible, and stays are always limited.

Presence at higher elevations is made possible by breathing oxygen from pressurized bottles (when $p(\mathrm{O_2})$ is nearly as great as $p_{\text{air, external}}$, $p(\mathrm{O_2})$ in the alveoli rises). This technique allows people to survive up to 12 km. With hyperventilation, the limit rises to 14 km. Modern airplanes fly up to that elevation but remain beneath it due to the danger of a sudden loss of pressure.

At elevations of more than 14 km people can only survive in pressure cabins or pressure suits (space suits). (Without protective measures, for example, bodily fluids will begin to boil beyond 20 km as $p_{\text{air}} < p_{\text{vapor pressure}}(\mathrm{H_2O})$ at 37°C).

1.3 Oxygen Transfer in the Brain

The supplying of oxygen by diffusion from capillaries in the human cerebral cortex can be presented using coaxial cylinders surrounding these capillaries (see Figure). Blood flows in the capillaries, and brain tissue is located in the outer cylinders. Such ?

cylinders lie in bundles, parallel to one another. Cell boundaries are permeable membranes to oxygen. Calculate the distribution of partial pressure of oxygen $p(r)$ in the external cylinder (in the brain tissue), using the diffusion equation in cylindrical coordinates (see Equation (1.1)). At capillary edge $r = R$ saturation pressure is p_s, and at the surface of the cylinder at $r = R_A$, the partial pressure of oxygen is minimal so that $\frac{dp}{dr}|_{r=R_A} = 0$. Consumption and material parameters of diffusion are contained in the quantity K, which is known. Considering stationary and axially symmetric relationships,

$$\frac{d^2p}{dr^2} + \frac{1}{r}\frac{dp}{dr} = K. \tag{1.1}$$

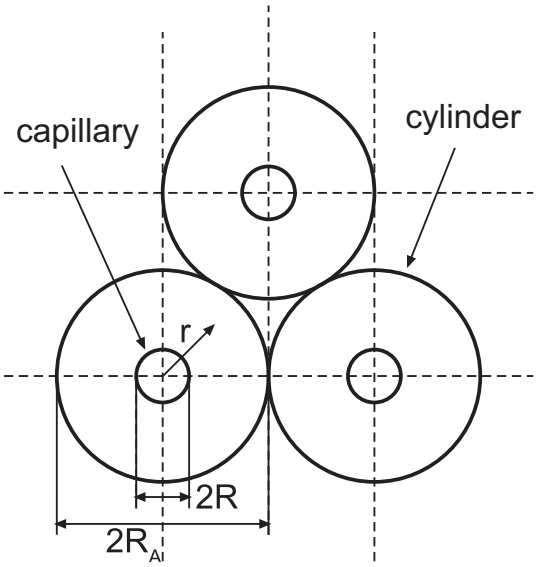

Fig. 1.1. Schema of a cross-section of the cerebral cortex, with its capillaries and their concentric cylinders.

! The differential equation

$$\frac{d^2p}{dr^2} + \frac{1}{r}\frac{dp}{dr} = K$$

is identical to

$$\frac{d}{dr}\left(r\frac{dp}{dr}\right) = K\,r.$$

Integrating twice gives

$$p(r) = \frac{1}{4}K\,r^2 + C_1 \ln r + C_2$$

with the integration constants C_1 and C_2. As at $r = R_A$ the partial pressure of oxygen should be minimal, $\frac{dp}{dr}|_{r=R_A} = 0$. This expression, and the boundary condition that at $r = R$ the saturation partial pressure of air occurs – $p(R) = p_S$ – gives $C_1 = -\frac{1}{2} K R_A^2$ and $C_2 = p_S - \frac{1}{4} K R^2 + \frac{1}{2} K R_A^2 \ln R$. Therefore,

$$p(r) = p_S + K \left[\frac{1}{4} \left(r^2 - R^2 \right) + \frac{1}{2} R_A^2 \ln \frac{R}{r} \right].$$

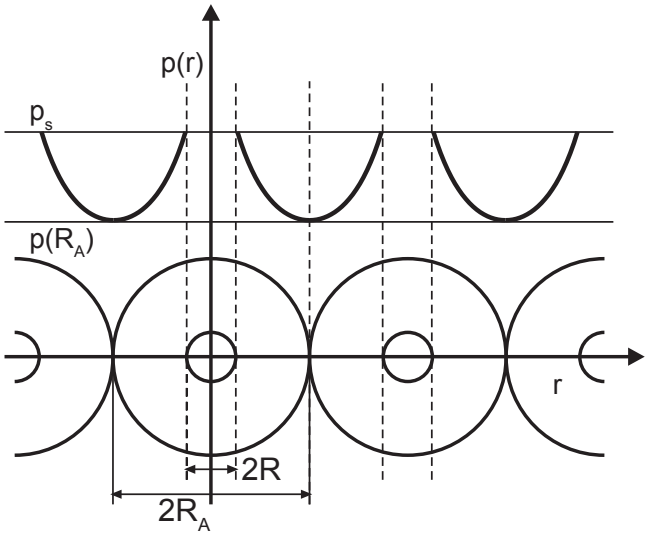

Fig. 1.2. The concentration $p(r)$ between the capillaries has its minima at R_A.

1.4 Photosynthesis

1. Of the total radiation power of the sun, $P_S = 2 \cdot 10^{17}$ W strike the Earth. What percent of this power is converted through photosynthesis if $m^*_{O_2} = 2 \cdot 10^{12}$ t/a are liberated? The chemical reaction equation of photosynthesis is ?

$$6\,CO_2 + 6\,H_2O \rightarrow C_6H_{12}O_6 + 6\,O_2\,.$$

   A Gibbs molar enthalpy of $\Delta G = +2{,}868$ kJ/mol is required.
2. Estimate the annual consumption of oxygen through human breathing $N^*_{O_2,\text{total}}$ at a global population of $n = 7$ billion. A person consumes $N^*_{O_2} = 1.1 \cdot 10^{22}$ molecules of oxygen per minute. What is the ratio of oxygen breathed in by people to the oxygen liberated by photosynthesis across the world?

! 1. The radiation power of the sun is $P_S = 2 \cdot 10^{17}$ W. In the course of a year, energy is

$$E_S = \tau P_S = (1\,\text{a}) \cdot \left(2 \cdot 10^{17}\,\text{J/s}\right) = 6.32 \cdot 10^{24}\,\text{J}.$$

The chemical reaction equation of photosynthesis

$$6\,CO_2 + 6\,H_2O \rightarrow C_6H_{12}O_6 + 6\,O_2 \quad \text{with } \Delta G = +2{,}868\,\text{kJ/mol}$$

says that for each iteration, a specific enthalpy of $\Delta G = 2{,}868\,\text{kJ/mol}$ is consumed and $N_{O_2\text{It}} = 6$ molecules of oxygen are liberated (see the Note on the opposite page). As such, the annual number of moles of oxygen generated through photosynthesis is

$$N^*_{O_2\text{Ph}} = \frac{m^*_{O_2}}{M_{O_2}} = \frac{\left(2 \cdot 10^{12}\,\text{t/a}\right)\left(10^6\,\text{g/t}\right)}{32\,\text{g/mol}} = 6.25 \cdot 10^{16}\,\text{mol/a},$$

with M_{O_2} as the molar mass of the oxygen molecule.
The total energy required per year is therefore E_{Ph}

$$\tilde{E}_{\text{Ph}} = \frac{N^*_{O_2\text{Ph}}\,\tau\,\Delta G}{N_{O_{2\text{It}}}} = \frac{\left(6.25 \cdot 10^{16}\,\text{mol/a}\right)(1\,\text{a})\,(2{,}868\,\text{kJ/mol})}{6}$$
$$= 2.987 \cdot 10^{22}\,\text{J}.$$

The proportion Φ of solar energy used in photosynthesis is therefore

$$\Phi = \frac{E_{\text{Ph}}}{E_S} \cdot 100\% = \frac{2.98 \cdot 10^{22}\text{J}}{6.25 \cdot 10^{24}\text{J}} \cdot 100\% = 0.473\%.$$

2. A person uses $N^*_{O_2} = 1.1 \cdot 10^{22}\,\text{1/min}$ molecules of oxygen each minute. This corresponds to

$$N^*_{O_2\text{mol}} = \frac{N^*_{O_2}}{N_A}$$

with N_A as Avogadro's number. Numerically,

$$N^*_{O_2\text{mol}} = \frac{1.1 \cdot 10^{22}\,\text{1/min}}{6.02 \cdot 10^{23}\,\text{1/mol}} = 1.81 \cdot 10^{-2}\,\text{mol/min}.$$

The total amount of oxygen $N^*_{O_2\text{total}}$ consumed annually by a world population of $n = 7 \cdot 10^9$ people is therefore

$$N^*_{O_2\text{total}} = n \cdot N^*_{O_2\text{mol}}.$$

Numerically,

$$N^*_{O_2\text{total}} = \left(7 \cdot 10^9\right)(0.01806\,\text{mol/min}) = 1.26 \cdot 10^8\,\text{mol/min}$$
$$= \left(1.26 \cdot 10^8\,\text{mol/min}\right)\left(5.26 \cdot 10^5\,\text{min/a}\right) = 6.65 \cdot 10^{13}\,\text{mol/a}.$$

The material ratio Ψ of inhaled oxygen to liberated oxygen is therefore

$$\Psi = \frac{N^*_{O_2\text{total}}}{N^*_{O_{2\text{Ph}}}} \cdot 100\% = \frac{6.65 \cdot 10^{13}}{6.25 \cdot 10^{16}} \cdot 100\% = 0.11\%.$$

Additional Note on the Reaction Equation:

$$6\,CO_2 + 6\,H_2O \rightarrow C_6H_{12}O_6 + 6\,O_2 \quad \text{with} \quad \Delta G = +2{,}868\ ^{kJ}/_{mol}.$$

Consider the molar Gibbs energy in the expression [$^{kJ}/_{mol}$]; this is the mol-specific energy that must be added to the chemical reactions each time to make them possible (if ΔG is negative, heat must be removed). It can be helpful to multiply this equation with the unit mol:

$$6\,\text{mol}\,CO_2 + 6\,\text{mol}\,H_2O \rightarrow 1\,\text{mol}\,C_6H_{12}\,O_6 + 6\,\text{mol}\,O_2.$$

With each iteration, $1\,\text{mol}\,C_6H_{12}O_6$ is produced. As a molar heat quantity of ΔG is required for each iteration, for $1\,\text{mol}\,C_6H_{12}O_6$ the reaction requires

$$\Delta E_Z = \Delta G \cdot \frac{1}{1}\,\text{mol} = 2{,}868\,\text{kJ}$$

and for the creation of $1\,\text{mol}\,O_2$

$$\Delta E_S = \Delta G \cdot \frac{1}{6}\,\text{mol} = 478\,\text{kJ}.$$

1.5 Erythrocytes: Oxygen Transport in the Body

1. How many molecules of oxygen $N^*_{O_2}$ are transported per minute in the blood if the minute breath volume of a human is $V^*_{O_2} = 10\,^{l}/_{min}$? The oxygen concentrations in inhaled and exhaled air are $c_{O_2\alpha} = 21$ Vol% and $c_{O_2\omega} = 16.5$ Vol% at pressure $p = 10^5$ Pa and temperature $T = 300$ K. ?
2. At saturation, a molecule of hemoglobin transports 4 molecules of oxygen. How many molecules of hemoglobin N_{HG} are in an erythrocyte in $V_B = 6\,l$ of blood, with an average blood circulation time of $\tau = 50$ s and with $N_{Ery} = 5{\cdot}10^6\ ^{1}/_{\mu l}$ erythrocytes in the blood?
3. What is the average life span τ_L of erythrocytes if $N^*_{Ery,\alpha} = 3 \cdot 10^6$ erythrocytes are generated in the body per second?

1. The number of oxygen molecules per unit time $N^*_{O_2}$ can be determined from the ideal gas equation. Here, it is !

$$pV^*_{O_2} = N^*_{O_2} kT$$

with k as the Boltzmann constant. Solving for $N^*_{O_2}$, we have

$$N^*_{O_2} = \frac{pV^*_{O_2}}{kT} = \frac{pV^* \Delta c_{O_2}}{kT}$$

with $\Delta c_{O_2} = c_{O_2\alpha} - c_{O_2\omega}$. Numerically,

$$N^*_{O_2} = \frac{10^5\,\text{Pa}\ 10\ ^{l}/_{min}\,(0.21 - 0.165)}{1.38 \cdot 10^{-23}\ ^{J}/_{K}\ 300\,\text{K}} = 1.09 \cdot 10^{22}\,\text{min}^{-1}.$$

2. As a hemoglobin molecule transports 4 molecules of oxygen, the flow of hemoglobin is

$$N^*_{HG} = \frac{N^*_{O_2}}{4} = \frac{1.087}{4} \cdot 10^{22}\,\text{min}^{-1} = 2.718 \cdot 10^{21}\,\text{min}^{-1}.$$

As 6 l of blood flow through the entire body in circulation time $\tau = 50$ s, blood flow is

$$V^*_B = \frac{V_B}{\tau} = \frac{6\,\text{l}}{50\,\text{s}} = 0.12\,\text{l/s} = 0.12\,\text{l/s}\,60\,\text{s/min} = 7.2\,\text{l/min}.$$

In a liter of blood there are $N_{Ery} = 5 \cdot 10^{12}$ erythrocyes, and the erythrocyte flow is

$$N^*_{Ery} = 7.2\,\text{l/min}\,5 \cdot 10^{12}\,\text{1/l} = 3.6 \cdot 10^{13}\text{min}^{-1}$$

This assumes that all erythrocytes circulate through the body in 50 s; they come into the lungs without an oxygen load, and are saturated with oxygen there. The ratio is then

$$\frac{N^*_{HG}}{N^*_{Ery}} = \frac{N_{HG}}{N_{Ery}} = \frac{2.718 \cdot 10^{21}}{3.6 \cdot 10^{13}} = 7.55 \cdot 10^7.$$

In an erythrocyte there are $N_{HG} = 7.55 \cdot 10^7$ hemoglobin molecules.[1]

3. For the erythrocytes, several rate equations apply. These say that the rate with which the number of erythrocytes in the body changes is equal to the difference between the rate of creation and destruction, which is proportional to the number of erythrocytes and inversely proportional to the lifespan τ_L (τ_L is constant).

$$\frac{dN_{Ery}}{dt} = -\frac{N_{Ery}}{\tau_L} + N^*_{Ery,a}.$$

At equilibrium, the number of erythrocytes does not change, and the erythrocyte creation rate is

$$N^*_{Ery,\alpha} = \frac{N_{Ery}}{\tau_L}.$$

Solving for the average life span τ_L , we have

$$\tau_L = \frac{N_{Ery}}{N^*_{Ery,\alpha}} = \frac{3 \cdot 10^{13}}{3 \cdot 10^6}\,\text{s} = 10^7\,\text{s} = 116\,\text{d}.$$

1.6 Network Theory of the Human Breathing Apparatus

? The laws of transport phenomena (mass flows, electric currents, water currents, and impulse flows) are of similar form and allow for many analogies. As such, they can also

1 Compare with values from the literature; E. Buddecke gives the mass of hemoglobin in an erythrocyte as (30–32) pg, and P. Karlson gives the molar mass of hemoglobin as 6.7000 g/mol. An average value for N_{HG} can then be calculated as $6.4 \cdot 10^7$.

be described using similar models. Due to relatively simple experiments and reasonable measurement techniques, the modeling of mechanical flow problems using analogous electrical quantities is especially popular. As a basic model, consider a charged capacitor with capacitance C that is discharged over a circuit with Ohm resistance R during time t. With such a model, the flow of breath in the lungs can also be described. The electric resistance R corresponds to the flow resistance of the lungs: $\frac{\Delta p}{V^*}$, with V^* as the flow of breath; the electric capacitance C corresponds to the expansibility of the lungs $\frac{\Delta V}{\Delta p}$.

1. What is the corresponding differential equation for the time dependence of the electric loading current $I\,(t)$ in an electrical system, and what is the solution with initial condition $I\,(t = 0) = I_0$?
2. What is the differential equation analogous to (1) for breath flow in the lungs, and its solution with breath volume V_0?
3. Is the time required to exhale 99% of the air inhaled longer for newborns with stiffer lungs than it is for adults?

[adults: $R_E = 0.15\ \frac{\text{kPa·s}}{\text{l}}$; $C_E = 2{,}000\ \frac{\text{ml}}{\text{kPa}}$; newborns: $R_N = 2.5\ \frac{\text{kPa·s}}{\text{l}}$; $C_N = 75\ \frac{\text{ml}}{\text{kPa}}$]

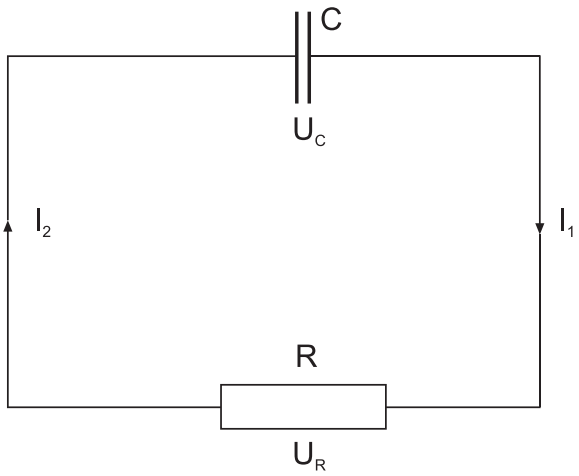

Fig. 1.3. Sketch of the principles of the electric model.

1. For the electric current,

$$I_1 = I_2 = I \tag{1.2}$$

and for the potentials,

$$U_C = -U_R. \tag{1.3}$$

As $U_C = \frac{Q}{C}$ with Q as the charge of the capacitor, and $U_R = IR$, we have

$$\frac{Q}{C} = -IR. \tag{1.4}$$

Taking the derivative gives the differential equation

$$\frac{dI}{dt} = -\frac{I}{RC}. \tag{1.5}$$

Separating variables and integrating gives

$$\int_{I_0}^{I} \frac{1}{I}\, dI = -\frac{1}{RC} \int_{0}^{t} dt$$

and

$$I(t) = I_0 \exp\left(-\frac{1}{RC}\, t\right). \tag{1.6}$$

2. Use the following analogies: the flow of breath corresponds to the electric current ($V^* \hat{=} I$); the intake volume of the lungs corresponds to the electric charge ($V \hat{=} Q$); lung pressure corresponds to electric potential ($p \hat{=} U$). The expansibility of the lungs corresponds to capacitance $C = \frac{\Delta V}{\Delta p}$. Therefore, (1.6) is here given analogously as

$$V = V_0 \exp\left(-\frac{1}{RC}\, t\right) = V_0 \exp\left(-\frac{1}{\frac{\Delta p}{V^*}\,\frac{\Delta V}{\Delta p}}\, t\right) = V_0 \exp\left(-\frac{V^*}{\Delta V}\, t\right). \tag{1.7}$$

3. We can then calculate time τ, at which 99% of the air inhaled has been exhaled, as

$$\tau = -RC \ln 0.01 = RC \ln 100 = 4.61\, RC.$$

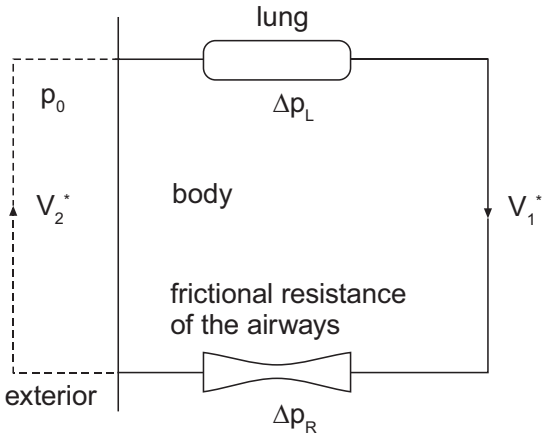

Fig. 1.4. Sketch of the principles of breath flow.

For adults, the value is

$$RC = R_E C_E = 0.15\,\text{kPa s}2.000\,{}^{\text{ml}}/_{\text{kPa}} = 0.3\,\text{s}$$

and for newborns:

$$RC = R_N C_N = 2.5\,\text{kPa s}75\,{}^{\text{ml}}/_{\text{kPa}} = 0.19\,\text{s}.$$

Therefore, we have $\tau_E = 1.38$ s for adults and $\tau_N = 0.86$ s for newborns. The time it takes to exhale inhaled air is less for infants than it is for adults. This means that infants breathe faster, but the quantity of air per breath is smaller for infants than it is for adults.

1.7 Transport Phenomena at the Cell Membrane

?

Oxygen from the air encounters the membrane surface of a cell. The oxygen must diffuse through a boundary layer located in front of the membrane. Consider the air as a two-component gas, comprised of O_2 (Index 1) and N_2 (Index 2). Nitrogen is the carrier gas. The following values are known: the concentration values of oxygen at the membrane surface c_{1M} and outside the boundary layer c_{1L}, the diffusion coefficients (both equal to D for the flows of oxygen and nitrogen), the membrane surface area A, and the boundary layer thickness δ.
Determine an equation to calculate the molar flow n_1^* – the flow of oxygen into the cell.
Note: If a gas component (1) diffuses through a boundary layer, the concentration of both component 1 and carrier gas (2) drops, as the sum of the molar concentrations remains constant. Due to this fall in concentration, the carrier gas diffuses away from the membrane; however, it is not expelled from the membrane, as the membrane is impermeable to the carrier gas. The additional contribution occurs through convection from the interior of the gas in the direction of the membrane. This flow brings additional component (1) with it, and so increases diffusion at the boundary layer.

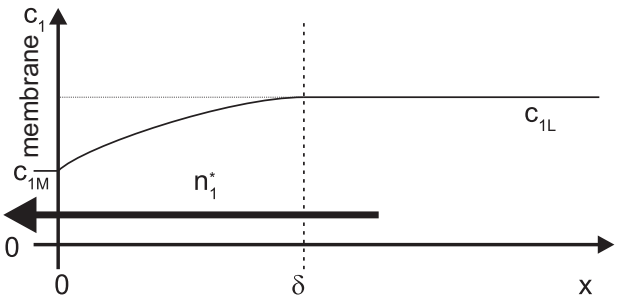

Fig. 1.5. The concentrations of oxygen within the cell ($x \leq 0$), in the boundary layer ($0 < x \leq \delta$), and in the air ($x > \delta$),as well as the consequent molar flow n_1^*.

! Diffusion is a purely molecular movement. Individual components of a mixture exchange places, though the total fluid that comprises the mixture remains at rest. Diffusion can, however, cause a reactive convection flow, as in the case discussed previously. Convection refers to the movement of the total mass. Generally, for the diffusion of component j, Fick's law in one axis holds:

$$n_j^* = -D\,A\,\frac{dc_j}{dx}. \tag{1.8}$$

By (1.8) the gradient $\frac{dc_j}{dx}$ causes a molar flow through surface A, which is perpendicular to the x-direction.

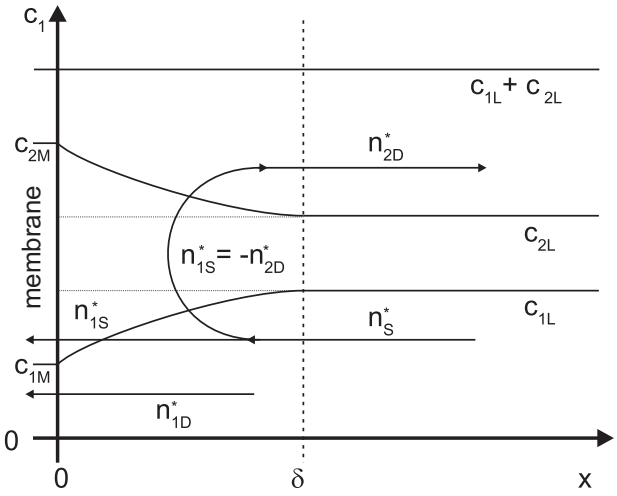

Fig. 1.6. The concentrations and flows in the transition region before the membrane.

The figure shows the behavior of concentration $c_j(x)$ for the component j (1 = oxygen; 2 = nitrogen). As a measure of concentration, we use the mole fraction

$$c_j = \frac{n_j}{\sum n_j}. \tag{1.9}$$

n_j is the number of moles of component j. x is the membrane separation coordinate. For a two-material system, we have

$$c_1(x) + c_2(x) = 1 \tag{1.10}$$

and therefore

$$\frac{dc_1}{dx} = -\frac{dc_2}{dx}. \tag{1.11}$$

From (1.8) we have, with A as membrane surface area,

$$\text{oxygen diffusion flow} \qquad n_{1D}^{*} = -DA\,\frac{dc_1}{dx} \tag{1.12a}$$

$$\text{nitrogen diffusion flow} \qquad n_{2D}^{*} = -DA\,\frac{dc_2}{dx}. \tag{1.12b}$$

Considering (1.11), nitrogen diffusion flow is also given as

$$n_{2D}^{*} = DA\,\frac{dc_1}{dx}. \tag{1.13}$$

This diffusive flow leads to nitrogen transport in the x-direction, away from the membrane. As, however, no nitrogen can be delivered out of the membrane, the diffusion causes a convective flow of nitrogen in the direction of the membrane; this is known as Stefan flow n_{2S}^{*}. As the total flow of nitrogen n_2^{*} at each position x on the boundary layer disappears, the Stefan flow must be exactly equal and opposite to the diffusive nitrogen flow:

$$n_{2S}^{*} = -n_{2D}^{*}. \tag{1.14}$$

Considering that the Stefan flow represents the flow of nitrogen, and by definition, only a portion of the total convection flow n_K^{*}, we have $n_{2S}^{*} = c_2 n_K^{*}$. Therefore,

$$n_K^{*} = \frac{1}{c_2}\,n_{2S}^{*}.$$

This flow n_K^{*} also transports oxygen. The proportion of oxygen n_{1S}^{*} is $c_1 n_K^{*}$, so that

$$n_{1S}^{*} = \frac{c_1}{c_2}\,n_{2S}^{*}$$

and in considering (1.14),

$$n_{1S}^{*} = -\frac{c_1}{c_2}\,n_{2D}^{*}. \tag{1.15}$$

Inserting (1.13) into (1.15), we have

$$n_{1S}^{*} = -\frac{c_1}{c_2} DA \frac{dc_1}{dx}. \tag{1.16}$$

The total flow of oxygen in the direction of the membrane in comprised additively of the convective portion n_{1S}^{*} and the diffusive potion n_{1D}^{*}:

$$n_1^{*} = n_{1S}^{*} + n_{1D}^{*}. \tag{1.17}$$

Inserting (1.16) and (1.12a) into (1.17), we have

$$n_1^{*} = -\frac{c_1}{c_2}\,DA\frac{dc_1}{dx} - DA\,\frac{dc_1}{dx} = -\left(1 + \frac{c_1}{c_2}\right) DA\,\frac{dc_1}{dx}.$$

Separating the variables and integrating over the boundary layer

$$\int_0^{\delta} n_1^* \, dx = -\int_{c_{1M}}^{c_{1L}} \left(1 + \frac{c_1}{c_2}\right) DA \, dc_1$$

we have, considering equation (1.10)

$$n_1^* \int_0^{\delta} dx = DA \int_{c_{1L}}^{c_{1M}} \frac{1}{1 - c_1} \, dc_1 .$$

Integration yields

$$n_1^* \delta = DA \, \ln\left(\frac{1 - c_{1M}}{1 - c_{1L}}\right).$$

The flow of oxygen n_1^* through the membrane is therefore

$$n_1^* = \frac{DA}{\delta} \, \ln\left(\frac{1 - c_{1M}}{1 - c_{1L}}\right) = \frac{DA}{\delta} \, \ln\left(\frac{c_{2M}}{c_{2L}}\right).$$

1.8 Dielectric Measurement of Exocytosis Processes

? In an experiment to calculate the capacitance C and the resistance R of a cell membrane, an alternating potential between intra- and extracellular space is applied using μ-electrodes. The time-dependence of current $I(t)$ is measured.

1. How can values for C and R be calculated from the function $I\,(t)$, and what is the complex impedance Z?
2. The membrane that surrounds a nerve cell with diameter $d = 100\ \mu\text{m}$ can be described for modeling purposes, to a first approximation, as a capacitor. The surface of the capacitor corresponds to the surface A of the cell, and the separation between the surfaces of different charge is membrane thickness $\delta = 10\ \text{nm}$. The cell membrane has dielectric constant ε. What is, in this model, the dependence of capacitance C on the geometric parameters and the dielectric constant of the membrane? The separation of the electrodes from the membrane should be ignored.
3. In exocytosis, materials are expelled from the interior of the cell. How does this method make the observation of such processes possible?

! 1. First, consider flow through the parallel circuit.

$$I = I_R + I_C. \tag{1.18}$$

With $I_R = \frac{U}{R}$ and $I_C = C \, \frac{dU}{dt}$ we have

$$I = \frac{U}{R} + C \, \frac{dU}{dt}, \tag{1.19}$$

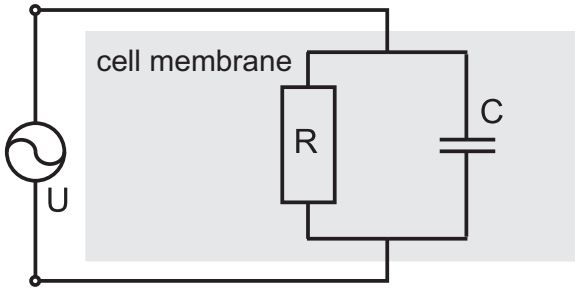

Fig. 1.7. Sketch of the equivalent electrical circuit for the membrane.

with $U(t) = U_0 e^{i\omega t}$ and $\frac{dU}{dt} = i\omega U(t)$

$$I = \frac{U}{R} + i\omega CU. \tag{1.20}$$

Therefore, the complex impedance is

$$Z = \frac{I}{U} = \left(\frac{1}{R} + i\omega C\right)^{-1}.$$

In Z, a phase relationship between I and U is coded; this can be determined by transferring Z into the Euler formulation of complex numbers:

$$Z = |Z|\, e^{i\varphi}.$$

φ is the phase

$$\tan\varphi = -\omega RC$$

and $|Z|$ is the apparent impedance

$$\begin{aligned} |Z| &= \sqrt{Z \cdot Z} = R(1 + R^2\omega^2C^2)^{-1/2} \\ &= R\left(1 + \tan^2\varphi\right)^{-1/2} = R\,\cos\varphi = -\frac{1}{\omega C}\,\sin\varphi. \end{aligned}$$

The apparent impedance is therefore

$$|Z| = \frac{U_{\text{eff}}}{I_{\text{eff}}} = R\,\cos\varphi = -\frac{1}{\omega C}\,\sin\varphi.$$

The resistance and capacity can then be calculated:

$$R = \frac{U_{\text{eff}}}{I_{\text{eff}}}\frac{1}{\cos\varphi}, \quad C = -\frac{I_{\text{eff}}}{U_{\text{eff}}}\frac{\sin\varphi}{\omega}.$$

2. The thickness $\delta \approx 10\,\text{nm}$ of the membrane is small in comparison to the diameter $d \approx 100\,\mu\text{m}$ of the nerve cell considered here, $\delta \ll d$. Locally, therefore, planar geometry is a good approximation, and the membrane can be described as a plate

capacitor with plate separation $a = \delta$. The surface of the capacitor plates A is equal to the surface area of the membrane $A_M = \pi d^2$, if considering a spherical cell. The capacitance of a plate capacitor is $C = \epsilon_0 \epsilon\, A/d$, and in the case above,

$$C = \epsilon_0 \epsilon \frac{A_M}{\delta} = \epsilon_0 \epsilon \frac{\pi d^2}{\delta},$$

with ϵ_0 as the dielectric constant of a vacuum, and ϵ as the dielectric number. A change in the thickness and the surface of the membrane leads to a change in capacitance C.

3. In exocytosis, vesicles from the interior of the cell are temporarily fused with the cell membrane. This changes the geometry of the membrane, and therefore, the capacitance.

1.9 Diffusion and Scale Qualities

? Consider oxygen entering into an amoeba and a blue whale in the case that for both organisms, material transfer occurs only through diffusion. The forms of the amoeba and the blue whale should be assumed to be spherical (diameter of the amoeba $d_A = 1\,\mu\text{m}$; blue whale $d_W = 13\,\text{m}$). The concentration of oxygen in water $c_o = 11\ \text{mg/l}$ is 10 times larger than at position $r = 0.1\,d$ in the organism. The oxygen is consumed at the center of the organism. As a material transfer mechanism, would diffusion alone be sufficient to maintain life in large animals like the whale? Assume that no oxygen is consumed along the diffusion path.
[diffusion constant of O_2 in the organism and in water: $D = 2.1 \cdot 10^{-9}\ \text{m}^2\text{s}^{-1}$, density of oxygen: $\rho_{o_2} = 1.429\ \text{kg/m}^3$]

! The diffusion equation, in general in spherical coordinates, is

$$\frac{\partial c_{O_2}}{\partial t} = D\,\nabla^2 c_{O_2} = \frac{d^2 c_{O_2}}{dr^2} + \frac{2}{r}\frac{dc_{O_2}}{dr},$$

in which derivatives with respect to the angular coordinate are set = 0, as isotropic relationships are assumed. In the stationary case, the distribution of concentration is constant, and the derivative with respect to time disappears. This familiar second-order differential equation with variable coefficients can be transformed into one with constant coefficients through the substitution $r = e^x$. It is then

$$\frac{d^2 c_{O_2}}{dx^2} + \frac{dc_{O_2}}{dx} = 0.$$

Integrating twice gives

$$c_{O_2} = A\,e^{-x} + B = \frac{A}{r} + B.$$

With boundary conditions $c(r = 0.1\,d) = \frac{c_0}{10}$ and $c(r = 0.5\,d) = c_0$ we have the integration constants $A = -0.112\,d\,c_0$ and $B = 1.22\,c_0$, and therefore the solution

$$c_{O_2} = c_0 \left(1.22 - 0.112\frac{d}{r}\right).$$

The concentration gradient in the radial direction is therefore, at the surface,

$$\left[\frac{dc_{O_2}}{dr}\right]_{r=\frac{d}{2}} = \frac{0.112\,c_o\,d}{d^2/4} = 0.45\,\frac{c_o}{d},$$

and is indirectly proportional to the diameter of the organism. The flow per unit area is, according to Fick's Law, proportion to the gradient. As the surface area increases with the square of the diameter, the total transport of oxygen through the surface rises linearly with the diameter. Consumption, however, rises cubically with weight under the assumption of constant energy use. This demonstrates that transport by diffusion, as used by amoebas, would not be sufficient to keep larger animals adequately supplied with oxygen. As such, the whale, like all higher animals, has a circulatory system that delivers oxygen to its organs.

2 Biomechanics

In biomechanics, the laws of classical mechanics are applied to biological systems. In this chapter we give particular consideration to the static characteristics and strength of the skeletal system. The bones that comprise this system are composite materials made of inorganic crystals and proteins that are assembled and dismantled by living cells. Because of this they are very adaptable; bone construction, for example, can be augmented when bones are under loads. These loads include external forces $\vec{F}$, the local effect of which will be discussed as stress (force per area). When forces apply perpendicularly to a surface dA they are referred to as normal stress σ; if they occur in the surface, they are called tangential or shear stress τ. General stress will be described using stress tensors $\underline{T}$.

Stresses cause deformation of the bones. So that a bone is not damaged, this deformation may not exceed an allowable limit. This limitation, in turn, requires that external loads not bring about a state of stress that causes an irreversible change in the form of the bone material, or destroys the bone (bone fracture). For the sake of simplicity, we primarily concentrate here only on cases of single-axis stress – either normal stress, or pure shear stress. The corresponding changes in form are pure strain (and compression), bending, shearing, or torsion. The critical stresses that may not be exceeded will also be characterized, along with the strength of bones.

The strain ϵ of a material body is the change in its length $\Delta 1$ under an axial load of value F with respect to the original length l ($\epsilon = \frac{\Delta l}{l}$). Strain ϵ is proportional to the applied normal stress $\sigma = \frac{F}{A}$ up to the critical stress σ_P. The relationship between stress σ and strain ϵ is $\sigma = E\epsilon$ for $\sigma \leq \sigma_P$. The proportionality factor E is called the tensile modulus (or Young's modulus). There is an analogous relationship for the shearing of a body. Here, due to a tangential force of magnitude F, shear stress $\tau = \frac{F}{A}$ is proportional to the shear angle γ up to the allowed stress τ_P ($\tau = G\gamma$ for $\tau \leq \tau_P$). The proportionality factor G is called the shear modulus. The relationships $\sigma = E\epsilon$ and $\tau = G\gamma$ are called Hooke's Laws for Strain and Shearing Stress, respectively. E and G are characteristics of materials, as are σ_P and τ_P; their values for bone material will be discussed. The stresses σ_P and τ_P mark the upper bound of Hooke's Law (proportionality boundaries). At higher values, the proportionality breaks down, and plastic deformation occurs in the bone. Even if the stresses lessen, a permanent deformation remains. If the stresses increase further, the bone will break at σ_B and τ_B. The region of plasticity is relatively small for bones, so strength against plastic deformation σ_P and τ_P can be set numerically equal to strength again breaking σ_B and τ_B.

The intensity of local stress is not only determined by the intensity of the external force, but also by its point of application. These are usually described as moments; the bending moment M_b, for example, corresponds to the product of the external force and the length of the lever arm. Bending stress $\sigma_b = \frac{M_b}{W_b}$ is generated, with the section

modulus

$$W_b = \frac{1}{e_R} \int x^2 dA.$$

For torsion, torque M_t produces torsional stress τ_t according to $\tau_t = \frac{M_t}{W_p}$, with the polar section modulus

$$W_p = \frac{1}{e_R} \int r^2 dA.$$

The section moduli are also calculated as integrals over all surfaces dA, weighted by the square of the distance from the reference axis; e_R is the distance of the boundary from the neutral axis. Stresses may not exceed the maximal values of bone strength for bending and torsion, either.

Bones must be able to bear the greatest possible forces and moments with the smallest possible deviations, and yet remain as light as possible. This optimization problem is solved by the body using "lightweight construction". The external parts of the bones are relatively dense, but internally they are, for the most part, porous throughout. Bone is structured as an extracellular matrix that is primarily comprised of calcium hydroxylapatite. This gives the bone resistance to compression. The rest of the bone is comprised principally of protein, which is primarily responsible for longitudinal strength against strain.

The forces that affect bones are body weight, and loads from outside the body. Additionally, there are also muscle forces that can apply torques through coupled action, and can lead to bending of the bones. An example is the skeletal muscle system. These muscles, with 40–50% of the entire body weight, are by far the body's heaviest organ. This is the muscle system that allows motion. The functional qualities of the skeletal muscles that allow for this motion result from bundled muscle fibers. Each muscle fiber is a long, cytoplasmic tube with diameters of 10–100 μm and lengths of 1–5 cm, without cell boundaries, so that a cell can have many hundreds of cell nuclei. These fibers usually extend throughout the entire muscle, and end in conjunctive tendons the bind the muscle to the bone. A muscle cell contains a large number of microfibrils that can change their length. They run parallel to one another along the longitudinal axis of the muscle, and are usually around 2.5 μm long.

A muscle generates its maximum force through isometric contraction – for example, in holding up a weight. When the muscle shortens under constant stress, its behavior is called isotonic contraction – for example, in lifting a weight. These different behaviors are illustrated by rest strain graphs. Here, a tensile force is applied to a muscle at rest, and the strain is measured. These graphs show non-Hookean behavior, and describe the natural elasticity of muscle fibres. The energy conversion efficiency η of muscle movement – the relationship of the mechanical work done to the chemical energy consumed – depends on the type of contraction. In isometric loading there is no motion in the direction of force, and so no mechanical work is done. The energy conversion efficiency is therefore $\eta = 0$. In isotonic loading, with a force that is less

than 30% of the maximum possible, there is an energy conversion efficiency on the order of $0.4 \leq \eta \leq 0.5$. The remaining chemical energy is converted into heat.

As bones need to be able to move in relation to one another, the body constructs joints. Because bones are not protected against friction, bone-to-bone contact is avoided by and bridged with cartilage. This material possesses a high resistance to compressive loads, with little friction. Additionally, the cartilage takes on a dampening role under shock loads. Coefficients of friction are lessened through joint fluidity; this avoids dry friction. Ligaments stabilize the joints, and also guide the tendons.

2.1 Achilles Tendon

With the help of the Achilles tendons, the main muscle of the leg is able to hold up the body of a person of mass $m = 50\,\text{kg}$ standing on one leg, at an angle between the foot and the surface of the floor of $\alpha = 20^\circ$. In this situation, what is the muscular force F_M if the length of the foot is $l = 13\,\text{cm}$ and the instep is $a = 10\,\text{cm}$? Assume that due to the anatomy of the foot (the ligaments), the tendons always act perpendicularly on the bones of the foot. If we assume that the muscular force acts as the strain force of a spring with spring constant $k = 10^3\,\text{N/cm}$, what is the required spring displacement s?

?

First, consider the geometry shown in the following diagram.

!

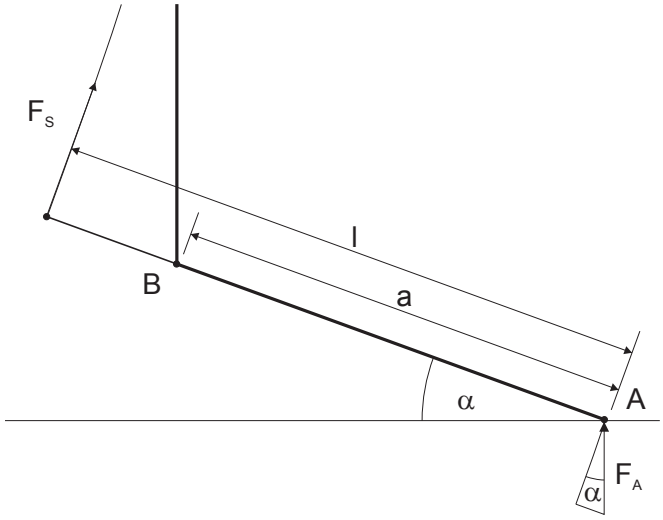

Fig. 2.1. The foot as a lever.

In static equilibrium, the following relationships must hold:

$$\sum_{i=1}^{n} \vec{F}_i = 0, \tag{2.1}$$

$$\sum_{j=1}^{m} \vec{M}_j = 0. \tag{2.2}$$

Here, the forces $\vec{F}_i$ acting upon a body from outside must also be considered, as well as the reaction forces that arise from a load. Internal forces cancel these out, and therefore do not enter into the calculation. From the first condition, we have the equilibrium reaction force $\vec{F}_A$ of the ground at Point A due to the weight of the person:

$$\vec{F}_G + \vec{F}_A = 0.$$

The reaction force $\vec{F}_A$ is opposite the weight force $\vec{F}_G$. As such, the magnitudes of F_A and F_G are equal. The second condition must hold for each surface point at which the force applies. Because of this, we can freely choose any point to formulate the sum of the moments such that they disappear. It is convenient to take the sum of the moments around Point B, as there, the weight force itself delivers no moment (the lever arm has length zero). Therefore,

$$F_S \cdot (l - a) - F_A \cdot a \cos\alpha = 0.$$

As $F_A = F_G$ and the force of the tendon F_S must be equal to the force of the muscle F_M, we have

$$F_M = \left(\frac{a}{l-a}\right) mg \cos\alpha.$$

Numerically

$$F_M = \frac{10}{3} \cdot 50\,\text{kg} \cdot 9.81\,\text{m/s}^2 \cos 20^\circ = 1{,}536\,\text{N}.$$

If we model the muscle as a spring that builds up its force F_M over displacement s, we find

$$F_M = ks$$

and therefore

$$s = \frac{F_M}{k} = \frac{1{,}536\,\text{N}}{10^3\,\text{N/cm}} = 1.54\,\text{cm}.$$

2.2 Bone Structures of the Ulna and Radius

? Consider a forearm held at 90° relative to the body. The hand holds a full mug of beer (volume $V = 1$ l; weight of the mug when empty $F_{GK} = 10$ N). The arm is $l = 50$ cm long. To model the problem, we shall take a round rod to represent the ulna and the radius, to which half of the forces applied to both bones will be allotted. How must this rod –

and therefore, the ulna and radius – be formed so that at each position x (length coordinate of the bone), strength (bending stress) is equal? What is the minimum diameter the bones must have at the elbow in order to hold the mug of beer steady?

The following two models of bones should be considered:

1. Solid rod
2. Hollow rod with diameter ratio $\frac{D}{d} = 2$, with D as the external diameter and d as the internal diameter.

We will ignore the weight of the bones themselves. The failure stress of the bone material is $\sigma_B = 100\,\text{MPa}$.

We can assume the solution of this integral:

$$\int z^2 \sqrt{a^2 - z^2}\, dz = -\frac{z}{4}\sqrt{(a^2 - z^2)^3} + \frac{a^2}{8}\left[z\sqrt{(a^2 - z^2)} + a^2 \arcsin\left(\frac{z}{a}\right)\right] + C.$$

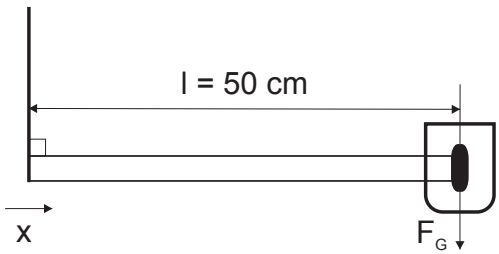

Fig. 2.2. The ulna and the radius are modeled as two rods. They are oriented at a right angle to the upper arm, and are loaded with a mug of beer at their far end.

1. Solid rod:

The shear force $\vec{F}$ is responsible for the load that acts at the end of the arm:

$$\vec{F} = \vec{F}_{GK} + \vec{F}_{GB}$$

with $\vec{F}_{GK}$ as the weight force of the mug and $\vec{F}_{GB}$ as the weight force of the beer. $F_{GB} = \varrho_B g V$ with V as the contents of the mug, and ϱ_B as the density of the beer. For ϱ_B, we can assume the density of water ϱ_W: $\varrho_B = \varrho_W = 1{,}000\,\text{kg/m}^3$
We have shear force

$$F = 10\,\text{N} + 1{,}000\,\text{kg/m}^3 \cdot 9.81\,\text{m/s}^2 \cdot 0.001\,\text{m}^3 = 19.81\,\text{N}.$$

Half of this shear force loads each of the bones, so that the rod force is $F_S = \frac{F}{2} = 9.9\,\text{N}$. As the rod is held steady, there is also a bending moment across the length of the rod: $M_b(x)$

$$M_b(x) = F_S\,(l - x)\,.$$

The bending moment is at its greatest at the fixing point ($x = 0$), the elbow:

$$M_{b,\max} = F_S l = 9.9\,\mathrm{N} \cdot 0.5\,\mathrm{m} = 4.95\,\mathrm{Nm}.$$

F_S and $M_b(x)$ together load the rod at each point x. However, because the length of the rod l is much greater than the rod radius D, only M_b is of measurable meaning for the stress state in the rod.[1] The bending moment causes an identical reaction moment at each point x according to its magnitude:

$$M_b^{\nabla}(x) = \int_A \sigma(z)\, z\, dA = \int_{-\frac{1}{2}D(x)}^{\frac{1}{2}D(x)} \sigma(z)\, z\, B(x,z)\, dz$$

with $B(z)$ as the width of the rod. The rod is round, and therefore

$$B(x,\, z) = \sqrt{\left[\frac{D(x)}{2}\right]^2 - z^2}.$$

The distribution of stress $\sigma\,(z)$ must be linear because the frontal areas of the rod remain undeformed under bending. This means that all "fibers" in the z direction are linearly squeezed or stretched by $\Delta l\,(z)$. The middle fibers remain unstretched. They are termed the "neutral fibers" (neutral axis). $\Delta l\,(z)$ is, therefore, a linear function. As Hooke's law $\sigma = E\varepsilon$ applies in the elastic region, with $\varepsilon\,(z) = \frac{\Delta l(z)}{l}$, the dependency $\sigma\,(z)$ must also be linear. The function $\sigma\,(z)$ is

$$\sigma\,(x, z) = \frac{2\sigma_0(x)}{D}\, z$$

with $\sigma_0(x)$ as the tension value at position $[x,\, z] = \left[x,\, \frac{D(x)}{2}\right]$. Therefore,

$$M_b^{\nabla}(x) = \frac{2\sigma_0(x)}{D(x)} \int_{-\frac{1}{2}D(x)}^{+\frac{1}{2}D(x)} z^2 \sqrt{\frac{D(x)}{2}^2 - z^2}\, dz,$$

and by symmetry,

$$M_b^{\nabla}(x) = 2\frac{2\sigma_0(x)}{D(x)} \int_0^{\frac{1}{2}D(x)} z^2 \sqrt{\left[\frac{D(x)}{2}\right]^2 - z^2}\, dz.$$

The integral

$$2 \int_0^{\frac{1}{2}D(x)} z^2 \sqrt{\left[\frac{D(x)}{2}\right]^2 - z^2}\, dz = J_a$$

1 In the case that $l \ll D$ we refer to a "slender" rod, and the deformation possible is curvature, to a good approximation. If $l/D \approx 1$, though, additional deformations appear, along with additional shear stresses.

is also written as the area moment of inertia J_a, and $\frac{J_a}{b} = W_a$ as the axial section modulus[2] with b as the distance of the neutral fibers from the boundary (edge) fibers. b is $\frac{1}{2}D(x)$ in the previous case. Therefore, we have

$$M_b^{\nabla}(x) = \frac{2\sigma_0(x)}{D(x)} J_a = \sigma_0(x)\, W_a.$$

The integration of $2\int_0^{\frac{1}{2}D(x)} z^2 \sqrt{\left[\frac{D(x)}{2}\right]^2 - z^2}\, dz$ yields (considering the integration solution given in the problem), for values J_a and W_a,

$$J_a = \frac{\pi D(x)^4}{64} \quad \text{and} \quad W_a = \frac{\pi D(x)^3}{32}.$$

And therefore

$$M_b^{\nabla}(x) = \frac{\pi}{32} D(x)^3 \sigma_0(x).$$

As $M_b(x)$ and $M_b^{\nabla}(x)$ must be equal, we have

$$F_S l \left(1 - \frac{x}{l}\right) = \frac{\pi}{32} D(x)^3 \sigma_0(x).$$

And therefore

$$\sigma(x) = \frac{32}{\pi D(x)^3} F_S l \left(1 - \frac{x}{l}\right).$$

As long as strength remains constant over x, $\sigma_0(x) = \text{constant}$, and is therefore not a function of x. Additionally, σ_0 cannot exceed the failure stress σ_B; with the condition that $\sigma_0 = \sigma_B$ the condition of minimum security is fulfilled. Therefore,

$$D^3(x) = \frac{32 F_S l}{\pi \sigma_B} \left(1 - \frac{x}{l}\right).$$

And the form of the bones becomes

$$D(x) = D_0 \sqrt[3]{1 - \frac{x}{l}}$$

with

$$D_0 = \sqrt[3]{\frac{32 M_{b,\max}}{\pi \sigma_B}}$$

as the diameter of the bone at the elbow $x = 0$.
With $M_{b,\max} = 4.95\,\text{Nm}$; $\sigma_B = 100\,\text{MPa} = 10^8\,\text{Pa}$ we have $D_0 = 7.96\,\text{mm}$.

2 Note that both expressions J_a and W_a are not moduli in the sense of force × lever arm, but rather are purely geometric quantities. J_a has unit m^4 and W_a has unit m^3.

Table 2.1. Bone diameter at different positions

	x [cm]	0	5	10	20	30	40	50
Solid rod	D_{solid} [mm]	8.0	7.7	7.4	6.7	5.9	4.7	0
Hollow rod	D_{hollow} [mm]	8.2	8.0	7.6	7.0	6.1	4.8	0

2. Hollow rod:
Here, the geometric quantities J_a and W_a change:

$$J_{a(\text{hollow})} = 2\left[\int_0^{\frac{1}{2}D(x)} z^2\sqrt{\frac{D(x)^2}{4}-z^2}\,dz - \int_0^{\frac{1}{2}d(x)} z^2\sqrt{\frac{d(x)^2}{4}-z^2}\,dz\right]$$
$$= \frac{\pi}{64}\left[D(x)^4 - d(x)^4\right]$$

$$W_{a(\text{hollow})} = \frac{\pi}{32}D(x)^3\left[1-(\frac{d}{D})^4\right].$$

With $\frac{d}{D} = 0.5$ we have

$$W_{a(\text{hollow})} = \frac{\pi}{32}D(x)^3 \cdot 0.9375.$$

As $M_b = W_a\sigma_B$, we have at position $x = 0$

$$M_{b,\max} = \frac{0.9375\,\pi}{32}D_0^3\,\sigma_B$$

and therefore

$$D_{0(\text{hollow})} = \sqrt[3]{\frac{32\,M_{b,\max}}{0.9375\cdot\pi\cdot\sigma_B}} = 1.03\,D_{0(\text{solid})} = 8.13\text{ mm}.$$

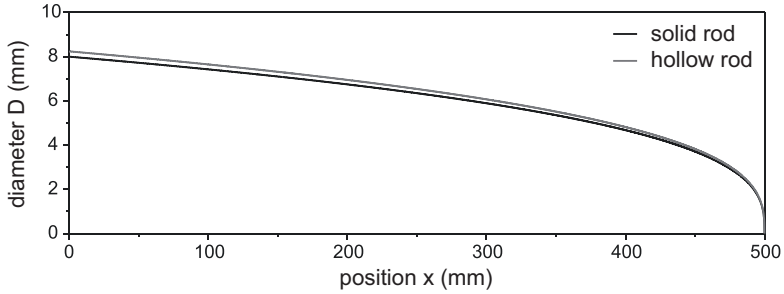

Fig. 2.3. The forms of the bones in comparison to one another.

Conclusion: At the same strength, the hollow rod has a diameter barely greater than that of the solid rod. Bones are therefore hollow in most cases. Advantages of this structure include a reduced amount of bone mass required, a reduction in dead weight, and more space for vessels and nerve fibers. The thickness of the arm bones is greater in adults than the value calculated here, as a human can hold more than a mug of beer.

2.3 Ski Bindings

Consider a ski binding that releases if the shear force $\vec{F}$ at the top of the binding exceeds a limit. Determine this limit, with a quadruple safety contingency ($\frac{\tau_B}{\tau_{\max}}$) against torsion fracture (four times maximum shear stress must be smaller than the fracture stress of bone). Assume that the bone structure, including the knee, in the human leg can be described as a round rod of length l and diameter d. This rod is held firm at its upper end. Assume that the rod has the physical properties of bone material. Also, determine the angle $\varphi_{\max}$ that the body has rotated relative to the axis of the skis at the moment at which the binding releases.
[rod: diameter $d = 4$ cm; length $l = 1$ m; failure stress of bone $\tau_B = 65$ MPa;
shear modulus of the bone mass $G = 3.7$ GPa
additionally: shoe size $s = 25$ cm; safety factor $\nu = 4$]

For the torque $\vec{M}_s$ that the ski binding exerts on the ski, we have

$$\vec{M}_s = \vec{F} \cdot \vec{s}. \tag{2.3}$$

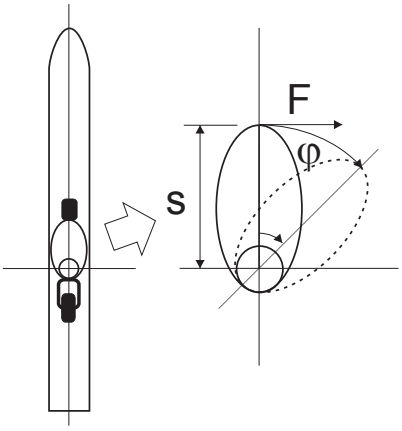

Fig. 2.4. The ski with the binding, from overhead.

Here, $\vec{F}$ is the shear force, and the length of the vector $\vec{s}$ corresponds to the shoe size. The torque that affects the leg is

$$M = \int_A \tau\,(r)\, r\, dA$$

with $\tau\,(r)$ as the shear stress distribution over a cross section of the rod. The distribution of stress $\tau(r)$ is, due to

$$\frac{\tau(r)}{\tau_0} = \frac{r}{R}$$

with $\tau_0 = \tau(r = R)$,

$$\tau\,(r) = \tau_0 \frac{r}{R}. \tag{2.4}$$

The element of area dA can be expressed using the radial coordinate r: $dA = 2\pi r dr$. Then the torque becomes

$$M = \tau_0 \left(\frac{2\pi}{R}\right) \int_0^R r^3 dr = \tau_0 W_P. \tag{2.5}$$

The polar section modulus W_P for a round, solid rod is

$$W_P = \frac{2\pi}{R} \int_0^R r^3\, dr = \left(\frac{\pi}{2}\right) R^3 = \left(\frac{\pi}{16}\right) d^3. \tag{2.6}$$

Therefore,

$$M = \frac{\pi \tau_0\, d^3}{16}. \tag{2.7}$$

The maximum allowable torque $M_{\max}$ can be determined from the condition that the maximum shear stress τ_0 multiplied by the safety factor υ must remain smaller than the failure stress τ_B of the bone, $\tau_0 \leq \upsilon\, \tau_B$:

$$M_{\max} = \frac{\pi \tau_B\, d^3}{16\, \upsilon}.$$

By setting this torque and the torque applied equal (2.3), $M_{\max} = M_s$, we have, for the release force,

$$F = \frac{\pi \tau_B\, d^3}{16\, \nu s} = 314.4\,\text{N}. \tag{2.8}$$

Geometrically – see Figure 2.5 – the twisting angle φ is related to the shear angle γ by

$$l\gamma = R\varphi = \frac{d}{2}\varphi \rightarrow \varphi = \frac{2\,l}{d}\gamma. \tag{2.9}$$

Therefore, the maximum twisting angle $\varphi_{\max}$ at which the ski binding releases is

$$\varphi_{\max} = \frac{2\,l}{d}\gamma_{\max}. \tag{2.10}$$

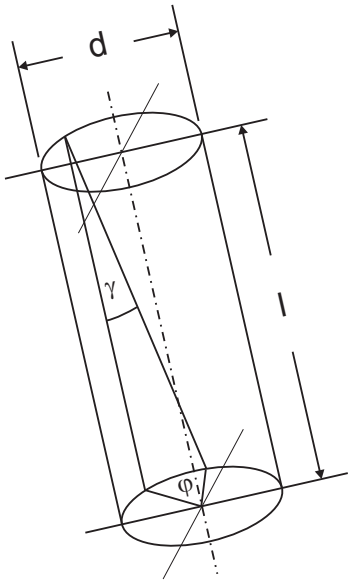

Fig. 2.5. The leg during torsion, with twisting angle φ and shear angle γ.

From Hooke's Law for torsion $\tau = G\gamma$, for $\tau < \tau_B$ with G as the shear modulus, we have

$$\gamma = \frac{\tau}{G} \quad \text{and} \quad \gamma_{\max} = \frac{\tau_B}{\nu G}. \tag{2.11}$$

Therefore, the maximum twisting angle is

$$\varphi_{\max} = 2\frac{\tau_B l}{\nu G d} \mathrel{\widehat{=}} \varphi^{\circ}_{\max} = 180^{\circ}\,\frac{\varphi_{\max}}{\pi} = 360^{\circ}\,\frac{\tau_B l}{\nu \pi G d}. \tag{2.12}$$

With $l = 1$ m; $G = 3.7$ GPa; $\tau_B = 65$ MPa and $d = 4$ cm we have

$$\varphi_{\max} = 360^{\circ}\,\frac{65\ \text{MPa} \cdot 1\ \text{m}}{4\pi \cdot 3.7\ \text{GPa} \cdot 0.04\ \text{m}} = 12.6^{\circ}.$$

In reality, the angle $\varphi_{\max}$ is significantly larger, because the leg – in spite of the assumption – is not fixed at the hip (ball-and-socket joint), and because the two parallel bones in the lower leg – tibia and fibula – permit greater rotational motion without harming the bones.

2.4 Elasticity of the Vertebrae

A man pulls on a rope tied to a wall with a force of $F = 200$ N (see figure). As a result, his spine begins to bend. Calculate this curvature – the deflection curve of the spine. The spine, fixed in place in the pelvis, is modeled as a straight elastic rod, orthogonal

?

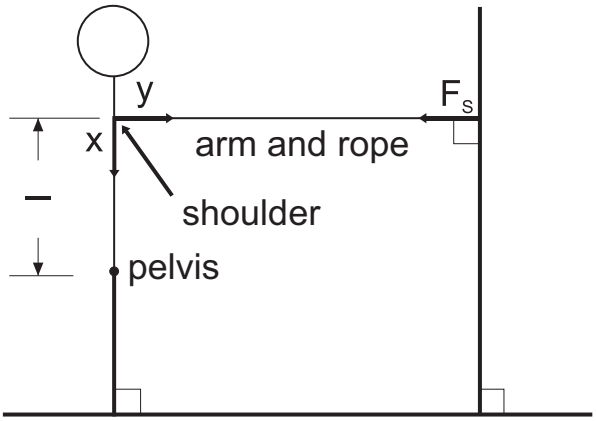

Fig. 2.6. Geometry for the determination of the deflection curve.

to the ground, with a square cross section. The pelvis remains at rest while the man pulls. The connection of the shoulders to the spine is fixed. What is the maximum deflection due to this load?
[Young's modulus of the spine (with the musculature) $E = 6.25\,\text{GPa}$ (effective value); length of the spine $l = 1\,\text{m}$; width of the square spine $b = 4\,\text{cm}$; failure stress of the bone material $\sigma_B = 120\,\text{N/mm}^2$]

! The external load on the spine is given by the force of the rope F_S, which arises to counter the pulling force F. This produces the x-dependent bending moment $M(x)$

$$M(x) = F_S\, x.$$

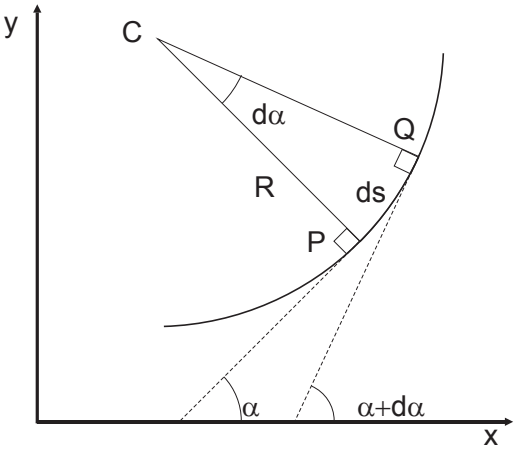

Fig. 2.7. Geometry for the determination of the deflection curve.

This moment leads to stresses in the spine that can, to a good approximation, be considered as pure normal stresses. So that the system remains static, the external moment must be equal and opposite to the internal moment. This is dependant on position – on the length coordinate x, as well as on the y coordinate:

$$dM\,(x, y) = \sigma(x)\, y\, dA.$$

Here, $\sigma(x) = \frac{2\sigma_0(x)}{b}\, y$ with $\sigma_0(x)$ as the tension on the upper boundary fibers of the spine. The element of area $dA = b\, dy$ is a cross sectional element of the spine. Therefore,

$$M(x) = \frac{2\sigma_0(x)}{b} \int_{-b/2}^{b/2} y^2 b\, dy = \frac{2\sigma_0(x)}{b}\, I_a$$

with the axial area moment of inertia

$$I_a = 2b \int_0^{b/2} y^2\, dy = b \left[\frac{y^3}{3} \right]_0^{b/2} = \frac{b^4}{12}.$$

The bending moment becomes

$$M(x) = \frac{2\sigma_0(x) I_a}{b}$$

and

$$\sigma_0(x) = \frac{M(x)\, b}{2\, I_a}.$$

The deflection curve can be described by the function $y(x)$. $y(x)$ is related to the radius of curvature $R(x)$.
We have

$$\tan\alpha = \frac{dy}{dx} = y'$$

and we can derive

$$\frac{d\alpha}{\cos^2\alpha} = y''\, dx.$$

Furthermore, we have $ds^2 = dx^2 + dy^2$, and therefore

$$\frac{ds}{dx} = \sqrt{1 + \left(\frac{dy}{dx}\right)^2} = \sqrt{1 + y'^2}.$$

With $d\alpha = \frac{ds}{R}$, we have, for the radius of curvature,

$$R = \frac{ds}{d\alpha} = \frac{ds}{dx}\frac{dx}{d\alpha}.$$

The relationship $\sin^2\alpha + \cos^2\alpha = 1$ can also be written in the form $\tan^2\alpha + 1 = \frac{1}{\cos^2\alpha}$, or, considering the terms mentioned above,

$$y'^2 + 1 = \frac{1}{\cos^2\alpha} = y''\frac{dx}{d\alpha}$$

$$R = \sqrt{1 + y'^2} \cdot \frac{(1 + y'^2)}{y''} = \frac{\left(1 + y'^2\right)^{3/2}}{y''}.$$

When considering the bending of bones, only small curvatures occur. For small curvatures, y' becomes small and y'^2 is even smaller, so we find, for the relationship between radius of curvature $R(x)$ and deflection curve $y(x)$,

$$R(x) = \frac{1}{y''(x)} \rightarrow y''(x) = \frac{1}{R(x)}.$$

In order to show how the radius of curvature depends on the load, we must consider the strain geometry according to Figure 2.8. For the distance of a point in the spine from the center of the circle that describes the curvature, we will use r. The load causes strain dl on the outermost fiber $r = R + \frac{b}{2}$, and compression $-dl$ on the innermost fiber $r = R - \frac{b}{2}$. The middle fibers of the spine $r = R$ remain undeformed (neutral fibers).

$$\frac{dx}{R} = \frac{dl}{\frac{b}{2}} = \frac{2\,dl}{b}.$$

As $\frac{dl}{dx} = \epsilon_0$ is the strain on the outermost fiber, we have

$$\frac{1}{R} = \frac{2\,\varepsilon_0}{b}.$$

Considering Hooke's Law $\sigma_0 = E\epsilon_0$ we have

$$\frac{1}{R} = \frac{2\,\sigma_0}{E\,b}.$$

Because $\frac{1}{R} = y''$ is valid for large radii of curvature, and for $\sigma_0 = \frac{M \cdot b}{2\,I_a}$ (see above), we have, for the second derivative of the deflection curve, the condition

$$y''(x) = \frac{M(x)}{I_a E}.$$

In the previous case, $M(x) = F_S x$, and $I_a = \frac{b^4}{12}$; therefore,

$$y'' = \frac{12\,F_S x}{b^4 E} = A\,x.$$

Then we have

$$y' = A\,\frac{x^2}{2} + B$$

and

$$y = A\,\frac{x^3}{6} + B\,x + C.$$

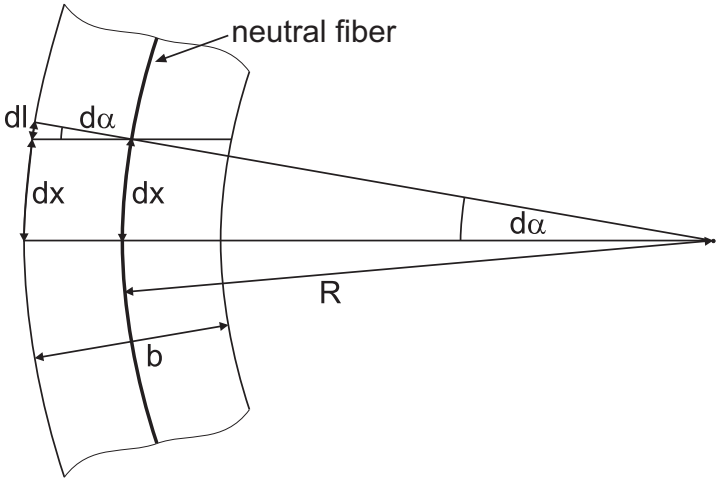

Fig. 2.8. Strain and compression of the material of the bones of the spine on both sides of the neutral fiber.

We have boundary conditions

$$y(l) = 0$$
$$y'(l) = 0,$$

which lead to

$$B = -\frac{A\,l^2}{2} = -\frac{6\,F_S l^2}{b^4 E}$$
$$C = -\frac{A\,l^3}{6} + \frac{A\,l^3}{2} = \frac{4\,F_S l^3}{b^4 E}.$$

The deflection curve is therefore

$$y(x) = \frac{2\,F_S}{b^4 E}\,x^3 - \frac{6\,F_S\,l^2}{b^4 E}\,x + \frac{4\,F_S\,l^3}{b^4 E}$$
$$= \frac{2\,F_S}{b^4 E}\left(x^3 - 3\,l^2 x + 2\,l^3\right).$$

As the maximum curvature occurs at $x = 0$, we have

$$y_{\max} = y(0) = \frac{4\,F_S l^3}{b^4 E}.$$

Numerically,

$$y_{\max} = \frac{4 \cdot 200}{0.04^4 \cdot 6.25 \cdot 10^9}\,\frac{\mathrm{N\,m^3}}{\mathrm{m^4 Pa}} = 5\,\mathrm{cm}.$$

Naturally, the solution is only valid if the bone material is not damaged by the load. The spine would break if the load exceeded the fracture stress σ_B at any point. The maximum stress that could be caused by the load given is $\sigma_{0,\max} = \sigma_0\,(l)$:

$$\sigma_{0,\max} = \frac{M\,(l)\,b}{2\,J_a} = \frac{F_S\,l\,b}{2\,\frac{b^4}{12}} = \frac{6\,F_S\,l}{b^3}.$$

Numerically,

$$\sigma_{0,\max} = \frac{6 \cdot 200 \cdot 1{,}000}{40^3}\,\frac{\mathrm{N\,mm}}{\mathrm{mm}^3} = 18.75\,\mathrm{N/mm^2}.$$

As the fracture stress of bone material is $\sigma_B = 120\,\mathrm{N/mm^2}$, we have demonstrated that $\sigma_{0,\max} \ll \sigma_B$. The bone can handle the load.

2.5 Lifting a Patient

? The lifting device at a hospital bed is comprised of a fixed frame to which a round steel bar with length $l = 1$ m is fixed perpendicularly (parallel to the ground). At the end of this bar is a triangular handle that makes standing up easier for the patient. We wish to find the necessary external diameter D, the deflection curve $y(x)$, and the maximum curvature $y_{\max}$ of the bar while considering its own weight for a $m_P = 100$ kg patient.

1. for a solid bar
2. for a tube with a ratio of the inner diameter to the outer diameter of $\frac{d}{D} = 0.95$.

Quadruple safety from the bar breaking is required.
[Material values for steel: Young's modulus $E = 206$ GPa; fraction stress $\sigma_B = 981$ MPa; density $\rho = 7{,}800\,\mathrm{kg/m^3}$]

! *Determination of the External Diameter*

1. Solid bar:
   The external load is given by the weight of the patient and the bar's own weight, and leads to the x-dependant bending moment $M(x)$

$$M(x) = M_P(x) + M_E(x).$$

   Here,

$$M_P(x) = m_P g\,(l - x)$$

   is the contribution of the patient's weight to the bending moment, and

$$M_E(x) = \varrho g A \int_x^l (l - x)\;dx = \frac{\pi}{8}\varrho g D^2\,(l - x)^2$$

   is the contribution of the bar's own weight. Under the assumption that the patient's entire weight is applied to the bar, we have

$$M(x) = g\,(l - x)\left\{m_P + \frac{\pi}{8}\varrho D^2\,(l - x)\right\}.$$

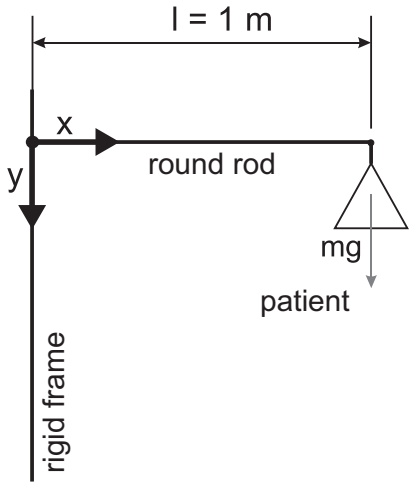

Fig. 2.9. Lifting device at the bed.

At position $x = 0$ the bending moment is at its greatest, which means that there, the load is greatest. $M_{\max}$ is then

$$M_{\max} = M\,(x = 0) = gl\left(m_P + \frac{\pi}{8}\varrho D^2 l\right).$$

This bending moment causes stresses in the bar that create an internal moment equal to the external moment. The contributions to this internal moment depend on position z, the coordinate in the vertical direction perpendicular to the neutral fiber:

$$dM\,(z) = \sigma z dA.$$

The position-dependant normal stress is $\sigma = \frac{2\sigma_0}{D}\,z$ and σ_0 is the value of the stress on the upper boundary fiber. The element of area is

$$dA = 2\sqrt{\frac{D^2}{4} - z^2}\,dz.$$

The bending moment becomes

$$M = \frac{4\sigma_0}{D}\int_{-D/2}^{D/2} z^2\sqrt{\frac{D^2}{4} - z^2}\,dz = \frac{8\sigma_0}{D}\int_{0}^{D/2} z^2\sqrt{D^2 - z^2}\,dz = \frac{2\sigma_0}{D}\,I_a.$$

I_a is the axial area moment of inertia

$$\begin{aligned} I_a &= 4\int_0^{D/2} z^2\sqrt{\frac{D^2}{4}-z^2}\,dz \\ &= 4\left[\frac{z}{4}\sqrt{\left(\frac{D^2}{4}-z^2\right)^3}+\frac{D^2}{32}\left(z\sqrt{\frac{D^2}{4}-z^2}+\frac{D^2}{4}\arcsin\frac{2z}{D}\right)\right]_0^{D/2} \\ &= \frac{D^4}{32}\arcsin 1 = \frac{D^4}{32}\frac{\pi}{2} = \frac{\pi D^4}{64}. \end{aligned}$$

Then,

$$M = \frac{2\sigma_0 I_a}{D} = \frac{\pi\sigma_0 D^3}{32}.$$

The stress σ_0 at position $x = 0$ cannot become greater than the allowed stress σ_{all}

$$\sigma_{\text{all}} = \frac{\sigma_B}{\nu}$$

with σ_B as the fracture stress of steel; ν is the safety factor. As such, the permissible internal moment is

$$M_{\text{all}} = \frac{\pi\sigma_B D^3}{32\nu}.$$

M_{all} is, however, equal to the external moment $M_{\max}$:

$$\frac{\pi\sigma_B D^3}{32\nu} = gl\left(m_P + \frac{\pi}{8}\varrho D^2 l\right)$$

or

$$D^3 - \frac{4\varrho g\nu l^2}{\sigma_B}D^2 = \frac{32\, m_P g l\nu}{\pi\sigma_B}.$$

Solving for the diameter of the bar, we have

$$\begin{aligned} D^3 - 0.00125\ \text{cm}\cdot D^2 &= 0.00004\ \text{cm}^3 \\ D &= 3.40\ \text{cm}. \end{aligned}$$

2. Hollow bar:
For the hollow bar, the contribution of the patient's weight remains the same. The contribution of the bar's own weight is

$$M_E = \frac{\pi}{8}\varrho_{ST} g D^2\left[1-\left(\frac{d}{D}\right)^2\right](l-x)^2$$

and for the total bending moment,

$$M_{\max} = g\left\{m_P + \frac{\pi}{8}\varrho D^2 l^2\left[1-\left(\frac{d}{D}\right)^2\right]\right\}.$$

The internal moment is

$$M_{\text{all}} = \frac{\pi\sigma_B}{32\nu}\left(1-\delta^4\right)D^3.$$

Using $M_{\max} = M_{\text{all}}$ we have

$$\frac{\pi\sigma_B}{32\nu}\left[1-\left(\frac{d}{D}\right)^4\right]D^3 = g\left\{m_P + \frac{\pi}{8}\varrho D^2 l^2\left[1-\left(\frac{d}{D}\right)^2\right]\right\}.$$

and in normal form,

$$D^3 - \left\{\frac{4\varrho g\nu l^2}{\sigma_B}\left[\frac{1-(\frac{d}{D})^2}{1-(\frac{d}{D})^4}\right]\right\}D^2 = \frac{32\, m_P g l\nu}{\pi\sigma_B[1-\left(\frac{d}{D}\right)^4]}.$$

Numerically in standard units,

$$D^3 - 0.00069 \qquad D^2 = 0.000219$$
$$D = 0.06\,\text{m} = 6\,\text{cm} \qquad \text{and} \qquad d = 5.70\,\text{cm}.$$

Calculation of the Deflection Curve and the Maximum Deflection

As discussed in the previous example, $y'' = \frac{M}{I_a E}$. As such we have for the

1. solid bar:

$$y'' = \frac{M(x)}{I_{aV}\, E}.$$

Here, the index V stands for quantities related to the solid bar. With $I_{aV} = \frac{\pi D^4}{64}$ and $M(x) = mg\,(l-x) + \frac{\pi D^2}{8}\, g\varrho\,(l-x)^2$ we have

$$A_V = \frac{64\, m_P g}{\pi D^4 E} = 7.3\cdot 10^{-2}\,\text{m}^{-2} \quad \text{and} \quad B_V = \frac{8\, g\varrho}{D^2 E} = 2.6\cdot 10^{-3}\,\text{m}^{-3}.$$

Therefore,

$$y'' = A_V\,(l-x) + B_V\left(l^2 - 2lx + x^2\right)$$
$$y' = A_V\left(lx - \frac{x^2}{2}\right) + B_V\left(l^2 x - lx^2 + \frac{x^3}{3}\right) + C$$
$$y = A_V\left(\frac{lx^2}{2} - \frac{x^3}{6}\right) + B_V\left(\frac{l^2x^2}{2} - \frac{lx^3}{3} + \frac{x^4}{12}\right) + Cx + D.$$

We have boundary conditions $y'(x = 0) = 0$ and $y(x = 0) = 0$, which lead to $C = D = 0$. The deflection curve is then

$$y(x) = \frac{1}{2}\, A_V\, x^2\left(l - \frac{x}{3}\right) + \frac{1}{2}\, B_V\, x^2\left(l^2 - \frac{2lx}{3} + \frac{x^2}{6}\right)$$

and the maximum deflection is

$$y_{\max} = y(x = l) = \frac{2}{3}\, A_V\, l^3 + \frac{1}{4}\, B_V l^4.$$

Numerically:

$$y_{\max} = 4.9\cdot 10^{-2}\,\text{m} + 6.5\cdot 10^{-4}\,\text{m} = 5\,\text{cm}.$$

2. tube:

$$y'' = \frac{M(x)}{I_{aR}E}.$$

The index R is related to the values of the hollow bar.
With $I_{aR} = \frac{\pi D^4}{64}[1 - (\frac{d}{D})^4]$ and $M(x) = m_P g(l - x) + \frac{\pi}{8} g D^2 \varrho\,[1 - (\frac{d}{D})^2]$ the deflection curve becomes

$$y(x) = \frac{1}{2}A_R x^2\left(l - \frac{x}{3}\right) + \frac{1}{2}B_R x^2\left(l^2 - \frac{2lx}{3} + \frac{x^2}{6}\right)$$

with $A_R = \frac{64 m_p g}{\pi D^4 E}\,[1 - (\frac{d}{D})^4] = 0.057\,\mathrm{m}^{-2}$ and $B_R = \frac{8g\varrho}{D^2 E}[\frac{1-(\frac{d}{D})^2}{1-(\frac{d}{D})^4}] = 0.00052\,\mathrm{m}^{-3}$. The maximum deflection is

$$y_{\max} = \frac{2}{3}A_R l^3 + \frac{1}{4}B_R l^4.$$

Numerically,

$$y_{\max} = 3.8 \cdot 10^{-2}\,\mathrm{m} + 2.2 \cdot 10^{-4}\,\mathrm{m} = 3.82\,\mathrm{cm}.$$

As can be seen, the maximum deflection of the tube is less than that of the solid bar.

2.6 Animal Proportions

? A mountain farmer would like to change from herding cattle to herding elephants. Above all, he does not want to give up the traditional "Almabtrieb" – driving the animals down from their mountain pastures into the valley in autumn – during which the animals wear bells around their necks. As the elephants have the same proportions as the cattle, but are twice as big, the farmer thinks the elephant bells can be twice as big while still exerting the same load on the neck. Is this correct? Assume that the animals are comprised of two spheres, with radius r for the head and R for the rigid body. These spheres are connected by a round, massless solid rod (length l, diameter D). Construct the relationship from the maximum tensions that occur in the necks of both animals. What consequences do the results have in relation to the maximum possible size of an animal?

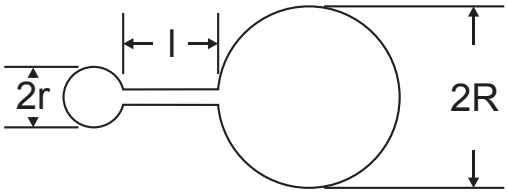

Fig. 2.10. Sphere–rod–sphere model of the head-neck-body of a cow and an elephant.

Due to geometric similarity, all length values for the cow and the elephant have the ratio 1 : 2. This means that for the radii of the bodies and heads, $R_E = 2R_R$, $r_E = 2r_R$; the same is true of the length and diameter of the neck. As such, we have, for the volume of the heads, !

$$\frac{V_E}{V_R} = \left(\frac{r_E}{r_R}\right)^3 = \left(\frac{2r_R}{r_R}\right)^3 = 2^3 = 8$$

and therefore,

$$V_E = 8\,V_R.$$

Under the assumption that both animals are of the same density, we have

$$m_E = 8\,m_R.$$

This yields the load on the head of each animal F_K as

$$F_{K,E} = 8F_{K,R}.$$

The stress distribution $\sigma(x)$ in the neck of the animal is (see Exercise 2.2)

$$\sigma(x) = \frac{32F_K l}{\pi D^3}\left(1 - \frac{x}{l}\right).$$

The maximum stress applied to body ($x = 0$) is

$$\sigma_{\max} = \frac{32}{\pi D^3}F_K l.$$

Therefore,

1. for the elephant

$$\sigma_{\max,E} = \frac{32}{\pi D_E^3}F_{K,E}l_E = \frac{32}{\pi\left(2D_R\right)^3}\,8F_{K,R}\,2l_R$$

2. for the cow

$$\sigma_{\max,R} = \frac{32}{\pi D_R^3}F_{K,R}l_R$$

And therefore,

$$\sigma_{\max,E} = 2\,\sigma_{\max,R}.$$

The maximum stress is therefore twice for the elephant what it is for the cow. However, the failure stress σB is equal for both animals, as their bones are comprised of the same material. This makes it clear that a geometric enlargement of the body has its limits. This is why, in nature, we do not find any geometric similarity in the neck area. In general, larger animals have a smaller neck length and an over-proportional thickness of neck vertebrae. This is the case with elephants with respect to cattle. As the elephants can no longer reach their food on the ground as easily, this may be the reason that elephants developed trunks. The principle is also relevant in considering

the size of the bells. The relationship of the weights of the cattle bell to the elephant bell is

$$\frac{F_{Gl,E}}{F_{Gl,R}} = \frac{\varrho_{Gl}\, g\, V_{Gl,E}}{\varrho_{Gl}\, g\, V_{Gl,R}} = \frac{V_{Gl,E}}{V_{Gl,R}} = \left(\frac{d_{Gl,E}}{d_{Gl,R}}\right)^3.$$

If the elephant bell has a doubled value,

$$d_{Gl,E} = 2\, d_{Gl,R},$$

and so,

$$\frac{F_{Gl,E}}{F_{Gl,R}} = 2^3 = 8.$$

The result is identical to the relationship of the loads on the head: the elephant bell weights eight times as much as the cattle bell. However, as the strength of the neck area (see above) does not rise directly with the increase of proportions, the farmer should not use larger bells for the elephants.

2.7 Bones of Uniform Strength

? How must a bone of uniform strength be designed if it is to be subjected to a load distributed evenly across its entire length l? As a model, use a horizontal beam of length l fixed on one side on which an evenly distributed load is resting. The cross section of the beam is rectangular; width b is constant, while height $h(x)$ should be adjusted so that the principal stress $\sigma(x)$ along the beam does not depend on x. Which figure of uniform strength is obtained? (Assume the end of the beam as the origin of the x axis.)

! For a body of uniform strength, bending stress is constant $\sigma(x) = \sigma_{\max}$. Bending stress is the ratio of bending moment M_B and section modulus W: $\sigma(x) = \frac{M_B(x)}{W(x)}$. Section modulus W can be calculated using the area moment of inertia I:

$$W = \frac{I}{e_R} = \frac{\frac{1}{12}bh^3}{\frac{h}{2}} = \frac{1}{6}bh^2.$$

e_R is the distance of the boundary fibers from the neutral fiber that runs through the focal point of the cross section of the beam. On one side of the neutral fiber compressive load dominates; on the other side, there is a tensile load. The bending moment M_B is the product of the force F and the lever arm. Here we must integrate so that for the beam fixed at one end, the force with uniform line load $f\,[\frac{\mathrm{N}}{\mathrm{m}}]$ increases linearly with x:

$$M_B(x) = \int_0^x dM_B(x) = \int_0^x dx\, F(x) = \int_0^x dx\, f \cdot x = \frac{1}{2}fx^2.$$

The line load is constant $f = \frac{F}{l}$, and the maximum bending moment is $M_B(l) = F\frac{l}{2}$. For the bending stress we have in total

$$\sigma(x) = \frac{M_B(x)}{W(x)} = \frac{\frac{1}{2} fx^2}{\frac{1}{6} bh^2(x)}; \quad \sigma_{\max} = \frac{\frac{1}{2} fl^2}{\frac{1}{6} bh^2_{\max}}.$$

The dependency on position x disappears if $h(x) \propto x$. Under this condition the body of uniform strength has the form of a triangle, and its height changes linearly with x.

2.8 Lifting Weights

If one bends forward to pick up a heavy object, the spine is more heavily loaded than if one lifts the object from the knees with a straight back. Use the model shown in Figure 2.11 to calculate the load on the spine if the object is $m = 20\,\text{kg}$. ?

In the model we make the simplifying assumption that the spine (shown as a beam with mass $M = 35\,\text{kg}$) bends primarily at the fifth lumbar vertebra. The supporting force comes from a group of muscles that are gathered here into one, secured at a distance of 2/3 of the length of the upper body. The angle between the spine and this fictitious muscle is $\alpha = 12^\circ$ (see Figure 2.11). Calculate the tensioning force F_S in the back muscle and the compressive force F_x that squeezes the spine together.

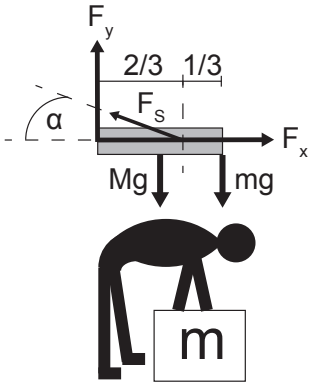

Fig. 2.11. Lifting weights.

First, consider the equality of forces in the vertical direction with $F_1 = Mg$ and $F_2 = mg$!

$$F_y + F_{S,y} - F_1 - F_2 = 0$$

and in the horizontal direction,

$$F_x - F_{S,x} = 0 \Leftrightarrow F_x = F_{S,x} = \frac{F_{S,y}}{\tan\alpha}.$$

For the torque (l is the length of the beam, and the origin is at the intersection of both forces F_x and F_y in the figure):

$$+\frac{2}{3}lF_{S,y} - \frac{l}{2}F_1 - lF_2 = 0.$$

Therefore,

$$F_{S,y} = \frac{3}{2}F_2 + \frac{3}{4}F_1 = \left(\frac{3}{2}\cdot 20\,\text{kg} + \frac{3}{4}\cdot 35\,\text{kg}\right)\cdot 9.81\,\frac{\text{m}}{\text{s}^2} = 551\,\text{N}.$$

The compressive force that presses on the spine is then

$$F_y = \frac{F_{S,y}}{\tan\alpha} = \frac{551\,\text{N}}{\tan 12^\circ} = 2{,}596\,\text{N}$$

and the tensional force in the back muscle is

$$F_S = \frac{F_{S,y}}{\sin\alpha} = \frac{551\,\text{N}}{\sin 12^\circ} = 2{,}654\,\text{N}.$$

The compressive load on the spine corresponds to a mass of 264 kg and the tensile force in the muscle corresponds to the weight of a mass of 271 kg, if a 20 kg mass is lifted in this manner.

3 Fluid Dynamics of the Circulatory System

Biofluid dynamics is concerned with the flows of bodily fluids, especially blood, through the cardiovascular system. The most important roles of this system are the supplying of the cells of the body with nutrients, and the removal of waste products. In addition to the network of blood vessels, the human body also has a lymphatic system that deals with materials that cannot enter the bloodstream through cell membranes due to their size. Lymph (lymphatic fluid) transports germs, along with other materials, to the lymph nodes, where they are rendered harmless. As such, the lymphatic system, along with the circulatory system, plays a central role in immune defense.

Blood is a relatively complex fluid, phenomenologically a suspension. It is comprised of red and white blood cells, and blood plasma as a carrier fluid in which a large number of materials are dissolved. Red blood cells (erythrocytes) transport oxygen, and white blood cells are responsible for immune defense. The blood cells can easily change their physical form. This characteristic lends blood a fluid elasticity. Such media are termed viscoelastic fluids. In spite of this, blood is often treated as a homogeneous fluid.

The most significant mechanical quantity in fluids, aside from fluid density ρ, is viscosity η. It is a measurement of the inner friction of a fluid when subjected to shearing forces. Unlike dry friction, fluid friction disappears in static conditions. Even with high viscosity, the velocity of a fluid remains finite as long as a force is applied. Shear stress, however, leads to a gradient of flow velocity $\dot{\gamma}$. For Newtonian fluids, shear stress τ and flow velocity gradient $\dot{\gamma}$ are proportional to one another: $\tau = \eta\dot{\gamma}$. For non-Newtonian fluids, η is a function of shear stress. Fluids in which viscosity decreases under increasing shear stress are termed pseudoplastic or viscoelastic. Table 3.1 gives an overview of typical measurements, flow velocities, and pressure gradients in different blood vessels.

Table 3.1. Typical flow parameters of vessels in the human body.

Bloodstream	**Diameter** $D = 2R$ [mm]	**Avg. Flow Velocity** w [m s^{-1}]	**Avg. Shear Rate** $\dot{\gamma}$ [s^{-1}]
aorta	25	0.48	155
artery	4	0.45	900
arteriole	0.05	0.05	8,000
capillary	0.008	0.001	1,000
venule	0.02	0.002	800
vein	5	0.1	160
vena cava	30	0.38	3,300

Although blood flow actually occurs in pulses, its mathematical treatment generally assumes stationary flow with an average flow velocity that remains constant over time. In this mathematical treatment of fluid flow problems, balance equations of mechanics are valid: continuity equations, conservation of momentum, and conservation of energy. Using the Newtonian formulation in the conservation of momentum equation yields, for a stationary process, the Navier–Stokes equation $\rho\,(\vec{w}\nabla)\,\vec{w} + \nabla p - \eta\nabla^2\vec{w} = 0$, which is important for fluid mechanics. In the context of estimation or approximate calculation, a special form of the conservation of energy equation is significant: the Bernoulli equation $p + \frac{\rho}{2}w^2 + \rho gh = \text{const}$. The Bernoulli equation is valid for continuous processes when friction is not taken into account. It describes the ideal case of frictionless flow.

For all flows, including blood flow in the veins, two distinctly different flow regimes occur: laminar and turbulent. The stream lines of laminar flow run parallel to one another, while those of turbulent flow appear stochastic. Each flow begins as laminar at low velocity, and suddenly breaks into turbulence while velocity is increasing. This is a stability problem. Without going into further details, it is still important to select criteria for the determination of flow regime. This can be accomplished by considering similitude theory, which has formulated relationships among constants for pipe flow using the flow-influencing quantities $(\Delta p,\ w,\ d,\ \rho,\ \eta)$. Here, the relationship for smooth pipe flow $Eu = f(Re)$ holds, with $Eu = \frac{\Delta p}{\rho w^2}$ and $Re = \frac{\rho w d}{\eta}$. The value of the Reynolds number has proven effective as a criterion for judging flow regime. For pipe flow, the laminar flow regime is stable when $Re < 2{,}300$; when $Re > 2{,}300$, turbulent flow occurs.

As a pump for blood, the heart's job is to deliver it to the body. From the perspective of fluid dynamics, the heart, as a double pump (two-chamber system), belongs to two coupled circuits: the pulmonary (lung) circulation, and the systemic (body) circulation. Its function is accomplished through a contraction of cardiac muscle. This contraction is termed cardiac systole, and relaxation is called cardiac diastole. The amplitude of average blood flow is calculated through the heart's frequency (heart rate), and the stroke volume. Resting heart rate is around 70 beats per minute, and rises sharply with physical exertion. Stroke volume can also be changed, for example, by the height of cardiac systole. Blood flow depends on many different internal and external factors. It is governed by an autonomous regulatory system in the body.

The calculation of the pulsing process is extremely complicated, and can only be accomplished under very idealizing assumptions. Considering the bloodstream as a rigid tube (in cylindrical coordinates), with radius R and blood as a Newtonian fluid, we have, for blood flow $\dot{m}$ under the assumption of a harmonic oscillation of the pressure gradient $\frac{dp}{dz}$ in steady state with frequency ω in complex notation (J_0 as a

first-order Bessel function)

$$\dot{m}(t) = \frac{\pi R^2}{i\omega} \cdot \frac{dp}{dz} \cdot \left[1 - \frac{J_0\left(r\sqrt{-i\,\frac{\omega\rho}{\eta}}\right)}{J_0\left(R\sqrt{-i\,\frac{\omega\rho}{\eta}}\right)} \right] \cdot e^{i\omega t}.$$

The assumption of a sinusoidal/cosinusoidal oscillation for the pressure gradient is a crude simplification of reality. Even so, the equation is both qualitatively and practically appropriate in describing blood flow. A full treatment of the phenomenon would require consideration of many other effects, like, for example, the elasticity of the blood vessels.

Arteriosclerotic changes often lead to disruptions in blood flow. Arterial occlusive diseases are of especially vital significance here. In most cases, plaque has built up in a blood vessel; this can develop into an acute blockage of flow and can significantly influence the flow behavior of the blood beyond a certain point. At that point, additional problems begin to occur simultaneously. The bloodstream gets smaller, and certain organs are no longer sufficiently supplied with oxygen and nutrients. Fatigue, and possibly pain in the area around the heart, are the results. Additionally, the occlusion causes the development of vortices and stagnant regions in the flow behind it. In these regions blood stagnates through local circular flow, which can lead to thrombosis. The situation can be addressed with medications that reduce the viscosity of the blood and strengthen the heart, or, at an advanced stage of the disease, with surgical intervention (for example, a bypass operation).

A number of illnesses change the viscosity of the blood significantly. As such, measurement of this viscosity can be used diagnostically. This requires the use of certain measuring devices. Today, in addition to the classic erythrocyte sedimentation rate method, there is a range of measurement techniques that allow for investigation of blood rheology in vivo.

3.1 From the Aorta to the Capillaries

Estimate the number of capillaries found in the human body. Take the diameter of the aorta to be $D = 2.5\,\text{cm}$. For the capillaries, an average diameter $d = 8\,\mu\text{m}$ can be assumed. All capillaries experience the same pressure gradient, six times higher than that in the aorta. ?

According to the Hagen–Poiseuille equation, volume flow under constant pressure gradient is !

$$V_i^* \propto D_i^4 \quad \text{and} \quad w_i \propto D_i^2.$$

Considering the different pressure gradients we have

$$\frac{w}{w_A} = 6\left(\frac{d}{D}\right)^2$$

with w_A as the flow velocity in the aorta and w as the flow velocity in the capillaries. We have the continuity equation

$$w_A A_A = NAw$$

with A_A as the average aorta cross section area and A for the average capillary cross section area. N is the number of capillaries

$$N = \frac{w_A A_A}{wA},$$

and therefore,

$$N = \frac{w_A}{w}\left(\frac{D}{d}\right)^2 = \frac{1}{6}\left(\frac{D}{d}\right)^4.$$

Numerically, we have

$$N = \frac{1}{6}\left(\frac{2.5}{8 \cdot 10^{-4}}\right)^4 = 1.6 \cdot 10^{13}.$$

3.2 The Blood as a Power Fluid

? Due to the elastic characteristics of the blood cells, blood demonstrates non-Newtonian behavior as it flows. This means that the dependence of shear stress τ on the shear rate $\dot{\gamma}$ is nonlinear. For such functions, a power equation approach is commonly used – for example, $\tau = k\dot{\gamma}^n$. For viscoelastic fluids (like blood), $n < 1$; for dilatant fluids, $n > 1$. For Newtonian fluids, $n = 1$ and $k = \eta$. k and n take on the roles of material qualities of the fluid. For blood in an artery of length L, under the assumption of a "power fluid" and under stationary relationships, we wish to find

1. shear stress distribution $\tau(r)$
2. velocity profile $w(r)$
3. flow rate V^*
4. average flow velocity $\bar{w}$
5. ratio of the maximum and minimum flow velocities $\frac{w_{\max}}{\bar{w}}$.

! 1. Consider the following cylindrical volume element $dV = \pi r^2 dz$.
Under stationary conditions, the sum of forces on the element of volume disappears

$$0 = F_P - F_R$$

with F_P as the compressive force and F_R as the friction force, which both act in the z-direction. Therefore,

$$0 = p\pi r^2 - \left[p + \left(\frac{\partial p}{\partial z}\right)dz\right]\pi r^2 - \tau 2\pi r dz.$$

Solving for τ, we find the distribution of shear stress by radial coordinate r in the artery:

$$\tau(r) = -\left(\frac{\partial p}{\partial z}\right)\frac{r}{2}.$$

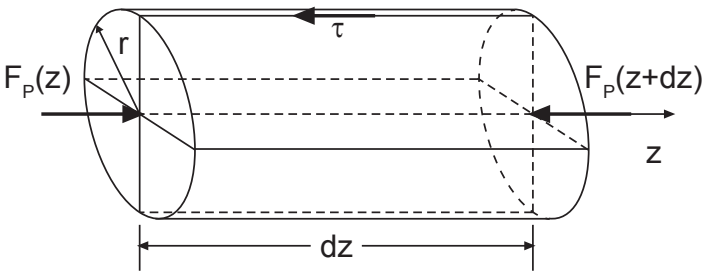

Fig. 3.1. Shear stress τ and compressive force F_P act on the cylindrical volume element dV.

As $\frac{\partial p}{\partial z}$ is not a function of z, $p\,(z)$ must be linear. Therefore, $\frac{\partial p}{\partial z}$ can also be substituted with $\frac{p_2-p_1}{z_2-z_1} = \frac{-\Delta p}{L}$, with $\Delta p = p_1 - p_2$. The distribution of stress is then

$$\tau\,(r) = \left(\frac{\Delta p}{L}\right)\frac{r}{2}.$$

2. For a power fluid, Ostwald de Waele's approach gives $\tau = k\dot{\gamma}^n$ with $\dot{\gamma}$ as the shearing gradient, which becomes $\dot{\gamma} = -\frac{dw}{dr}$ for axial flows in cylindrical geometries. The sign is negative because velocity is decreasing in the r-direction. Therefore,

$$\tau = k\left(-\frac{dw}{dr}\right)^n.$$

Introducing the power approach into the shear stress distribution, we have $k(-\frac{dw}{dr})^n = (\frac{\Delta p}{L})\frac{r}{2}$, and therefore,

$$w = -\left[\left(\frac{\Delta p}{L\,2\,k}\right)\right]^{\frac{1}{n}}\int r^{\frac{1}{n}}dr.$$

Integration leads to the velocity distribution $w(r)$

$$w(r) = -\left[\frac{n}{1+n}\left(\frac{\Delta p}{2kL}\right)^{\frac{1}{n}}\right]r^{\frac{1+n}{n}} + C$$

$$= C - Br^{\frac{1+n}{n}} \quad \text{with} \quad B = \frac{n}{1+n}\left(\frac{\Delta p}{2kL}\right)^{\frac{1}{n}}.$$

For $r = \frac{D}{2}$, $w = 0$ due to wall adhesion, so that from this condition the integration constant C can be determined. From $0 = C - B(\frac{D}{2})^{\frac{1+n}{n}}$ we have

$$C = B\left(\frac{D}{2}\right)^{\frac{1+n}{n}}$$

and

$$w(r) = B\left[-r^{\frac{1+n}{n}} + \left(\frac{D}{2}\right)^{\frac{1+n}{n}}\right] = B\left(\frac{D}{2}\right)^{\frac{1+n}{n}}\left[1 - \left(\frac{2r}{D}\right)^{\frac{1+n}{n}}\right].$$

After back substitution of B we have $w(r)$ as

$$w(r) = \frac{n}{1+n}\left(\frac{\Delta p}{2\,kL}\right)^{\frac{1}{n}}\left(\frac{D}{2}\right)^{\frac{1+n}{n}}\left[1-\left(\frac{2r}{D}\right)^{\frac{1+n}{n}}\right].$$

3. For volume throughput, volume flow is V^*. For V^* we have

$$\begin{aligned} V^* &= 2\pi \int_0^{D/2} r\, w(r)\, dr \\ &= 2\pi \frac{1+n}{n}\left[\left(\frac{\Delta p}{2kL}\right)^{\frac{1}{n}}\right]\left(\frac{D}{2}\right)^{\frac{1+n}{n}} \int_0^{D/2}\left[1-\left(\frac{2r}{D}\right)^{\frac{1+n}{n}}\right] dr \\ &= \frac{n\pi}{1+3n}\left(\frac{\Delta p}{2kL}\right)^{\frac{1}{n}}\left(\frac{D}{2}\right)^{\frac{1+3n}{n}}. \end{aligned}$$

4. Average velocity $\bar{w}$ is an assumed velocity, constant over r, that makes throughput equal: $w(r)$. Therefore, for average velocity, we have

$$\bar{w}A = V^*$$

with A as the flow cross section. A is a circular cross section for the artery, with $A = \frac{\pi D^2}{4}$. Therefore, we have for $\bar{w}$

$$\bar{w} = \frac{n}{1+3n}\left(\frac{\Delta p}{2\,kL}\right)^{\frac{1}{n}}\left(\frac{D}{2}\right)^{\frac{1+n}{n}}.$$

5. Flow velocity is at its maximum in the center at $r = 0$. Therefore,

$$w_{\max} = w(r=0) = \frac{n}{1+n}\left(\frac{\Delta p}{2\,kL}\right)^{\frac{1}{n}}\left(\frac{D}{2}\right)^{\frac{1+n}{n}}.$$

We have the ratio $\frac{w_{\max}}{\bar{w}}$

$$\frac{w_{\max}}{\bar{w}} = \frac{1+3n}{1+n}.$$

For $n = 1$ and $k = \eta$ we have, using the equations above, the corresponding solutions for Newtonian fluids

$$w(r) = \frac{\Delta p D^2}{16\eta L}\left[1-\left(\frac{2r}{D}\right)^2\right]$$

$$V^* = \frac{\pi \Delta p D^4}{128\eta L} \quad \text{(Hagen–Poiseuille).}$$

As such, for Newtonian fluids, average velocity is $\bar{w} = \frac{\Delta p D^2}{32\eta L}$, maximum velocity in the capillaries is $w_{\max} = \frac{\Delta p D^2}{16\eta L}$, and the ratio of these velocities is $\frac{w_{\max}}{\bar{w}} = 2$.

3.3 Branching

Consider a model of the arterial system in which, after a certain length L, the artery splits into two branches of equal diameter. The largest arterial diameter is $D = 2.5$ cm.

1. By what factor Φ must the diameter D_n change from level to level if at each level, the reduction in pressure is to remain constant?
2. By what factor Ψ does flow velocity change from level to level?
3. After how many levels N is diameter D_N just 25 μm?

1. For each level, pressure drop is

$$\Delta p = \Delta p_n = \Delta p_{n+1} = \text{const}$$

with $n = 1, 2, 3, ..., N$. From the Hagen–Poiseuille equation, $V^* = \frac{\pi D^4}{128\eta}\left(\frac{\Delta p}{L}\right)$ and therefore,

$$\frac{\Delta p}{L} = \frac{128\eta V^*}{\pi D^4}$$

$$\left(\frac{\Delta p}{L}\right)_n = \frac{128\eta V_n^*}{\pi D_n^4}$$

$$\left(\frac{\Delta p}{L}\right)_{n+1} = \frac{128\eta V_{n+1}^*}{\pi D_{n+1}^4}.$$

We can also obtain the ratios of the diameters of two levels, one following the other

$$\left(\frac{D_n}{D_{n+1}}\right)^4 = \frac{V_n^*}{V_{n+1}^*}.$$

Due to continuity, the amount of material flowing through an artery in the nth level must be equal to the amount of material flowing through both subsequent arteries, $V_n^* = 2V_{n+1}^*$. Therefore,

$$\frac{D_{n+1}}{D_n} = \left(\frac{1}{2}\right)^{1/4} = 0.84 = \Phi.$$

2. For the flow velocities of the individual branches, due to $w_n A_n = w_{n+1} A_{n+1}$, we have the condition

$$\frac{w_n}{w_{n+1}} = \frac{A_{n+1}}{A_n} = \left(\frac{D_{n+1}}{D_n}\right)^2 = \left(\frac{1}{2}\right)^{1/2} = 0.71 = \Psi.$$

3. After N branches the diameter ratio is: $\frac{D_N}{D} = \left(\frac{D_{n+1}}{D_n}\right)^N$. And so,

$$N = \frac{\log\left(\frac{D_N}{D}\right)}{\log\left(\frac{D_{n+1}}{D_n}\right)} = \frac{\log\left(\frac{D_N}{D}\right)}{\log(\Phi)}.$$

With $D = 2.5\,\text{cm}$ and $D_N = 25\,\mu\text{m}$ we have

$$N = \frac{\log\left(\frac{0.025}{25}\right)}{\log\,(0.84)} = \frac{\log\left(10^{-3}\right)}{-0.075} = \frac{-3}{-0.075} = 40.$$

After 40 levels, the arteries are only 25 μm thick.

3.4 Bypass

? Due to a "calcification", a patient's aortic diameter D has narrowed to 2 cm. The resulting loss of pressure leads to a life-threatening decrease in blood flow. As such, a bypass operation will be performed: an additional vessel will be added to the aorta, so that blood flow can return to its normal level. What must the diameter d of the bypass be so that the drop in pressure Δp_V and the flow rate V^* reach the values of a healthy aorta? Stationary and laminar conditions should be assumed.
[pressure drop in the healthy aorta $\Delta p_V = \Delta p_{V\text{norm}} = 87.6\,\text{Pa}$; blood flow $V^* = V^*_{\text{norm}} = 7\ {}^{\text{l}}/_{\text{min}}$; aorta length $l = 40\,\text{cm}$; blood viscosity $\eta = 1.8 \cdot 10^{-2}\,\text{Pa} \cdot \text{s}$]

! Using the Hagen–Poiseuille equation, we have

$$\Delta p_V = \frac{128\eta V^*_{\text{norm}} l}{\pi D^4}.$$

After the OP, the bloodstream V^*_{norm} splits into two branches (V^*_{By} is the flow of blood through the bypass, and V^*_A is the flow through the aorta)

$$V^*_{\text{norm}} = V^*_A + V^*_{By} = \frac{\pi \Delta p_{V\text{norm}}}{128\, l\, \eta}\left(d^4 + D^4\right).$$

Solving for bypass diameter:

$$d^4 = \frac{128\eta V^*_{\text{norm}} l}{\pi \Delta p_{V\text{norm}}} - D^4$$

$$d = \sqrt[4]{\frac{128 \cdot 1.8 \cdot 10^{-2}\,\text{Pa} \cdot \text{s} \cdot 7\ {}^{\text{l}}/_{\text{min}} \cdot 40\,\text{cm}}{\pi \cdot 87.6\,\text{Pa}} - 2^4\text{cm}^4} = 2.19\,\text{cm}.$$

3.5 Hemorheometry Using a Rotating Sphere Viscometer

? The viscosity of blood (blood plasma) can be measured using a rotating sphere viscometer. This system is comprised of an inner solid sphere that rotates concentrically with angular frequency n within a hollow sphere; a shearing load occurs in the space between the spheres. The driving torque M is measured, in its dependency on

angular frequency $M(n)$. The rotating sphere viscometer is especially well suited for hemorheometry because the fluid chamber is isolated from the atmosphere. The diameter of the inner solid sphere is d, and the diameter of the outer hollow sphere is D. We want to find the evaluation relationships for the determination of the function $\eta(\dot{\gamma})$ function for a rotating sphere system with a very narrow gap ($\delta = {}^{d}/_{D} \approx 1$), with $\dot{\gamma} = f(n)$ and $\eta = f(M, n)$. The shear rate $\dot{\gamma}$ is, in spherical coordinates, $\dot{\gamma} = -r\frac{\partial}{\partial r}(\frac{w_\varphi}{r})$.

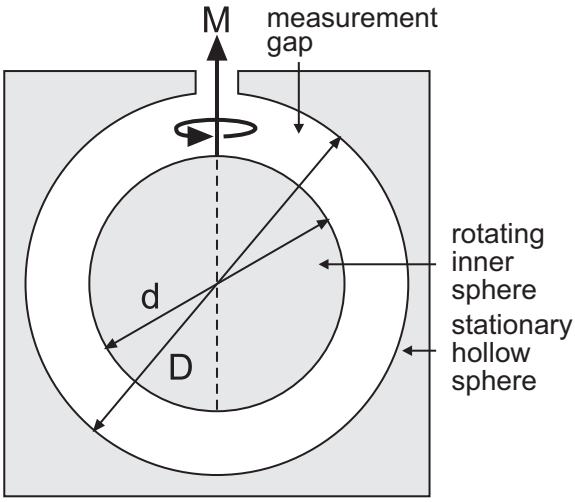

Fig. 3.2. Geometry of a rotating sphere viscometer.

The velocity field $\vec{w}$ in the sphere gap can be described as $\vec{w}\left(w_r, w_\varphi, w_\vartheta\right)$; (r, φ, ϑ) are spherical coordinates (r – radial length; φ – azimuthal angle; ϑ – polar angle). For $\delta = {}^{d}/_{D} \rightarrow 1$ (very narrow gap), the three-dimensional rotational flow occurs, approximately, in a single layer flow (shear flow) $\vec{w}\left(w_\varphi, 0, 0\right)$ with $w_\varphi = w_\varphi(r, \vartheta)$. The equation of motion is

$$\frac{D}{Dt}\vec{w} = [\vec{\nabla} \cdot \underline{\underline{\sigma}}]$$

with $\frac{D}{Dt}$ as substantial derivative and $\underline{\underline{\sigma}}$ as the stress tensor. As only the φ-components of the equation of motion contribute, considering the narrow gap the equation of motion takes the form

$$\frac{\partial \sigma_{r\varphi}}{\partial r} + 3\frac{\sigma_{r\varphi}}{r} = 0. \tag{3.1}$$

The component $\sigma_{r\varphi}$ of the stress tensor is, due to the shear flow, identical to the shear stress τ. Furthermore, $\sigma_{r\varphi} = \tau$. From the equation of motion (3.1) we have, after integrating over r, the relationship $\tau = \frac{C}{r^3}$; for fluids for which the Newtonian approach is

sufficient, this leads to the equation

$$\dot{\gamma} = \frac{C}{\eta r^3}. \tag{3.2}$$

The shear rate $\dot{\gamma}$ for rotation flow with flow direction φ that experiences shear stress in the r direction is

$$\dot{\gamma} = -r\frac{\partial}{\partial r}\left(\frac{w_\varphi}{r}\right)$$

and yields, considering $\tau = \eta\dot{\gamma} = \frac{C}{r^3}$,

$$-\eta r\frac{\partial}{\partial r}\left(\frac{w_\varphi}{r}\right) = \frac{C}{r^3}.$$

This leads to the differential equation

$$d\left(\frac{w_\varphi}{r}\right) = -\left(\frac{C}{\eta r^4}\right)dr$$

with solution

$$\frac{w_\varphi}{r} = \left(\frac{C}{3\eta r^3}\right) + B.$$

Because the inner sphere rotates with angular velocity ω and the outer sphere remains at rest, the boundary conditions are

$$w_\varphi\,(r = {}^{d}/_{2}) = \frac{d}{2}\omega\,\sin\vartheta$$

and

$$w_\varphi\,(r = {}^{D}/_{2}) = 0.$$

Therefore, for B and C, we have the correspondence equations

$$\omega\sin\vartheta = B + \left(\frac{8C}{3\eta d^3}\right) \quad \text{und} \quad 0 = B + \left(\frac{8C}{3\eta D^3}\right).$$

Therefore,

$$C = \frac{3\eta d^3\omega\sin\vartheta}{8\left(1-\delta^3\right)} \quad \text{und} \quad B = -\frac{\delta^3\omega\sin\vartheta}{1-\delta^3}.$$

C substituted in (3.2) yields

$$\dot{\gamma}\,(r,\vartheta) = \frac{3}{8}\left(\frac{d}{r}\right)^3\frac{\omega\sin\vartheta}{1-\delta^3}.$$

The shearing gradient at the surface of the inner sphere $\dot{\gamma}(\frac{d}{2},\vartheta) = \dot{\gamma}_d$ is

$$\dot{\gamma}_d\,(\vartheta) = 3\omega\left(\frac{\sin\vartheta}{1-\delta^3}\right) = 6\pi n\left(\frac{\sin\vartheta}{1-\delta^3}\right).$$

$\dot{\gamma}_d$ depends on ϑ. That means that for each angle ϑ, other $\dot{\gamma}_d$ values exist that correspond to the driving torque M over the entire shear region of the inner sphere ($0 \leq \vartheta \leq \pi$). An average shear rate across the entire shear region $\dot{\gamma}_{\text{eff}}$ is

$$\dot{\gamma}_{\text{eff}} = \frac{6\,n}{1-\delta^3} \int_0^{\pi} \sin\vartheta \, d\vartheta = -\frac{6n}{1-\delta^3} \cos\vartheta|_0^{\pi}$$

Therefore, for the evaluation equation for the shear rate dependent on speed n, we have the relationship

$$\dot{\gamma} = \frac{12\,n}{1-\delta^3}. \tag{3.3}$$

The driving torque is calculated from the $\sigma_{r\varphi}$ components of the stress tensor for $r = {}^{d}/_{2}$, which is identical to the shearing stress on the surface of the inner sphere $\tau_d = \tau\,({}^{d}/_{2})$, as

$$M = \frac{\pi d^3}{2}\tau_d \int_0^{\frac{\pi}{2}} \sin^2\vartheta \, d\vartheta = \frac{\pi^2 d^3}{8}\tau_d.$$

For a Newtonian fluid with flow function $\tau = \eta\dot{\gamma}$ we have, considering (3.3),

$$M = 2\pi^2 \eta n \left(\frac{d^3}{1-\delta^3}\right).$$

Solving for η, we have the evaluation equation for the determination of viscosity from the measured values M and n:

$$\eta = \frac{1-\delta^3}{2\pi^2 d^3}\left(\frac{M}{n}\right) \approx \frac{1-\delta^3}{20\,d^3}\left(\frac{M}{n}\right). \tag{3.4}$$

With (3.3) and (3.4), we obtain, from M and n, the curve $\eta\,(\dot{\gamma})$; from this, using $\tau = \eta \cdot \dot{\gamma}$, the flow curve can also be calculated.

3.6 Flow Coefficients

The dimensionless coefficients *Re* (Reynolds number) and *Eu* (Euler number) are defined, for capillary flow, as

$$Re = \frac{d\,w\,\rho}{\eta} \qquad \text{and} \qquad Eu = \frac{\Delta p}{\rho\,w^2}$$

with w as the average flow velocity in the capillary, d as the diameter of the capillary, ρ as the density of the fluid, η as the dynamic viscosity, and Δp as the pressure drop along the length of the vessel l. The Hagen–Poiseuille equation can be written in dimensionless form using these constants. What advantages does this form have?

! The Hagen–Poiseuille equation is

$$V^* = \frac{\pi d^4 \Delta p}{128 \eta l}$$

Volume flow is $V^* = wA = \frac{w\pi d^2}{4}$. Therefore,

$$\frac{w\pi d^2}{4} = \frac{\pi d^4 \Delta p}{128\,\eta l}$$

This gives pressure difference

$$\Delta p = \frac{32\,l\eta w}{d^2} = 32\left(\frac{l}{d}\right)\left(\frac{\eta w}{d}\right).$$

Dividing both sides by ϱw^2, we find that

$$\frac{\Delta p}{\varrho w^2} = 32\left(\frac{l}{d}\right)\left(\frac{\eta}{\varrho w d}\right)$$

and

$$Eu = 32\left(\frac{l}{d}\right) Re^{-1}$$

With $Eu' = \left(\frac{d}{l}\right) Eu$ as the modified Euler number, we also have

$$Eu' = \frac{32}{Re}$$

In the subject literature, in addition to the Euler number, a coefficient of equal value exists that is written as tube friction coefficient λ; $\lambda = \frac{\Delta p}{\frac{\varrho}{2} w^2} \frac{d}{l}$. With λ, the relationship between λ and Re is given as

$$\lambda = \frac{64}{Re}.$$

As the Hagen–Poiseuille equation only applies to laminar capillary flow ($Re \leq 2{,}300$), $Eu' = {}^{32}/_{Re}$ (that is, $\lambda = {}^{64}/_{Re}$) is only valid in this case. When considering turbulence, other functional dependencies apply[1] that must be determined using experimental validations of models. In planning and evaluating these experiments, the dimensionless form is very advantageous, as the number of variables is reduced from 5 to 2. To calculate the function $Eu' = f(Re)$ (that is, $\lambda = f(Re)$), we only need to vary Re, and to measure Eu' (that is, λ). This is most simply done by changing the flow velocity w. If, on the other hand, the dimension-dependent form of the function with $\Delta p = f(w, d, l, \varrho, \eta)$ had to be used, we would have to vary w, d, l, ϱ, and η in many different trials.

---

1 for example, by Blasius: $\lambda = 0.316\,(Re)^{-0.25}$ for $2{,}300 \leq Re \leq 10^5$; by Nikuradse: $\lambda = 0.0032 + 0.22(Re)^{-0.24}$ for $10^5 \leq \mathrm{Re} \leq 3 \cdot 10^6$

Additionally, the dimensionless form allows for "model transfer". This method allows measured data obtained from an experiment to be scaled up significantly. Here, the following condition applies: all the constants that describe a problem must correspond in the model, and in the main executions (Π-theory of Buckingham). If, for example, a researcher attempted to investigate blood flow through an experiment using water, he would need to consider in evaluating the data

$$Re_B = Re_W \quad \text{and} \quad Eu_B = Eu_W.$$

3.7 Narrowing of the Aorta

In an investigation, a pathological change of the flow cross section of the aorta of a patient is diagnosed. The free diameter is seen using X-ray imaging to be narrowed to $d = 1\,\text{cm}$. Estimate the resulting loss in pressure Δp_v in the aorta. The flow should be assumed to be laminar and under stationary relationships. Inertial effects should be ignored. ?

Note: In the calculation, consider that a circular hole is the boundary value of a hyperboloid. In using hyperbolic coordinates here, the coordinate of the wall hyperbola goes to zero. Therefore, first calculate the general loss of pressure in flow through a hyperbola in hyperbolic coordinates, and concretize Δp_v by the numerical calculation of the hole-like narrowing.

[average blood viscosity: $\eta = 0.018\,\text{Pa} \cdot \text{s}$; blood flow: $V^* = 7\,{}^{\text{l}}/_{\text{min}}$]

In Figure 3.3 the geometry of the hyperbolic narrowing in the (xz)-plane of a Cartesian coordinate system at the origin is presented. The narrowed point has separation $2a$; the focus distance is $2e$. !

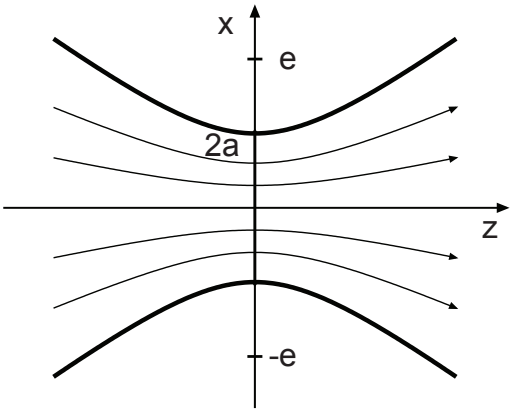

Fig. 3.3. Hyperbolic flow lines in the region of the narrowing.

The equation of the wall hyperbola in the (xz)-plane is

$$\frac{x^2}{a^2} - \frac{z^2}{e^2 - a^2} = 1.$$

Confocal hyperbolas and ellipses are defined as

$$\frac{x^2}{e^2\left(1-\tau^2\right)} - \frac{z^2}{e^2\tau^2} = 1 \quad \text{with } \tau_0 \le \tau \le 1 \text{ [hyperbolas]}$$

and

$$\frac{x^2}{e^2\left(1+\sigma^2\right)} + \frac{z^2}{e^2} = 1 \quad \text{with } 0 \le \sigma \le \infty \text{ [ellipses]},$$

where $\tau_0 = \sqrt{1 - \frac{a^2}{e^2}}$. The confocal hyperbolas and ellipses are orthogonal to one another; σ and τ are the coordinates of these curves. For the blood flow, the Navier–Stokes equation gives in this case

$$\eta\vec{\nabla} \times \vec{\nabla} \times \vec{w} + \vec{\nabla}p = 0.$$

Using the following transformation relationships

$$\vec{W} = \frac{\vec{w}e^2}{V^*} \qquad X = \frac{x}{e}$$

$$\hat{\nabla} = e\vec{\nabla} \qquad Y = \frac{y}{e}$$

$$P = \frac{pe^3}{\eta V^*} \qquad Z = \frac{z}{e}$$

the Navier–Stokes equation can be written dimensionlessly as

$$\hat{\nabla} \times \hat{\nabla} \times \vec{W} + \hat{\nabla}P = 0.$$

The surfaces created are now given by the following equations:

$$\frac{X^2 + Y^2}{1+\sigma^2} + \frac{Z^2}{\sigma^2} = 1 \quad \text{rotation ellipsoid}$$

$$\frac{X^2 + Y^2}{1-\tau^2} - \frac{Z^2}{\tau^2} = 1 \quad \text{rotation hyperboloid.}$$

Using the transformation formulae

$$X^2 = \left(1+\sigma^2\right)\left(1-\tau^2\right)\cos^2\varphi$$
$$Y^2 = \left(1+\sigma^2\right)\left(1-\tau^2\right)\sin^2\varphi$$
$$Z^2 = \sigma^2\tau^2$$

we can calculate the metric coefficients as

$$g_{\sigma\sigma} = \frac{\sigma^2+\tau^2}{1+\sigma^2}; \qquad g_{\tau\tau} = \frac{\sigma^2+\tau^2}{1-\tau^2}; \qquad g_{\varphi\varphi} = \left(1+\sigma^2\right)\left(1-\tau^2\right).$$

For the surface element of an ellipsoid we have the relationship $dA = \sqrt{g_{\sigma\sigma} g_{\varphi\varphi}}\, d\varphi d\tau$, and for the section of the ellipsoidal element on the interior of the wall hyperbola, we have the throughput relationship

$$-\oint W_\sigma dA = 1.$$

Here, we consider the portion of the narrowing that acts against flow in the $+\sigma$ – Richtung direction. From the continuity equation

$$\hat{\nabla} \cdot \overrightarrow{W} = \frac{1}{\sqrt{g_{\sigma\sigma} g_{\tau\tau} g_{\varphi\varphi}}} \left[\frac{\partial}{\partial \sigma} \left(\sqrt{g_{\tau\tau} g_{\varphi\varphi}}\, W_\sigma \right) + \frac{\partial}{\partial \tau} \left(\sqrt{g_{\sigma\sigma} g_{\varphi\varphi}}\, W_\tau \right) \right] = 0$$

we can see that the components of the velocity vector $\overrightarrow{W}$ can be calculated from a flow function Ψ:

$$W_\sigma = -\frac{1}{\sqrt{g_{\tau\tau} g_{\varphi\varphi}}} \frac{\partial \Psi}{\partial \tau}$$

$$W_\tau = +\frac{1}{\sqrt{g_{\sigma\sigma} g_{\varphi\varphi}}} \frac{\partial \Psi}{\partial \sigma}.$$

Forming the rotation of the dimensionless Navier–Stokes equations, and inserting into the resulting equation

$$\hat{\nabla} \times \hat{\nabla} \times \hat{\nabla} \times \overrightarrow{W} = 0$$

the expressions for W_σ and W_τ, we have the differential equation

$$D^4 \Psi = 0.$$

Here, $D^4 \Psi = D^2 \left(D^2 \Psi \right)$ is, with the differential operator,

$$D^2 = \frac{1}{g_{\sigma\sigma}} \frac{\partial^2}{\partial \sigma^2} + \frac{1}{g_{\tau\tau}} \frac{\partial^2}{\partial \tau^2}.$$

To solve this differential equation, we can use an approach in the form $\Psi = m(\tau)$. The throughput relationship is satisfied most easily by using this approach. Substitution gives

$$D^4 \Psi = \frac{1}{\left(\sigma^2 + \tau^2\right)^3} \left[4 \left(1 - \tau^2\right) (1 + \sigma)^2 \frac{d^2 m}{d\tau^2} - 4\tau \left(1 - \tau^2\right) \left(1 + \sigma^2\right) \frac{d^3 m}{d\tau^3} \right] +$$
$$+ \frac{1 - \tau^2}{\sigma^2 + \tau^2} \frac{d^4 m}{d\tau^4}.$$

As the differential equation must hold for all σ- and τ-values, we have the relationships

$$\frac{d^4 m}{d\tau^4} = 0 \quad \text{and} \quad \frac{d^2 m}{d\tau^2} - \tau \frac{d^3 m}{d\tau^3} = 0,$$

whose common solution, considering the boundary condition $\overrightarrow{W}(\tau = \tau_0) = 0$, is

$$\Psi = C\left(\tau^3 - 3\tau_0^2\tau\right)$$

The constant C can be calculated by considering the throughput condition

$$C = \frac{1}{2\pi\left(1 - 3\tau_0^2 + 2\tau_0^3\right)}.$$

This makes the velocity field of the blood flow $\overrightarrow{W}$

$$\overrightarrow{W} = (W_\sigma, 0, 0) \quad \text{with } W_\sigma = \frac{-3C\left(\tau^2 - \tau_0^2\right)}{\sqrt{\left(1 + \sigma^2\right)\left(\sigma^2 + \tau^2\right)}}.$$

As we can see, the stream lines run along the confocal hyperbolas. To calculate the loss in pressure along the axis of rotation, $\overrightarrow{W}$ must be substituted into the dimensionless Navier–Stokes equation. Solving for $\hat{\nabla}P$, this is then $\hat{\nabla}P = -\hat{\nabla} \times \hat{\nabla} \times \overrightarrow{W}$, and in component description,

$$\frac{\partial P}{\partial \sigma} = +\sqrt{\frac{g_{\sigma\sigma}}{g_{\tau\tau}g_{\varphi\varphi}}}\frac{\partial}{\partial \tau}\left[\sqrt{\frac{g_{\varphi\varphi}}{g_{\sigma\sigma}g_{\tau\tau}}}\frac{\partial}{\partial \tau}\left(\sqrt{g_{\sigma\sigma}}W_\sigma\right)\right]$$

$$\frac{\partial P}{\partial \tau} = -\sqrt{\frac{g_{\tau\tau}}{g_{\sigma\sigma}g_{\varphi\varphi}}}\frac{\partial}{\partial \sigma}\left[\sqrt{\frac{g_{\varphi\varphi}}{g_{\sigma\sigma}g_{\tau\tau}}}\frac{\partial}{\partial \sigma}\left(\sqrt{g_{\sigma\sigma}}W_\sigma\right)\right]$$

We can now express the pressure gradient on the axis of rotation as

$$\frac{\partial P}{\partial \sigma}\Big|_{\tau=1} = -\frac{12\,C}{\left(1 + \sigma^2\right)^2}.$$

and, after integration of the loss in pressure,

$$P(\sigma)\,|_{\tau=1} = P_\infty - 6\,C\left(\frac{\sigma}{1 + \sigma^2} + \arctan\sigma\right)$$

and the total loss in pressure

$$\Delta P = 24\,C\int_0^\infty \frac{1}{\left(1 + \sigma^2\right)^2}\,d\sigma = \frac{3}{1 - 3\tau_0^2 + 2\tau_0^3}$$

between $+\infty \leq \sigma \leq -\infty$. As we are considering here a spasmodic narrowing, we can set $\tau_0 = 0$, and in the case $\tau_0 \to 0$ the hyperboloid degenerates to a circular hole with radius $e = a = \frac{d}{2}$. Therefore, the dimensionless loss in pressure becomes $\Delta P = 3$, or, dimensionally,

$$\Delta p_V = \frac{3\eta V^*}{a^3} = \frac{24\eta V^*}{d^3}.$$

Numeric evaluation yields

$$\Delta p_V = \frac{24 \cdot 0.018\ \text{Pa} \cdot \text{s} \cdot 7\ {}^{\text{l}}/_{\text{min}}}{1\ \text{cm}^3} = \frac{24 \cdot 0.018\ \text{Pa} \cdot \text{s} \cdot 7\ {}^{\text{l}}/_{\text{min}}}{60\ {}^{\text{s}}/_{\text{min}} \cdot 1{,}000\ {}^{\text{l}}/_{\text{m}^3} \cdot 0.01^3\ \text{m}^3} = 50.4\ \text{Pa}.$$

In the scope of this treatment, inertial effects were ignored. These are, however, responsible for the vortices that frequently arise behind narrowings. These can further increase pressure loss (see also Exercise 3.8). Vortices are especially dangerous in the blood stream because blood within them stagnates. This leads to danger of blood clots, which can cause thrombosis.

3.8 Stepwise Narrowing of the Aorta

?

Consider the loss in pressure of a narrowing of the aorta according to the image; the diameter narrows from $d_1 = 2.5\,\text{cm}$ to $d_2 = 1\,\text{cm}$. Calculate the resulting loss in pressure Δp_v in the aorta for the case in which this loss in pressure occurs only due to vortices. Ignore fluid friction. Make sure to consider that directly after the narrowing, the effective flow cross section is further restricted due to inertial effects to A'. The size of this restriction is described by the contraction number k, which is defined as the ratio $\frac{A'}{A_2}$; k is dependent on the Reynolds number $Re = \frac{\varrho_{\text{blood}} d_2 w_2}{\eta_{\text{blood}}}$ and the ratio $\Phi = \frac{A_2}{A_1}$. Modeling experiments define this dependency as $k = 4.6 \cdot 10^{-3}\, Re\, \Phi$. The average blood flow of the patient is determined to be $V^* = 7\ {}^{\text{l}}/_{\text{min}}$. For the solution, assume stationary relationships.
[blood density $\rho_{\text{blood}} = 1{,}050\ {}^{\text{kg}}/_{\text{m}^3}$, blood viscosity $\eta_{\text{blood}} = 0.018\ \text{Pa} \cdot \text{s}$]

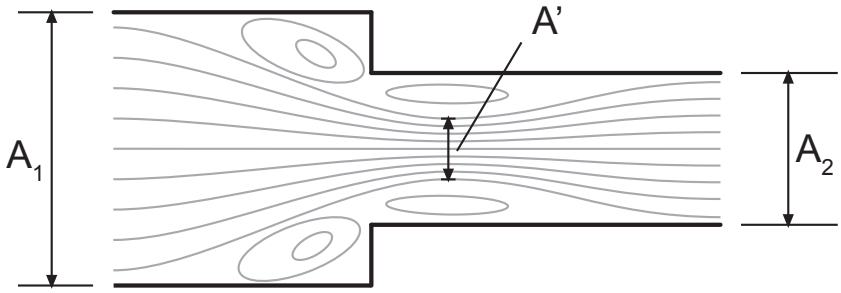

Fig. 3.4. Stepwise narrowing in the cross-section of an artery

!

Due to the sharp-edged, right-angle narrowing, the flow lines cannot follow the 90° edge lines directly. Instead, they describe a continuous trajectory, and vortices arise as stagnant zones. Additionally, due to the inertia of the fluid, flow is further reduced relative to the geometric narrowing by a cross-sectional area A'. The creation of vortices due to this narrowing means a loss of mechanical energy, which corre-

sponds to a drop in pressure of Δp_V. This drop in pressure is the difference between the pressure that would enter into a new cross section of the aorta without vortex creation (represented by the Bernoulli pressure p_{2B}), and the actual pressure p_2. As such, point 2 is chosen, where the blood can flow again without hindrances. As the drop in pressure before the narrowing contributes to the experimentally obtained contraction number k, to determine the drop in pressure, only the flow behind the narrowing is considered (here, flow spreads out again); the pressures p' and p'_B in the most narrow flow cross section A' can be assumed to be equal.

$$\Delta p_V = p_{2B} - p_2. \tag{3.5}$$

Ideal pressure p_{2B} can be expressed using the Bernoulli equation, and the real pressure p_2 can be described using the momentum equation. The Bernoulli equation is

$$p_{2B} + \frac{\rho_{\text{blood}}}{2} w_2^2 = p'_B + \frac{\rho_{\text{blood}}}{2} w'^2.$$

Therefore,

$$p_{2B} - p'_B = \frac{\rho_{\text{blood}}}{2} w_2^2 \left(\frac{w'^2}{w_2^2} - 1 \right). \tag{3.6}$$

The momentum equation (single-axis and stationary) is

$$0 = m^* \left(w' - w_2 \right) + A_2 \left(p' - p_2 \right).$$

Considering $m^* = \rho_{\text{blood}} A_2 w_2$, $p_2 - p'$ becomes

$$p_2 - p' = \frac{\rho_{\text{blood}}}{2} w_2^2 \left(\frac{2w'}{w_2} - 2 \right). \tag{3.7}$$

(3.6) and (3.7) substituted into (3.5) yield, considering $p' = p'_B$, the pressure drop Δp_V

$$\begin{aligned} \Delta p_V &= \frac{\rho_{\text{blood}}}{2} w_2^2 \left[\left(\frac{w'}{w_2} \right)^2 - 2\frac{w'}{w_2} + 1 \right] \\ &= \frac{\rho_{\text{blood}}}{2} w_2^2 \left(\frac{w'}{w_2} - 1 \right)^2. \end{aligned}$$

As the continuity equation is $V = w' A' = w_2 A_2$, we have

$$\frac{w'}{w_2} = \frac{A_2}{A'} = \frac{1}{k}$$

with k as the contraction number. From the relationship $k = 4.6 \cdot 10^{-3}\, Re\, \Phi$ we have, with $Re = \frac{w_2 \varrho_{\text{blood}} d_2}{\eta_{\text{blood}}} = 850$ and $\Phi = \frac{A_2}{A_1} = \frac{0.8}{4.9} = 0.16$, the value $k = 0.63$.

This value can be used to calculate the loss in pressure Δp_V due to the narrowing:

$$\Delta p_V = \frac{\rho_{\text{blood}}}{2} \left(\frac{V^*}{A_2} \right)^2 \left(\frac{1}{k} - 1 \right)^2.$$

Numerically, with $\rho_{\text{blood}} = 1{,}050\,\text{kg/m}^3$; $V^* = 7\,\text{l/min} = 2.33 \cdot 10^{-4} m^3/s$; $A_2 = 0.8\,\text{cm}^2$, and $k = 0.63$, the drop in pressure is $\Delta p_V = 384\,\text{Pa}$.

3.9 Blood Pressure in the Aorta

What is the loss in pressure due to fluid friction in the aorta of a healthy person? To perform the calculation, assume stationary relationships and laminar flow. Is this last condition justified? What is the loss in pressure due to friction in relation to the loss in pressure due to narrowing of the aorta? As an estimate of pressure loss from narrowing, assume the sum value of spasmodic and stepped narrowing corresponding to the preceding exercises.
[aorta diameter $D = 2.5\,\text{cm}$; aorta length $l = 40\,\text{cm}$; blood viscosity $\eta = 0.018\,\text{Pa s}$; blood flow $V^* = 7\ {}^{\text{l}}/_{\text{min}}$]

?

The loss of pressure in the aorta Δp_A can be calculated from the Hagen–Poiseuille equation, if laminar conditions apply. This is the case if the Reynolds number is $Re < 2{,}300$. The Reynolds number is

!

$$Re = \frac{\rho w D}{\eta} = \frac{\rho D V^*}{\eta A} = \frac{4}{\pi}\frac{\rho}{\eta}\frac{V^*}{D}.$$

Numerically, with $D = 2.5\,\text{cm}$, Re is $l = 40\,\text{cm}$; $V^* = 7\ {}^{\text{l}}/_{\text{min}}$; $\eta = 0.018\,\text{Pa} \cdot \text{s}$, and $\rho = 1{,}050\ {}^{\text{kg}}/_{\text{m}^3}$

$$Re = 337.$$

This fulfills the criteria for laminar flow, and we can use the Hagen–Poiseuille equation.

$$V^* = \frac{\pi D^4}{128\,\eta}\frac{\Delta p_A}{l}.$$

Solving for Δp_A,

$$\Delta p_A = \frac{128\,\eta l}{\pi D^4} V^* = \Delta p_A = 360\,\text{Pa}.$$

If there is narrowing in the aorta with pressure drop due to friction (see Exercise 3.7) $\Delta p_{VR} = 50.4\,\text{Pa}$ and due to turbulence (see Exercise 3.8 $\Delta p_{VW} = 384\,\text{Pa}$), the drop in pressure rises to

$$\Delta p = \left(\Delta p_A + \Delta p_{VR} + \Delta p_{VW}\right) = 360\,\text{Pa} + 50.4\,\text{Pa} + 384\,\text{Pa} = 794.4\,\text{Pa}.$$

The ratio of the drop due to narrowing to the drop due to friction in the aorta is

$$\frac{\Delta p_V}{\Delta p_A} = \frac{794.4\,\text{Pa}}{360\,\text{Pa}} = 2.2.$$

As is clear, the loss of pressure more than doubles due to this massive narrowing.

3.10 Pulsatile Blood Flow

? Consider pulsing blood flow. Calculate blood flow strength V_S^*

1. for the case in which the heart rate of a patient has dropped to $\omega_S = 50\,\mathrm{min}^{-1}$ (normal value $\omega = 70\,\mathrm{min}^{-1}$), and compare this result with the stationary value for the same pressure gradient p';
2. for another patient with heart flutter (a disturbance in the rhythm of the heart, with a suddenly elevated heart rate).

For the solution, start with the distribution of velocity

$$w(r,t) = \frac{p' e^{i\omega t}}{i\omega\rho}\left[1 - \frac{J_0\left(r\sqrt{-i\frac{\rho\omega}{\eta}}\right)}{J_0\left(R\sqrt{-i\frac{\rho\omega}{\eta}}\right)}\right]$$

and calculate $w(r,t)$ to a second-order approximation. The r coordinate is the distance of a particle of blood from the axis of a blood vessel. This allows us to calculate the average velocity $\bar{w}$ and to compare it with the corresponding relationship from the Hagen–Poiseuille equation. The average velocity $\bar{w}$ corresponds to an average over r, which, in the middle of a pulse, creates the same throughput as the velocity profile $w(r,\,t)$ (weighted average).
[blood density $\rho = 1{,}050\,\mathrm{kg/m^3}$; blood viscosity $\eta = 0.018$ Pa s; aorta radius $R = 1.25$ cm]

! Before the average velocity can be calculated, the Bessel function $J_n(x)$ in the existing equation for $w(r,t)$ should be developed in a series. We have

$$J_n(x) = \frac{x^n}{2^n\Gamma(n+1)}\left[1 - \frac{x^2}{2(2n+2)} + \frac{x^4}{8(2n+2)(2n+1)} - \ldots + \ldots\right].$$

and the Bessel function of zero order $J_0(x)$ is

$$J_0(x) = \frac{1}{\Gamma(1)}\left[1 - \frac{x^2}{4} + \frac{x^4}{16} - \ldots + \ldots\right]$$

Considering that the gamma function is $\Gamma(1) = 1$ in the desired approximation,

$$J_0(x) \approx 1 - \frac{x^2}{4}.$$

The ratio of the Bessel function in the exit equation is then

$$\frac{J_0\left(r\sqrt{-i\frac{\rho\omega}{\eta}}\right)}{J_0\left(R\sqrt{-i\frac{\rho\omega}{\eta}}\right)} = \frac{4\eta + i\,r^2\rho\omega}{4\eta + i\,R^2\rho\omega}.$$

Substituting this in the solution for $w(r,t)$ we have

$$w(r,t) = p' e^{i\omega t}\left[\frac{\left(R^2 - r^2\right)}{4\eta + i\,\left(\rho\omega R^2\right)}\right].$$

p' is the peak of the periodic pressure gradient. Considering the Euler formula for complex numbers $e^{iz} = \cos\, z + i\, \sin\, z$ we have

$$w\,(r,t) = p'\left[\frac{\left(R^2 - r^2\right)}{4\eta + i\,\left(\rho\omega R^2\right)}\right][\cos\,(\omega t) + i\,\sin\,(\omega t)]$$
$$= p'\frac{R^2}{4\eta}\,\frac{\left[1 - \left(\frac{r}{R}\right)^2\right][\cos\,(\omega t) + i\,\sin\,(\omega t)]}{1 + i\,\frac{\rho\omega R^2}{4\eta}}.$$

The value $\frac{\rho\omega R^2}{\eta}$ that occurs in the equation can be understood as a Reynolds number constructed with the pulse frequency, and is abbreviated as $\widetilde{Re}$. Therefore,

$$w(r,t) = \frac{p'R^2}{4\eta}\,\frac{\left\{\left[1 - \left(\frac{r}{R}\right)^2\right]\right\}\{\cos\,(\omega t) + i\,\sin\,(\omega t)\}}{1 + i\,\frac{1}{4}\widetilde{Re}}.$$

For the oscillation, only the real portion of this complex expression is relevant. We must expand using the complex conjugate denominator $1 - i\,\frac{1}{4}\widetilde{Re}$; the real portion is then

$$w\,(r,t) = \frac{p'R^2}{4\eta}\left[1 - \left(\frac{r}{R}\right)^2\right]\,\frac{\cos\,(\omega t) + \frac{1}{4}\widetilde{Re}\,\sin\,(\omega t)}{1 + \frac{1}{16}\widetilde{Re}^2}.$$

As can be seen, we are dealing with a superimposed sin/cosine oscillation over time t with a parabolic dependence of radius r, that corresponds to the velocity profile of Hagen–Poiseuille $w(r) = \frac{p'R^2}{4\eta}[1-(\frac{r}{R})^2]$ at $\omega = 0$. The average velocity $\bar{w}$ is, with balance,

$$\frac{2\bar{w}\,A}{\omega} = \int_A \int_t w\,(r,t)\,dA\,dt$$

with the cross-sectional area A of the aorta. As $A = \pi R^2$ and $dA = 2\pi r dr$, we have

$$\bar{w} = \frac{2\,p'}{4\,\eta}\int_0^R 2\,\frac{\omega}{2}\int_0^{\frac{\pi}{2\omega}} r\left[1 - \left(\frac{r}{R}\right)^2\right]\frac{\cos\,(\omega t) + \frac{1}{4}\,\widetilde{Re}\,\sin\,(\omega t)}{1 + \frac{1}{16}\,\widetilde{Re}^2}\,dr\,dt.$$

Because the variables r and t occur separately in the equation, we can integrate independently over dr and dt:

$$\bar{w} = \frac{p'R^2}{8\,\eta}\,\frac{\omega}{1 + \frac{1}{16}\,\widetilde{Re}^2}\int_0^{\frac{\pi}{2\omega}} \cos\,(\omega t) + \frac{1}{4}\,\widetilde{Re}\,\sin\,(\omega t)\,\,dt$$
$$= \frac{p'R^2}{8\,\eta}\,\frac{\omega}{1 + \frac{1}{16}\,\widetilde{Re}^2}\left[\frac{\sin\,(\omega t) - \frac{1}{4}\,\widetilde{Re}\,\cos\,(\omega t)}{\omega}\right]_0^{\frac{\pi}{2\omega}}$$
$$= \frac{p'R^2}{8\,\eta}\left[\frac{1 + \frac{1}{4}\,\widetilde{Re}}{1 + \frac{1}{16}\,\widetilde{Re}^2}\right].$$

The average velocity $\bar{w}_{HP}$ by the Hagen–Poiseuille is

$$\bar{w}_{HP} = \frac{p' R^2}{8\,\eta}.$$

And the ratio $\Theta = \frac{\bar{w}}{\bar{w}_{HP}}$ becomes

$$\Theta = \frac{1 + \frac{1}{4}\,\widetilde{Re}}{1 + \frac{1}{16}\,\widetilde{Re}^2}$$

1. In the case of a disruption in heart function with heart rate reduced to $\omega_S = 50\,\mathrm{s}^{-1}$ we have blood stream strength

$$V_S^* = \pi\,\overline{w}_S R^2 = \frac{\pi p' R^4}{8\,\eta}\left[\frac{1 + \frac{1}{4}\,\widetilde{Re}_S}{1 + \frac{1}{16}\,\widetilde{Re}_S^2}\right] \quad \text{with } \widetilde{Re}_S = \frac{\rho \omega_S R^2}{\eta}.$$

   Hagen–Poiseuille gives

$$V_{HP}^* = \frac{\pi p' R^4}{8\,\eta}$$

   and therefore, the ratio

$$\frac{V_S^*}{V_{HP}^*} = \left[\frac{1 + \frac{1}{4}\,\widetilde{Re}_S}{1 + \frac{1}{16}\,\widetilde{Re}_S^2}\right].$$

   With $\omega_S = 50\,\mathrm{min}^{-1}$, $\widetilde{Re}_S = 7.6$, and

$$\frac{V_S^*}{V_{HP}^*} = \left[\frac{1 + \frac{1}{4}\,7.6}{1 + \frac{1}{16}\,7.6^2}\right] = 0.63\cdot$$

   Due to the disturbance in heart function, the blood stream strength of the patient (considering the approximation) is 63% smaller than in the case of a stationary calculation using Hagen–Poiseuille.

2. Heart rate disruptions due to heart flutters lead to $\omega \to \infty$ and therefore also $\widetilde{Re} \to \infty$. As such, the expression $\frac{V_S^*}{V_{HP}^*}$ is unknown. Using Hospital's rule, we have

$$\lim_{\widetilde{Re} \to \infty}\left(\frac{V_S^*}{V_{HP}^*}\right) = \lim_{\widetilde{Re} \to \infty}\left(\frac{\frac{1}{4}}{\frac{1}{8}\,\widetilde{Re}}\right) = \lim_{\widetilde{Re} \to \infty}\left(\frac{2}{\widetilde{Re}}\right) = 0;$$

   that is, when $\widetilde{Re} \to \infty$ blood flow is $V_S^* \to 0$. This gives rise to a life-threatening situation that can lead to cardiac infarction if countermeasures, like the use of a defibrillator, are not immediately taken.

3.11 Cardiac Output

To estimate cardiac output, assume that the average systolic pressure of the left ventricle is $p_{lv} = 100\,\text{mm Hg}$, and that of the right ventricle is $p_{rv} = 15\,\text{mm Hg}$. The heart has a volume of $V = 300\,\text{ml}$ and the stroke volume of a ventricle is 70 ml. ?

1. Assuming that the volume of the ventricle is shifted against a constant systolic pressure during a heartbeat, what is the mechanical work done by the heart per heartbeat?
2. What is the average power at heart rate ν of 72 beats per minute? What is the power density?
3. Is the power density from section (b) achievable with an aquarium pump? The pump has volume $V = 0.2\,\text{l}$, and can carry 10 l of water to a height of $h = 6.12\,\text{m}$ per minute.
4. Up until now, we have ignored that blood pumped out must be accelerated. What is the percent portion of the work of acceleration with respect to the total work? The expulsion velocity is $v = 0.5\,\frac{\text{m}}{\text{s}}$, and the density of blood is $\rho = 1.05\,\frac{\text{kg}}{\text{l}}$.

!

1. The mechanical work is comprised of the contributions of the left and right ventricles: $W = W_{\text{lV}} + W_{\text{rV}}$. The unit still used in medicine mm Hg – the Torr – corresponds to 133.32 Pa. With $W = pV$ we have

$$W_{\text{lV}} = 100 \cdot 133.32\,\text{Pa} \cdot 0.070 \cdot 10^{-3}\text{m}^3 = 0.93\,\text{J}$$
$$W_{\text{rV}} = 15 \cdot 133.32\,\text{Pa} \cdot 0.070 \cdot 10^{-3}\text{m}^3 = 0.14\,\text{J}.$$

2. The average power is

$$P = W_{\text{ges}}\nu = (0.93 + 0.14)\,\text{J} \cdot \frac{72\,{}^{1}/_{\text{min}}}{60\,{}^{\text{s}}/_{\text{min}}} = 1.28\,\text{W}$$

and the power exerted per volume is

$$\frac{P}{V} = \frac{1.28\,\text{W}}{300\,\text{ml}} = 4.27\,\frac{\text{kW}}{\text{m}^3}.$$

3. The power of the aquarium pump is calculated from the discharge $V^* = V\nu = 10\frac{\text{l}}{\text{min}}$ as

$$P = W\nu = mgh \cdot \nu = \rho gh \cdot V^* = 10^3\,\frac{\text{kg}}{\text{m}^3} \cdot 9.81\,\frac{\text{m}}{\text{s}^2} \cdot 6.12\,\text{m} \cdot \frac{10 \cdot 10^{-3}\text{m}^3}{60\,\text{s}} = 10\,\text{W}.$$

For power density, we have

$$\frac{P}{V} = \frac{10\,\text{W}}{0.2 \cdot 10^{-3}\,\text{m}^3} = 50\,\frac{\text{kW}}{\text{m}^3}.$$

The power density would suffice; the difficulty in developing an artificial heart lies elsewhere.

4. The acceleration work is

$$W_B = \frac{1}{2}mv^2 = \frac{1}{2}\rho V v^2 = \frac{1}{2}\cdot 1.05\,\frac{\text{kg}}{\text{l}}\cdot 2\cdot 0.070\,\text{l}\cdot 0.5^2\,\frac{\text{m}^2}{\text{s}} = 0.018\,\text{J}.$$

Its portion of the total work done is only

$$\frac{W_B}{W_B + W} = \frac{0.018\,\text{J}}{0.018\,\text{J} + 1.073\,\text{J}} = 0.016 = 1.6\%.$$

3.12 Mitral Valve Opening Surface

? The pressure difference between the front and back sides of the closed mitral valve of a human heart is 2 mm Hg. Additionally, the heart index, the ratio of the heart minute volume to the body surface area A_0, is $q = 3.5\,\frac{\text{l}}{\text{m}^2\,\text{min}}$. What is the opening surface of the mitral valve for a person that weighs $m = 75$ kg and is $l = 170$ cm tall?

To solve the problem, use the continuity equation $V^* = \bar{w}\cdot A$ as well as the modified DuBois formula for an approximate calculation of the surface area of the body:

$$A_0 = k\cdot\sqrt{m\cdot l},$$

with constant $k = 0.167\,\sqrt{\frac{\text{m}^3}{\text{kg}}}$. V^* is the volume flow (volume per time) of blood with average velocity $\bar{w}$ through a surface A.

! Using the heart index q and the DuBois formula, we have, for volume flow V^*

$$\begin{aligned} V^* &= A_0 q = 0.167\,\sqrt{\text{m}^3/\text{kg}}\cdot\sqrt{75\,\text{kg}\cdot 1.7\,\text{m}}\cdot 3.5\,\frac{\text{l}}{\text{m}^2\,\text{min}} \\ &= 6.6\,\frac{\text{l}}{\text{min}} = 1.1\cdot 10^{-4}\,\frac{\text{m}^3}{\text{s}}. \end{aligned}$$

With a rapid opening of the mitral valve, we can assume that the entire pressure difference Δp is available for propulsion. The pressure difference is

$$\Delta p = \rho_{\text{Hg}}\cdot g\cdot\Delta h = 13.6\cdot 10^3\,\frac{\text{kg}}{\text{m}^3}\cdot 9.81\,\frac{\text{m}}{\text{s}^2}\cdot 2\cdot 10^{-3}\text{m} = 266.8\,\text{Pa}.$$

Considering the Bernoulli equation $\frac{1}{2}\rho\bar{w}^2 = \Delta p$ we have, for average flow velocity $\bar{v}$

$$\bar{w} = \sqrt{\frac{2\,\Delta p}{\rho}} = \sqrt{\frac{2\cdot 266.8\,\text{Pa}}{1.08\cdot 10^3\,\text{kg/m}^3}} = 0.7\,\frac{\text{m}}{\text{s}}.$$

As the blood only flows out during half of the cardiac cycle, we have, as an estimate of the surface of the mitral valve,

$$A = \frac{2\cdot V^*}{\bar{w}} = \frac{2\cdot 1.1\cdot 10^{-4}\text{m}^3\text{s}}{0.7\,\text{m s}} = 3.14\cdot 10^{-4}\text{m}^2 = 3.14\,\text{cm}^2.$$

3.13 Dialysis

A device used for dialysis operates on the principle of ultrafiltration. The blood at the membrane is required to have an excess pressure of $\Delta p = 10^5$ Pa. Before the blood flows back into the body of the patient, this pressure difference must be mitigated. This is achieved by the use of N capillaries of length $L = 0.5$ m connected in parallel. All capillaries have the same diameter d. The shear stress at the capillary walls may not exceed $\tau_R = 25$ Pa, in order to avoid the risk of hemolysis. The volumetric flow is $\dot{V} = 5 \cdot 10^{-6}$ m³/s. The fluidic properties of the blood can be modeled using the Rabinowitsch approach[2], which relates the shear stress τ and fluid velocity gradient $\dot{\gamma}$ for various fluids by choice of appropriate constants a and c by a third order polynomial

$$\frac{\dot{\gamma}}{c} = \frac{\tau}{a} + \left(\frac{\tau}{a}\right)^3.$$

Assuming that the relevant parameters are $a = 1.2$ Pa and $c = 12$ 1/s, how many capillaries are required and how large should be their diameter?

Since the shear stress at the capillary wall is $\tau_R = \Delta p \frac{d}{4L}$, we can write for the diameter

$$d = 4L\frac{\tau_R}{\Delta p} = 4 \cdot 0.5 \cdot \frac{25\cdot}{10^5}\,\text{m} = 5 \cdot 10^{-4}\text{m} = 0.5\,\text{mm}.$$

The volumetric flow $\dot{V}_I$ through one capillary can be calculated using, with fluid velocity $w(r)$,

$$\dot{V}_I = 2\pi \int_0^{\frac{d}{2}} r w(r)\, dr.$$

Integrating by parts yields

$$\dot{V}_I = \pi \left[\frac{d^2}{4} w\left(r = \frac{d}{2}\right) - \int_0^{\frac{d}{2}} r^2 dw \right],$$

and due to $w\left(r = \frac{d}{2}\right) = 0$ it follows that

$$\dot{V}_I = -\pi \int_0^{\frac{d}{2}} r^2 dw = -\pi \int_0^{\frac{d}{2}} r^2 \frac{dw}{dr}\, dr = \pi \int_0^{\frac{d}{2}} r^2 \dot{\gamma}\, dr = \pi \int_0^{\frac{d}{2}} r^2 f(\tau)\, dr \tag{3.8}$$

Since the shear stress distribution can be assumed to be linear $\tau = \tau_R \frac{2}{d} r$ and thus

$$\frac{d\tau}{dr} = \frac{2\tau_R}{d} \rightarrow dr = \frac{d}{2\tau_R} d\tau \tag{3.9}$$

2 The Rabinowitsch model describes, similar to the potential law of fluids, the correlation between the shear rate τ and velocity gradient $\dot{\gamma}$ for some fluids

and because $\tau^2 = \tau_R^2 \frac{4}{d^2} r^2$

$$r^2 = \frac{d \cdot \tau^2}{4 \tau_R^2}. \tag{3.10}$$

Substitution of Equation (3.9) and Equation (3.10) into Equation (3.8) yields

$$\dot{V}_I = \frac{\pi}{8} \left(\frac{d}{\tau_R} \right)^3 \int_0^{\tau_R} \tau^2 f(\tau)\, d\tau.$$

Using the Rabinowitsch approach, the expression for $\dot{V}_I$ is

$$\begin{aligned} \dot{V}_I &= \frac{\pi}{8} \left(\frac{d}{\tau_R} \right)^3 c \int_0^{\tau_R} \tau^2 \left[\frac{\tau}{a} + \left(\frac{\tau}{a} \right)^3 \right] d\tau = \frac{\pi}{8} \left(\frac{d}{\tau_R} \right)^3 c \left(\frac{\tau_R^4}{4a} + \frac{\tau_R^6}{6a} \right) \\ &= \frac{\pi}{8} d^3 c \left(\frac{\tau_R}{4a} + \frac{\tau_R^3}{6a} \right) = \frac{\pi}{8} \left(5 \cdot 10^{-4} \right)^3 12 \left(\frac{25}{4 \cdot 1.2} + \frac{25^3}{6 \cdot 1.2} \right) \mathrm{m^3/s} \\ &= 77 \, \mathrm{cm^3/min}. \end{aligned}$$

Thus, the number of capillaries N is

$$N = \frac{\dot{V}}{\dot{V}_I} = \frac{5 \cdot 10^{-6}}{1.28 \cdot 10^{-6}} = \frac{5}{1.28} = 4.$$

4 The Senses

For humans, in addition to the senses of taste and smell, the senses of sight and hearing are the most important. We take in the greatest portion of our information through sight, which is made possible by both the eyes and a part of the brain. Light strikes the eye, which then sends a nerve impulse to the brain where it is transformed into usable information. The eye itself is comprised of the cornea, the anterior chamber, the lens, the iris with the pupil, the vitreous humor, the retina, and the optical nerve. Using its musculature as well as the eyelids and the tear (lachrymal) glands, the eye is able to adapt to changing requirements. The eyeball is comprised of a gelatinous fluid that is 98% water. The remaining 2% is primarily collagen and hyaluronan, which bind the water. The intraocular pressure is between 2 and 3 kPa greater than that of the surroundings. The ocular fluid is constantly refreshed in order to ensure a high optical quality. The cornea, with its high transparency, is constantly wetted with lachrymal fluid; this keeps its surface smooth and removes debris.

Incident light is refracted by the cornea and lens; their curvatures are the most important part of the lensing mechanism of the eye. The lens itself is flexible across a certain range; this allows the eye to focus on specific objects. The iris with the pupil, a variable aperture, contributes to adaptation to brightness and focusing at different depths. Images are generated on the retina, and are converted into electrical nerve impulses by the optical cells. The retina is the site of the blind spot, and the macula lutea. The latter lies in the optical center of the eye and has the greatest density of optical cells. As such, the sharpest images are created at it. The blind spot is the position at which the optical nerve and the blood vessels connect to the eye. Here there are no sensory cells, and no sensory perception occurs. Everywhere else, though, the retina contains sensory cells. There are two kinds of photoreceptors: rods and cones. Rods detect brightness and darkness, and cones detect colors. They are primarily concentrated in the macula, and the best perception of color occurs there. There are significantly more rods than cones, especially in the outer regions of the retina. The field of sight of a human eye extends from roughly -60° to $+120^\circ$ horizontally, and from roughly -75° to $+60^\circ$ vertically. Because both eyes' regions of vision overlap in humans, we can also perceive distances within this range.

The lensing effect in the eye is due principally to the curved cornea and the lens. Each surface layer contributes a component of refraction, which can be described with the lens formula $\frac{n_1}{g} + \frac{n_{N+1}}{b} = \sum_{i=1}^{N} \frac{n_{i+1}-n_i}{r_i}$, with g as the object distance, b as the image distance, n as the index of refraction, and r_i as the radius of curvature of the boundary layer. The term $\frac{\Delta n}{r}$ is called the refractivity or optical power, with unit (m^{-1}). In optics, this unit is also called the diopter (dpt).

Like every system of lenses, even a healthy eye has a number of optical imperfections. Among them are the spherical and chromatic aberrations. The former manifests itself in the dark, when the pupil diameter is large. Under these conditions, the sig-

nals of multiple neighboring sensory cells are “averaged” to produce a signal strong enough for perception. The chromatic aberration refers to the fact that blue light is refracted more sharply than red light. In the wavelength range of 400–700 nm, the error is around 2 dpt. For most sensory cells, though, the difference in the index of refraction is too small to be noticeable. Another flaw comes from the fact that images are only sharp in the vicinity of the macula. However, because (as explained above) there are many more sensory cells there than in rest of the retina, the image can still be detected with sharp resolution.

The change in the index of refraction is due to a deformation of the lens known as accommodation. At rest, the lens is kept tense by suspending ligaments, and is relatively flat; as such, the index of refraction is small. This allows distant objects to be seen in clear focus. If the ciliary muscle is contracted, the ligaments slacken and the lens curves more steeply; the index of refraction rises, and the focal point moves closer to the eye. While children can see objects that are relatively close (around 7 cm) clearly, for adults, this distance grows with age as the flexibility of the lens decreases. Because the lens is made of extracellular material, it does not regenerate itself. This is why many older people need reading glasses to assist with accommodation. Nearsightedness occurs when the focal length is too short, and the image appears in the interior of the eye rather than on the retina. In this case, a diverging lens is required (negative diopters). Farsightedness requires that the focal length be shortened in order to project the image on the retina. In this case, glasses feature a converging lens.

The eye is sensitive to a range in wavelengths of 380 to 780 nm. This portion of the spectrum corresponds well with the spectrum of solar radiation that occurs at the surface of the Earth. Both the sensitivity of the sensory cells and absorption in the entire eye play roles in the dependency of sensory perception on wavelength. Short--wave light is almost completely absorbed before reaching the retina, as water and all molecular materials absorb relatively strongly in the ultraviolet range and at larger wavelengths. In the process, a portion of the optical energy absorbed is re-radiated in the form of florescent light. Because this florescent light appears as a diffuse background, it disturbs the remaining sensory perception. Nearly half of the light left over is scattered, and is lost as far as sensory perception is concerned. In the sensory cells, a portion of the incident light is absorbed; the maximum absorption depends on the type of sensory cell and total brightness, at a wavelength between 400 and 600 nm.

Processing images, which occurs in the visual center of the brain, is extremely complicated. The brain receives necessary information through the optical nerve, which transmits it from the light-sensitive cells (rods and cones). A portion of the visual cortex is present in the retina as three layers of neurons, which can be thought of as an “appendage” of the brain. The action potentials of the sensory cells are transmitted from place to place by neurons. Directly after these sensory cells are the bipolar cells. These activate the nerve fibers, which can be divided into an “on-channel” and an “off-channel”. In the “on-channel”, exposure to light causes a rise in the frequency of spontaneous discharge; in the off-channel, discharge is suppressed. Most signals

to the brain utilize both on- and off-channels. This has the advantage that in average lighting, not all neurons need to work at half power. The horizontal cells modulate signal transmission. Further processing occurs within the brain itself. The nerve fibers run from different parts of the retina to the corresponding parts of the brain; the nerves from the right side of both eyes run through the optic chiasm to the right half of the brain, and vice versa. The visual cortex is located in the rear of the brain. The brain also controls the orientation of the eye and makes sure that the central portions of images are formed on the macula.

The fact that we see our surroundings in color relies on both the dependency on wavelength of absorption, scattering, and reflection of light by materials, and on the ability of the eye to selectively detect different wavelengths of light using the cones. Depending on the relative stimulation of different kinds of cones, color effects occur in the brain. In addition to the encoding of color and spatial data, there are also neurons that react specifically to motion – to changes in information. These signals serve, for example, to turn the eye in the direction of motion.

Because the constituent elements of information processing only develop in early childhood, strabismus (constantly crossing the eyes) must be dealt with at that age to avoid degeneration of the optical nerves. In addition, it has become possible to replace individual visual cells. An "artificial retina" system is comprised of a camera and an electronic component that is implanted into the eye; the system stimulates the optical nerves directly, according to the video feed.

The sense of sound occurs when sound waves are transmitted through the ears to the auditory nerves. The ear is comprised of three parts: outer ear, middle ear, and inner ear. The ears create two cavities that begin at the temporal bone and lead deep into the skull, where the nerve fibers that deliver the signals to the brain are located. Sound waves are variations in air pressure. The amplitudes of these variations are termed sound pressure. The frequency range of human hearing stretches from $\nu = 16\,\mathrm{Hz}$ to $20\,\mathrm{kHz}$. From the quietest but still audible $2\,\mathrm{kHz}$ sound up to the pain threshold, the range extends over $\Delta p_{eff} = 20\,\mu\mathrm{Pa}$ to $20\,\mathrm{Pa}$. At the hearing threshold ($20\,\mu\mathrm{Pa}$), intensity is $I_0 \approx 10^{-12}\,\mathrm{W/m^2}$; at the pain threshold, it is roughly $I_{\max} \approx 1\,\mathrm{W/m^2}$. Hearing perceives sound pressure somewhat logarithmically. As such, it makes sense to use a logarithmic sound pressure scale. Using reference pressure Δp_0, the definition of sound level is $L = 20 \cdot \log(\frac{\Delta p}{\Delta p_0}) = 10 \cdot \log(\frac{I}{I_0})$. If we take the sensory boundary of human hearing as a baseline, then we have $\Delta p_0 = 20\sqrt{2}\,\mu\mathrm{Pa} = 28.3\,\mu\mathrm{Pa}$. The sonic value calculated is measured in decibels (dB). In addition to this parameter there is another measurement, the phon, that takes into account the physiological impact of the volume. The two values are not linearly related.

The outer ear is comprised of the pinna (auricle) and the outer auditory canal, with the eardrum at the end. This membrane divides the outer ear from the middle ear. Transfer of sound occurs through the eardrum, and the three adjoining auditory ossicles: the malleus (hammer), the incus (anvil), and the stapes (stirrup). The stapes

is connected to the oval window, behind which is the inner ear. This is comprised of the bony labyrinth; its voids are filled with a fluid, the perilymph. The sensory cells are located between the individual chambers of this region, and transform movements of the membranes into nerve impulses. Additionally, the inner ear contains three archways in which is located the vestibular system. The outer ear serves to amplify sounds, and to filter incoming sound waves according to their direction. In the middle ear impedance matching of the air to the perilymph occurs. Without this impedance matching, the middle ear would only be able to transmit around 1% of the energy received by the outer ear to the inner ear. The inner ear conducts an analysis of the frequency and amplitude of the sound waves, and the signals are then processed in the cerebral cortex. A relatively narrow canal, the Eustachian tube, connects the middle ear to the pharynx. It serves to keep air pressure equal on both sides of the eardrum.

The detection of pitch and volume is accomplished by different sensory cells in the ear, lending further importance to the transfer mechanisms of wave propagation. The acoustic oscillations of the air are converted multiple times before they are processed as nerve impulses. First, a membrane oscillation begins at the eardrum; it is transmitted from the eardrum through the mechanical connections of the auditory ossicles to the membrane of the oval window. This creates fluid waves in the cochlea, and through the membranous labyrinth, in the endolymph as well. This leads to the oscillation of additional membranes in the cochlea – the basilar and tectorial membranes. The relative movements of these two membranes generate a displacement of hair cells. The magnitude of this displacement is transmitted to the brain as a nerve impulse. The mechanical characteristics of the transport media, like membrane elasticity and mass, viscosity of the fluids, dampening behaviors, and reflections determine the pitch and the extent of oscillation propagation. As such, high-frequency waves penetrate deeper into the cochlea than low-frequency ones. The signals released from the rear nerve cells are interpreted by the brain as higher pitches. The brain determines spatial orientation by using the difference in intensity of the sound waves between both ears, as well as differences in phase.

In addition to the transmission path of the sound waves, sound waves are also directly transmitted through the bones of the skull. This sound transfer mechanism, termed bone conduction, bypasses the outer and middle ears and transports the sound waves through oscillations of the skull. It does not usually perform a significant role in hearing, as bone does not conduct nearly as much sound as air.

As they grow older, many people suffer to a greater or lesser extent from difficulties in hearing. There are many causes of this phenomenon. Hearing loss can often only be corrected through the use of hearing aids, which strengthen the amplitude of sound waves arriving at the ear. As most devices strengthen the entire spectrum of sound waves linearly, they significantly reduce the differentiation and weighting of signals that healthy ears can achieve.

4.1 Information Processing

To read an assigned section of this book, a student needs 15 min. The section contains 3,000 words in total [Wt], with an average of 7 characters [Sz] each. ?

1. What is the flow of information, if the informational content of a character is 1.5 bit?
2. What amount of time t_{theo} would the student need to grasp the meaning of the text if, in processing the information, he reaches the maximum information capacity of they eye $C = 3 \cdot 10^6$ bit/s?

!

1. If reading $N = 3{,}000$ Wt with $s = 7$ Sz/Wt requires $t = 15$ min, then, under the assumption that information content is $i = 1.5$ bit/Sz, information flow is

$$I^* = \frac{N\,s\,i}{t} = \frac{(3{,}000\ \text{Wt})\,(7\ \text{Sz/Wt})\,(1.5\ \text{bit/Sz})}{15\ \text{min}} = 2{,}100\ \text{bit/min} = 35\ \text{bit/s}.$$

2. With the maximum information capacity of the eye as $C = 3 \cdot 10^6$ bit/s, for the theoretical amount of time we have

$$t_{\text{theo}} = \frac{I}{C}.$$

With

$$I = 3{,}000 \cdot 7 \cdot 1.5 = 31{,}500\ \text{bit}$$

we have

$$t_{\text{theo}} = \frac{31{,}500\ \text{bit}}{3 \cdot 10^6\ \text{bit/s}} = 10.5\ \text{ms}.$$

4.2 Glasses

In a simple model of the eye, the convex lens L takes the place of the combination of the cornea and the lens in the eye. At a distance of $l = 2$ cm is the retina R, assumed to be a flat screen. The lens L projects an object G at distance $d = 30$ cm onto the retina, but refraction is too strong. In order to achieve a sharp projection of this object, the retina must be located $\delta = 5$ mm closer to the lens of the eye. To obtain a sharp image, refraction should be reduced by wearing glasses Z, which provide an additional lens at a distance of $s = 1.2$ cm from L. ?

1. What must the focal distance f_Z of lens Z be to project a sharp image on the retina?
2. In order to see a sharp image without glasses, the distance of the object $GL = d$ can be changed by d' while keeping image distance ($LR = l$) constant. At what distance d' must the object be placed so that L projects a sharp image on R?

! 1. Because the lens of the eye is convex, for refraction, we have

$$\frac{1}{f_L} = \frac{1}{d} + \frac{1}{l-\delta}.$$

Therefore, for the focal distance we have

$$f_L = \frac{d\,(l-\delta)}{d+l-\delta}.$$

Numerically, this is $f_L = \frac{30(2-0.5)}{30+2-0.5}$ cm = 1.43 cm. We need a concave lens in the glasses, as we need to reduce refraction. For the combination of lenses (eye and glasses) we have, for the notional refraction, $\frac{1}{f_{ZL}}$, and therefore for the focal distance f_{ZL}

$$\frac{1}{f_{ZL}} = \frac{1}{g} + \frac{1}{b} \qquad \text{and} \qquad f_{ZL} = \frac{g\,b}{b+g}.$$

The geometry of the optical path gives

$$g + b = d + l, \qquad \text{so that} \qquad b = d + l - g$$

$$\frac{B}{G} = \frac{b}{g} \quad \text{and} \quad \frac{B}{G} = \frac{l-\delta}{d} \qquad \text{and therefore} \qquad b = g\left(\frac{l-\delta}{d}\right)$$

with B as the size of the image, G as the size of the object, and b and g as the image and object distances. We then have

$$d + l - g = g\left(\frac{l-\delta}{d}\right) \qquad \text{and} \qquad d + l = \left(1 + \frac{l-\delta}{d}\right) g$$

and therefore

$$g = \frac{d+l}{1+\frac{l-\delta}{d}} \qquad \text{and} \qquad b = \frac{d+l}{1+\left(\frac{d}{l-\delta}\right)}.$$

Numerically, we have, with $l = 2$ cm; $d = 30$ cm; $\delta = 0.5$ cm $\rightarrow$ $g = \frac{32}{1+\frac{1.5}{30}}$ cm = 30.48 cm, and $b = \frac{32}{1+\frac{30}{1.5}} = 1.52$ cm and finally

$$f_{ZL} = \frac{30.48 \cdot 1.52}{1.52 + 30.48}\,\text{cm} = 1.45\,\text{cm}$$

For the combination of lenses we have the lens formula

$$\frac{1}{f_{ZL}} = \frac{1}{f_Z} + \frac{1}{f_L} - \frac{s}{f_Z f_L}$$

From this expression, the focal distance of the glasses f_Z can be eliminated:

$$f_Z = \frac{(f_L - s)\,f_{ZL}}{f_L - f_{ZL}}$$

With $s = 1.2$ cm, using the assumptions above, we have

$$f_Z = \frac{(1.43 - 1.2)\,1.43}{1.43 - 1.45}\,\text{cm} = -18.125\,\text{cm}$$

2. If the object distance is changed by d', a sharp image can be projected on the retina. Then we have

$$\frac{1}{f_L} = \frac{1}{d'} + \frac{1}{l}$$

Therefore,

$$\frac{1}{f_L} = \frac{1}{d'} + \frac{1}{l-\delta} = \frac{(l-\delta)+d}{d\,(l-\delta)}.$$

and finally

$$d' = \left[\frac{d+l-\delta}{d\,(l-\delta)} - \frac{1}{l}\right]^{-1}.$$

We can evaluate d' as $\rightarrow d' = [\frac{31.5}{30\cdot 1.5} - \frac{1}{2}]\,\mathrm{cm}^{-1} = [0.7 - 0.5]^{-1}\,\mathrm{cm} = 5\,\mathrm{cm}$.

4.3 Geometry of Glasses Lenses

For a pair of glasses, a lens is to be ground from glass with index of refraction $n = 1.4$. The refraction is $D = 2$ diopters. The diameter of the lens is $a = 5\,\mathrm{cm}$. If the lens has radii of curvature r_1 and r_2, as well as thickness d, its refraction is given as

$$D = (n-1)\left(\frac{1}{r_1} + \frac{1}{r_2}\right) + \left\{\frac{(n-1)^2}{n}\,\frac{d}{r_1 r_2}\right\}.$$

1. What radii of curvature must the surfaces on both sides have if they are to be exactly equal?
2. How wide will the lens be at its thickest point?
3. Would treating the lens as a "thin lens" in this case have been reasonable?

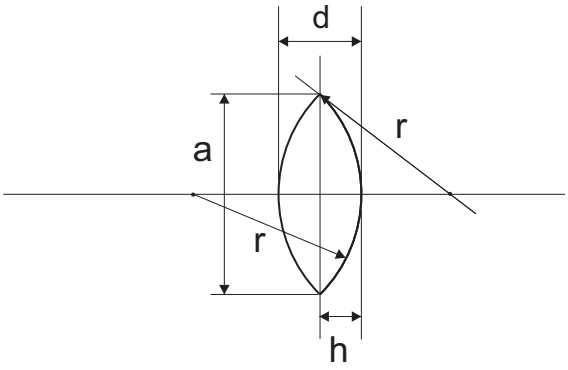

Fig. 4.1. Bi-convex spherical lens with radius of curvature r.

1. The radii of curvature are equal, so with $r_1 = r_2 = r$ we have

$$D = \frac{2\,(n-1)}{r} + \frac{(n-1)^2}{n}\frac{d}{r^2}. \tag{4.1}$$

From the Pythagorean Theorem we have

$$(r-h)^2 + \left(\frac{a}{2}\right)^2 = r^2$$

$$h = r - \sqrt{r^2 - \left(\frac{a}{2}\right)^2}$$

$$d = 2\,h = 2\,r - 2\sqrt{r^2 - \left(\frac{a}{2}\right)^2}. \tag{4.2}$$

(4.2) in (4.1) gives

$$D = \frac{2\,(n-1)}{r} + \frac{(n-1)^2}{n}\left[2r - 2\,\frac{\sqrt{r^2 - \left(\frac{a}{2}\right)^2}}{r^2}\right]$$

$$= \frac{2\,(n-1)}{r} + 2r\,\frac{(n-1)^2}{nr}\left[1 - r^2\sqrt{1 - \left(\frac{a}{2r}\right)^2}\right].$$

The solution can be found by iteration: $D = 2$ diopters gives $r = 0.4$ m.

2. For the thickest point d of the lens we have (4.2)

$$d = 2\,r - 2\sqrt{r^2 - \left(\frac{a}{2}\right)^2}.$$

Numerically,

$$d = 0.8\,\text{m} - 2\sqrt{(0.4)\,\text{m}^2 - \left(\frac{0.05\,\text{m}}{2}\right)^2} = 0.001564\,\text{m} = 1.564\,\text{mm}.$$

3. With a thin lens, the thickness of the lens is negligible in comparison to the radius of curvature. In addition, the radius of curvature is sufficiently large that the second term of the equation, which scales quadratically with the inverse of the radius of curvature, becomes insignificant. In this case, the equation for refraction reduces to

$$D = (n-1)\,\frac{2}{r_D}.$$

If we use this equation to calculate the radius of curvature, we have

$$r_D = \frac{D}{2\,(n-1)} = 0.25\,\text{m} = 0.6\,\text{r},$$

a discrepancy of 40%. The equation for a thin lens does not give a good approximation in this case.

4.4 Optical Illusions

A fisherman stands on a riverbank. In the water, a fish is swimming away from him at depth $t = 1\,\text{m}$ beneath the water's surface. The fisherman thinks that the fish is $l = 2\,\text{m}$ long and assumes that its tail fin is $s = 8\,\text{m}$ away from him horizontally. The fisherman's line of sight is $h = 2\,\text{m}$ above the surface of the water. How big is the fish in reality?
[index of refraction of water $n_W = \frac{4}{3}$]

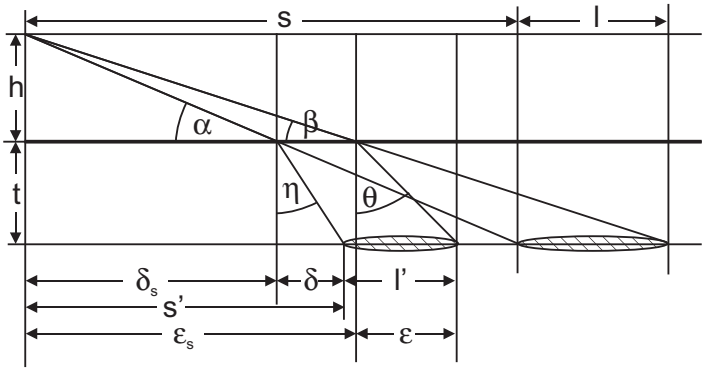

Fig. 4.2. Optical path at the water-air boundary layer. The shaded ellipses represent the fish at its actual and apparent positions.

We calculate the angle as

$$\tan\beta = \frac{h+t}{l+s} \quad \text{and therefore} \quad \beta = \arctan\left(\frac{h+t}{l+s}\right) = \arctan\left(\frac{3\,\text{m}}{10\,\text{m}}\right) = 16.7^\circ$$

$$\tan\alpha = \frac{h+t}{s} \quad \text{and therefore} \quad \alpha = \arctan\left(\frac{h+t}{s}\right) = \arctan\left(\frac{3\,\text{m}}{8\,\text{m}}\right) = 20.6^\circ$$

and by Snell's law

$$\frac{\sin\gamma}{\sin\gamma'} = \frac{n_W}{n_L}$$

with n_W as the index of refraction of water and n_L as the index of refraction of air; γ is the angle of incidence and γ' is the angle of reflection relative to the perpendicular. From this we have

$$\frac{\sin(90^\circ - \alpha)}{\sin\eta} = \frac{4}{3}$$

and therefore

$$\eta = \arcsin\left[\frac{3\sin(90^\circ - 20.6^\circ)}{4}\right] = 44.6^\circ.$$

For the ray to the fisherman's head, we have

$$\frac{\sin\left(90^\circ - \beta\right)}{\sin\theta} = \frac{4}{3}$$

and

$$\theta = \arcsin\left[\frac{3\sin\left(90^\circ - 16.7^\circ\right)}{4}\right] = 45.9^\circ$$

$$\tan\eta = \frac{\delta}{t} \qquad \text{and} \qquad \tan\alpha = \frac{h}{\delta_S}$$
$$s' = \delta_s + \delta \qquad \text{and} \qquad s' + l' = \varepsilon_s + \varepsilon.$$

Additionally,

$$s' = \frac{h}{\tan\alpha} + t\,\tan\eta = 6.32\ \text{m} \qquad \text{and} \qquad s' + l' = \frac{h}{\tan\beta} + t\,\tan\theta = 7.70\ \text{m}.$$

And therefore, the true length is

$$l' = \left(s' + l'\right) - s' = 7.7\ \text{m} - 6.32\ \text{m} = 1.38\ \text{m}.$$

4.5 Retina Implantation

? The retina of a human eye can be compared to a square CCD sensor with edge length measuring $d_{\text{CCD}} = 1$ cm and with 5 megapixelx of display.

1. What is the separation d_{CCD} between the centers of the CCD cells in comparison to the average separation d_N of the cones in the retina?
2. What are the minimum detectable angles of incidence θ_{CCD} and d_N if the retina, or CCD cells, are 2 cm in front of the iris?
3. A vertical segment comprised bright and dark lines of equal width strikes the retina. What is the minimum width D of these lines such that they can be resolved by the retina and the CCD?

!

1. The edge length of the CCD is d_{CCD}, and along an edge, there are $\sqrt{5}\cdot 10^3$ pixels with sensory cell separation of $d_{\text{CCD}} = \frac{1\ \text{cm}}{\sqrt{5}\cdot 10^3} = 4.5\ \mu\text{m}$. The average separation $\bar{d}_N$ between receptors in the retina is $\bar{d}_N = 6.6\ \mu\text{m}$. Therefore,

$$\frac{d_{\text{CCD}}}{d_N} = \frac{4.5}{6.6} = 0.68.$$

2. The angle of incidence for the CCD is $\theta_{\text{CCD}} = \frac{4.4\ \mu\text{m}}{2\ \text{cm}} = 220\ \mu\text{rad}$, and for the retina: $\theta_N = \frac{6.6\ \mu\text{m}}{2\ \text{cm}} = 330\ \mu\text{rad}$.
3. For the width of the lines, $D \geq 2\,d$. This means that D_N for the retina must be at least $D_N = 13.2\ \mu\text{m}$; for the CCD, it must be at least $D_{\text{CCD}} = 8.8\ \mu\text{m}$.

4.6 Threshold of Vision of the Human Eye

The absolute energy threshold E_S of the human eye (energy of an incident flash of light that immediately leads to a sensation of sight) is, according to measurements of a light wave with $\lambda = 510\,\text{nm}$, $4.0 \cdot 10^{-17}\,\text{J}$. ?

1. How many quanta of light are necessary to cause sensation of sight in this situation?
2. We can correct this number by considering the following reductions to it: reflection at the cornea 4%, scattering in the optical media of the eye 50%, absorption in the rhodopsin 20%.

!

1. The energy of a photon of wavelength $\lambda = 510\,\text{nm}$ is

$$E = h\nu = \frac{hc}{\lambda} = \frac{6.626 \cdot 10^{-34}\,\text{J s} \cdot 3 \cdot 10^{8}\,\text{m/s}}{510 \cdot 10^{-9}\,\text{m}} = 3.898 \cdot 10^{-19}\,\text{J}.$$

   The energy threshold, therefore, corresponds to

$$N = \frac{E_S}{E} = \frac{4.0 \cdot 10^{-17}\,\text{J}}{3.898 \cdot 10^{-19}\,\text{J}} = 103$$

   photons.
2. This seems like very few; however, it is only the number of photons that strike the surface of the eye. After reflection at the cornea only 99 light quanta remain, and due to absorption and scattering in the eye only 49 light quanta actually arrive at the retina. Of these, 10 are absorbed by rhodopsin. Amazingly, these are sufficient to allow the eye to sense the light!

4.7 Visual Angle and Resolution

Due to diffraction phenomena, the eye has a limited physical capacity for optical resolution. Two points of an object will only be perceived as separate from each other if the visual angle does not fall below a minimum value. The visual angle can be made greater if the object is brought closer to the eye. The ability to reduce the distance between the eye and the object is limited by the eye's accommodation. In order to be able to see clearly, a minimum distance between the object and the eye must be maintained; this minimum distance can only be reduced with the assistance of a convex lens. ?

1. Which cardinal point of the optical system of the eye must align with the image-side focal point of a thin convex lens so that the visual angle of the eye aided by the lens is not dependent on the position of the object? The object has size G and is located within the simple focal distance f of the lens.

2. How close must the object be brought to the eye (to the opposing center point M of the optical system of the eye) if, with accommodation of ∞, a sharp image will be produced? The focal distance of the lens is 5 cm.
3. What is the angular magnification $V = \frac{\tan\alpha'}{\tan\alpha}$ (angle magnification) with respect to the conventional visual range of 250 mm? α' is the visual angle of the aided eye, and α is the visual angle of the unaided eye.
4. What would the value of the image scale $M = \frac{G'}{G}$ be for the convex lens if the image was at $\frac{f}{2}$? Use the expression for thin lenses.

!

1. The object-side node M of the optical system of the eye must align with the image-side focal point of the thin convex lens. If $g \leq f$, then the visual angle σ' of the aided eye does not depend on the position of the object (see Figure 4.3).
2. An eye at infinite accomodation sees a sharp image if the beams of light enter the eye in parallel. This corresponds to $b = \infty$, and from the lens equation we have

$$\frac{1}{f} = \frac{1}{g} + \frac{1}{b}.$$

This is the case when the object is located at the focal point: $g = f$. M is located, according to section (a), at the image-side focal point of the convex lens; as given in the exercise, it is 5 cm away. According to Figure 4.3, the object can be brought up to $2 \cdot f = 10$ cm to the object-side node of the eye.

3. For the visual angle with the lens, we have

$$\tan\alpha' = \frac{G}{f}$$

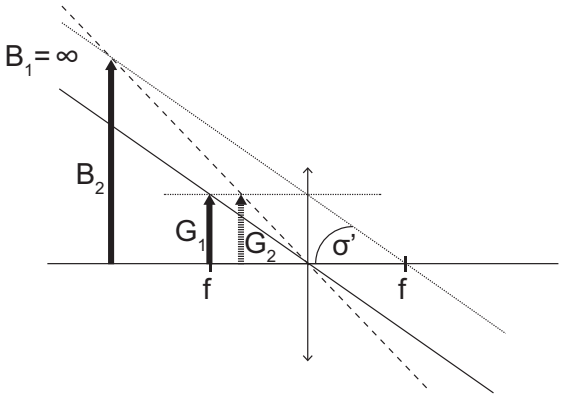

Fig. 4.3. Construction of the images of two objects of equal size $G_{1,2}$. B_i is the image size of object i, and f are the focal distances of the lens (designated as the line with the double arrow). In the case of object 1, located exactly at the focal point of the lens, the image is infinitely far away. σ' is the visual angle of the eye.

and for the visual angle of the unaided eye,

$$\tan\alpha = \frac{G}{250\,\text{mm}}.$$

As such, the angular magnification is:

$$V = \frac{\tan\alpha'}{\tan\alpha} = \frac{\frac{G}{f}}{\frac{G}{250\,\text{mm}}} = \frac{250\,\text{mm}}{50\,\text{mm}} = 5.$$

4. In order to calculate the image scale, we can use the lens equation (see part (2)) and the ray law

$$\frac{G}{B} = \frac{g}{b},$$

As $g = \frac{f}{2}$,

$$\frac{1}{b} = \frac{1}{f} - \frac{1}{\frac{f}{2}} = -\frac{1}{f}$$

and the image scale is

$$|M| = \left|\frac{B}{G}\right| = \left|\frac{b}{g}\right| = \frac{\frac{1}{f}}{\frac{f}{2}} = 2.$$

4.8 The Aphakic Eye

1. In order to calculate the refraction of the cornea and the lens, we will use values for the indices of refraction and radii of curvature of the schematic eye according to Gullstrand (see Figure 4.4). ?
2. Many maladies of the eye require the removal of the lens, after which the *aphakic eye* remains. Does the image of an infinitely distant image appear on the retina, or somewhere else (at a certain distance away from the retina)? Where does the image of an object closer to the eye appear?

[index of refraction of air $n_0 = 1$; index of refraction for the cornea $n_K = 1.376$; index of refraction for the vitreous humor $n_W = 1.336$; index of refraction for the lens $n_L = 1.414$; radius of curvature of the apex of the cornea $r_1 = 7.7$ mm; radius of curvature of the cornea $r_2 = 6.8$ mm]

1. With the values given !

$$n_0 = 1$$
$$n_K = 1.376$$
$$n_W = 1.336$$
$$r_1 = 7.7\,\text{mm}$$
$$r_2 = 6.8\,\text{mm}$$

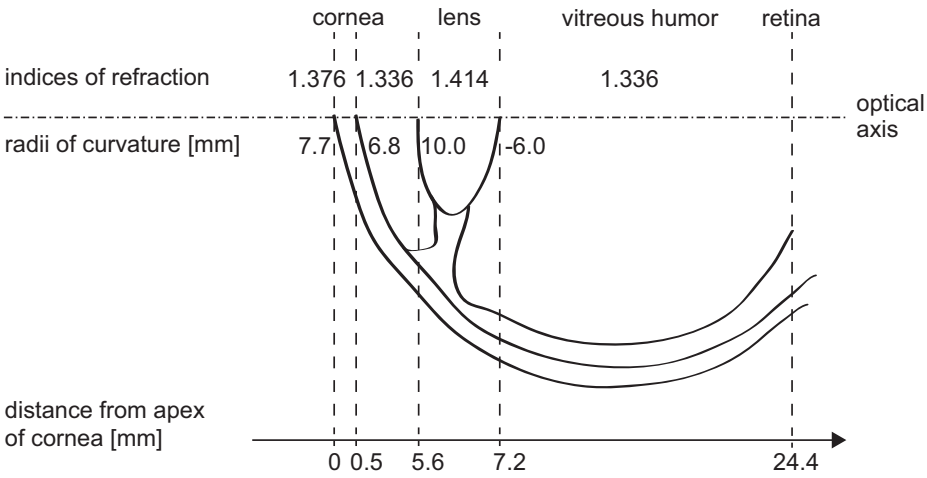

Fig. 4.4. Gullstrand's schematic eye.

we have, for refraction according to Gullstrand,

$$D_K = \frac{n_K}{f_K} = -\frac{n_0}{g} + \frac{n_W}{b}$$

$$D_K = \frac{n_K - n_0}{r_1} + \frac{n_W - n_K}{r_2}$$

$$D_K = \frac{1.3776 - 1}{7.7\ \text{mm}} + \frac{1.336 - 1.376}{6.8\ \text{mm}} = 0.04295\ {}^{1}/_{\text{mm}} = 42.95\ \text{dpt}.$$

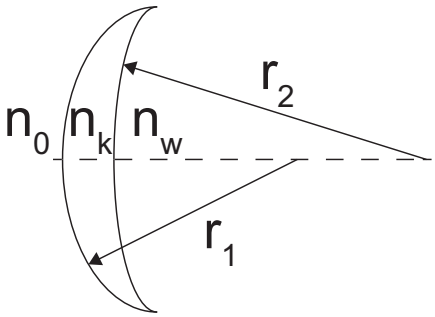

Fig. 4.5. Model of the cornea. n_i are the respective indices of refraction; r_i are the radii of curvature of the lens surfaces.

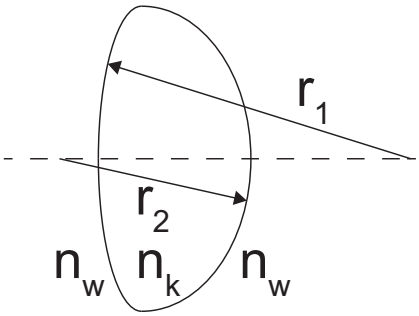

Fig. 4.6. Model of the lens. n_i are the respective indices of refraction; r_i are the radii of curvature of the lens surfaces.

2. We must take into account that the radius of curvature r_2 must be counted as negative. The refraction of the lens is therefore

$$D_L = \frac{n_L}{f_L} = \frac{n_L - n_W}{r_1} + \frac{n_W - n_L}{r_2}$$
$$D_L = \frac{1.414 - 1.336}{10\,\text{mm}} + \frac{1.336 - 1.414}{-6\,\text{mm}} = 0.0208\ {}^{1}/_{\text{mm}} = 20.8\,\text{dpt}.$$

In total, we have

$$D = D_K + D_L = 42.95\,\text{dpt} + 20.8\,\text{dpt} = 63.75\,\text{dpt}.$$

For an object infinitely far away ($g = \infty$),

$$b = f = f_K = \frac{n_K}{D_K} = \frac{1.376}{42.95\,\text{dpt}} = 32\,\text{mm}.$$

The image is 32 mm − 24.4 mm: 8 mm behind the retina (if more fluid were there). Closer objects would be resolved even further back.

4.9 Threshold of Hearing, and Thermal Motion in Comparison

?

We can compare the intensity of a sound wave at the threshold of hearing at $f = 1\,\text{kHz}$ with the intensity of a sound wave propagating in the eardrum, at $T = 20\,^{\circ}\text{C}$ and the same frequency. The sound wave at the threshold of hearing corresponds to a deflection amplitude $\chi_0 = 0.11$ Å which transports an energy of $k_B T$ per period. The surface area of the eardrum is $A = 0.5\,\text{cm}^2$. The speed of sound is $c = 330\ {}^{\text{m}}/_{\text{s}}$, and the density of the air is $\rho = 1.3\ {}^{\text{kg}}/_{\text{m}^3}$. If the pain threshold is at 120 dB, how much higher is the intensity in comparison to the threshold of hearing? By what factor do the deflection χ and pressure amplitude Δp vary?
[Note: the energy density of the sound wave is $W = \frac{1}{2}\rho\omega^2\chi^2$]

!

Due to thermal effects, the sound wave at frequency f has the intensity $I = \frac{P}{A} = \frac{3fk_BT}{2A}$. With $f = 1\,\text{kHz}$ and the values provided for $A = 0.5\,\text{cm}^2$ and $T = 293\,\text{K}$ the intensity is

$$I = 9.09 \cdot 10^{-14}\ {}^{\text{W}}/_{\text{m}^2}.$$

The intensity of a 1 kHz sinusoidal sound wave at the threshold of hearing is

$$I_0 = Wc = \frac{1}{2}\rho_L c\left(2\pi f\chi_0\right)^2 = 10^{-12}\ {}^{\text{W}}/_{\text{m}^2}.$$

The ratio to the threshold of hearing $({}^{I}/_{I_0})_H$ becomes

$$({}^{I}/_{I_0})_H = 9.09 \cdot 10^{-2}.$$

Therefore,

$$\begin{aligned} & I \propto \chi^2 \quad \text{and} \quad \chi \propto p \\ \rightarrow\ & I \propto p^2 \quad \text{and} \quad I \propto \Delta p^2 \end{aligned}$$

$$\begin{aligned} L &= 10 \log \left(I/I_0 \right) \\ &= 20 \log \left(\Delta p/\Delta p_0 \right) \\ &= 20 \log \left(\chi/\chi_0 \right). \end{aligned}$$

Therefore, we have

$$\begin{aligned} I/I_0 &= 10^{L/10} \\ \Delta p/\Delta p_0 = \chi/\chi_0 &= 10^{L/20}. \end{aligned}$$

As L has the value $L = L_S = 120\,\text{dB}$ at the pain threshold, we have the following relationships:

$$\begin{aligned} \left(I/I_0 \right)_S &= 10^{L_S/10} = 10^{12} \\ \left(\chi/\chi_0 \right)_S = \left(\Delta p/\Delta p_0 \right)_S &= 10^{L_S/20} = 10^6. \end{aligned}$$

4.10 Sound Propagation

? A mountain guide observes an avalanche at a distance. He perceives two noises, one after the other. One propagates through the air; the other, through the ground. Two seconds pass between the sounds. How far away did the avalanche occur if the speeds of sound in air and in the ground are $c = 330\ \text{m/s}$ and $c_G = 4{,}000\ \text{m/s}$ respectively?

! We have

$$c_G = \frac{s}{t} \qquad \text{and} \qquad c = \frac{s}{t + \Delta t}$$

with s as the path of the sound, t as the time between the avalanche and the arrival of the first sound, and Δt as the time between the first and second sounds. For s we have, from the second equation,

$$s = ct + c\Delta t.$$

Introducing t from the first equation, we have

$$s = \frac{c}{c_G} s + c\Delta t = \frac{c c_G}{c_G - c} \Delta t = \frac{330\ \text{m/s} \cdot 4{,}000\ \text{m/s}}{(4{,}000 - 330)\ \text{m/s}} 2\,\text{s} = 719\,\text{m}.$$

4.11 Loudspeakers

At full volume, a loudspeaker can produce sounds with frequencies from 30 Hz to 18 kHz with steady intensity; the maximum deviation from the average value of the sound level in this range is 3 dB. By what factor does the intensity change relative to the average value at maximum deviation? ?

Average intensity I_1 gives average sound level L_{I_1}. For I_2 we have !

$$L_{I_2} = L_{I_1} + 3\,\text{dB},$$

and

$$L_{I_2} - L_{I_1} = 10\,\log\frac{I_2}{I_0} - 10\,\log\frac{I_1}{I_0} = 10\,\log\frac{I_2}{I_1} = 3\ \text{dB}.$$

Therefore,

$$\log\frac{I_2}{I_1} = 0.3,$$

and

$$\frac{I_2}{I_1} = 10^{0.3} \approx 2.$$

±3 dB corresponds to a doubling – that is, a halving of the intensity.

4.12 Threshold of Hearing

Calculate the maximum displacement of air molecules in a sound wave of frequency 1 kHz at the threshold of hearing. ?
[threshold f hearing at 1 kHz : $10^{-12}\ \text{W/m}^2$]

With a sinusoidal waveform of frequency f we can write the displacement of the sound wave as !

$$\chi(x,t) = \chi_0\,\sin(\omega t - kx),$$

with χ_0 as the amplitude of the wave (and therefore as the maximum displacement), and $\omega = 2\pi f$. The velocity $v(x,t)$ of the particles can be written as a time-dependent derivative:

$$v(x,t) = \frac{\partial}{\partial t}\chi(x,t) = \chi_0\omega\cos(\omega t - kx).$$

The corresponding kinetic energy density is

$$w_{kin} = \frac{1}{2}\rho v^2 = \rho\chi_0^2\omega^2\cos^2(\omega t - kx),$$

with ρ as the density of the medium. We assume that the average density does not change significantly throughout the wave. At the threshold of hearing the amplitude is so small that this is a very reasonable assumption. The average density of the kinetic energy is given by the average value of $\langle\cos^2\rangle = \frac{1}{2}$. In addition, considering the

elastic energy that delivers the same contribution on average, the total energy density becomes

$$w = \rho\chi_0^2\omega^2.$$

The intensity of a wave is generally equal to the product of energy density and propagation velocity:

$$I = wc = c\rho\chi_0^2\omega^2.$$

Solving for χ_0, we have

$$\chi_0 = \frac{1}{\omega}\sqrt{\frac{2I}{\rho_0 c}} = \frac{1}{2\pi 10^3 \mathrm{s}^{-1}}\sqrt{\frac{2\cdot 10^{-12}}{1.3\,343}\frac{\mathrm{W m^3 s}}{\mathrm{m^2\,kg\,m}}} = 1.1\cdot 10^{-11}\mathrm{m}.$$

4.13 Sound Interference with Point Sources

? At an open-air concert, two subwoofers are placed next to the stage, at a distance of $d = 10$ m from one another, to amplify the bass. Where should someone who dislikes the bass stand? What about someone who prefers loud bass? Determine an expression that describes all maxima and minima of intensity in the audience (in Cartesian coordinates). The preferred locations for both groups of the public are on certain arrays of curves. What kind of curved form is appropriate?
[sound velocity in air $c = 330$ m/s; frequency of the bass $f = 68$ Hz]

! For wavelength λ we have

$$\lambda = \frac{c}{f} = \frac{330\ \mathrm{m/s}}{68\ \mathrm{Hz}} = 4.85\ \mathrm{m}.$$

The path difference Δl between the sound waves determines whether they interfere to produce a maximum or a minimum. If Δl is a multiple of the sound wavelength, a maximum is produced, and $\Delta l = n\lambda$ (with $n = 0, 1, 2, \ldots$). Minima occur at $\Delta l = (n+\frac{1}{2})\lambda$. Those audience members that prefer loud bass should stand on the lines of the maxima, and the others should stand at the minima. As all the points of these arrays of curves have the same difference in distance from two fixed points, we must be dealing with hyperbolas. As proof, consider a triangle with vertices at both loudspeakers $(-\frac{d}{2}, 0)$, $(\frac{d}{2}, 0)$ and in the middle of the audience (x, y). The two edges that do not run along the stage have length l_1 from $(-\frac{d}{2}, 0)$ to (x, y) and l_2 from $(\frac{d}{2}, 0)$ to (x, y). Therefore, for the amplitudes of the sound waves at (x, y) we have

$$l_1 = \sqrt{(d/2 + x)^2 + y^2} \qquad \text{and} \qquad l_2 = \sqrt{(d/2 - x)^2 + y^2}.$$

The path-length difference is therefore

$$\Delta l = \sqrt{(x - d/2)^2 + y^2} - \sqrt{(x + d/2)^2 + y^2}.$$

For the maxima,

$$\Delta l = \frac{2\pi}{k} n = \lambda n.$$

This equation can be written in the normal form

$$\frac{x^2}{a^2} - \frac{y^2}{b^2} = 1$$

of a hyperbola.

4.14 Echolocation

Echolocation is a form of sensory perception of certain animals, like bats. These animals emit sound waves that are reflected by obstacles. The reflected signal is recognized by the animal. The wave sent out by a bat for echolocation has a frequency of 50 kHz. What is its wavelength λ, and how long does it take for the bat to receive a signal reflected from an obstacle 20 m away?
[bulk modulus of air $k = 1.41 \cdot 10^5$ Pa; density of air $\rho = 1.3\ {}^{\mathrm{kg}}/_{\mathrm{m}^3}$]

For longitudinal waves, we have $c = \sqrt{\frac{k}{\rho}}$ for sound velocity. As such, c in the air becomes

$$c = \sqrt{\frac{1.41 \cdot 10^5\ {}^{\mathrm{N}}/_{\mathrm{m}^2}}{1.3\ {}^{\mathrm{kg}}/_{\mathrm{m}^3}}} = 329\ {}^{\mathrm{m}}/_{\mathrm{s}}.$$

Because $\lambda = \frac{c}{f}$, we have

$$\lambda = \frac{329\ {}^{\mathrm{m}}/_{\mathrm{s}}}{5 \cdot 10^4\ \mathrm{Hz}} = 6.6\ \mathrm{mm}.$$

The signal travels the distance s from the bat to the obstacle twice. It requires

$$T = \frac{2s}{c} = \frac{2 \cdot 20\ \mathrm{m}}{329\ {}^{\mathrm{m}}/_{\mathrm{s}}} = 0.12\ \mathrm{s}.$$

4.15 Impedance Matching

So that the sound waves that enter the ear are not too attenuated by the time they reach the inner ear, impedance matching occurs at the eardrum. The sound pressure at the oval window is raised by a factor α relative to that at the eardrum through the lever action of the malleus and incus. Calculate the improvement in transmission through this mechanism relative to the situation without impedance matching.

1. From the conservation of energy, expressed as $I_e = I_r + I_t$, as well as the continuity expression for the displacement, $\chi_e + \chi_r = \chi_t$ (see Figure 4.7) we can express transmission as $T := \frac{I_t}{I_e} = \frac{4Z_1Z_2}{(Z_1+Z_2)^2}$.

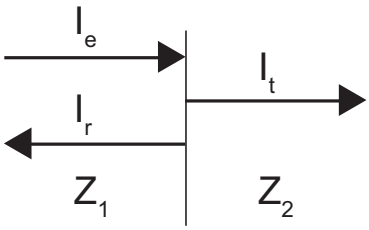

Fig. 4.7. In the region of the incident (e) and reflected (r) wave, impedance is Z_1, and in the region of the transmitted (t) wave it is Z_2.

2. Show that the sound pressure that proceeds from the oval window is raised by the factor $\alpha := \frac{F_1}{F_2} \cdot \frac{l_1}{l_2}$ relative to the sound pressure at the eardrum. $F_1 = 55\,\text{mm}^2$ is the surface area of the eardrum, which is connected to the handle of the malleus; $F_2 = 2.8\,\text{mm}^2$ is the surface area of the oval window, and $\frac{l_1}{l_2} = 1.3$ is the ratio of the lever arms of the incus and the handle of the malleus.
3. Correct the formula from Part 1 to take into account the amplification factor α. Note: the amplification factor changes the continuity expression for the displacement to $\chi_e + \chi_r = \alpha \cdot \chi_t$.
4. What percent of the intensity of the incident sound would be transmitted without impedance matching? By what percent does the transmission coefficient T change through impedance matching? For wave impedance of the air, we have $Z_1 = 414\,\text{kg/m}^2\text{s}$, and for that of the lymph fluid in the inner ear, we have $Z_2 = 10^5\,\text{kg/m}^2\text{s}$.

! 1. Continuity requirements for the intensity:

$$I_i = I_t + I_r.$$

With $Z = \rho_0 c$ and

$$I = \frac{1}{2}\rho_0 v_0^2 c = \frac{1}{2} Z \omega^2 \chi_0^2$$

we have

$$\frac{1}{2} Z_i \omega^2 \chi_e^2 = \frac{1}{2} Z_r \omega^2 \chi_r^2 + \frac{1}{2} Z_t \omega^2 \chi_t^2.$$

With $Z_e = Z_r = Z_1$ and $Z_t = Z_2$ we obtain by rearranging

$$Z_1 \left(\chi_e^2 - \chi_r^2 \right) = Z_2 \chi_t^2. \tag{4.3}$$

Together with the continuity requirement for the displacements

$$\chi_e + \chi_r = \chi_t$$

we obtain

$$\begin{aligned} Z_1\left(\chi_e^2 - \chi_r^2\right) &= Z_2\left(\chi_e + \chi_r\right)^2 \\ Z_1\left(\chi_e - \chi_r\right)\left(\chi_e + \chi_r\right) &= Z_2\left(\chi_e + \chi_r\right)^2 \\ Z_1\left(\chi_e - (\chi_t - \chi_e)\right) &= Z_2\chi_t \\ 2Z_1\chi_e &= (Z_1 + Z_2)\chi_t \\ \chi_t &= \frac{1}{Z_1 + Z_2} \cdot 2Z_1 \cdot \chi_i. \end{aligned}$$

For transmitted intensity, it follows that

$$\begin{aligned} I_t &= \frac{1}{2}Z_2\omega^2\chi_t^2 = \frac{1}{2}Z_2\omega^2\frac{4Z_1^2\chi_e^2}{\left(Z_1 + Z_2\right)^2} \\ &= \frac{1}{2}Z_1\omega^2\chi_e^2 \cdot \frac{4Z_1Z_2}{\left(Z_1 + Z_2\right)^2} = I_i \cdot \frac{4\,Z_1Z_2}{\left(Z_1 + Z_2\right)^2}. \end{aligned}$$

2. The force on the eardrum is

$$F_1 = \Delta p_e \cdot A_1$$

and on the oval window in the middle ear

$$F_2 = \Delta p_i \cdot A_2,$$

where Δp_e and Δp_i refer to the corresponding pressure amplitudes. The auditory ossicles transform the forces into torques. With lever arms l_1 and l_2 we have

$$\begin{aligned} F_1 l_1 &= F_2 l_2 \\ \Delta p_e\, A_1\, l_1 &= \Delta p_i\, A_2\, l_2. \end{aligned}$$

Solving for Δp_i we obtain the pressure at the oval window:

$$\Delta p_i = \Delta p_e \frac{A_1}{A_2}\frac{l_1}{l_2} = \alpha \cdot \Delta p_e.$$

The amplifying factor α by which the sound pressure is increased is

$$\alpha = \frac{55}{2.8} \cdot 1.3 = 25.5.$$

3. The solution method is like that in (a), but this time, the amplifying factor α is considered for the displacement. Its continuity condition is

$$\chi_e + \chi_r = \alpha \cdot \chi_t.$$

Substituting into (4.3) yields

$$\begin{aligned} Z_1\left(\chi_e - \chi_r\right)\left(\chi_e + \chi_r\right) &= Z_2\frac{1}{\alpha^2}\left(\chi_e + \chi_r\right)^2 \\ Z_1\left(2\chi_e - \alpha \cdot \chi_t\right) &= Z_2\frac{1}{\alpha^2} \cdot \alpha\chi_t \\ 2Z_1\chi_e &= \chi_t\left\{\frac{Z_2}{\alpha} + \alpha Z_1\right\} \end{aligned}$$

and therefore,

$$\chi_t = \frac{2Z_1\alpha}{\{Z_2 + \alpha^2 Z_1\}} \cdot \chi_e.$$

Substituting again into the equation for transmitted intensity, we have

$$I_t = \frac{1}{2} Z_2 \omega^2 \chi_t^2 = \frac{1}{2} Z_2 \omega^2 \chi_e^2 \frac{4Z_1^2\alpha^2}{(Z_2 + \alpha^2 Z_1)^2}$$

$$= I_e \frac{4Z_1 Z_2 \cdot \alpha^2}{(Z_2 + \alpha^2 Z_1)^2}.$$

4. Without impedance matching, only

$$\frac{I_t}{I_e} = \frac{4 \cdot 414 \cdot 10^5}{(414 + 10^5)^2} = 0.016 = 1.6\,\%$$

of the intensity would be transmitted. Impedance matching increases this value by

$$\frac{I_t}{I_e} = \frac{4 \cdot 414 \cdot 10^5 \cdot (25.5)^2}{(414 \cdot (25/5)^2 + 10^5)^2} = 0.79 = 79\,\%.$$

In actuality, this value is between 40 % and 60 %.

4.16 Acoustic Pain Threshold

? If a jet 30 m away starts up, the sound level is $L = 140$ dB SPL – above the pain threshold. Is this pain the same that one would experience if one were to dive without compensating for pressure (e.g., by swallowing)? To answer this question, calculate the depth at which the incremental pressure in the water corresponds to the effective value of sound pressure of the jet at startup.

! Sound level L is a logarithmic measure of sound pressure relative to $p_0 = 20 \cdot 10^{-6}$ Pa

$$L := 20 \cdot \log_{10}\left(\frac{\Delta p_{\text{eff}}}{20 \cdot 10^{-6}\,\text{Pa}}\right).$$

The effective value of the sound pressure at sound level 140 dB is therefore

$$\Delta p_{\text{eff}} = p_0 \cdot 10^{\frac{L}{20}} = 20 \cdot 10^{-6}\,\text{Pa} \cdot 10^7 = 200\,\text{Pa}.$$

At water depth h we have pressure $p_w = \rho g h$. The pressure required is therefore reached at a depth of

$$h = \frac{p_w}{\rho g} = \frac{\Delta p_{\text{eff}}}{\rho g} = \frac{200\,\text{Pa}}{10^3\,\text{kg/m}^3 \cdot 9.81\,\text{m/s}^2} = 20.4\,\text{mm}.$$

The sound pressure at the pain threshold corresponds to the pressure at water depth 2 cm. As we do not experience any pain in water at this depth, this is not the cause of pain beyond the pain threshold.

5 Electric Currents, Fields, and Potential

Bioelectric signals originate in potential differences between the interiors and exteriors of biological cells. These differences arise due to differing ion concentrations. The lipid bilayer of a cell is only a few nanometers thick, and is electrically insulating. As such, capacitance is very high, typically on the order of magnitude of $1\,\frac{\mu F}{cm^2}$. The membranes of muscle and nerve cells contain proteins that create important ion channels between the tails and heads of the lipid bilayer. The permeability of these channels to ions like K^+, Na^+, Ca^{2+}, and Cl^- can be controlled. In addition, there are other selective channels for certain types of ions. Transport through these channels occurs either due to electrostatic forces, or through diffusion due to concentration gradients. There are also protein structures – known as ion pumps – that can pump ions against the direction of passive transport, from the interior to the exterior or vice versa. Energy must be consumed to do so, while passive transport occurs on its own and does not require additional energy. There are also proteins that function as gatekeepers and allow or prevent passive transport. The most import ion pumps are the Na^+/K^+ pumps, which continuously transport potassium ions into the interior of cells and deliver sodium ions to the exterior. The concentration of potassium ions within the cell is notably higher, while for sodium ions, the situation is reversed. Ultimately, all of these processes give rise to the resting membrane potential that characterizes the quiescent state of a cell. Na^+, K^+, and Cl^- are primarily responsible for the resting membrane potential; their concentrations can differ by a factor of 10 to 30. The potential difference ΔU can be calculated using the Goldmann equation:

$$\Delta U = \frac{k_B T}{e} \cdot \ln\left(\frac{P_K c_K^e + P_{Na} c_{Na}^e + P_{Cl} c_{Cl}^i}{P_K c_K^i + P_{Na} c_{Na}^i + P_{Cl} c_{Cl}^e}\right).$$

The weighting factors P_i are designated motility or permeability. The superscript indexes e and i signify whether the respective value corresponds to the exterior or the interior of the cell. Because the motility of a potassium ion is roughly 30 times greater than that of a sodium ion, the influence of the K^+ ions is usually dominant.

The permeability of cells can be influenced by external factors, like electric fields (conductive stimulation) or the presence of certain chemical messengers (non-conductive stimulation). When the ion channels open, ion motility through the channels rises to such an extent that the mechanisms of passive transport overwhelm the active pumping mechanisms. Consequentially, resting potential rises rapidly. Generally, the Na^+ channels open more quickly than the K^+ channels, which can lead to a short-term "overshoot" of the membrane potential into positive territory. After this rapid depolarization of the cell, a state of equilibrium is restored again by the ion pumps.

The stimulation of a cell can be transmitted by nerve fibers. There are two types of stimulus conduction: continuous and saltatory. If the nerve fibers do not have a myelin sheath, current flow occurs continuously in the immediate environment. Myelinated

nerve fibers, on the other hand, are encased in an insulating lipid layer – the myelin sheath. At intervals of a few millimeters, these are interrupted by nodes of Ranvier (sheath gaps); the potential change jumps from one gap to the next, and is therefore substantially faster than continuous stimulus conduction.

A cell specialized for stimulus conduction is called a nerve cell (neuron). These cells can be separated into three segments: the dendrites, which serve as receptors, the neurite (axon and nerve fibers), which function as effectors, and the perikaryon (soma), which, as the cell body, forms the central region for cell metabolism. In the central nervous system the axons are generally bound together with bundles of fibers; in the peripheral nervous system, to nerve fibers and nerves. The nervous system is tasked with transmitting information as a sequence of action potentials. In order to do this, the information must be transmitted to other neurons. This transmission occurs through structures that are generally known as synapses. For electric synapses, stimulus transfer occurs through tunnel-like connections between the synapses; for chemical synapses, stimuli are transferred with the assistance of neurotransmitters across gaps. The sources of electromagnetic fields that arise along the axons can be modeled as electric quadrupoles. The electric processes behind the synapses can be described as electric dipoles. As signals from this kind of source fall off very quickly as distance from the source increases, and as they are generally stochastically distributed, these signals can only be measured when they add up due to anatomic conditions. If, for example, 10^5 nerve cells in one square millimeter of the cerebral cortex fire simultaneously, electric potentials of only around 10 μV (which can be seen using an EEG (electroencephalogram)), or magnetic flux densities of around 100 fT, arise at the scalp. In comparison, the electric depolarization of the heart leads to a signals a hundred times greater as measured by an EKG (electrocardiogram).

Because the four chambers of the heart (right and left atrium and ventricle) work together in a coordinated manner, there is a nervous cardiac conduction system in the heart in addition to the cardiac muscle cells (myocardium). The sinoatrial node works largely autonomously, and is both the control center and the origin of impulses. The release of an impulse can be influenced from the central nervous system through the sympathetic and parasympathetic nervous systems. The impulse spreads from the sinoatrial node to the neighboring cardiomyocytes of the atria, and after around 40 milliseconds, the impulse reaches the atrioventricular (AV) node in the center of the heart. The AV node delivers the impulse through the bundle of His, which transmits it along both of its branches to the Purkinje fibers. The impulse progresses relatively quickly through these both ventricles. There, impulse transfer slows back down to normal speed due to the absence of specialized cells.

Using an electrocardiogram (EKG) we can observe this transmission of the electrical impulse. Electric potentials, weakened across the extracellular fluid, are measured on the surface of the body. These potentials are roughly in the range of a millivolt (for which there are standard derivations). The most recognizable EKG signals are found when the lead electrodes are attached to the right forearm (–) and the left foot (+). A

grounding electrode is attached to the right foot in order to suppress external perturbations. In addition to this normal EKG, a vectorcardiogram can also be produced. Each cell stimulated functions as an electric dipole, and the vector sum of all cells stimulated at a point in time yields the resulting electric dipole (also termed the integral vector or cardiac vector). If multiple normal EKGs are combined, the position of this cardiac vector can be followed in time. The direction of the largest cardiac vector (the R wave in the EKG) defines the electric axis of the heart. Generally, this corresponds with the heart's anatomical condition. As such, the condition of the heart when altered by illness in a characteristic way can be determined.

5.1 Nerve Conduction in the Giant Axons of Squid

?

The mechanism of nerve stimulation and conduction has been investigated in the giant axons of squid. The diameter of these cylindrical giant axons is $d = 0.5\,\text{mm}$. The interior of an axon, the axoplasm, can be considered as a passive electrical conductor and an ion reservoir. The concentrations of sodium and potassium ions in the axoplasm are $c^i_{\text{Na}} = 50\,\text{mol/dm}^3\ \text{Na}^+$ and $c^i_{\text{K}} = 400\,\text{mol/dm}^3\ \text{K}^+$, and in the extracellular medium $c^e_{\text{Na}} = 460\,\text{mol/dm}^3\ \text{Na}^+$ and $c^e_{\text{K}} = 10\,\text{mol/dm}^3\ \text{K}^+$. Stimulation takes place principally at the nerve membrane.

We can use the Goldman equation to find the solution:

$$\Delta U = \frac{kT}{e} \ln\left(\frac{p_{\text{K}} c^e_{\text{K}} + p_{\text{Na}} c^e_{\text{Na}}}{p_{\text{K}} c^i_{\text{K}} + p_{\text{Na}} c^i_{\text{Na}}}\right).$$

1. Measurements of isotope flow gave the permeability ratio (relative motility) $\frac{P_{\text{K}}}{P_{\text{Na}}} = 15$. What is the resting potential? ($T = 300\,\text{K}$)
2. For a passive cable, voltage U_0 applied at one end drops off exponentially with length, $U = U_0 e^{-x/l}$, with decay distance $l = \sqrt{\frac{r R_m}{2 R_i}}$. What percent of an applied voltage U_0 is still measurable at the end of a $l = 1\,\text{cm}$ giant axon if it is treated as a passive cable? The specific resistance of the axoplasm is $R_i = 30\,\Omega\text{m}$, and the specific resistance of the sheath is $R_m = 700\,\Omega\,\text{cm}^2$.

!

1. Here, the Goldmann equation is

$$\begin{aligned}\Delta U &= \frac{kT}{e} \ln\left(\frac{p_{\text{K}} c^e_{\text{K}} + p_{\text{Na}} c^e_{\text{Na}}}{p_{\text{K}} c^i_{\text{K}} + p_{\text{Na}} c^i_{\text{Na}}}\right) = \frac{kT}{e} \ln\left(\frac{c^e_{\text{Na}} + \frac{p_{\text{K}}}{p_{\text{Na}}} c^e_{\text{K}}}{c^i_{\text{Na}} + \frac{p_{\text{K}}}{p_{\text{Na}}} c^i_{\text{K}}}\right) \\ &= \frac{1.38 \cdot 10^{-23}\,\text{J/K} \cdot 300\,\text{K}}{1.6 \cdot 10^{-19}\,\text{C}} \cdot \ln\left(\frac{460\,\text{mol/dm}^3 + 15 \cdot 10\,\text{mol/dm}^3}{50\,\text{mol/dm}^3 + 15 \cdot 400\,\text{mol/dm}^3}\right) \\ &= -59.4\,\text{mV}.\end{aligned}$$

2. The decay distance is

$$l = \sqrt{\frac{rR_m}{2R_i}} = \sqrt{\frac{0.25 \cdot 10^{-3}\text{m} \cdot 700 \cdot 10^{-4}\ \Omega\text{m}^2}{2 \cdot 30\ \Omega\text{m}}} = 5.4 \cdot 10^{-4}\text{m}.$$

and therefore,

$$\frac{U\,(x = 0.01\text{ m})}{U_0} = e^{-\frac{0.01\text{ m}}{5.4 \cdot 10^{-4}\text{m}}} = 9 \cdot 10^{-9} = 9 \cdot 10^{-7}\%.$$

5.2 Nerve Stimulation

? Nerve stimulation changes the difference in potential across the neural pathway by $\Delta U = 100\,\text{mV}$, principally due to an influx of Na^+ ions into the nerve fibers. How many Na^+ ions N_{Na^+} per unit area of the cell membrane are necessary to charge a membrane with capacitance $C = 1\,\mu\text{F/cm}^2$ by the amount ΔU?

! The necessary charge is

$$Q^+ = C \cdot \Delta U = 10^{-6}\,\text{F/cm}^2 \cdot 0.1\,\text{V} = 10^{-7}\,\text{C/cm}^2,$$

corresponding to

$$N_{Na^+} = \frac{Q^+}{e} = 6.25 \cdot 10^{11}\,\text{ions/cm}^2.$$

5.3 Electrical Model of a Cell Membrane

? Consider a piece cut from the cell membrane. Boundary effects should be ignored. The cell membrane has a specific conductivity of $\sigma_M = 10^{-10}(\Omega\,\text{cm})^{-1}$, dielectric constant $\varepsilon_M = 8$, and thickness $d_M = 7.5\,\text{nm}$. On both sides of the membrane are two boundary layers with equal specific conductivity $\sigma_P = \sigma_I = 10^{-2}(\Omega\,\text{cm})^{-1}$. The thickness of these layers is $d_P = 50\,\text{nm}$ and $d_I = 100\,\text{nm}$ respectively, and their capacitance is negligible.

1. What is the simplest possible equivalent circuit diagram that captures these passive electrical characteristics?
2. What are the resistance and capacitance that occur in this equivalent circuit diagram if the area of the membrane surface considered is $A = 1\,\mu\text{m}^2$?

1. Equivalent electrical circuit diagram:

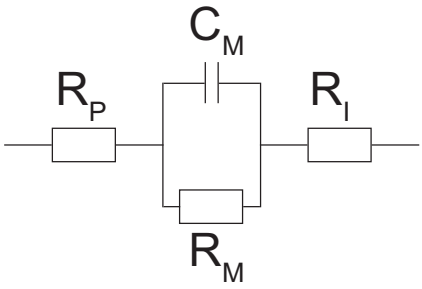

Fig. 5.1. R_P is in series with $(C_M||R_M)$ and R_I.

2. Generally,

$$R = \frac{\rho l}{A} = \frac{l}{\sigma A}.$$

For the individual resistances, considering $\frac{1}{\Omega\,\mathrm{cm}} = 10^2 \frac{1}{\Omega\mathrm{m}}$ and $\mathrm{A} = 1\,\mu\mathrm{m}^2 = 10^{-12}\,\mathrm{m}^2$, we have:

$$R_P = \frac{d_P}{A\sigma_P} = \frac{50 \cdot 10^{-9}\ \mathrm{m}}{10^{-12}\ \mathrm{m}^2 \cdot {}^1/_{\Omega\mathrm{m}}} = 5 \cdot 10^4 \Omega$$

$$R_I = \frac{d_I}{A\sigma_I} = \frac{100 \cdot 10^{-9}\mathrm{m}}{10^{-12}\ \mathrm{m}^2 \cdot {}^1/_{\Omega\mathrm{m}}} = 1 \cdot 10^5 \Omega$$

$$R_M = \frac{d_M}{A\sigma_M} = \frac{7.5 \cdot 10^{-9}\ \mathrm{m}}{10^{-12}\ \mathrm{m}^2 \cdot 10^{-8}\ {}^1/_{\Omega\mathrm{m}}} = 7.5 \cdot 10^{11}\ \Omega.$$

For the capacitance, we use the assumption of a plate capacitor:

$$C_M = \varepsilon_0 \varepsilon_r \frac{A}{d_M} = 8.854 \cdot 10^{-12}\ \mathrm{F/m} \cdot 8 \cdot \frac{10^{-12}\ \mathrm{m}^2}{7.5 \cdot 10^{-9}\ \mathrm{m}} = 9.44 \cdot 10^{-15}\ \mathrm{F}.$$

5.4 Measurement of Cell Membrane Potentials

At a nerve cell, the membrane potential U_M of a cell membrane in the quiescent state shall be measured (see Diagram 5.2).

1. What is the relationship of the potential measured, U_x, to the membrane potential U_M, if $R_i = 20\,\mathrm{k}\Omega$, $R_E = 50\,\mathrm{k}\Omega$, and $R_{i,V} = 1\,\mathrm{M}\Omega$?
2. What is $\frac{U_x}{U_M}$ if $R_E \gg R_{i,V}$?
3. What is U_M in case (1) if the reading from the measurement instrument is 40 mV?

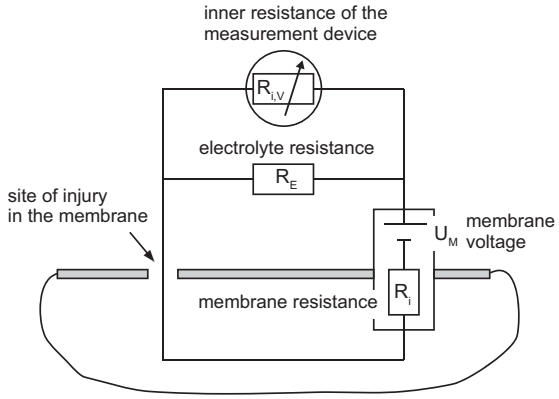

Fig. 5.2. Measurement of cell membrane potentials.

! 1. From the equivalent circuit diagram we have

$$R_x = R_E || R_{i,V} = \frac{1}{\frac{1}{R_E} + \frac{1}{R_{i,V}}} = \frac{R_E R_{i,V}}{R_E + R_{i,V}} = \frac{50\,\text{k}\Omega \cdot 1{,}000\,\text{k}\Omega}{50\,\text{k}\Omega + 1{,}000\,\text{k}\Omega} = 47.6\,\text{k}\Omega.$$

For the potentials,

$$\frac{U_x}{U_M} = \frac{U_x}{U_i + U_x} = \frac{R_x I}{(R_i + R_x) I} = \frac{47.6\,\text{k}\Omega}{20\,\text{k}\Omega + 47.6\,\text{k}\Omega} = 0.704.$$

2. If $R_E \gg R_{i,V}$, then $R_x \approx R_{i,V}$ and therefore we have

$$\frac{U_x}{U_M} \approx \frac{R_{i,V}}{R_i + R_{i,V}} = \frac{10^3\text{k}\Omega}{20\,\text{k}\Omega + 10^3\text{k}\Omega} = 0.98.$$

3. The membrane potential U_M with measured potential $U_x = 40$ mV is

$$U_M = \frac{U_x}{0.704} = \frac{40\,\text{mV}}{0.704} = 56.82\,\text{mV}.$$

5.5 EKG and Cardiac Dipole

? In the diagram, the equilateral Einthoven triangle and the corresponding standard leads I, II, and III for the EKG are portrayed. $\vec{M}$ is the dipole component of the cardiac vector in the plane of the equilateral triangle that is formed by the lead points R, L, and F. A planar coordinate system (r, θ) is assumed, with the origin at the center of the triangle, where direction $\theta = 0$ corresponds to the direction of the cardiac dipole (this is shown in Figure 5.3). Under this configuration, we have for the dipole potential

$$\varphi_D = \frac{|\vec{M}| \cos\theta}{4\pi\varepsilon_r\varepsilon_0 r^2} = K \cos\theta.$$

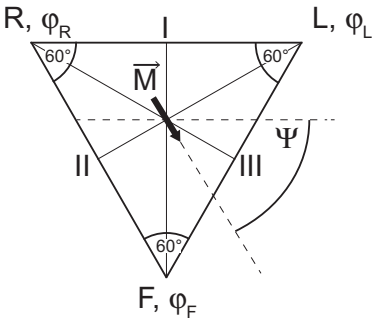

Fig. 5.3. EKG and cardiac dipole. I is the lead between the right arm and the left arm, II is between the right arm and the left leg, and III is between the left arm and the left leg. The direction $\theta = 0$ is, in this diagram, equal to that of the cardiac dipole $\vec{M}$.

1. Calculate the three potentials U_I, U_{II}, U_{III} as a function of Ψ (see diagram).
2. How do potentials $|U_I| : |U_{II}|$ behave, with the standard leads, for a normal position with $\Psi = 60^\circ$ and a left position with $\Psi = -45^\circ$?

1. For the angle used in the solution, consider Figure 5.4. From these, we have:

$$\varphi_D(\theta) = K \cos\theta.$$

$$\cos(\theta_L) = \cos(360^\circ - \Psi - \alpha) = \cos(-\Psi - \alpha) = \cos(\Psi + \alpha)$$

$$2\alpha + \beta = 180^\circ \; ; \; \beta/2 = 60^\circ \; ; \; \Rightarrow \alpha = 30^\circ$$

$$\theta_R = 360^\circ - \Psi - (\alpha + \beta) = 360^\circ - \Psi - 150^\circ.$$

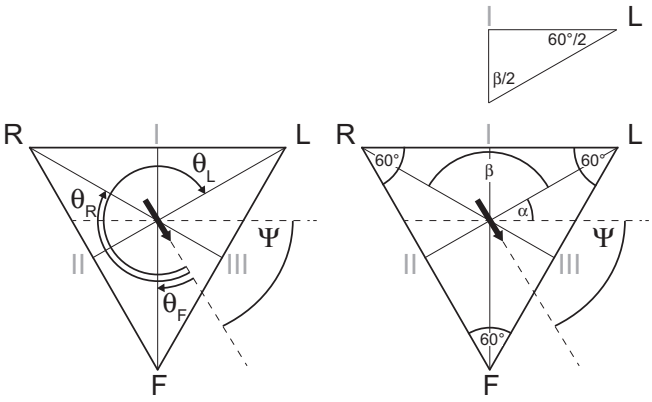

Fig. 5.4. On the right, the angles α and β used in the solution are indicated; on the left are the angles used for the calculation of the dipole potentials θ_F, θ_R, and θ_L.

For potential U_I:

$$
\begin{aligned}
U_I &= \varphi_L - \varphi_R \\
U_I &= K\cos\theta_L - K\cos\theta_R \\
U_I &= K\cos(\Psi + 30^\circ) - K\cos(\Psi + 150^\circ) \\
U_I &= K\left\{\cos\Psi\cos 30^\circ - \sin\Psi\sin 30^\circ - \cos\Psi\cos 150^\circ + \sin\Psi\sin 150^\circ\right\} \\
U_I &= K\left\{\frac{\sqrt{3}}{2}\cos\Psi - \frac{1}{2}\sin\Psi - \left(-\frac{\sqrt{3}}{2}\right)\cos\Psi + \frac{1}{2}\sin\Psi\right\} \\
U_I &= K\sqrt{3}\cos\Psi.
\end{aligned}
$$

Analogously, we have

$$
\begin{aligned}
U_{II} &= K\left\{\cos(\Psi + 150^\circ) - \cos(\Psi + 270^\circ)\right\} \\
U_{II} &= -K\left\{\frac{\sqrt{3}}{2}\cos\Psi + \frac{3}{2}\sin\Psi\right\}
\end{aligned}
$$

and

$$
\begin{aligned}
U_{III} &= K\left\{\cos(\Psi + 270^\circ) - \cos(\Psi + 30^\circ)\right\} \\
U_{III} &= K\left\{\frac{3}{2}\sin\Psi - \frac{\sqrt{3}}{2}\cos\Psi\right\}.
\end{aligned}
$$

The sum of all three parts is therefore

$$
\begin{aligned}
U_I + U_{II} + U_{III} &= K\left\{K\sqrt{3}\cos\Psi - \frac{\sqrt{3}}{2}\cos\Psi - \frac{3}{2}\sin\Psi + \frac{3}{2}\sin\Psi - \frac{\sqrt{3}}{2}\cos\Psi\right\} \\
&= 0.
\end{aligned}
$$

2. From the above, we have

$$
\frac{|U_I|}{|U_{II}|} = \frac{|K\sqrt{3}\cos\Psi|}{|-K\left(\frac{\sqrt{3}}{2}\cos\Psi + \frac{3}{2}\sin\Psi\right)|}.
$$

Normal position

$$
\frac{|U_I|}{|U_{II}|} = \frac{\sqrt{3}\cos\ 60^\circ}{\frac{\sqrt{3}}{2}\cos\ 60^\circ + \frac{3}{2}\sin\ 60^\circ} = \frac{1}{2}.
$$

Left position

$$
\frac{|U_I|}{|U_{II}|} = \frac{\sqrt{3}\cos\left(-45^\circ\right)}{\frac{\sqrt{3}}{2}\cos\left(-45^\circ\right) + \frac{3}{2}\sin\left(-45^\circ\right)} = \frac{2\sqrt{3}}{|\sqrt{3}\cdot -3|} = 2.73.
$$

Cabrera circle: the electrical cardiac axes correspond to the anatomical cardiac axes; therefore, the condition of the heart can be determined by using a vectorcardiogram. Certain illnesses are connected to atypical heart conditions.

5.6 Electric Shock

If more than 100 mA pass through a person's chest, cardiac death is the most likely result. ?

1. Estimate the resistance of the human body from hand to hand by calculating the conductivity of a "physiological solution" of 9 g NaCl in a liter of water. (ion motility in an aqueous solution at 18°C: $\mu^+(\mathrm{Na}) = 4.6\cdot10^{-8}\,\mathrm{m^2/Vs}$; $\mu^-(\mathrm{Cl}) = 6.85\cdot10^{-8}\,\mathrm{m^2/Vs}$.) The distance from hand to hand is $l = 1.5$ m, and the cross section at the narrowest point is $A = 10\,\mathrm{cm}^2$.
2. What potentials can become dangerous for a person?
3. Why are people often advised to keep one hand in their pocket (or on their back) when working on open electric devices?

1. The conductivity σ is the relationship of current density j and electric field strength E. The current density is the product of the volume charge density ρ and the average velocity $\bar{v}$ of the charge carrier: !

$$\sigma = \frac{j}{E} = \frac{\rho\bar{v}}{E}.$$

The average velocity, in turn, is the product of the total ion motility μ_{tot} and the field strength. The total ion motility is the sum over the contributions of the individual ions; this sum is itself dependent on charge Z, particle density n, and motility μ:

$$\sigma = \frac{\rho\cdot\mu_{\mathrm{tot}}E}{E} = \rho\mu_{\mathrm{tot}} = \left(Z_+n_+\mu_+ + Z_-n_-\mu_-\right).$$

When NaCl dissolves in water, the quantity and charge of both ions are numerically equal in the solution:

$$n_+ = n_- =: n\,; \quad Z_+ = Z_- =: e.$$

Therefore, we have conductivity

$$\sigma = ne\left(\mu_+ + \mu_-\right)$$

In order to determine the number of charge carriers from the given mass m and the volume of the solution V, we will use the relative molar masses m_{mol} of sodium and chlorine, and calculate, using the Avogadro constant N_A:

$$m = N_{\mathrm{mol}}\cdot m_{\mathrm{mol}} = N_{\mathrm{mol}}\cdot\left(m_{\mathrm{mol}}(\mathrm{Na}) + m_{\mathrm{mol}}(\mathrm{Cl})\right)$$

$$N_{\mathrm{mol}}(\mathrm{NaCl}) = \frac{9\,\mathrm{g}}{22.990\,\mathrm{g/mol} + 35.453\,\mathrm{g/mol}} = 0.154\,\mathrm{mol}$$

$$n = \frac{N}{V} = \frac{N_AN_{\mathrm{mol}}}{V} = \frac{6.022\cdot10^{23}\,\mathrm{1/mol}\cdot0.154\,\mathrm{mol}}{10^{-3}\mathrm{m}^3} = 9.27\cdot10^{25}\mathrm{m}^{-3}$$

$$\sigma = 9.27\cdot10^{25}\mathrm{m}^{-3}\cdot1.6\cdot10^{-19}\mathrm{C}\cdot(4.6+6.85)\cdot10^{-8}\,\mathrm{m^2/Vs} = 1.698\,\mathrm{1/\Omega m}.$$

Therefore, resistance is

$$R = \frac{\rho l}{A} = \frac{l}{\sigma A} = \frac{1.5\ \text{m}}{1.698\ {}^{1}/_{\Omega\text{m}} \cdot 10^{-3}\text{m}^2} = 883\ \Omega.$$

2. When one's hands are wet, contact resistance can be ignored. The potentials that are dangerous for people are, then, relatively small:

$$U_{\text{crit}} = RI_{\text{crit}} = 883\ \Omega \cdot 0.1\ \text{A} = 88.3\ \text{V}.$$

3. If one is working on an open electrical device with both hands, current can pass through the heart if an electric shock occurs. That can lead to dangerous heart flutters. If one only touches the device with one hand, the danger is lessened.

6 Heat

Biothermics deals with the thermodynamic processes of living organisms in interaction with their environments. A healthy person generates a nearly constant amount of heat over time, which must be dissipated so that body temperature remains constant. For a healthy person, the normal internal body temperature is $T_i = 37.2\,^{\circ}\mathrm{C}$ with variation ΔT_i within small bounds ($\Delta T_i = \pm 0.5\,^{\circ}\mathrm{C}$). Inflammation in the body can cause elevated temperatures. The upper bound of survivable temperature is $42.8\,^{\circ}\mathrm{C}$, as at that point, proteins denature. The lower bound is $27\,^{\circ}\mathrm{C}$. The body attempts to maintain the desired core temperature as long as possible (for example, by losing heat in the case of a fever or physical exertion through increased blood circulation and sweating; in the case of hypothermia, by retaining heat through reduced circulation in the skin). Under normal conditions, the temperature of the surrounding environment T_a is lower than the internal temperature of the body T_i. As such, there is a natural flow of heat out of the body's core into the external environment. Additional sources of heat can also develop in the body through radiation or laser therapy. The heat created by these sources over time must be dissipated, too. The transfer mechanisms available to do so are thermal conduction and convection. Both heat transport phenomena, conduction and convection, are dependent on physical matter. While in thermal conduction a molecular process occurs in which the exterior of the matter remains at rest, convection is a macroscopic process in which the movement of the matter itself does the work of heat transfer.

In thermal conduction, the quantity of heat dQ that is transferred over time dt through surface A is designated heat flux density $\dot{q} = \frac{dQ}{A\,dt}$. This term can be related to the temperature gradient $\vec{\nabla}T$ using the thermal conduction coefficient λ, yielding $\dot{q} = -\lambda\vec{\nabla}T$ (Fourier's approach). This leads to the general thermal conduction equation

$$\frac{\partial T}{\partial t} = \frac{\lambda}{\rho c_W}\nabla^2 T.$$

Here, ρ is the density of the thermoconductive body tissue, and c_W is its specific heat. In the general case of the body under stationary conditions, the thermal conduction equation can be solved as a boundary value problem. Considering n layers of tissue from the center of the body to the skin, with thermal conduction coefficient λ_j, layer density δ_j, and skin temperature T_H, we find for heat flux density $\dot{q}$ the relationship

$$\dot{q} = \frac{T_i - T_H}{\sum\limits_n \frac{\delta_j}{\lambda_j}}.$$

Heat convection occurs only in moving fluids; in organisms, these are primarily blood and air. The individual particles of fluid transport not only mass, but also the enthalpy that they contain. At phase boundary layers, like at the surface of the skin, both transfer mechanisms – conduction and convection – occur. This is termed heat transfer.

This process is very complex, and is described as $\dot{q} = \alpha \Delta T$ with heat transfer coefficient α and temperature difference $\Delta T = T_H - T_a$. The entire heat transfer phenomenon is captured in the heat transfer coefficient α. It is not a pure quantity like λ, but a function of the material characteristics of the fluid, the geometry of the phase boundary layer, and the fluid dynamics and thermal relationships of the system. Using it, for example, the sensation of temperature experienced by the skin (termed sensible heat) can be determined from the value of α. In a subzero temperature environment, everyone feels colder when the wind is blowing than when it is not. Due to the large number of variables that determine α, it is wise to use a dimensionless characterization to address the problem according to the laws of analogy. Under these conditions there arises a dependency in the form $Nu = f\,(Re, Pr, Gr)$ with Nusselt number $Nu = \frac{\alpha l}{\lambda}$, Reynold number $Re = \frac{w l \rho}{\eta}$, Prandtl number $Pr = \frac{c_W \eta}{\lambda}$, and Grashof number $Gr = \frac{g \beta \rho^2 d^3 \Delta T}{\eta^2}$. The quantity l is the characteristic geometric length; λ is the thermal conductivity, ρ the density, η the dynamic viscosity, c_W the specific heat, and β the coefficient of volume expansion; λ, ρ, η, c_W, and β are all related to the fluid and represent its material characteristics. The flow velocity w describes the condition of the flow, and the temperature difference $\Delta T = T_H - T_a$ describes the thermal environment. In the literature there are a range of criteria-dependent equations for this function that are applicable in many different circumstances. In addition to these mechanisms, heat transfer can also occur through thermal radiation. This radiation requires no transmission medium, and follows the Stefan-Bolzmann Law $\dot{q} = C\,T^4$ with radiation constant C and absolute temperature of the radiating surface T. The body's own thermal radiation does not play a significant roll in dissipating heat from its core. However, the thermal radiation that originates with sun – especially infrared radiation – is quite important. It plays a crucial role in determining the temperature of the surroundings, upon which the magnitude of heat loss is dependent.

6.1 Skiwear

? To protect himself from the cold, a skier wears a $s = 4\,\text{cm}$-thick down parka. The parka has an inner and outer surface area of $A_D = 2\,\text{m}^2$; the surface temperature is $T_D = -15\,^\circ\text{C}$. In this case, what is the heat flow Φ? How does Φ change if the parka gets so wet in freezing rain that the down lining shrinks to 1/4 of its original width, and the thermal conductivity of the down rises 20 – fold? What is the skin temperature T_S in both cases, if internal body temperature remains constant at $T_i = 37.4\,^\circ\text{C}$?
[thermal conductivity coefficients: down feathers $\lambda_D = 0.025\,\text{W/K m}$; human tissue and skin $\lambda_S = 0.2\,\text{W/K m}$; temperature boundary layer thickness in the skin and tissue $d = 4.5\,\text{cm}$ (estimated)]

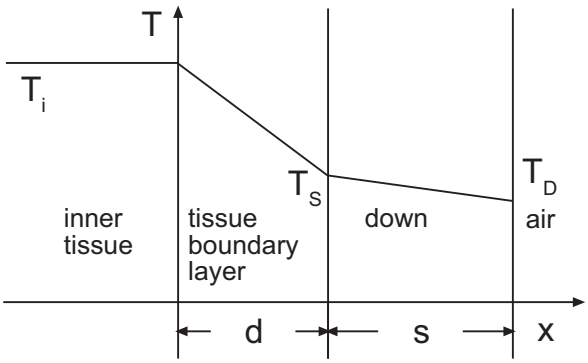

Fig. 6.1. Temperature profile of the skin and clothing.

We assume that the skin and clothing form two layers without any space between them, as shown in Figure 6.1. In the steady state, we have

!

– heat flow in the body

$$\Phi_B = \frac{\lambda_S A_S}{d} (T_i - T_S) \tag{6.1}$$

– heat flow in the down parka

$$\Phi_D = \frac{\lambda_D A_D}{s} (T_S - T_D) . \tag{6.2}$$

In each layer, heat flow is the same

$$\Phi_B = \Phi_D = \Phi,$$

so that with (6.1) and (6.2), we have two equations that we can use to determine the desired quantities Φ and T_S. We then obtain

$$\Phi = \frac{T_i - T_D}{\frac{d}{\lambda_S A_S} + \frac{s}{\lambda_D A_D}} \quad \text{and} \quad T_S = T_i - \frac{T_i - T_D}{1 + \frac{s}{d}\frac{\lambda_S A_S}{\lambda_D A_D}}.$$

Evaluating numerically, we get

– in dry conditions

$$\Phi_t = \frac{37.4 - (-15)}{\frac{0.045}{0.2 \cdot 2} + \frac{0.04}{0.025 \cdot 2}} \text{ W} = 57 \text{ W}$$

$$T_{S_t} = (37.4 - 6.5) \,^\circ\text{C} = 30.9 \,^\circ\text{C}.$$

– in freezing rain

$$\Phi_n = 428 \text{ W}$$

$$T_{S_n} = -10.7 \,^\circ\text{C}.$$

Due to its altered thermal conductivity, 7.5 times greater than in dry conditions, the parka's insulating effect becomes correspondingly weaker. In the rain, skin temperature is critical – at –10.7 °C the skin is prone to frostbite. In addition, after a period of time, the body will no longer be able to maintain its 37.4 °C core temperature. Fatigue and exhaustion will result.

6.2 Heat Loss

? The human body is continually losing heat through thermal conduction, as the temperature of the body is generally higher than the temperature of its surroundings.

1. Determine the heat flow from an unclothed person under the following assumptions: let the surface area of the body be $A = 1.60\,\mathrm{m}^2$; skin temperature $T_S = 30\,^\circ\mathrm{C}$; inner body temperature $T_i = 37.4\,^\circ\mathrm{C}$; the tissues that border the skin and in which there is a temperature gradient shall be $\delta = 4.5\,\mathrm{cm}$ thick; let the thermal conductivity of human tissue be $\lambda_S = 0.2\,\mathrm{W/m{\cdot}K}$.
2. During physical exertion, a higher rate of heat dissipation is necessary than when resting; this is because as performance increases, so does heat generation within the body. Measurements of an athlete showed that after a workout, 250 W must be dissipated from the body. How does the body react to this situation?

! 1. The general heat transfer equation

$$\frac{\partial T}{\partial t} = a\,\nabla^2 T$$

reduces, in this stationary, one-dimensional situation, to

$$0 = \frac{d^2T}{dx^2}$$

with x in the direction of the heat flow Φ. Integrating, we obtain

$$dT = C_1 \qquad \text{und} \qquad T = C_1 x + C_2.$$

Considering the boundary conditions $T = T_i$ for $x = 0$ and $T = T_S$ for $x = \delta$, we have the following conditional equations for constants C_1 and C_2:

$$T_i = C_2 \qquad \text{and} \qquad T_S = C_1\delta + T_i,$$

which lead to $C_1 = \frac{T_S - T_i}{\delta}$. Using this, we describe the temperature distribution $T(x)$ as

$$T(x) = \frac{T_S - T_i}{\delta}\,x + T_i.$$

Fourier gives heat flow as

$$\Phi = -\lambda_S A \frac{dT}{dx}.$$

Substituting the temperature distribution, we have

$$\Phi = \frac{\lambda_S A}{\delta} \left(T_i - T_S\right).$$

Using $\lambda_S = 0.2\ ^{\mathrm{W}}/_{\mathrm{m\cdot K}}$; $A = 1.6\ \mathrm{m}^2$; $\delta = 0.045\ \mathrm{m}$; $T_i = 37.4\ ^{\circ}\mathrm{C}$ and $T_S = 30\ ^{\circ}\mathrm{C}$, we have

$$\Phi = \frac{1.6\ \mathrm{m}^2 0.2\ ^{\mathrm{W}}/_{\mathrm{m\cdot K}}}{0.045\ \mathrm{m}} (7.4\ \mathrm{K}) = 52.62\ \mathrm{W}.$$

2. During physical exertion, the heat dissipation across the skin that was calculated in Exercise 6.1 is not enough to cool the body. The body reacts by sweating (loss of heat through the evaporation of sweat), and stronger breathing (utilization of additional surface area in the lungs). If that is not sufficient, the body must be cooled through additional means so that body temperature does not rise too high.

Part II: **The Physics of Diagnostics and Therapy**

7 X-Ray Diagnostics and Computer Tomography

Shortly after the discovery of X-rays by Wilhelm Conrad Röntgen on November 8, 1895, their significance to medical diagnostics was recognized. Using these diagnostic techniques, the part of the body under investigation is irradiated with X-rays; the attenuated radiation is then detected behind the body. As this attenuation is determined by the electron density in living beings, it is influenced principally by heavy atoms. Due to this effect, for example, bones are markedly different from the soft tissue that surrounds them. This tissue, in turn, can be further investigated through the introduction of contrast agents (as in, for example, coronary angiography). The first digital system of projection radiography was digital subtraction angiography (DSA), with which a clean image of the network of vessels can be obtained. In computer tomography (CT), many different projection X-ray recordings can be taken by rotating the source of the X-rays and the detector around the object under investigation. From these readings, a three-dimensional image that represents electron density is calculated.

An X-ray tube is comprised of a high-vacuum tube in which a heatable cathode and an anode are located. Between the cathode and the anode, a voltage U of 10–150 kV is usually applied, and a current of 1–2,000 mA. Due to the thermoelectric effect, electrons flow out from the cathode. These electrons are accelerated through the high voltage. When the beam of electrons strikes the anode, X-rays are created. The majority of these incident electrons transfers their energy through interaction with the electron shells of the anode material, which heats up as a result. A small portion of the electrons is slowed down in the field of the atomic nuclei of the anode material. The greatest possible frequency of this bremsstrahlung is achieved if the entire kinetic energy of the electrons $E_{\text{kin}} = eU$ is completely converted into the energy of a photon: $f_{\max} = \frac{E_{\text{Photon}}}{h} \stackrel{!}{=} \frac{E_{\text{kin}}}{h} = \frac{eU}{h}$. The bremsstrahlung spectrum of an X-ray tube is continuous up to this boundary frequency. If an atom is ionized by an incident electron, the gap that occurs can be filled by energetically higher-positioned electrons. This is the origin of the characteristic radiation through the transition of outer-shell electrons to vacant spaces. The energy released through this process is radiated away in the form of X-rays with discrete energy, and is known as characteristic radiation.

To investigate human tissue, not all portions of the X-ray spectrum are appropriate. The long-wave portion is immediately absorbed in the first layer of tissue. This contributes to radiation damage, but not to the image in the detector. As such, filers are employed to absorb this "weak" X-ray radiation.

The classical method of detecting X-rays is the use of X-ray films. These are comprised of a carrier foil with emulsion layers that contain silver bromide crystals. As X-ray quanta strike these layers, the bromine ions are oxidized, and electrons are liberated. These electrons are captured at seeds, and neighboring silver ions are reduced. These silver seeds are developed and fixed. The advantage of X-ray films is their excellent spatial resolution; their disadvantage is the relatively high dose of radiation

required. In a film-foil system, therefore, the emulsion is surrounded by an amplifying foil with a layer of luminescent material. The luminescent light that occurs in this layer illuminates the film. The advantage of this method is a dose amplification by a factor of 10 to 20; concurrently, though, the sharpness of the image is somewhat reduced. Additional options include the introduction of imaging plates, selenium films, or solid-state detectors (scintillators).

The absorption of an X-ray in a thin object can be described through microscopic absorbers; for each of these, a designated surface σ, the cross section, is completely covered by the radiation. Integration over many such thin layers yields the Lambert-Beer law, which describes the entire attenuation of the intensity I of the X-ray through an object with thickness d:

$$I = I_0 e^{-\mu d}.$$

In this equation, μ is the (linear) attenuation coefficient. This is the inverse of the average penetration depth $\bar{x} = 1/\mu$. As the interaction of X-rays with the tissue is affected by electron density, the attenuation coefficient is, in first approximation, proportional to the density ρ of the tissue:

$$\mu = n\sigma = \frac{N_A \rho}{m_{\text{mol}}} \sigma$$

(N_A: Avogadro constant, m_{mol}: molar mass of the material). Frequently, the mass attenuation coefficient μ/ρ is used when discussing the attenuation of X-rays. The energy deposited per unit mass by the ionizing radiation is designated as the dose D.

Image quality is the contribution of the imaging system to the quality of an X-ray image. It can be described physically by the image sharpness, contrast, noise, and by the artifacts that can occur.

The sharpness of an image is limited by several effects: geometric diffuseness that results from the finite limits of X-ray focus, image converter blurriness due to scattering effects, blurriness due to movement, and absorption blurriness, as radiation attenuation does not vary in discrete steps. Spatial resolution can refined through the use of a modulation transfer function (MTF). Very generally, a linear transfer system may be characterized by the impulse response $h(x, y)$ of the system. Its two-dimensional Fourier transform is called the (complex) transfer function $H(k_x, k_y)$. The MTF is the value of the normalized transfer function:

$$\text{MTF} = \frac{\left|H(k_x, k_y)\right|}{|H(0,0)|}.$$

If this (measured) MTF is presented graphically, the resolution capacity is the intercept with a straight line that represents just-perceivable contrast. In practice, it is very important that the entire MTF of a system is divisible into the individual MTFs of the parts of the system. In this manner, complicated systems like X-ray image enhancers can be analyzed more easily.

In the interaction of X-rays with tissue, the radiation is not just attenuated; in addition to useful radiation, diffuse scattered radiation is also generated, primarily due to Compton scattering (at the energies employed in X-ray diagnostics). The scattered radiation does not contribute to the formation of an image, and reduces the contrast of the image. If D_1 and D_2 are two neighboring dose values in a measured dosage profile, the contrast is given as $K = \frac{|D_1 - D_2|}{D_1 + D_2}$. Using the useful radiation (dose D_N) and the scattered radiation (dose D_S) , the total radiation contrast can be calculated: $K_G = \frac{1}{1+\alpha} \cdot K_N$. In this expression, $\alpha := \frac{2D_S}{D_{1,N} + D_{2,N}}$ in the region of the thorax typically has the value $\alpha(\text{thorax}) \approx 2$, and in the abdomen, around $\alpha(\text{abdomen}) \approx 7$. In order to reduce scattered radiation, screens are inserted that are comprised of alternating regions of interspacing material (which are transparent to X-rays) and lead slats (which absorb X-rays). The scattered radiation screen is characterized by geometric quantities, like the height and thickness of the lead slats and of the interspacing material, as well as the number of lead slats per millimeter. The most important physical quantity is selectivity $S := \frac{T_N}{T_S}$, which shows the relationship between the transparency to useful radiation $T_N := D_{N,\text{in}}/D_{N,\text{out}}$ and to scattered radiation $T_S := D_{S,\text{in}}/D_{S,\text{out}}$, and is, therefore, a measurement of the quality of the screen. The selectivity can have values in the range from 5 to 15 according to the radiation energy employed. Through the use of the radiation screen, the parameter α can be reduced by $1/S$, and total radiation contrast can be elevated.

Image noise has a number of causes, but the greatest contribution comes from quantum noise. It results from the statistical nature of X-ray radiation. The probability distribution to measure x quanta is given as a Poisson distribution $p(x) = \frac{\mu^x e^{-\mu}}{x!}$. As such, with even irradiation, the number x of photons striking the detector fluctuates around the average value μ, with variance $\sigma^2 = \mu$. As quantum noise is characteristic of nature, it cannot be removed by any X-ray image intensifier, no matter how good. Therefore, specification by what factor the noise is made worse by quantum noise is important to judge the quality of an image-producing system. The detective quantum efficiency (DQE) is defined as the ratio of the square of the signal-noise ratio (SNR) when exiting relative to that when entering, and is consequently always less than 1. For values in a Poisson distribution, $\text{SNR} = \frac{\mu}{\sqrt{\mu}} = \sqrt{\mu}$, and therefore,

$$\text{DQE} := \frac{\text{SNR}_{\text{out}}^2}{\text{SNR}_{\text{in}}^2} = \frac{\mu_{\text{out}}}{\mu_{\text{in}}}.$$

Just like MTF, the DQE of an entire system is the product of its component systems.

Computer tomography (CT) employs the same physical principle as projection X-ray. However, multiple individual projection images are taken, and a three-dimensional image of electron density is calculated by using a computer and rear projection. Iterative reconstruction was used in the early days of CT. Today, it is only used in nuclear diagnostics. Instead, filtered rear projection is employed. The idea here is to describe an arbitrary, integrable function $g(x, y)$ through all straight line integrals over the definition region of g. Due to the redundant information, not all of these line

integrals are necessary; this makes application of the technique in CT possible. The aggregate of all projections

$$p(\xi, \Theta) := \int_{-\infty}^{+\infty} d\eta \, g(x, y)$$

is described as a Radon transform. ξ, η here stand for the coordinates of a coordinate system rotated around Θ, relative to that of the object. The image function $g(x, y)$ desired is found using

$$g(x, y) = \frac{1}{2\pi} \int_0^{\pi} d\Theta \, \left\{ p(\xi, \Theta) \star FT^{-1} \{|k|\} \right\}.$$

In the integrand, the convolution of $p(\xi, \Theta)$ is next to the core of the convolution, the inverse Fourier transform of the function $f(k) = |k|$. This filtering function cannot be solved in general, and only yields actual filters under a bandwidth boundary of the signal. The convolution core is, however, independent from the angle of projection, and as such all measured projections are convoluted with the same core. This allows for the possibility of replacing the core with a modified filtering function. In this manner, for example, smoothing and high-resolution filters can be used in rear projection, and therefore, in image production.

7.1 Bouguer–Lambert Law

?

1. Deduce an expression for the line probability density for the absorption of a photon (probability of absorption per penetration depth $\omega = \frac{w}{\Delta x}$) that penetrates a block with frontal area A at a right angle. The block is made of a mixture of materials i, with densities ρ_i; molar masses M_i and an effective cross section σ_i.
2. Calculate the dependence on location of the intensity $I(x)$ of incident radiation for propagation through the block. The intensity of the incident radiation is I_0. Also, show that the effective absorption coefficient μ is equal to the sum of the absorption coefficients of the individual materials.
3. Consider a sphere of radius $R = 2\,\text{cm}$ that undergoes irradiation. Behind the sphere is a screen at a right angle to the direction of radiation. The absorption coefficient of the sphere's material is $\mu = 0.2\,\text{cm}^{-1}$. What does the relative intensity profile $i(r) = \frac{I(r)}{I_{\max}}$ on the screen look like?

!

1. For the absorption probability, we have

$$w = \frac{\text{surface of absorber}}{\text{total area}} = \frac{A_{\text{abs}}}{A}.$$

The total area over which the photon can be absorbed can be calculated using the line density $\frac{N_i}{V} A$, weighted with the effective cross section and the penetration

depth Δx for all the materials of the block.

$$A_{\text{abs}} = \sum_i \frac{N_i}{V} A \Delta x \sigma_i$$

with N_i as the number of particles of material i. Therefore for N_i, for the probability of absorption, we have

$$w = \sum \frac{N_i}{V} \Delta x \sigma_i,$$

in relation to the penetration depth,

$$\omega = \frac{w}{\Delta x} = \sum \frac{N_i}{V} \sigma_i.$$

From the definition of the molar mass

$$M_i = \frac{N_A}{N_i} m_i$$

we have, for particle density,

$$n_i = \frac{N_i}{V} = \frac{\rho_i N_i}{m_i} = \frac{\rho_i N_A}{M_i}.$$

The probability of absorption per penetration depth is therefore

$$\omega = \frac{w}{\Delta x} = \sum \frac{\rho_i N_A}{M_i} \sigma_i.$$

For ω, the designation of absorption coefficient μ_i is also useful.

2. The intensity I of a photon ray with photon energy E_γ and with photon flux Φ (number of photons per area and per time) is

$$I = E_\gamma \Phi.$$

For photons with frequency ν and flux $\Phi = \frac{d^2}{dtdA} N_\gamma$, we have through substitution

$$I = h\nu \frac{d^2}{dtdA} N_\gamma.$$

As the photon beam propagates through the block, the intensity after distance dx (the x-axis is the propagation axis of the photons) changes by

$$dI = I(x + dx) - I(x),$$

and the number of photons corresponding to dN_γ

$$dN_\gamma = N(x + dx) - N_\gamma(x).$$

As the number of photons can only change through interaction with the material of the block, dN_γ must be, through absorption probability

$$w = \frac{\text{interacting photons}}{\text{total incident photons}}$$

(with respect to ω) expressed as

$$dN_\gamma = -dx\,\omega N_\gamma(x)$$

and

$$N_\gamma(x+\delta x) = N_\gamma(x) - dx\omega N_\gamma(x).$$

Therefore, we have the first-order differential equation

$$\frac{dN_\gamma}{dx} = -\omega N_\gamma(x) = -\mu N_\gamma(x)$$

with effective absorption coefficient $\mu = \sum \mu_i = \sum \omega_i = \sum \frac{\rho_i N_A}{M_i}\sigma_i$.

By employing the "intensity operator": $\hat{I} = h\nu\frac{d^2}{dtdA}$, we have the differential equation

$$\frac{dI}{dx} = -\mu I$$

with the known exponential function as the solution:

$$I = I_0 e^{-\mu x}.$$

3. The distance that the beam travels between its source and detection can be divided into three elements: distance L_1 from source to sphere surface, distance within sphere d, and separation L_2 from the discharge from the sphere to the screen. First, consider distance d. This is for a beam that runs parallel to the equatorial plane at distance r

$$d(r) = \begin{cases} 2\sqrt{R^2 - r^2} & r \le R \\ 0 & r > R \end{cases}$$

with R as the radius of the sphere. The entire distance that the beam travels is therefore

$$D = L_1(r) + d(r) + L_2(r).$$

It encounters the material with absorption probabilities μ_0 on paths L_1 and L_2, and μ on path d (total path L). As such, we have, for the intensity of the beam on the detector

$$\begin{aligned} I(r) &= I_0 e^{-\mu_0 L_1} e^{-\mu d} e^{-\mu_0 L_1} \\ &= I_0 e^{-\mu_0 (L-d)} e^{-\mu d}. \end{aligned}$$

As such, a beam that missed the sphere has the highest intensity (if $\mu > \mu_0$)

$$I_{\max} = I_0 e^{-\mu_0 L}.$$

The relative intensity profile is therefore described as

$$\begin{aligned} \frac{I(r)}{I_{\max}} &= \frac{I_0 e^{-\mu_0 (L-d)} e^{-\mu d}}{I_0 e^{-\mu_0 L}} \\ &= e^{\mu_0 d} e^{-\mu d}. \end{aligned}$$

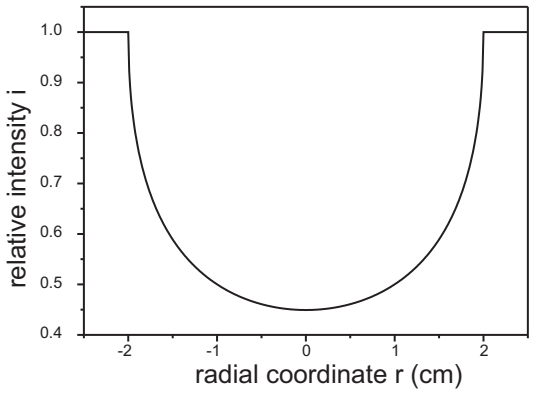

Fig. 7.1. Relative intensity on the screen, dependent on radial coordinate r.

As absorption in the paths outside of the sphere should be neglected, we can set $\mu_0 = 0$. Therefore,

$$i(r) = \frac{I(r)}{I_{\max}} = e^{-\mu d} = \exp\left(-2\mu\sqrt{R^2 - r^2}\right).$$

A beam on the x-axis will have the minimum relative intensity, as here, beam path is $d = 2R$

$$i_{\min}(r) = \frac{I_{\min}}{I_{\max}} = 0.45.$$

7.2 X-Ray Tubes

An X-ray tube is comprised of an evacuated bulb in which are located a cathode as a thermal source of electrons, and an anode made of tungsten. During operation, there is a potential difference between cathode and anode of 100 kV, and an electric current of 100 mA is flowing. In this system, 1% of the electric power is used for the creation of X-rays. How many electrons strike the anode each second? What is the power emitted as X-ray radiation? How long can the X-ray tube work without the anode fusing? How can this amount of time be lengthened?
[mass of the anode $m = 74$ g; tungsten: specific heat $c_p = 0.33$ J/kg K; melting temperature $T_S = 3{,}000$ K]

For the electric charge we have $|Q| = Ne$ with N as the number of electrons that strike the anode. Therefore,

$$|I| = \frac{d|Q|}{dt} = \frac{dNe}{dt} = e\frac{dN}{dt}$$

and therefore,

$$\frac{dN}{dt} = \frac{|I|}{e} = \frac{0.1\ \text{A}}{1.6 \cdot 10^{-19}\ \text{C}} = 6.25 \cdot 10^{17}\ \text{s}^{-1}.$$

Thermal power P_{th} is

$$P_{th} = P_{el} - P_R$$

with P_{el} as the power of the incident electrons, and P_R as the power lost through X-ray radiation. We have $P_{el} = UI$ and $P_R = \eta P_{el}$ with $\eta = 0.01$. Therefore,

$$P_R = 0.01\, UI = 0.1\,\text{kW},$$
$$P_{th} = UI\,(1 - 0.01) = 9.9\,\text{kW}.$$

The quantity of heat Q_S that would raise the anode from the temperature of the surroundings T_0 to melting temperature T_S is

$$Q_S = mc_p\,(T_S - T_0) \approx 0.074\,\text{kg}\,0.33\,\text{J/kg K}\,(3{,}000\,\text{K} - 293\,\text{K}) = 66.1\,\text{J}.$$

The time τ until melting is given by the ratio

$$\tau = \frac{Q_S}{P_{th}} = \frac{66.1\,\text{Ws}}{9.9\,\text{kW}} = 6.67\,\text{ms}.$$

The X-ray tube can only be driven in pulses. A longer driving time can be reached by using a larger anode mass (1 to 2 kg), or by using water cooling.

7.3 Spectrum of an X-Ray Tube

?

1. Describe the function of an X-ray tube.
2. The spectrum of an X-ray tube is continuous, but is truncated at a certain wavelength (λ_{min}). In general, a number of characteristic peaks also appear in the spectrum. Explain the origin of these phenomena. How can the boundary wavelength (λ_{min}) be calculated easily?

!

1. An X-ray tube is comprised of an evacuated bulb in which a voltage is applied across a glowing cathode and an anode. The glowing cathode emits electrons, which are accelerated by this voltage and which strike the anode. The electrons are slowed down in the anode, and emit X-rays.
2. The continuous portion is due to bremsstrahlung. The electrons are slowed down by the atomic nuclei in the anode (kinetic energy of the electrons is transformed into radiation). The maximum radiation energy (the energy of a γ) is determined by the voltage applied: if an electron with maximum kinetic energy Ve^- is suddenly slowed down, a photon with $\lambda_{\text{min}} = \frac{hc}{Ve^-}$ is emitted. The bremsstrahlung adds a significant contribution to the X-ray spectrum, and can be influenced by changes in the acceleration voltage. A higher acceleration voltage yields a smaller λ_{min}.

7.4 Intensity Attenuation

When a patient's upper leg is absorbing X-rays, the X-ray, after leaving the X-ray tube with original intensity $I_0 = 4\ \mathrm{W/m^2}$, passes through the following layers: ?

- layer of air, of distance $x_L = 30$ cm; attenuation coefficient $\mu_L = 0.001\ \mathrm{cm^{-1}}$;
- soft tissue of thickness $x_{W_1} = 7$ cm; attenuation coefficient $\mu_W = 0.18\ \mathrm{cm^{-1}}$;
- bone, with a diameter of $x_K = 2$ cm; attenuation coefficient $\mu_K = 1.6\ \mathrm{cm^{-1}}$;
- soft tissue of thickness $x_{W_2} = 6$ cm.

What is the intensity of the X-ray when it strikes the photo plate?
[Note: the bone should be considered to be solid, not hollow]

Intensity I_{LW} after travel through the air, at the boundary layer (air | soft tissue) !

$$\begin{aligned} I_{LW} &= I_0 \exp\left(-\mu_L x_L\right) \\ &= 4.0\ \mathrm{W/m^2} \exp\left(-0.001\ \mathrm{cm^{-1}} \cdot 30\ \mathrm{cm}\right) = 3.88\ \mathrm{W/m^2}. \end{aligned}$$

Intensity I_{WK} after the first layer of soft tissue, at the next boundary layer (soft tissue | bone)

$$I_{WK} = I_{LW} \exp\left(-\mu_W x_{W_1}\right) = 3.88\ \mathrm{W/m^2}\, e^{-1.26} = 1.1\ \mathrm{W/m^2}.$$

Intensity I_{KW} after the bone, at the next boundary layer (bone | soft tissue)

$$I_{KW} = I_{WK} \exp\left(-\mu_K x_K\right) = 1.1\mathrm{W/m^2} e^{-3.2} = 0.045\ \mathrm{W/m^2}.$$

Intensity I_P after the second layer of soft tissue, at the photo plate

$$I_P = I_{KW} \exp\left(-\mu_W x_{W_2}\right) = 0.045\ \mathrm{W/m^2} e^{-1.08} = 0.015\ \mathrm{W/m^2}.$$

or, in total,

$$\begin{aligned} I_p &= I_0 \exp\left\{-\left[\mu_L x_L + \mu_W \left(x_{W1} + x_{W2}\right) + \mu_K x_K\right]\right\} \\ &= 4.0\ \mathrm{W/m^2} \exp\left\{-\left[0.03 + 0.18\ (7 + 6) + 3.2\right]\right\} = \\ &= 4.0\ \mathrm{W/m^2} \exp\ (-5.57) = 0.015\ \mathrm{W/m^2}. \end{aligned}$$

7.5 Contrast

1. Formulate a simple expression for the contrast C between the two image regions A and B (see Figure). ?
2. The intensity of the transmitted rays I_a, I_b can be found as the sum of primary and scattered components ($I = P + S$). How does the contrast change under the assumption that the scattered radiation has the same intensity in both cases?

3. In order to be able to differentiate clearly between two regions in an X-ray image, a contrast of $C \geq 0.3$ is necessary. If this contrast does not occur at first, it can be achieved through the introduction of the contrast agent iodine. The isotope $^{131}_{53}\mathrm{J}$ is used. Estimate the minimum concentration of iodine $c_J = \frac{N_J}{N_B}$, introduced by injecting iodine into the blood stream, that is necessary to be able to distinguish a vein from the soft tissue that surrounds it.

[blood $\mu_B = 0.17\,\mathrm{cm}^{-1}$; soft tissue $\mu_W = 0.18\,\mathrm{cm}^{-1}$; diameter of the vein $d = 1\,\mathrm{mm}$; charge number of blood $Z_B = Z_a = 7$]

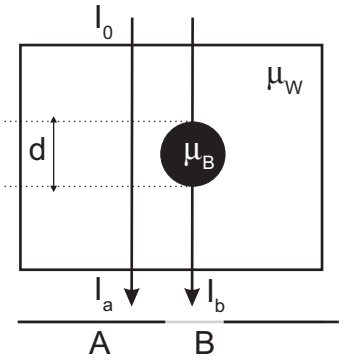

Fig. 7.2. Different beam paths in tissue; one of the beams strike a circular region with absorption coefficient μ_B.

! 1. The (Weber) contrast[1] C is defined as

$$C = \left| \frac{I_b - I_a}{I_a} \right| . \tag{7.1}$$

For image region A, we have, with I_0 as the original intensity

$$I_a = I_0 \exp\left(-\mu_B x\right) . \tag{7.2}$$

1 alternative: Michelson contrast

$$C_M = \left| \frac{I_b - I_a}{I_a + I_b} \right| = \left| \frac{\exp(-d\Delta\mu) - 1}{\exp(-d\Delta\mu) + 1} \right| .$$

Expanding as a series for $\gamma = d\Delta\mu$ yields:

$$C_M = C_M(0) + \frac{dC_M}{d\gamma}\gamma + \ldots \cong \left| -\frac{1}{2}\gamma \right| = \left| \frac{d\Delta\mu}{2} \right| .$$

For small d and $\Delta\mu$, this give the half-Weber contrast.

For region B

$$I_b = I_0 \exp\left[-\mu_B (x-d) - \mu_W d\right] = I_0 \exp\left[-x\mu_B - d(\mu_W - \mu_B)\right]$$
$$= I_0 \exp\left(-d\Delta\mu\right) \exp\left(-\mu_B x\right) = I_0 \exp\left(-d\Delta\mu\right) \exp\left(-\mu_B x\right)$$

with $\Delta\mu = \mu_W - \mu_B$. Therefore, contrast C is

$$C = \left|\exp(-d\Delta\mu) - 1\right|. \tag{7.3}$$

For the estimate, the consideration of small $d\Delta\mu$ is sufficient. As such, the term $\exp\left(-d\Delta\mu\right)$ can be decomposed and disregarded after the second term. We have

$$\exp\left(-d\Delta\mu\right) \cong 1 - d\Delta\mu. \tag{7.4}$$

(7.4) substituted in (7.3) yields

$$C \cong \left|1 - d\Delta\mu - 1\right| = \left|d\Delta\mu\right|.$$

2. For the change in contrast ΔC, we have

$$\Delta C = C_{mS} - C_{oS}, \tag{7.5}$$

in which C_{mS} is the contrast with scattering, and C_{oS} is the contrast without scattering. The total intensity I is then

$$I_a = P_a + S_a \quad \text{and} \quad I_b = P_b + S_b$$

with P for primary radiation and S for scattered radiation. In the case that $S_a = S_b = S$, (7.5) is, considering (7.1),

$$\Delta C = \left|\frac{P_b - P_a}{P_a + S}\right| - \left|\frac{P_b - P_a}{P_a}\right| = -\frac{2P_a^2 + P_a S + P_b S}{P_a\left(P_b + S\right)}. \tag{7.6}$$

Because all values are positive in (7.6), the numerical value of ΔC is negative. This means that the contrast with scattering is lower that the contrast without scattering. [2].

2 For Michelson contrast, we have contrast change

$$\Delta C_M = \left|\frac{P_b - P_a}{P_b + P_a + 2S}\right| - \left|\frac{P_b - P_a}{P_a + P_a}\right|$$
$$= \frac{\left|P_b^2 - P_a^2\right| - \left|\left(P_b + P_a + 2S\right)\left(P_b - P_a\right)\right|}{\left(P_a + P_a\right)\left(P_b + P_a + 2S\right)}$$
$$= \frac{\left|P_b^2 - P_a^2\right| - \left|\left(P_b^2 - P_a^2 + 2S\left(P_b - P_a\right)\right)\right|}{\left(P_a + P_a\right)\left(P_b + P_a + 2S\right)}.$$

3. To ensure acceptable differentiability, contrast must be $C > 0.3$. For $d = 1$, therefore, $\Delta\mu$ must have at least the value

$$\Delta\mu_{\min} = \frac{C_{\min}}{d} = \frac{0.3}{0.1\,\text{cm}} = 3\,\text{cm}^{-1}.$$

For blood, $\mu_B = 0.17\,\text{cm}^{-1}$, and for soft material $\mu_W = 0.18\,\text{cm}^{-1}$. Therefore, $\Delta\mu = 0.01\,\text{cm}^{-1}$. This means that in this case, assured differentiability is not possible. As such, the contrast agent iodine 53 is introduced into the blood. The amount N_J that is sufficient to achieve a C_{min} value of $0.3\,\text{m}^{-1}$ depends on the amount of blood $N_1 = N_B$. The ratio $\frac{N_J}{N_B}$ is the desired concentration c_J. For the attenuation coefficient μ_i and charge number Z_i of component i, the proportionality relationship is:[3] $\mu_i \propto N_i Z_i^{4.5}$. Therefore,

$$\frac{\mu_J}{\mu_B} = \left(\frac{N_J}{N_B}\right)\left(\frac{Z_J}{Z_B}\right)^{4.5} = c_J\left(\frac{Z_J}{Z_B}\right)^{4.5}.$$

With $Z_J = 53$ and $Z_B = 7$, we have

$$c_j = \frac{1}{9.0 \cdot 10^4}\left(\frac{\mu_J}{\mu_B}\right).$$

Considering the corresponding parameter space (positive), we can differentiate between two cases.

Case 1. $P_b > P_a$

$$\begin{aligned}\Delta C_M &= \left|\frac{P_b - P_a}{P_b + P_a + 2S}\right| - \left|\frac{P_b - P_a}{P_a + P_a}\right| \\ &= \frac{P_b - P_a}{P_b + P_a + 2S} - \frac{P_b - P_a}{P_a + P_a} \\ &= \frac{-2S\,(P_b - P_a)}{(P_a + P_a)\,(P_b + P_a + 2S)} \\ &< 0.\end{aligned}$$

Case 2. $P_b < P_a$

$$\begin{aligned}\Delta C_M &= \left|\frac{P_b - P_a}{P_b + P_a + 2S}\right| - \left|\frac{P_b - P_a}{P_a + P_a}\right| \\ &= -\frac{P_b - P_a}{P_b + P_a + 2S} + \frac{P_b - P_a}{P_a + P_a} \\ &= \frac{2S\,(P_b - P_a)}{(P_a + P_a)\,(P_b + P_a + 2S)} \\ &< 0.\end{aligned}$$

As is clear, the second term in the numerator is greater than the first in both cases; this means that the Michelson contrast also inherently declines.

3 According to "Effekte der Physik und ihre Anwendungen" by Ardenne, Musoil, and Klemrad, the dependency varied between $Z^{4.6}$ for light atoms and Z^4 for heavy atoms; here, we will assume a power of 4.5 for simplicity.

As $\mu_J - \mu_W = \Delta\mu_{min} = 3\,\mathrm{cm}^{-1}$ we have $\mu_J = 3\,\mathrm{cm}^{-1} + \mu_W = 3.18\,\mathrm{cm}^{-1}$.
This yields[4] for c_J

$$c_j = \frac{1}{9.0 \cdot 10^4}\left(\frac{3.18}{0.17}\right) = 2.1\,‰.$$

7.6 Scattered Radiation

The proportion of scattered radiation in an X-ray imaging sequence is around 80%. Assume that the differences in dosage of useful radiation across the entire field are very small. The contrast is to be improved through the use of a grate. ?

1. What is the total radiation contrast without the grate (relative to the contrast without scattered radiation K_N)?
2. If the grate used has a transparency to useful radiation of $T_N = 60\%$, and a transparency to scattered radiation of $T_S = 5\%$, what is the improvement in contrast?

1. S: scattered radiation; N: useful radiation; G: total radiation. For the total radiation contrast K_G we have !

$$K_G = K_N \frac{1}{1+\alpha}$$

with

$$\alpha = \frac{2D_S}{D_{1N} + D_{2N}}.$$

D_{1N} and D_{2N} are two neighboring doses of useful radiation, and D_S is the dose of scattered radiation. If the proportion of scattered radiation, as set forth in the problem, comprises 80% of the total radiation, then 20% of this total remains available as useful radiation. Considering the approximation given that the differences in doses of useful radiation are very small – $D_{1N} \approx D_{2N}$ – we have

$$\alpha \approx \frac{2D_S}{2D_N} = \frac{D_S}{D_N} = \frac{D_S/D_G}{D_N/D_G} = \frac{80\%}{20\%} = 4.$$

$$\Rightarrow K_G = K_N/5 = 0.2 \cdot K_N.$$

4 In the case of Michelson contrast,

$$\Delta\mu_{\mathrm{min}} = \frac{2}{d} C_{\mathrm{Min}} = 6\,\mathrm{cm}^{-1}$$

and therefore

$$c_j = \frac{1}{9.0 \cdot 10^4}\left(\frac{6.18}{0.17}\right) = 4.0\,‰.$$

2. The selectivity of the grate is

$$S = \frac{T_N}{T_S} = \frac{60\%}{5\%} = 12.$$

Therefore, for the total radiation contrast, we have

$$K_G = K_N \frac{1}{1 + \alpha/S} = K_N \frac{1}{1 + 4/12} = 0.75 \cdot K_N.$$

7.7 Quantum Noise of an X-Ray Image Intensifier

? Calculate the quantum noise of an X-ray image intensifier at dose power (dose per time) of 0.1 $\frac{\mu Gy}{s}$, pixel size 0.2 mm · 0.2 mm, and exposure time 0.45 s per image. From the calibration measurement, the conversion factor γ of the energy dose (in [Gy]) expressed as the number of quanta per mm is known:

$$\gamma = 2 \cdot 10^4 \frac{\text{quanta}}{\text{mm}^2 \mu\text{Gy}}$$

Assume a Poisson distribution, and calculate the quantum noise and the relative error

1. for incident quanta
2. for the number of quanta actually attested if the absorption at the entrance window is 10%, and the effective absorptance of CsJ for the energy used is 70%
3. for the photons of visible light after conversion, under the assumption that 3,000 ± 100 $^{\text{photons}}/_{\text{X-ray quantum}}$ are generated.

! 1. We have

$$\frac{\#\text{quanta}}{\text{pixel} \cdot \text{s}} = 2 \cdot 10^4 \frac{\#}{\text{mm}^2 \mu\text{Gy}} \cdot (0.2\,\text{mm})^2 \cdot 0.1 \frac{\mu\text{Gy}}{\text{s}} = 80 \frac{\#}{\text{pixel} \cdot \text{s}}.$$

For the exposure time, we have, for the number of quanta per pixel,

$$N = 80 \frac{\#}{\text{pixel} \cdot \text{s}} \cdot 0.45\,\text{s} = 36 \frac{\#}{\text{pixel}}.$$

For a Poisson distribution we have

$$\sigma_N = \sqrt{N}$$

and therefore,

$$N = 36 \pm 6$$

and

$$\sigma_{N,\text{rel}} = \frac{6}{36} = 0.167 = 16.7\%.$$

2. After the window and absorption of 10% the number of quanta is

$$N_{\text{n.F.}} = 0.9\,\text{N} = 32.4.$$

The number of attested quanta is then

$$N_{\text{attest.}} = 0.7 \cdot N_{\text{n.F.}} = 22.7.$$

and

$$N_{\text{attest.}} = 22.7 \pm \sqrt{22.7} = 22.7 \pm 4.8$$

and

$$\sigma_{N_{\text{attest.}},\text{rel}} = \frac{4.8}{22.7} = 0.211 = 21.1\%.$$

3. At a quantum yield of

$$A = (3{,}000 \pm 100)\,\frac{\#\text{photons}}{\text{X-ray quantum}}$$

we have

$$N_{\text{Ph}} = A \cdot N_{\text{attest.}} = 3{,}000 \cdot 22.7 = 68{,}100$$

photons created. Using the Gaussian error propagation method, we determine

$$\sigma_{N_{\text{Ph}}} = \sqrt{N_{\text{attest.}}^2 \sigma_A^2 + A^2 \sigma_{N_{\text{attest.}}}^2} = \sqrt{22.7^2 \cdot 100^2 + 3{,}000^2 \cdot 4.8^2} = 14{,}578.$$

$$N_{\text{Ph}} = 68{,}100 \pm 14{,}578.$$

$$\sigma_{N_{\text{Ph,rel}}} = \frac{14{,}578}{68{,}100} = 0.214 = 21.4\%.$$

7.8 Fourier Reconstruction of an Image

Consider the reconstruction of an image from the projections measured. The two-dimensional Fourier transform of the image $g(x, y)$ is $G(k_x, k_y)$. It can be reconstructed from the one-dimensional Fourier transform $P(k, \Theta)$ of the projections measured $p(\xi, \Theta)$, ?

$$P(k, \Theta) = \int_{-\infty}^{+\infty} d\xi\; p(\xi, \Theta)\, e^{-i2\pi k\xi},$$

and for a slice through the two-dimensional Fourier transform $G(k_x, k_y)$ at angle Θ: $G(k, \Theta) = P(k, \Theta)$. Show that the inverse two-dimensional Fourier transform

$$g(x, y) = \frac{1}{(2\pi)^2} \iint_{-\infty}^{+\infty} dk_x dk_y\, G(k_x, k_y)\, e^{+i2\pi(xk_x + yk_y)}$$

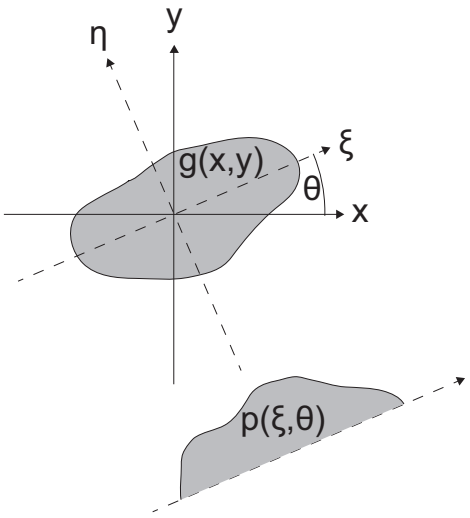

Fig. 7.3. Example of a projection measurement $p(\xi, \theta)$.

is given by

$$g(x, y) = \frac{1}{2\pi} \int_0^{\pi} d\Theta \left\{ p(\xi, \Theta) * FT^{-1}\{|k|\} \right\}$$

In the expression, $FT^{-1}\{|k|\}$ is the inverse Fourier transform of the function $f(k) = |k|$, and $*$ is the convolution of the two functions. (Note: the Cartesian coordinates k_x, k_y must be converted into polar coordinates)

$$g(x, y) = \frac{1}{(2\pi)^2} \int_{-\infty}^{\infty} dk_x \int_{-\infty}^{\infty} dk_y G(k_x, k_y) e^{i2\pi(xk_x + yk_y)}.$$

! With polar coordinates

$$k_x = k \cos\theta; \qquad k_y = k \sin\theta$$

and the Jacobian determinant

$$|J| = \det \begin{pmatrix} \frac{\partial k_x}{\partial k} & \frac{\partial k_y}{\partial k} \\ \frac{\partial k_x}{\partial \theta} & \frac{\partial k_y}{\partial \theta} \end{pmatrix} = |k|(\cos^2\theta + \sin^2\theta) = |k|$$

we have

$$g(x,y) = \frac{1}{(2\pi)^2}\int_{-\pi}^{\pi} d\theta \int_{0}^{\infty} dk\,|k|\,G(k\cos\theta, k\sin\theta)e^{i2\pi k(x\cos\theta + y\sin\theta)}$$

$$= \frac{1}{(2\pi)^2}\int_{-\pi}^{\pi} d\theta \int_{0}^{\infty} dk\,|k|\,G(k,\theta)e^{i2\pi k(x\cos\theta + y\sin\theta)}$$

$$= \frac{1}{(2\pi)^2}\int_{-\pi}^{\pi} d\theta \int_{0}^{\infty} dk\,|k|\,P(k,\theta)e^{i2\pi k(x\cos\theta + y\sin\theta)}.$$

With

$$x = \xi\cos\theta - \eta\sin\theta,$$
$$y = \xi\sin\theta + \eta\cos\theta$$

we have

$$g(x,y) = \frac{1}{(2\pi)^2}\int_{-\pi}^{\pi} d\theta \int_{0}^{\infty} dk\,|k|\,P(k,\theta)e^{i2\pi k\xi}$$

$$= \frac{1}{(2\pi)^2}\int_{0}^{\pi} d\theta \int_{-\infty}^{\infty} dk\,|k|\,P(k,\theta)e^{i2\pi k\xi}$$

$$= \frac{1}{2\pi}\int_{0}^{\pi} d\theta \left\{\frac{1}{2\pi}\int_{-\infty}^{\infty} dk\,|k|\,P(k,\theta)e^{i2\pi k\xi}\right\}$$

$$= \frac{1}{2\pi}\int_{0}^{\pi} d\theta \left\{FT^{-1}(P(k,\theta)\cdot|k|)\right\}$$

$$= \frac{1}{2\pi}\int_{0}^{\pi} d\theta \left\{FT^{-1}(P(k,\theta)) \star FT^{-1}(|k|)\right\}$$

$$= \frac{1}{2\pi}\int_{0}^{\pi} d\theta \left\{p(\xi,\theta) \star FT^{-1}(|k|)\right\}.$$

7.9 Radon Transform of a Circular Object

We wish to find the Radon transform $p(\Theta, s)$ of a circular object at angle $\Theta = 0$ (that is, the projection in this direction). Within the circle with radius R, the corresponding function should have the value $f(x,y) = a$, and outside of it, the function should be zero. What form does the Radon transform have for $a = \frac{1}{2}$, and for any other values $a > 0$? ?

! For the function, we have:

$$f(x, y) = a \qquad \text{for} \quad x^2 + y^2 \leq R^2$$
$$f(x, y) = 0 \qquad \text{outside}$$

Therefore, for the projection at angle $\Theta = 0$, we have:

$$p(0, x) = \int_{-\sqrt{R^2-x^2}}^{+\sqrt{R^2-x^2}} dy\, a = a \cdot 2\sqrt{R^2 - x^2} \qquad \text{für} \quad |x| \leq R$$
$$p(0, x) = 0 \qquad \text{für} \quad |x| > R$$

If $a = \frac{1}{2}$, then

$$p(0, x) = \sqrt{R^2 - x^2}$$

describes a half-circle with radius R. Otherwise, this is half of an ellipse.

7.10 Beam Hardening and Partial Volume Artifacts in CT

?

1. Explain, as shown in Figure 7.4, the origin of beam hardening artifacts in CT. The emission spectrum of the X-ray tube is marked as 1 in the diagram, and the arrow perpendicular to it shows the median of the distribution. The mass attenuation coefficient μ/ρ of the (homogeneously) irradiated body is also indicated. It is assumed that the emission spectrum is valid for the first half of the path of the X-ray through the body; for the second half, the spectrum labeled 2 is valid. Why does the "median" of the distribution shift after the X-ray has passed through a portion of the body, as depicted in this crude model?
2. What is the origin of partial volume artifacts in CT? Consider a region within one pixel (the underlying voxel of the object) that possesses two different X-ray attenuation coefficients. Also, discuss the two cases shown on the right in Figure 7.4. For the solution, it is sufficient to only consider one incident beam direction in the upper case, while in the lower case irradiation from two directions, 1 and 2, should be discussed.

!

1. The median shifts due to the absorption of the X-ray in the body (here, in the first half). Especially weak X-rays are absorbed. Two different medians (for halves 1 and 2) also have, as in the diagram, different values for μ, although (according to the assumption) we are considering a homogeneous material. The value for μ/ρ for the second half corresponds to the value that is obtained for harder X-rays. This is the origin of the term *beam hardening artifact*.

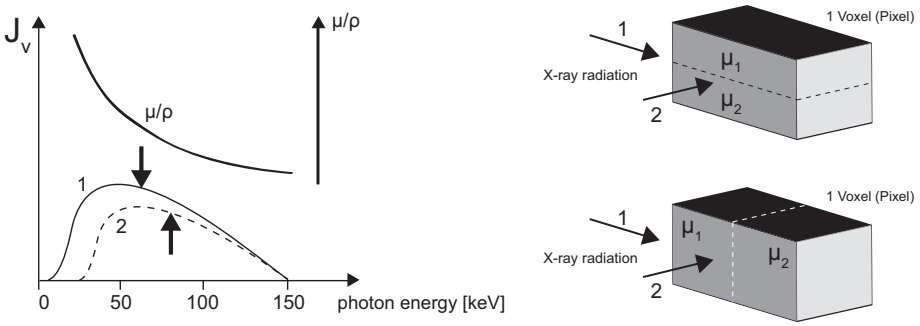

Fig. 7.4. Left: spectra of X-ray tubes. Right: The occurrence of partial volume artifacts. In both cases (above and below), a pixel is presented with two regions, each of a different X-ray attenuation coefficient μ_i. The arrows show the direction of incident X-rays (1 and 2 mare two projections at different times).

2. In the upper portion of Figure 7.4, for the irradiation direction indicated, the total X-ray power at the detector is

$$J_D = \frac{J_0}{2}\left(e^{-\mu_1 l} + e^{-\mu_2 l}\right). \tag{7.7}$$

In the lower portion of the image 7.4, the X-ray power at the detector for radiation from direction 1 is

$$J_D = J_0 e^{-(\mu_1+\mu_2)l/2} = J_0 e^{-\bar{\mu} l} \tag{7.8}$$

and for radiation from direction 2, the solution is again expression (7.7). The different outcomes (7.7) and (7.8) lead to the conclusion that in the second case, different projections lead to different attenuations for the same pixel (partial volume artifact).

7.11 Modulation Transfer Function of a CT Scanner

The (one-dimensional) impulse response (point spread function) of the detector of a CT-scanner is box-shaped, with width a_D: ?

$$h_D(x) = \Theta(x - 0) - \Theta(x - a_D).$$

1. Find the complex transfer function $H(k)$ and the modulation transfer function (MTF) of this detector.
2. The impulse response for the X-ray tube in the CT scanner should have the same form as that of the detectors, but with width a_R. What is the MTF of the entire system, detector and tube?

3. The geometric significance of a_D and a_T can be seen in Figure 7.5. The separation between tube and detector is $d = 30\,\text{cm}$, the focus value in the tube is $F = 1\,\text{mm}$, the size of the detector is $D = 0.7\,\text{mm}$, and the distance between the X-ray tube and the center of rotation (the black point in Figure 7.5) is $r = 10\,\text{cm}$. What are the effective focus values of the tube (a_T) and the detector (a_D) in this case?
4. At what distance r_{opt}, measured in units of d, is the minimum focus value $a_{\min}$ (maximum resolution) achieved? Make the general assumption that the focus of the tube is twice as large as the diameter of the detector – $F = 2D$.

! 1. The complex transfer function is, in general,

$$H(k) := \int_{-\infty}^{\infty} dx\, h(x) e^{-ikx}.$$

For the detector, this becomes

$$\begin{aligned} H_D(k) &= \int_{-\infty}^{\infty} dx\, \{\Theta(x-0) - \Theta(x-a_D)\}\, e^{-ikx} = \int_0^{a_D} dx e^{-ikx} \\ &= \frac{1}{-ik}\left[e^{-ikx}\right]_0^{a_D} = \frac{1}{-ik}\left(e^{-\frac{ika_D}{2}} - 1\right) \\ &= \frac{1}{-ik} e^{-\frac{ika_D}{2}} \left(e^{-\frac{ika_D}{2}} - e^{+\frac{ika_D}{2}}\right) = e^{-\frac{ika_D}{2}} \frac{\sin\left(\frac{ka_D}{2}\right)}{\frac{k}{2}}. \end{aligned}$$

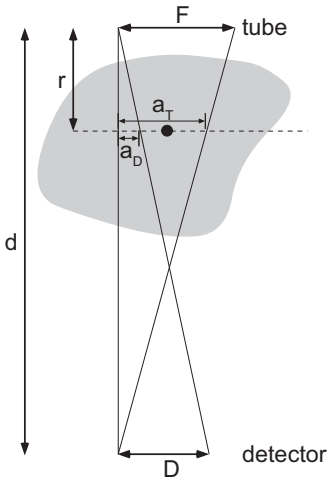

Fig. 7.5. Schematic diagram of beam path in a CT system.

For the MTF, consider the boundary case

$$|H_D(0)| = \left| \lim_{k\to 0} \frac{\sin\left(\frac{ka_D}{2}\right)}{\frac{k}{2}} \right| \cdot \left| e^{-\frac{ika_D}{2}} \right| = \left| \lim_{k\to 0} \frac{\frac{d}{dk}\sin\left(\frac{ka_D}{2}\right)}{\frac{d}{dk}\frac{k}{2}} \right|$$

$$= \left| \lim_{k\to 0} \frac{a_D}{\cos(\frac{ka_D}{2})} \right| = a_D.$$

Therefore,

$$\mathrm{MTF}_D(k) = \frac{|H_D(k)|}{|H_D(0)|} = \left| e^{-\frac{ika_D}{2}} \cdot \frac{\sin\left(\frac{ka_D}{2}\right)}{\frac{k}{2}} \right| = a_D \left| \frac{\sin\left(\frac{ka_D}{2}\right)}{\frac{ka_D}{2}} \right|.$$

The MTF is a normalized sinc function.

2. The great advantage in using the MTF as the descriptor is that it can be multiplied into a whole

$$\mathrm{MTF}_{\mathrm{ges}} = \mathrm{MTF}_D \cdot \mathrm{MTF}_R = \left| \frac{\sin\left(\frac{ka_D}{2}\right)}{\frac{ka_D}{2}} \right| \cdot \left| \frac{\sin\left(\frac{ka_R}{2}\right)}{\frac{ka_R}{2}} \right|.$$

3. From the beam intercept laws as applied to the diagram, we have

$$a_D = D\,\frac{r}{d} = \frac{7\cdot 10^{-4}\mathrm{m}\cdot 0.1\ \mathrm{m}}{0.3\ \mathrm{m}} = 2.33\cdot 10^{-4}\mathrm{m} = 0.23\ \mathrm{mm},$$

$$a_T = F\,\frac{(d-r)}{d} = 10^{-3}\mathrm{m}\,\frac{(0.3-0.1)\ \mathrm{m}}{0.3\ \mathrm{m}} = 0.67\ \mathrm{mm}.$$

4. r_{opt} is determined if $a_D = a_T$:

$$a_D = a_T,$$
$$\frac{Dr}{d} = \frac{F(d-r)}{d},$$
$$r = 2\,(d-r) = \frac{2}{3}d.$$

8 Ultrasound

Ultrasound refers to sound waves with frequencies beyond the threshold of hearing, from around 16 kHz up. Although sound frequencies of up to 1 GHz are technically producible today, medical diagnostics primarily makes use of frequencies in the range of a few megahertz. This is because below 2 MHz resolution is too slight, while with frequencies above around 10 MHz, absorption in the tissue is too strong.

In ultrasound diagnostics, ultrasonic waves of low power are directed into the human body. In water and in human tissue, these waves propagate with a speed of sound of around 1,500 m/s, and as such, their wavelengths at frequencies of a few MHz are in the range of $\lambda < 1$ mm. As a result, the ultrasound can be focused, reflected, scattered, and absorbed in the tissue, analogously to an optical beam. If the regions of interest in the tissue differ in any of these effects, imaging is possible (at least in principle). Through the interaction of the coupled waves with the environment, ultrasonic signals arise that are recorded in diagnostic application and are analyzed. These signals are used to produce ultrasound images, to characterize tissues, for the biometry of organs, and also to understand how bodily functions are taking place. Ultrasound diagnostics has a number of advantageous characteristics: it is non-invasive and painless, can be completed relatively quickly and without special preparation of the patient, and is relatively cost-effective. While the method was originally used to complement other methods of investigation, ultrasound diagnostics is delivering more and more of its own findings today.

While with the diagnostic use of ultrasound, the body is very likely not to be affected, the effects of ultrasound on organs and tissue are used in therapeutic contexts. The sound wave transports energy and momentum, and acts in a targeted way on the intended region of the body. This process employs mechanical friction and thermal effects; in addition, under certain condition, is can influence physico-chemical reaction processes.

The propagation of sound waves takes place through the action of pressure waves in a medium. With a change in pressure p, a corresponding change in density occurs:

$$\left.\frac{\partial p}{\partial \rho}\right|_{\rho_0} = \frac{1}{\kappa \rho_0}.$$

In the expression, ρ_0 is the equilibrium value of density ρ without the sound wave, and κ is the compressibility. Instead of the compressibility, the compression modulus $K = \frac{1}{\kappa}$ is also used. In order to describe the propagation of the sound, the displacement $\chi(\vec{r}, t)$ of the molecules by the sound wave can be observed. For small oscillations in pressure, propagation can be described by the wave equation

$$\frac{\partial^2 \chi}{\partial t^2} = c^2 \cdot \Delta \chi.$$

In the expression, $c = \frac{1}{\sqrt{\kappa \rho_0}}$ is the phase velocity of the sound wave.

In medical applications, the wavelengths λ of ultrasound waves are in the range of 1 mm to 40 µm. As these wavelengths are frequently small in comparison the dimension being investigated, sound propagation in the x-direction can be described to a good approximation as plane waves: $\chi(x,t) = \chi_0 \sin(\omega t - kx)$. The amplitude of the velocity $v = \frac{\partial \chi}{\partial t}$ of the air molecules is termed the sound particle velocity: $v_0 = \omega \chi_0$.

An analogous wave equation to the molecular displacement χ can also be found for the density and the pressure. Inserting a plane wave for pressure demonstrates that the sound particle velocity v_0 is proportional to the sound pressure Δp:

$$\Delta p_0 = \rho_0 c \cdot v_0 = Z \cdot v_0$$

Sound impedance Z plays a role in ultrasound similar to that of impedance in electro-technology (there, Δp_0 corresponds to voltage U and v_0 to current I). As such, Z is also described as wave resistance. In fluids and gases, sound pressure and sound particle velocity are in phase, and Z is a real quantity. In air and water, impedance is $Z_{\text{air}} = 430\ \text{Ns/m}^3$ and $Z_{\text{water}} = 1.46 \cdot 10^6\ \text{Ns/m}^3$ respectively.

The energy density of the sound wave is

$$w = \frac{1}{2}\rho_0 v_0^2 = \frac{1}{2}\frac{\Delta p_0^2}{\rho_0 c^2}.$$

This yields, for intensity,

$$I = wc = \frac{1}{2Z}\Delta p_0^2.$$

Ultrasound diagnostics are used primarily to investigate soft tissues with low shearing stiffness. As such, consideration of longitudinal waves suffices. In solid bodies like bones, however, transverse waves can also occur. These will not be considered here.

Incident sound waves with intensity I_e are partially reflected (intensity I_r) and partially transmitted (intensity I_t) at a boundary layer between two regions with different sound impedances Z_1 and Z_2. With perpendicular incidence, the transmission coefficient is calculated as $T := \frac{I_t}{I_e} = \frac{4Z_1Z_2}{(Z_1+Z_2)^2}$, and the reflection coefficient is $R := \frac{I_r}{I_e} = \frac{(Z_1-Z_2)^2}{(Z_1+Z_2)^2}$. At incidence at angle θ_1 relative to the plumb line from the boundary layer, the law of refraction $\frac{\sin\theta_1}{\sin\theta_2} = \frac{c_1}{c_2}$, like in geometric optics, also applies; θ_2 is the angle of the transmitted wave relative to the plumb line, and c_i is the corresponding phase velocity. Similarly, at reflection at an acoustically dense medium ($Z_2 > Z_1$), a phase change of the wave by π occurs; at reflection at an optically thin medium, it does not. Furthermore, with sound transmission, there are also interference effects. As such, acoustic impedance matching can also be carried out here in order to couple the sound waves between two regions with very different sound impedance characteristics without loss. To do so, the thickness of the layer must correspond to a fourth of the sound wavelength, and the impedance of the antireflex layer must be $Z_{ar} = \sqrt{Z_1 Z_2}$. As in optics, one or more boundary surfaces can be used to focus ultrasound waves. If an ultrasound wave meets an obstacle of dimensions comparable to its wavelength, deflection effects occur.

The sound wave experiences attenuation during its propagation. In a homogeneous medium the intensity of the wave falls off exponentially: $I(x) = I_0 e^{-\mu x}$. The attenuation coefficient μ is generally comprised of an absorption component and a scattering component: $\mu = \mu_{\text{Abs}} + \mu_{\text{scat}}$. In sound absorption, sound energy is changed into other forms of energy (heat above all). In scattering at inhomogeneities of size d, the dependency of the attenuation coefficient on frequency f differs according to the scattering region. In the *geometric region* ($d \gg \lambda$), μ is independent of frequency (diffuse scattering); in the *stochastic region*, $\mu \sim f^2$ generally applies, and in the *Rayleigh region*, $\mu \sim f^4$.

In an ultrasound transducer, coupled sound waves in the body are created and the returning echo is detected. The piezoelectric effect is used to change acoustic signals into electric signals. In certain materials, an elastic deformation leads to a change in the electric polarization, and therefore to an electric potential. This principle is used in the detection of sound waves. In reverse, through the application of electric potential, sound waves can be created using a piezoelectric crystal. The sound field created depends on the geometry of the ultrasonic transducer, and can be influenced by lenses or through the simultaneous use of individual piezocrystals in an array.

Using ultrasound diagnostics, reflection or transmission measurements can be accomplished. To produce images (echography, sonography), the reflected signals that arise after short, directed sound impulses are usually used in processing. Amplitude modulation employs echolocation techniques. Using the temporal delay between the transmission of the impulse and the echo, or between echoes themselves, the duration of the sound can be calculated; using this value, the sound path and the distance to the origin of the echo signal can be determined. With brightness modulation, the echo intensity is transformed into brightness. Through the movement of the ultrasound head, an image in the direction of motion of the sound is created. This can be traced by hand, or followed by automatic mechanical or electrical systems. Through the combination of several two-dimensional images, if information on position is also registered, a three-dimensional image can be created.

Doppler ultrasound employs the Doppler effect to measure the velocity of a fluid – for example, blood in the heart or in the blood vessels. The blood cells correspond to moving transmission sources, and therefore, the frequency shift of the sound wave at flow velocity v and angle α between flow direction and the direction of the incident sound wave is described as $\frac{\Delta f}{f} = \frac{2v}{c} \cos\alpha$. With Doppler ultrasound measurements in continuous wave mode, separate senders and receivers in the measurement head are used. If the distance to the source of the Doppler signal is also to be calculated, the pulse-Doppler technique can be used. In it, the same pulses as in sonography are used, and the frequency shift of the reflected signals is also detected.

8.1 Doppler Ultrasound

? A Doppler ultrasound measurement device is used to measure the flow velocity of blood in an artery. The emitting and simultaneously receiving instrument is brought to the skin above the artery to be investigated, at angle $\alpha = 45^\circ$; the artery has a flow diameter of $d = 1.7\,\text{cm}$ (see Figure). In this case, a blood cell located exactly in the flow axis of the artery is struck with ultrasound. The frequency of the emitted sound wave is $f = 5.5\,\text{MHz}$. The Doppler device shows the response to have a frequency shift of $|\Delta f| = 920\,\text{Hz}$. The flow character of blood should be considered Newtonian (blood density is $\rho = 1{,}050\,\text{kg/m}^3$; viscosity is $\eta = 0.018\,\text{Pa s}$).

1. What is the velocity v of the blood cell being investigated? The speed of sound is $c = 1{,}500\,\text{m/s}$.
2. Under normal conditions, an average velocity of around $v_N = (0.8–0.9)\,\text{m/s}$ occurs in the artery in question. What conclusions can be drawn from the results of the inquiry?

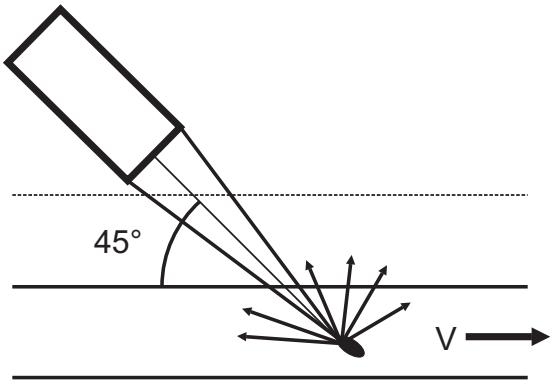

Fig. 8.1. Measurement assembly used to calculate the flow velocity of blood by Doppler ultrasound.

! 1. The frequency of the wave emitted is $f = 5.5 \cdot 10^6\,\text{Hz}$. The blood cell that reflects the wave is moving with velocity v in the artery. Here, the sender is stationary, and the reflector (the blood cell) is moving. From the frame of reference of the particle in which it is at rest, the frequency is then

$$f' = f\left(1 - \frac{v}{c}\cos\alpha\right)$$

with c as the speed of sound. This is also the frequency of the scattered wave in the frame of reference of the particle. The receiver registers the frequency

$$f'' = \frac{f'}{1 + \frac{v}{c}\cos\alpha} = f\left(\frac{1 - \frac{v}{c}\cos\alpha}{1 + \frac{v}{c}\cos\alpha}\right),$$

that is, as frequency shift

$$\Delta f = f'' - f = f\left(\frac{1-x}{1+x} - 1\right) = f\left(\frac{1-x-1-x}{1+x}\right) = f\left(-\frac{2x}{1+x}\right),$$

with $x = \frac{v}{c}\cos\alpha$. Solving for $x = \frac{v}{c}\cos\alpha$ yields

$$\frac{v}{c}\cos\alpha = \frac{\frac{\Delta f}{f}}{2 - \frac{\Delta f}{f}}$$

and therefore, for velocity,

$$v = \left(\frac{c}{\cos\alpha}\right)\left(\frac{\frac{\Delta f}{f}}{2 - \frac{\Delta f}{f}}\right) = \left(\frac{1{,}500\ m/s}{0.71}\right)\left(\frac{\frac{920}{5.5\cdot 10^6}}{2 - \frac{920}{5.5\cdot 10^6}}\right) = 0.17\ \text{m/s}.$$

2. As the blood cell observed is located in the axis of the artery, the flow velocity of the blood cell, under laminar, Newtonian conditions, is twice a great as the average velocity v_m. As such, $v_m = 0.085$ m/s. Obviously, $v_m \approx v_N$, velocity in the normal region. Although the assumption of laminar flow is justified, it can be tested by considering the Reynolds number, which must be less than $Re_G = 2{,}300$ for laminar conditions. In this case, it is

$$Re = \frac{\rho d v_m}{\eta} = \frac{1{,}050 \cdot 0.017 \cdot 0.1}{0.018} = 99.2 \ll Re_G \rightarrow \text{laminar!}$$

8.2 Impedance Matching for Sound Waves

Between the ultrasound device and the skin, a special transition layer is usually applied to achieve the highest possible transmission of energy between layers of different impedance. This is known as impedance matching. The sound waves have the form

?

$$p_n = p_{n_i} + p_{n_r} = A_n e^{i(wt-kx)} + B_n e^{i(wt+kx)}. \tag{8.1}$$

Considering the corresponding continuity conditions for pressure p and particle velocity $\dot{\chi}$, for the boundary surfaces shown in the diagram between the three layers with impedances Z_1, Z_2, and Z_3, show that for the transmission coefficient T for sound at layer thickness $l = \frac{\lambda_2}{4}$ (with λ_2 as the wavelength of the sound in the transmission medium 2), the following expression is valid:

$$T = \frac{Z_1 A_3^2}{Z_3 A_1^2} = 1, \quad \text{if } Z_2^2 = Z_1 Z_3. \tag{8.2}$$

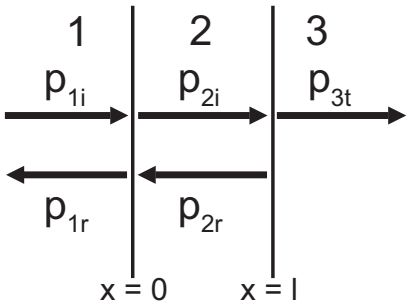

Fig. 8.2. Separating layer (2) increases the efficiency of sound transfer from (1) to (3). Here, p_{ni} stands for incident sound waves, and p_{nr} stands for reflected waves.

! For pressure wave $p = p_0 + p\,(t, x)$, at boundary surface (a|b), the continuity condition is

$$p_a = p_b$$
$$p_{ai} + p_{ar} = p_{bi} + p_{br}.$$

The index i stands for the incident wave; the index r stands for the reflected wave, and therefore,

$$A_a\, e^{i(\omega t - k_a x)} + B_a\, e^{(i\omega t + k_a x)} = A_b\, e^{i(\omega t - k_b x)} + B_b\, e^{i(\omega t + k_b x)}$$
$$A_a e^{-ik_a x} + B_a e^{ik_a x} = A_b e^{-ik_b x} + B_b e^{ik_b x}.$$

At the boundary surface (1|2) $x = 0$, and so

$$A_1 + B_1 = A_2 + B_2. \tag{8.3}$$

At the boundary surface (2|3) $x = l$, and therefore

$$A_2 e^{-ik_2 l} + B_2 e^{ik_2 l} = A_3 e^{-ik_3 l}. \tag{8.4}$$

$B_3 = 0$, as after the third layer, the wave goes on forever. For particle velocity $\dot{\eta}$, at boundary layer (a|b), the continuity condition is

$$\dot{\chi}_a = \dot{\chi}_b.$$

From the definition of acoustic impedance $Z_a = \frac{p_a}{\dot{\eta}_a}$, we have

$$\dot{\chi}_a = \frac{p_{ai} - p_{ar}}{Z_a}.$$

And therefore,

$$\frac{p_{ai} - p_{ar}}{Z_a} = \frac{p_{bi} - p_{br}}{Z_b}.$$

At boundary surface (1|2) with $x = 0$ we have

$$\frac{A_1 - B_1}{Z_1} = \frac{A_2 - B_2}{Z_2},$$

or

$$Z_2 (A_1 - B_1) = Z_1 (A_2 - B_2). \tag{8.5}$$

At boundary surface (2|3) with $x = l$, we have

$$\frac{A_2 e^{-k_2 l} - B_2^{ik_2 l}}{Z_2} = \frac{A_3 e^{-ik_3 l}}{Z_3}$$

that is,

$$Z_3 \left(A_2 e^{-k_2 l} - B_2 e^{ik_2 l}\right) = Z_2 A_3 e^{-ik_3 l}. \tag{8.6}$$

Using (8.3) and (8.5) after eliminating B_1 with $\frac{Z_a}{Z_b} = \gamma_{a,b}$ we have

$$A_1 = \frac{1}{2}\left[(1 + \gamma_{1,2}) A_2 + (1 - \gamma_{1,2}) B_2\right]. \tag{8.7}$$

Using (8.4) and (8.6), correspondingly,

$$A_2 = \frac{1}{2} e^{ik_2 l} (1 + \gamma_{2,3}) A_3. \tag{8.8}$$

Substituting A_2 from (8.8) into (8.7) and solving this equation for B_2, we have

$$B_2 = \frac{1}{2} e^{-k_2 l} (1 - \gamma_{2,3}) A_3. \tag{8.9}$$

A combination of (8.8) and (8.9) yields

$$A_1 = \frac{1}{4} A_3 \left[(1 + \gamma_{1,2})(1 + \gamma_{2,3}) e^{ik_2 l} + (1 - \gamma_{1,2})(1 - \gamma_{2,3}) e^{-k_2 l}\right]$$

or

$$A_1 = \frac{1}{2} A_3 \left[(1 + \gamma_{1,3}) \cos\, k_2 l + i (\gamma_{1,2} + \gamma_{2,3}) \sin\, k_2 l\right] \quad \text{with } \gamma = \gamma_{1,2}\gamma_{2,3}.$$

For $l = \frac{\lambda_2}{4}$ we have $k_2 l = \frac{\pi}{2}$, so

$$\frac{A_1}{A_3} = \frac{1}{2}\left[i (\gamma_{1,2} + \gamma_{2,3})\right],$$

$$\left|\frac{A_3}{A_1}\right|^2 = \frac{4}{(\gamma_{1,2} + \gamma_{2,3})^2}. \tag{8.10}$$

Expanding (8.8) with $\gamma_{1,3}$ we obtain the transmission coefficient

$$T = \frac{4\gamma_{1,3}}{(\gamma_{1,2} + \gamma_{2,3})^2} = \frac{4\gamma_{1,3}}{\gamma_{1,2}^2 + \gamma_{2,3}^2 + 2\gamma_{1,3}}. \tag{8.11}$$

This can only be $T = 1$ if the denominator from [8.8] is equal to $4\,\gamma_{1,3}$! This means that

$$\gamma_{1,2}^2 + \gamma_{2,3}^2 = 2\gamma_{1,3}$$

or

$$\left(\frac{Z_1}{Z_2}\right)^2 + \left(\frac{Z_2}{Z_3}\right)^2 = 2\,\frac{Z_1}{Z_3}.$$

Rearranging yields the equation

$$Z_2^4 + Z_1^2 Z_3^2 - 2\,Z_2^2 Z_3 Z_1 = 0$$

that is,

$$Z_2^2 = Z_3 Z_1 \pm \sqrt{Z_3^2 Z_1^2 - Z_1^2 Z_3^2} = Z_3 Z_1.$$

8.3 Bats

? A bat moves at $v_F = 5.75\ \mathrm{m/s}$. The bat encounters a mosquito moving at $v_M = 3.5\ \mathrm{m/s}$. The bat emits a sound wave of frequency $f_F' = 51\ \mathrm{kHz}$. What frequency is registered by the bat if the sound wave is reflected by the mosquito?

! In the bat's frame of reference, we have

$$f_F' = f\left(\frac{c + v_F}{c}\right)$$

with f as the frequency in the laboratory frame of reference. The frequency f_r' of the reflected wave in the mosquito's frame of reference is

$$f_r' = f_F'\left(\frac{c + v_M'}{c}\right)$$

with $v_M' = v_F + v_M$. For the frequency f_r'' of the reflected wave in the bat's frame of reference, we have

$$f_r'' = f_r'\left(\frac{c}{c - v_M}\right) = f_F'\left(\frac{c + v_M'}{c - v_M}\right).$$

With $c = 330\ \mathrm{m/s}$; $f_F' = 51\ \mathrm{kHz}$; $v_F = 5.75\ \mathrm{m/s}$; $v_M = 3.5\ \mathrm{m/s}$; and $v_M' = 9.25\ \mathrm{m/s}$ we find the numerical value

$$f_r'' = 51\ \mathrm{kHz}\left(\frac{330 + 9.25}{330 - 9.25}\right) = 53.94\ \mathrm{kHz}.$$

53.94 kHz is the frequency that the bat receives from the mosquito.

8.4 Ultrasound Transducer Array

? An ultrasound transducer is comprised of $N = 5$ individual responsive piezoelectric

crystals that are brought together perpendicular to the direction of an outgoing wave at a distance of $\Delta d = 0.25\,\text{cm}$ from one another. These transducers create sound with a frequency of $f = 310\,\text{kHz}$, which is focused in the tissue of a patient at a distance of $d = 5\,\text{cm}$ perpendicular to the crystal arrangement. What must the phase φ_n of the individual waves that exit the crystals be? That is, what time delay τ_n of the driving signal must be chosen? Assume that the middle crystal lies at the focus of the next one. The tissue has the qualities of water ($c = 1{,}500\,\text{m/s}$).

Each crystal is a point source, and the sound waves emitted from them have a displacement that depends on the distance to the source and the phase: !

$$u_n \propto e^{-i\left(-kr_n+\phi_n\right)}.$$

The distance to the desired point of focus is $r_n = \sqrt{d^2 + (n \cdot \Delta d)^2}$.
At the focus,

$$U = \sum_{n=-\frac{N}{2}}^{\frac{N}{2}} u_n \propto \sum_n e^{-i\left(-kr_n+\phi_n\right)}.$$

The intensity is $I \propto U^2$, and I is maximized when U is maximized. This is the case when φ is chosen so that $e^{-i\left(-kr_n+\phi_n\right)} = 1$; that is,

$$kr_n + \phi_n = 0.$$

Therefore, the phases must be chosen as

$$\phi_n = -k\sqrt{d^2 + (n \cdot \Delta d)^2}$$

Calculating the phase shift φ_n with respect to the middle element, we have

$$\varphi_n = \phi_n - \phi_0 = -k\sqrt{d^2 + (n \cdot \Delta d)^2} - kd$$

or $\varphi_0 = 0$, $\varphi_{\pm 1} = -0.081$, and $\varphi_{\pm 2} = -0.324$. The phase shift corresponds to a temporal delay of

$$-\tau_n = -\frac{\varphi_n}{\omega} = -\frac{\varphi_n}{2\pi f}.$$

$$\tau_1 = -41\,\text{ns},$$

$$\tau_2 = -166\,\text{ns}.$$

This corresponds to $\tau_{\pm 1} = -41\,\text{ns}$ and $\tau_{\pm 2} = -166\,\text{ns}$ – a negative time delay. The signals must be emitted earlier.

8.5 Material of an Ultrasonic Lens

? A useful ultrasonic lens must have the lowest possible reflection, and the highest possible index of refraction n. Assume that the lens is located in water, and that sound strikes it perpendicularly (that is, assume a small opening angle of the sound bundle, and a thin lens). Which of the materials listed should be chosen for the lens? To answer the question, calculate both the relative index of refraction $n = \frac{\sin\alpha_1}{\sin\alpha_2}$ (index 1: lens, index 2: water), as well as the corresponding degree of reflectance $R = \frac{I_r}{I_e}$.

Table 8.1. Density and sound velocity of different materials.

Material	Density $\rho \cdot 10^{-3}$ [kg/m³]	Sound Velocity c [m/s]
Water	1.00	1,480
Iron	7.90	5,000
Aluminium	2.71	5,200
Glass FK 1	2.27	4,900
Polystyrene	1.06	1,800
Plexiglass	1.18	1,840

! With index 1 (lens) and index 2 (water), the index of refraction is

$$n = \frac{\sin\alpha_1}{\sin\alpha_2} = \frac{c_1}{c_2}.$$

For perpendicular incidence, the degree of reflectance is then

$$R = \frac{(Z_1 - Z_2)^2}{(Z_1 + Z_2)^2}.$$

With $Z = \rho c$, the values in Table 8.2 can be obtained. As the index of refraction should be maximized, and the degree of reflectance minimized, the optimal materials are glass and polystyrene.

Table 8.2. Indices of refraction and degrees of reflectance of materials.

Material	n	R
Iron	3.4	0.86
Aluminium	3.5	0.66
Glass FK 1	3.3	0.59
Polystyrene	1.2	0.02
Plexiglass	1.2	0.04

8.6 Measurement of the Lens of the Eye using Ultrasonic Pulse-Echo Technique

?

Ultrasonic pulse-echo technique can be used to measure the thickness D of the lens of the eye. In the method, ultrasonic pulses are received by an oscilloscope. How thick is the lens if two pulses are registered by the oscilloscope with a time delay of $\Delta t_1 = 2\,\mu s$? A third pulse is detected by the oscilloscope $\Delta t_2 = 17.26\,\mu s$ after the second pulse, originating with a foreign body in the eye. How deep is this object in the eye if distance from the apex of the cornea to the lens is $d = 5.6$ mm (see 4.4)? The average velocity of sound in the lens is $\bar{c} = 1{,}630$ m/s, and the speed of sound in water is $c_{H_2O} = 1{,}480$ m/s.

!

From Figure 8.3 we have

$$2D = \bar{c} \cdot \Delta t_1.$$

Therefore,

$$D = \frac{\bar{c} \cdot \Delta t_1}{2} = \frac{1{,}630\ \text{m/s} \cdot 2 \cdot 10^{-6}\text{s}}{2} = 1.63\ \text{mm}.$$

Additionally,

$$2x = c_{H_2O} \cdot \Delta t_2$$

and

$$x = \frac{c_{H_2O} \cdot \Delta t_2}{2} = \frac{1{,}480\ \text{m/s} \cdot 17.26 \cdot 10^{-6}\ \text{s}}{2} = 12.77\ \text{mm}.$$

The separation between the foreign body and the apex of the cornea is therefore

$$y = 5.6\ \text{mm} + D + x = (5.6 + 1.63 + 12.77)\ \text{mm} = 20\ \text{mm}.$$

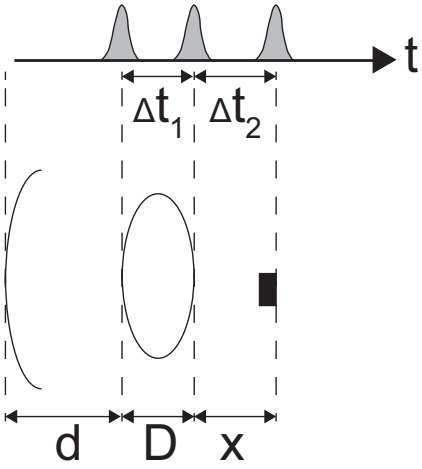

Fig. 8.3. Experimental setup and time sequence of the pulses. On the left is the cornea; in the middle is the lens, and the black box on the far right represents the foreign body in the eye.

8.7 Ultrasound Transducers

? A high-frequency generator emits an effective power of 150 W through the excitation of an ultrasonic quartz. This electro-acoustic transducer works at efficiency $\eta = 60\%$. The diameter of the quartz plate of the transducer is $d = 80$ mm.

1. What is the maximum ultrasonic intensity that can be produced by the transducer (with equal distribution over the surface of the transducer)?
2. The frequency of the device is $\nu = 900$ kHz. What is the effective value of the (alternating) pressure in the air, and in the muscles (ignore reflections)? Use: $Z_{\text{air}} = 43\,\text{g/cm}^2\text{s}$, $Z_{\text{muscle}} = 1.63 \cdot 10^5\,\text{g/cm}^2\text{s}$; $c_{\text{air}} = 331\,\text{m/s}$, $c_{\text{muscle}} = 1{,}568\,\text{m/s}$. Is this device intended for therapeutic use?

! 1. We have

$$P_{US,\max} = \eta P_{el} = 0.6 \cdot 150\,\text{W} = 90\,\text{W}.$$

$$I_{\max} = \frac{P_{US,\max}}{A} = \frac{90\,\text{W}}{\pi \cdot 40^2\,\text{mm}^2} = 17{,}905\,\text{W/m}^2 = 1.79\,\text{W/cm}^2.$$

2. The effective value of the alternating pressure can be found from

$$I = \frac{1}{2Z}\Delta p^2 = \frac{1}{Z}\Delta p_{\text{eff}}^2$$

leading to

$$\begin{aligned}\Delta p_{\text{eff}}^2(\text{air}) &= \sqrt{IZ} = \sqrt{430\,\text{kg/m}^2\text{s} \cdot 1.79 \cdot 10^4\,\text{W/m}^2} \\ &= 2{,}774\,\text{N/m}^2 = 0.028 \cdot 10^5\,\text{Pa} = 0.028\,\text{bar} = 28\,\text{mbar}\end{aligned}$$

$$\begin{aligned}\Delta p_{\text{eff}}^2(\text{muscles}) &= \sqrt{IZ} = \sqrt{1.63 \cdot 10^6\,\text{kg/m}^2\text{s} \cdot 1.79 \cdot 10^4\,\text{W/m}^2} \\ &= 170{,}813\,\text{N/m}^2 = 1.71 \cdot 10^5\,\text{Pa} = 1.71\,\text{bar}.\end{aligned}$$

The device is intended for use in muscle massage and therapy.

9 Nuclear Magnetic Resonance

Nuclear magnetic resonance imaging shows concentrations of nuclear spin. In medical applications, the nuclei in question are almost always hydrogen nuclei (^{1}H, protons), and the following discussion will be limited to these. Normally, both nuclear spin states are degenerate. If an external magnetic field $\vec{B}_0$ is applied, these split due to the nuclear Zeeman effect by an energy difference $\Delta E = \gamma \cdot B_0$. The gyromagnetic ratio γ of the nucleus gives the ratio of the magnetic moment $\vec{\mu}$ to the nuclear spin $\vec{I}\hbar$ coupled to it: $\vec{\mu} = \gamma \vec{I}\hbar$. For protons with $I = \frac{1}{2}$, $\gamma(^1\mathrm{H}) = 2.675 \cdot 10^8 \frac{\mathrm{rad}}{\mathrm{T \cdot s}}$. To encourage transitions between these two energy levels an alternating magnetic field is applied; its frequency ν_{rf} satisfies the resonance condition $h\nu_{\mathrm{rf}} = \hbar\omega_{\mathrm{rf}} \stackrel{!}{=} \Delta E = \gamma B_0 = \hbar\omega_0$. This alternating magnetic field $\vec{B}_1$ must be oriented perpendicular to the static field $\vec{B}_0 = B_0 \cdot \vec{e}_z$. In units of frequency, $\gamma(^1\mathrm{H}) \approx 43 \frac{\mathrm{MHz}}{\mathrm{T}}$; this gives, for the typical fields used in clinical applications of $B_0 = 1.5$ T, a resonant frequency of around $\nu_0 \approx 65$ MHz. ω_0, or $\nu_0 = \frac{\omega_0}{2\pi}$, is also known as the Larmor frequency.

Torque $\vec{T} = \vec{\mu} \times \vec{B}$ affects the magnetic moment $\vec{\mu}$ of the protons in a magnetic field $\vec{B}$. As the torque corresponds to the temporal change in the magnetic angular momentum $\hbar\vec{I}$, the equation of motion $\frac{d\vec{\mu}}{dt} = \vec{\mu} \times \gamma\vec{B}$ results. Because the macroscopic magnetization $\vec{M}$ is the vector sum of the magnetic moments of all protons by volume, the magnetization is given as

$$\frac{d\vec{M}}{dt} = \vec{M} \times \gamma\vec{B} = \vec{M} \times \vec{\omega}.$$

The solution to this equation of motion describes a precession of the magnetization around the magnetic field.

If the entire volume V of a biologic sample with spin density $n = \frac{N}{V}$ is brought into a Zeeman field $\vec{B}_0 = B_0 \cdot \vec{e}_z$, an equilibrium state of magnetization $\vec{M}_0 = M_0 \cdot \vec{e}_z$ occurs due to the unequal occupation of the nuclear energy levels of the protons in thermal equilibrium (at temperature T). This magnetization is proportional to the magnetic field:

$$M_0 = n \cdot \frac{(\hbar\gamma)^2 I(I+1)}{k_B T} \cdot B_0.$$

If this equilibrium magnetization is inverted by using an alternating field of a certain amplitude and duration – a π-pulse – then the angular momentum disappears, and no precession occurs. However, a slow change of the magnetization in the direction towards the equilibrium state does take place, and can be described as a function of time by the equation

$$M_z = M_0(1 - e^{-\frac{t}{T_1}}).$$

The transverse components M_x and M_y remain = 0. The characteristic time T_1 for this process is termed the longitudinal relaxation time.

If the equilibrium magnetization is pulsed through the application of a $\frac{\pi}{2}$-pulse in the $x-y$-plane perpendicular to the static magnetic field, the resulting magnetization precesses in the $x-y$ plane according to $M_x = M_0 \cdot \cos(\omega_0 t + \varphi)$, $M_y = -M_0 \cdot \sin(\omega_0 t + \varphi)$, and $M_z = 0$ around $\vec{B}_0 = B_0 \cdot \vec{e}_z$. Additionally, there is also a slow change in the amplitude of the magnetization in direction to the equilibriums state, as $M_x = M_y = 0$. This process can generally be described as exponential damping:

$$M_x = M_0 \cdot \cos(\omega_0 t + \varphi) \cdot e^{-\frac{t}{T_2}}, \quad M_y = -M_0 \cdot \sin(\omega_0 t + \varphi) \cdot e^{-\frac{t}{T_2}}.$$

The corresponding time constant T_2 is termed the transverse relaxation time.

This attenuation of the x- and y-components is subject to the conservation of energy. One contribution comes from the slightly different precession speeds of the individual magnetic moments. As the magnetization is the vector sum of these moments, this dephasing of the individual spins leads to a decay in the transverse magnetization. The origin of the differing precession speeds, and therefore of the dephasing, lies in locally fluctuating microscopic fields; influences like slight inhomogeneities ΔB_0 in the static magnetic field, which lead to slightly different resonant frequencies, also play a part. In total, the transverse relaxation rate is $\frac{1}{T_2^*} = \frac{1}{T_2} + \frac{\gamma \cdot \Delta B_0}{2}$. Independently, after the $\frac{\pi}{2}$-pulse, the M_z-components return again.

If the transverse and longitudinal relaxations are considered, the equations of movement for the magnetization – the Bloch equations – are

$$\begin{aligned}
\frac{dM_x}{dt} &= M_y \omega_o - \frac{M_x}{T_2}, \\
\frac{dM_y}{dt} &= -M_x \omega_0 - \frac{M_y}{T_2}, \\
\frac{dM_z}{dt} &= -\frac{(M_z - M_0)}{T_1}.
\end{aligned}$$

In order to induce the nuclear spins, an alternating magnetic field $\vec{B}_1$ oriented perpendicular to the Zeeman field must be applied. In order to create this, a pulse of alternating current with this frequency is sent through a coil. Because the excitation must be resonant, the necessary frequencies are in the radio-frequency region. Assuming that a solenoid coil is oriented in the x-direction, $\vec{B}_1(t) = 2B_1 \cos(\omega_{\mathrm{rf}} t + \phi)\, \vec{e}_x$. If the linear alternating field $\vec{B}_1(t)$ is decomposed into two rotating components opposite one another, only the portion of the field that precesses around $\vec{B}_0$ in the same direction as the spin is able to cause excitation. As such, the effective amplitude of the RF field $\vec{B}_1(t)$ in the case of a simple coil is just B_1. To improve efficiency, the coil is usually connected to an oscillating circuit. If power P is introduced to an oscillating circuit with Q factor Q and excitation volume V, then, for the amplitude of the alternating field, $B_1 \sim \sqrt{\frac{PQ}{V\omega_0}}$; the resonance frequency of the oscillating circuit corresponds to the Larmor frequency ω_0 of the spin. If the strength of the alternating field is fixed, the duration of the RF irradiation by which the equilibrium magnetization is effected is

determined. This then rotates under irradiation around the $\vec{B}_1$-direction according to the precession equation. The angle of the magnetization with the z-axis (Zeeman field) at time t after the beginning of the irradiation is $\theta = \omega_1 t = \gamma B_1 t$. If the duration of the irradiation is chosen so that $\theta = \frac{\pi}{2}$, then the irradiation is termed a $\frac{\pi}{2}$- or 90°-pulse and the magnetization, at the end of the RF pulse, lies in the x-y-plane. Similarly, the pulse is termed a π- or 180°-pulse if the angle of rotation is $\theta = \pi$. For typical $\vec{B}_1$ field strengths at the order of magnitude of a few mT, the necessary pulse durations for protons are in the range of μs.

The excited spins can be detected by using the Faraday effect through a receiver coil. A time-variant magnetization of the sample yields a time-dependent potential, according to Faraday's law of induction: $U \sim \frac{d\Phi}{dt}$. In this expression Φ is the magnetic flux through the coil, which is determined by the spin density. Due to the time dependency, the signal is also proportional to ω_0, and only the transverse components of the magnetization contribute (linearly) to the signal.

According to the Bloch equations, a signal is expected after the application of a $\frac{\pi}{2}$-pulse to a spin system in thermal equilibrium:

$$s(t) = s_0 \cos\left(\omega_0 t + \varphi\right) \cdot e^{-\frac{t}{T_2}}.$$

The dephasing of the spin can be partially undone by using an RF pulse of a certain duration and direction. If this rephasing pulse is applied after time $T_E/2$ after the end of the excitation pulse, a slowly building signal is observed that reaches a maximum after total time T_E; this is termed (spin) echo. After this maximum, the signal dephases again. The application of multiple rephrasing pulses allows an entire sequence of signals to be detected with just one excitation pulse. This saves a considerable amount of time in comparison to the repeated application of excitation pulses with direct detection, as, in this case, the researcher must wait between measurements each time until the equilibrium magnetization is established again. This gain in time is especially important in imaging through the use of magnetic resonance.

After an excitation pulse, all the nuclear spins in the receiver coil contribute to the signal. As such, location coding of the signals received is necessary in all three spatial dimensions. This leads to the use of a magnetic field gradient, which can, through the use of individual selectable gradients that can be turned on an off in a targeted manner (pulsed gradients). If, for example, an additional linear gradient field $\vec{B}(\vec{r}) = \vec{B}_0 + G_z \cdot z \cdot \vec{e}_z$ is applied parallel to the static magnetic field during the excitation of the nuclear spins, the resonant frequency of the spin in the sample changes linearly along the z-axis. Only the spatial region where the resonant frequency is equal to that of the incident RF field is excited, and contributes to the signal. Because, using this method, a layer can be selected, G_z is termed the slice selection gradient. Through the finite excitation bandwidth of the RF pulse, which is inversely proportional to the duration of the pulse τ_p, the thickness D of the selected layer can be determined: $\frac{1}{D} = \frac{\gamma}{2\pi} \cdot G_z \cdot \tau_\mathrm{p}$. In order to achieve a uniform excitation of the layer, the excitation pulses take the

form $\frac{\sin x}{x}$ with respect to time, corresponding to a rectangular function with respect to frequency.

By using a layer selection gradient during the excitation of the nuclear spins, a slice is selected from the object under investigation for imaging. Location encoding in the x- and y-directions is achieved through frequency/phase encoding gradients. The frequency encoding gradient is switched on as the signal is read, and is therefore called readout gradient. If this is switched in the x-direction, the precession frequency of the spin is position-dependent along this axis. If a Fourier transform of the signal is carried out, signals from different x-regions emerge at different locations in the spectrum. As such, the different portions of the signal can be connected to their corresponding locations. In order to form a three-dimensional image, the direction of the readout gradient can be changed, and multiple one-dimensional images can be combined with the assistance of projection reconstruction algorithms. Today, phase encoding is generally used in the other spatial direction (y). An experiment with the same layer selection gradient and readout gradient is repeated, and a phase encoding gradient is switched on in the y-direction at a particular point in the experiment. In each repetition, the strength of this phase encoding gradient is changed, and a new spectrum is observed. If, for example, 128 points are desired for the image in the y-direction, the experiment must be repeated 128 times as the phase encoding gradient is varied from original value $-G_y$ stepwise through zero up to $+G_y$.

The classic experiment, and workhorse in the day-to-day operations of a clinic, is the spin echo sequence. Because this method gives the best image quality it is frequently used as a reference for other methods. With other pulse sequences, a portion of the image quality or resolution is sacrificed, usually in order to achieve quicker image production. In spin echo sequencing a selective $\frac{\pi}{2}$-pulse is first applied, with a layer selection gradient. Then, for a short time, a phase encoding gradient is switched on following a selective π-pulse for echo creation. During the uptake of the signal, the readout gradient is switched on. The time from the middle of the excitation pulse to the echo's maximum is termed the echo time T_E. This experiment is repeated with different phase encoding gradient values after time T_R, during which the state of equilibrium can be re-established, until data observation for an entire layer image is complete. Typical values for digital resolution are 128, 256, or even 512 phase coding steps (and therefore points). T_E is in the range of 10–100 ms, and T_R is 0.5–3 s. If relaxation is considered, the signal amplitude of the echo is

$$S = S_0 \cdot e^{-\frac{T_E}{T_2}} \cdot (1 - e^{\frac{T_R}{T_1}}).$$

The parameters T_E and T_R can be selected, while T_1 and T_2 are determined by the sample (the tissue). If, for example, $T_R \approx T_1$ is chosen, and $T_E \ll T_2$, then the contrast of the image is most significantly influenced by the tissue parameter T_1. In choosing this T_1-weighting, the structure of the tissue can be imaged especially well. By choosing $T_R \gg T_1$ and $T_E \approx T_2$, T_2 is weighted heavily; under this condition the image is very sensitive to pathological processes in which a relatively large amount of water is present

in the tissue. For several investigations in the head or the spine regions, a pure proton density image is sometimes desired. In this case, choose $T_R \gg T_1$ and $T_E \ll T_2$. A high proton density will then have high brightness in the image. In addition to the values chosen for pulse sequence parameters, contrast media can also be used. In combination with a wide range of specialized pulse sequences, this yields enormous flexibility and versatility of MRI (magnetic resonance imaging) for medical investigations.

Analogous to the Fourier transform with respect to time, which leads to a frequency spectrum, a Fourier transform can also be carried out with respect to location. This is especially useful with MRI because the location frequencies k_x and k_y are, according to

$$k_{x,y} = \gamma \cdot \int dt\, G_{x,y}(t),$$

functions of the magnetic field gradients in the corresponding spatial directions. As such, the signal can be described as

$$S(k_x, k_y) = \int dx \int dy\, M_T(x, y) \cdot e^{-i(k_x \cdot x + k_y \cdot y)}.$$

The transverse magnetization $M_T(x, y)$ desired can be calculated through the back-transformation of the signal in k-space. An individual scan with a constant readout gradient (x-direction) corresponds to a row in k-space. In spin echo experiments, the data matrix in k-space is filled in line by line along the k_x-axis as scans progress. Image reconstruction yields a periodic image. As this periodicity is of no interest in MRI, the image region is limited to one period, the field of view (FOV). The width of this region is given by the increment Δk in k-space: $\mathrm{FOV} = \frac{2\pi}{\Delta k}$. The resolution of the image is given by the maximum value $k_{\max}$ in k-space: $\delta x = \frac{2\pi}{k_{\max}}$. The same holds for the other spatial direction y. The image information is distributed over the entire k-space, but the data in the center of the k-space have deep location frequencies (k-values), and therefore contribute information strongly to the signal-noise relationship; they contain, however, no image details. The data at the edges of k-space contain, due to their high location frequencies, information on fine structures. Due to these relationships, filters can also be used before image reconstruction, in order to enhance or suppress certain information present in the raw data. As the use of filters requires advanced knowledge of the details of their effects, only unfiltered data is generally used in everyday clinical studies.

Artifacts in MRI images have a wide range of possible origins. Motion artifacts occur due to the involuntary or physiological movement of the patient during the imaging process. Inhomogeneity artifacts occur due to faults in the devices and susceptibility effects within the body. Digital image artifacts stem from the reconstruction of the image with the assistance of Fourier transforms.

In addition to the conventional spin-echo method, gradients can be used to create an echo signal instead of a π-pulse. There are two families of pulse sequences in MRI that are based on either the spin-echo, or the gradient-echo. From these, a wide range

of pulse sequences have been developed, each with specific advantages and disadvantages. In addition to the possibility of drastically reducing the duration of the process relative to the spin-echo experiment, experiments have also been developed to investigate dynamic parameters like the motion of water molecules. These methods even allow for differentiation between diffuse and directed motion. Furthermore, through the use of hyperpolarized gases, very strong signals can be read from the lungs, and in vivo spectroscopy can be carried out. An additional and prominent area of application is functional imaging (fMRI), in which the change of signals in dependency on specific activities is observed. This allows for glimpses of how the brain functions. The foundation of these techniques is the BOLD effect (blood oxygen level dependency). Hemoglobin molecules that are bound to oxygen are diamagnetic; those without oxygen are paramagnetic. This has an effect on the signal; as such, for example, local oxygen consumption in the brain – which indicates increased activity – is made visible.

9.1 Zeeman Effect and Nuclear Spin Resonance

? Calculate:

1. The resonant frequency f of the NMR transition of protons in a magnetic field of $B = 3\,\mathrm{T}$.
2. The wavelength of photons that cause these transitions. In what range of the electromagnetic spectrum do these wavelengths occur?

! 1. For resonance with Zeeman splitting ΔE, for a proton with magneton μ_P,

$$\Delta E = \hbar\omega = hf = 2\,\mu_P B.$$

Solving for frequency yields

$$f = \frac{2\,\mu_P B}{h}.$$

Numerically, with $\mu_P = 2.79\mu_N = 1.4 \cdot 10^{-26}\,\mathrm{J/T}$, $B = 3\,\mathrm{T}$ and the Planck constant $h = 6.6 \cdot 10^{-34}\,\mathrm{Js}$ we find the resonant frequency

$$f = \frac{2\left(1.4 \cdot 10^{-26}\,\mathrm{J/T}\right) 3\,\mathrm{T}}{6.6 \cdot 10^{-34}\,\mathrm{Js}} = 127\,\mathrm{MHz}.$$

2. The wavelength is

$$\lambda = \frac{c}{f} = \frac{3 \cdot 10^8\,\mathrm{m/s}}{127\,\mathrm{MHz}} = 2.36\,\mathrm{m}.$$

This wavelength is in the radio frequency region of the spectrum, in the very high frequency (VHF) range.

9.2 Magnetization and its Relaxation

From the equation of motion for the angular momentum $\frac{d\vec{I}}{dt} = \vec{\mu}\times\vec{B}$, derive the equation of motion for magnetization $\vec{M}$.
[μ is the magnetic moment, and B is the magnetic field]

1. in a static magnetic field along the z-axis.
2. Additionally, in an RF field that rotates in the xy-plane with angular frequency ω. Relaxation processes can be ignored.
3. The equations should be modified so that the longitudinal and transverse relaxation times T_1 and T_2 are considered. What is described by these times?

1. For the torque,

$$\vec{\tau} = \frac{d\vec{I}}{dt} = \vec{\mu} \times \vec{B}.$$

The magnetic moment $\vec{\mu}$ can be expressed using $\vec{\mu} = \gamma\vec{I}$ with γ as the gyromagnetic ratio, leading to

$$\frac{d\vec{\mu}}{dt} = \gamma\frac{d\vec{I}}{dt} = \gamma\left(\vec{\mu} \times \vec{B}\right) = \gamma\begin{pmatrix} \mu_y B_z - \mu_z B_y \\ \mu_z B_x - \mu_x B_z \\ \mu_x B_y - \mu_y B_x \end{pmatrix}.$$

For $\vec{B} = \begin{pmatrix} 0 \\ 0 \\ B_0 \end{pmatrix}$ we have

$$\vec{\mu} \times \vec{B} = \begin{pmatrix} \mu_y B_0 \\ -\mu_x B_0 \\ 0 \end{pmatrix} = B_0\begin{pmatrix} \mu_y \\ -\mu_x \\ 0 \end{pmatrix}.$$

Therefore, the equation of motion is

$$\frac{d\vec{\mu}}{dt} = \gamma B_0\begin{pmatrix} \mu_y \\ -\mu_x \\ 0 \end{pmatrix}.$$

2. For

$$\vec{B} = \begin{pmatrix} B_1 \cos(\omega t) \\ B_1 \sin(\omega t) \\ B_0 \end{pmatrix}$$

we have

$$\vec{\mu} \times \vec{B} = \begin{pmatrix} \mu_y B_0 - \mu z B_1 \sin(\omega t) \\ \mu_z B_1 \cos(\omega t) - \mu_x B_0 \\ \mu_x B_1 \sin(\omega t) - \mu_y B_1 (\cos\omega t) \end{pmatrix}.$$

In a coordinate system that rotates around the z-axis with angular frequency ω,

$$B_{\text{eff}} = B_0 + B_1(\omega t) + \frac{\omega}{\gamma} = \begin{pmatrix} B_1 \\ 0 \\ B_0 + \frac{\omega}{\gamma} \end{pmatrix}$$

and therefore

$$\frac{d\vec{\mu}}{dt} = \gamma \begin{pmatrix} \mu_y \left(B_0 + \frac{\omega}{\gamma}\right) \\ \mu_z B_1 - \mu_x \left(B_0 + \frac{\omega}{\gamma}\right) \\ -\mu_y B_1 \end{pmatrix}.$$

3. Here,

$$\frac{d\vec{\mu}}{dt} = \gamma \begin{pmatrix} \mu_y B_0 - \mu_z B_1 \sin(\omega t) \\ \mu_z B_1 \cos(\omega t) - \mu_x B_0 \\ \mu_x B_1 \sin(\omega t) - \mu_y B_1 \cos(\omega t) \end{pmatrix} + \begin{pmatrix} -\frac{\mu_x}{T_2} \\ -\frac{\mu_y}{T_2} \\ -\frac{\mu_z - \mu_0}{T_1} \end{pmatrix}.$$

The longitudinal relaxation time T_1 describes the decay of the z-components of the magnetization to their equilibrium values. The transverse relaxation time T_2 describes the decay of the x- and y-components.

9.3 NMR Pulses and the Rotating Coordinate System

? In a laboratory frame of reference, the following magnetic field is applied:

$$\vec{B} = B_0 \begin{pmatrix} 0 \\ 0 \\ 1 \end{pmatrix} + B_1 \begin{pmatrix} \cos(\omega_{RF} t + \varphi) \\ 0 \\ 0 \end{pmatrix}. \tag{9.1}$$

1. What is the corresponding effective magnetic field $\vec{B}_{\text{eff}}$ in a coordinate system rotating with the Larmor frequency ω_L?
2. What happens if ω_{RF} is resonant? What role does the phase φ of the RF field play?
3. How long does it take for the magnetization to rotate by 90° and 180° if the RF field has an amplitude of $B_1 = 10^{-4}$ T?

! 1. Express the magnetization $\vec{M}$ using the unit vectors $\hat{i}$, $\hat{j}$, $\hat{k}$:

$$\vec{M} = M_x \hat{i} + M_y \hat{j} + M_z \hat{k}$$

and then,

$$\frac{d\vec{M}}{dt} = \frac{\partial M_x}{\partial t}\hat{i} + M_x \frac{\partial \hat{i}}{\partial t} + \frac{\partial M_y}{\partial t}\hat{j} + M_y \frac{\partial \hat{j}}{\partial t} + \frac{\partial M_z}{\partial t}\hat{k} + M_z \frac{\partial \hat{k}}{\partial t}.$$

For the partial derivatives with respect to time of the unit vectors, we have

$$\frac{\partial \hat{i}}{\partial t} = \omega \times \hat{i} \qquad \frac{\partial \hat{j}}{\partial t} = \omega \times \hat{j} \qquad \frac{\partial \hat{k}}{\partial t} = \omega \times \hat{k}.$$

$$\left(\frac{d\vec{M}}{dt}\right)_{\text{static}} = \left(\frac{d\vec{M}}{dt}\right)_{\text{rot}} + \vec{\omega} \times \vec{M}.$$

As $(\frac{d\vec{M}}{dt})_{\text{static}} = \gamma\, \vec{M} \times B$, we have

$$\left(\frac{d\vec{M}}{dt}\right)_{\text{rot}} = \gamma \vec{M} \times \vec{B} - \vec{\omega} \times \vec{M} = \gamma \vec{M} \times \left(\vec{B} + \frac{\vec{\omega}}{\gamma}\right) = -\gamma(\vec{B}_{\text{eff}} \times \vec{M})$$

and therefore,

$$B_{\text{eff}} = \vec{B} + \frac{\vec{\omega}}{\gamma}.$$

For $\frac{\vec{\omega}}{\gamma} = -\vec{B}_0$, $\vec{B}_{\text{eff}}$ becomes

$$\vec{B}_{\text{eff}} = \vec{B}_1 \cos(\omega_{RF}\, t).$$

In the laboratory frame of reference, $\vec{B}_{\text{eff}}$ is

$$\vec{B}_{\text{eff}} = B_1 \begin{pmatrix} \cos(\omega_{RF}\, t + \varphi) \\ 0 \\ 0 \end{pmatrix}.$$

Transforming the x- and y-components into a rotating coordinate system yields

$$\vec{B}_{\text{eff}} = B_1 \begin{pmatrix} \cos(-\omega_L\, t) & \sin(-\omega_L\, t) \\ \sin(-\omega_L\, t) & \cos(-\omega_L\, t) \end{pmatrix} \begin{pmatrix} \cos(\omega_{RF}\, t + \varphi) \\ 0 \end{pmatrix}$$

$$= B_1 \begin{pmatrix} \cos(\omega_L\, t) & \cos(\omega_{RF}\, t + \varphi) \\ -\sin(\omega_L\, t) & \cos(\omega_{RF}\, t + \varphi) \end{pmatrix}.$$

Using trigonometric identities, this becomes

$$\cos(\omega_L\, t)\cos(\omega_{RF}\, t + \varphi) = \frac{1}{2}\left[\cos\left[(\omega_L + \omega_{RF})\; t + \varphi\right] + \cos\left[(\omega_L - \omega_{RF})\; t - \varphi\right]\right],$$

$$\sin(\omega_L\, t)\cos(\omega_{RF}\, t + \varphi) = \frac{1}{2}\left[\sin\left[(\omega_L + \omega_{RF})\; t + \varphi\right] + \sin\left[(\omega_L - \omega_{RF})\; t + \varphi\right]\right].$$

The values with $(\omega_L + \omega_{RF})\, t$ are not resonant, and can therefore be ignored. Then

$$\vec{B}_{\text{eff}} = \frac{1}{2} B_1 \begin{pmatrix} \cos[(\omega_L - \omega_{RF})t - \varphi] \\ -\sin[(\omega_L - \omega_{RF})t - \varphi] \end{pmatrix}.$$

2. In the resonant case, $\omega_L = \omega_{RF}$. Then

$$\vec{B}_{\text{eff}} = \frac{1}{2} B_1 \begin{pmatrix} \cos(-\varphi) \\ -\sin(-\varphi) \end{pmatrix} = \frac{1}{2} B_1 \begin{pmatrix} \cos\varphi \\ \sin\varphi \end{pmatrix}.$$

$\vec{B}_{\text{eff}}$ is constant in a rotating coordinate system. φ describes the direction of $\vec{B}_{\text{eff}}$ in the x-y-plane.

3. For ω we have

$$\omega = \frac{d\Theta}{dt} = -\gamma B_1.$$

The flip angle is therefore

$$\Theta(t) = \int_0^t (-\gamma B_1)\, dt = \left|-\gamma B_1 t\right|.$$

The required pulse duration is

$$t = \frac{\Theta}{\gamma B_1}.$$

For $\Theta = \pi$, $t = t_{180^\circ} = \frac{\pi}{\gamma B_1}$ and for $\Theta = \pi/2$, $t = t_{90^\circ} = \frac{t_{180^\circ}}{2}$.
With $\gamma = 2.675 \cdot 10^8\ \mathrm{rad/Ts}$ and $B_1 = 1 \cdot 10^{-4}\ \mathrm{T}$ we have

$$t_{180^\circ} = \frac{\pi}{(2.675 \cdot 10^8\ \mathrm{1/Ts})\,(1 \cdot 10^{-4}\ \mathrm{T})} = 120\ \mu\mathrm{s},$$

$$t_{90^\circ} = \frac{t_{180^\circ}}{2} = 60\ \mu\mathrm{s}.$$

9.4 Fat Signal Suppression through Inversion Recovery

? In a simple measurement technique to determine relaxation time T_1 the following sequence of pulses is used:

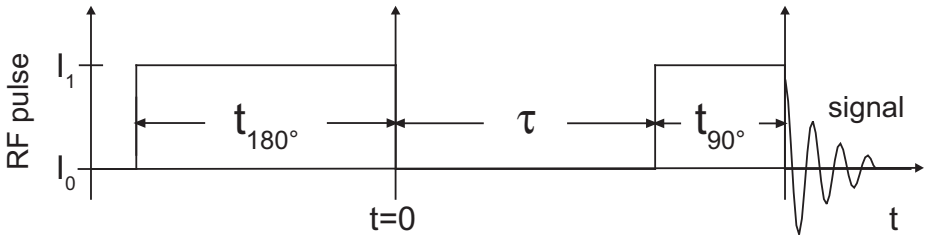

Fig. 9.1. The pulse sequence.

1. What pulse duration t_{180° must be chosen for amplitude B_1 of the RF field to invert the magnetization? How long should the second pulse be in the same field to create the maximum signal?
2. What is the time dependency of the magnetization $M_z(t)$ after the 180°-pulse if the system is in equilibrium before the first pulse?
3. What must τ be so that z-magnetization is $M_z(\tau) = 0$?

4. Tissue comprised of water (${}_{\mathrm{H_2O}}T_1 = 1.2\,\mathrm{s}$) and fat (${}_{\mathrm{fat}}T_1 = 260\,\mathrm{ms}$) is to be investigated.
   (a) Why will image reconstruction in the MRI be made more difficult by the presence of fat within the tissue, with respect to frequency coding?
   (b) How can the methods here be used to suppress the signal from the fat? How strongly will the signal of water be suppressed in the process?

1. Equilibrium is

$$M\left(-t_{180^\circ}\right) = \begin{pmatrix} 0 \\ 0 \\ M_0 \end{pmatrix}.$$

The first pulse inverts this state

$$M(0) = \begin{pmatrix} 0 \\ 0 \\ -M_0 \end{pmatrix}.$$

The pulse lengths are

$$t_{180^\circ} = 2\,t_{90^\circ} = \pi\left(\gamma B_1\right)^{-1}.$$

2. The equation of motion for the z-component is

$$\dot{M}_z = -\left(\frac{M_z - M_0}{T_1}\right).$$

For $M_z(0) = -M_0$ the solution is

$$M_z\,(t) = M_0\left(1 - 2\,e^{-t/T_1}\right).$$

3. Using the condition $M_z\,(\tau) = 0$ we have

$$0 = M_0\left(1 - 2\,e^{-\tau/T_1}\right) \quad \Rightarrow \quad 2\,e^{-\tau/T_1} = 1.$$

Solving for τ

$$\tau = T_1 \ln 2.$$

4. Due to differing material characteristics, the z-magnetizations of fat and water decay with different time constants.
   (a) Due to the influence of chemical shifting on the location coding, two overlaid images that are spatially displaced are produced in the MRI image reconstruction.
   (b) If the 90°-pulse is applied at exactly the moment at which the z-magnetization of the fat disappears (${}_{\mathrm{fat}}M_z = 0$), only the remaining magnetization of the water in the (x, y)-plane will be captured. Only a weakened signal can be measured, but it is not disturbed by signals from fat in other parts of the sample.

$$\tau = {}_{\mathrm{fat}}T_1 \ln 2.$$

$$_{H_2O}M_z(\tau) = M_0\left(1 - 4e^{-_{fat}T_1/_{H_2O}T_1}\right) = 72\%\ M_0.$$

As the signal measured is proportional to the magnetic flux through the receiver coil, and therefore to magnetization, the signal from water is reduced by 28%.

9.5 Gradient Echo

? There are two large families of MRI pulse sequences: those based on spin echoes, and those that use gradient echoes to produce signals. The signal of a gradient echo experiment is given by

$$S = S_0 e^{-\frac{T_E}{T_2^*}}\left(1 - e^{-\frac{T_R}{T_1}}\right).$$

Here, T_E is the echo time, and T_R is the repetition time.

1. Describe the process of such an experiment according to the pulse diagram.
2. If this sequence of pulses is used in an MRI experiment, what must the parameters T_E and T_R be to obtain a T_1-weighting? What is this T_1 weighting generally used to do?
3. How would a T_2^*-weighting be accomplished, and what would it be used to do?
4. What is PD (proton density) weighting, and how must the parameters be chosen to achieve it?

! 1. The initialization pulse of length t_{init} breaks the magnetization out of equilibrium.

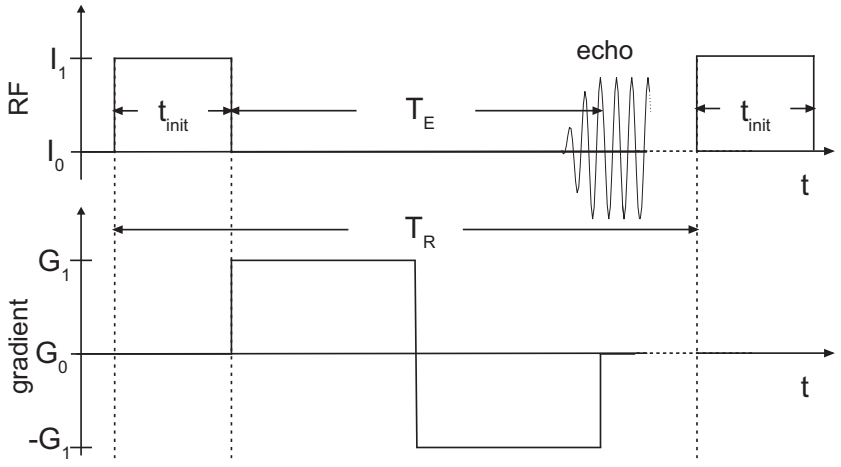

Fig. 9.2. Pulse sequence of a gradient echo experiment. Above: radiofrequency pulses. Below: serial magnetic field gradient.

Directly after this pulse, the gradient with strength G_1 is applied. After time $\frac{1}{2}T_E$ after the end of the initialization pulse, the polarity of the gradient is flipped, so that after another period of time $\frac{1}{2}T_E$ the echo maximum is achieved. After the echo there is a waiting period in which the magnetization can relax, until the sequence is carried out again. The repetition time T_R describes the amount of time that passes between repetitions of the initialization pulse. As such, the time parameters can be used to achieve weighting with respect to the time constants T_1 and T_2^* for signal production.

2. If T_E is set to be as small as possible, $S \approx S_0(1 - e^{-\frac{T_R}{T_1}})$. This means that the contrast between different T_1 is expressed strongly. Long T_1-times are expected with fluids, while tissues usually have a short T_1. As such, an edema (swelling) or a region full of blood will produce a dark image, while the neighboring tissue will be light. T_E set as small as possible is, however, not the optimum. (An optimization can only be achieved through effective pulse sequencing.)
3. If T_R is set long, so that the T_1-relaxation can go on as long as possible, it is possible to determine the contrast of T_2^*. Fluids tend to show up light with T_2^*-weighting, while tissues comprised of water and fat are resolved in shades of gray. Usually, undesired substances in the patient show up bright; as such, T_2^*-weighting is often used in diagnosing illnesses.
4. S_0 is proportional to M_{xy}, which again depends on the z-magnetization at the beginning of the 90°-pulse. Here, the equilibrium magnetization, which is proportional to proton density, also plays a role (see also Exercise 9.6).
   If T_E is chosen to be short, and T_R to be long, a signal is obtained that primarily depends on S_0 (M_{xy}). This weighting was especially frequently used in the early days of MRI, when T_2^*-weighting took too much time. PD weighting can be used to differentiate between cortical bones and meniscus.

9.6 Contrast in MRI Imaging

In an MRI experiment, tissue with different T_1- and T_2-times in two different regions, but the same proton density throughout, is to be investigated. In inversion recovery preparation, the z-magnetization is first recorded (at time $t = 0$, the magnetization of both regions is rotated by 180°). After time T, a 90°-pulse is applied. ?

1. Determine an expression for the Michelson contrast $C = \frac{I_2 - I_1}{I_2 + I_1}$ of the signal measured (after the 90°-pulse) of the two regions of tissue. Show that the contrast, depending on measurement time t (the time difference $t - T$), is

$$C(t - T) = \frac{1 - \xi e^{-\frac{t-T}{\phi}}}{1 + \xi e^{-\frac{t-T}{\phi}}}.$$

Using the parameters given, derive expressions for ξ and ϕ. Note that the receiver coil detects xy-magnetization.

2. In an inversion recovery experiment on the human brain, the inversion time is (T) 200 ms. How long must the measurement time (time after the 90°-pulse until the next inversion) be at a minimum, if a contrast of at least 80% between gray material (${}_AT_1 = 600$ ms, ${}_AT_2 = 100$ ms) and cerebrospinal fluid (${}_BT_1 = 1155$ ms, ${}_BT_2 = 145$ ms) is desired?

!

1. Solving the Bloch equation for M_z (first in analogy to Exercise 9.4),

$$\frac{dM_z}{dt} = \frac{M_0 - M_z}{T_1}.$$

Boundary conditions: $M_z(t = 0) = {}_iM_z$ and M_0 is the equilibrium magnetization

$$\frac{dM_z}{M_0 - M_z} = \frac{1}{T_1}dt,$$

$$\ln \frac{M_0 - M(t)}{M_0 - {}_iM_z} = -\frac{t}{T_1},$$

$$M_0 - M(t) = (M_0 - {}_iM_z)\, e^{-\frac{1}{T_1}}.$$

Due to the complete inversion at time $t = 0$ we have ${}_iM_z = -M_0$, and therefore,

$$M(t) = M_0 \left(1 - e^{-\frac{t}{T_1}}\right) + {}_iM_z e^{-\frac{t}{T_1}}.$$

2. Due to the array of coils in MRI tomography, the signal I is proportional to the value of xy-magnetization: $I \propto |M_{xy}|$. In order to make the z-magnetization visible, the signal is captured with a 90°-pulse at time T in the xy-plane. This means that $M_{xy} = M_z(T)$, which leads to the expression

$$M_{xy}(t) = \left(M_0 \left(1 - e^{-\frac{T}{T_1}}\right) + {}_iM_z e^{-\frac{T}{T_1}}\right) e^{-\frac{t-T}{T_2}}.$$

For both materials with different T_1 and T_2, there are, therefore, different signal strengths and corresponding contrast:

$$I_A(t) = \left({}_AM_0 \left(1 - e^{-\frac{T}{AT_1}}\right) + {}_{iA}M_z e^{-\frac{T}{AT_1}}\right) e^{-\frac{t-T}{AT_2}},$$

$$I_B(t) = \left({}_BM_0 \left(1 - e^{-\frac{T}{BT_1}}\right) + {}_{iB}M_z e^{-\frac{T}{BT_1}}\right) e^{-\frac{t-T}{BT_2}}.$$

To isolate numerator and denominator of the contrast,

$$\begin{aligned} I_B - I_A = &\left({}_AM_0 \left(1 - e^{-\frac{T}{AT_1}}\right) + {}_{iA}M_z e^{-\frac{T}{AT_1}}\right) e^{-\frac{t-T}{AT_2}} \\ &- \left({}_BM_0 \left(1 - e^{-\frac{T}{BT_1}}\right) + {}_{iB}M_z e^{-\frac{T}{BT_1}}\right) e^{-\frac{t-T}{BT_2}}. \\ I_B + I_A = &\left({}_AM_0 \left(1 - e^{-\frac{T}{AT_1}}\right) + {}_{iA}M_z e^{-\frac{T}{AT_1}}\right) e^{-\frac{t-T}{AT_2}} \\ &+ \left({}_BM_0 \left(1 - e^{-\frac{T}{BT_1}}\right) + {}_{iB}M_z e^{-\frac{T}{BT_1}}\right) e^{-\frac{t-T}{BT_2}}. \end{aligned}$$

The equilibrium magnetization is calculated using the proton density $M_0 = \sum \mu \propto \rho_{p^+}$. If the proton density is the same for both materials, and both components begin with inverted z-magnetization,

$$I_B - I_A = {}_AM_0\left(1 - 2e^{-\frac{T}{AT_1}}\right)e^{-\frac{t-T}{AT_2}} - {}_BM_0\left(1 - 2e^{-\frac{T}{BT_1}}\right)e^{-\frac{t-T}{BT_2}},$$
$$I_B + I_A = {}_AM_0\left(1 - 2e^{-\frac{T}{AT_1}}\right)e^{-\frac{t-T}{AT_2}} + {}_BM_0\left(1 - 2e^{-\frac{T}{BT_1}}\right)e^{-\frac{t-T}{BT_2}},$$

$$\begin{aligned}\frac{I_B - I_A}{I_B + I_A} &= \frac{{}_AM_0\left(1 - 2e^{-\frac{T}{AT_1}}\right)e^{-\frac{t-T}{AT_2}} - {}_BM_0\left(1 - 2e^{-\frac{T}{BT_1}}\right)e^{-\frac{t-T}{BT_2}}}{{}_AM_0\left(1 - 2e^{-\frac{T}{AT_1}}\right)e^{-\frac{t-T}{AT_2}} + {}_BM_0\left(1 - 2e^{-\frac{T}{BT_1}}\right)e^{-\frac{t-T}{BT_2}}} \\ &= \frac{\left(1 - 2e^{-\frac{T}{AT_1}}\right)e^{-\frac{t-T}{AT_2}} - \frac{{}_BM_0}{{}_AM_0}\left(1 - 2e^{-\frac{T}{BT_1}}\right)e^{-\frac{t-T}{BT_2}}}{\left(1 - 2e^{-\frac{T}{AT_1}}\right)e^{-\frac{t-T}{AT_2}} + \frac{{}_BM_0}{{}_AM_0}\left(1 - 2e^{-\frac{T}{BT_1}}\right)e^{-\frac{t-T}{BT_2}}} \\ &= \frac{1 - \frac{\left(1-2e^{-\frac{T}{BT_1}}\right)}{\left(1-2e^{-\frac{T}{AT_1}}\right)}e^{-\left(\frac{1}{BT_2} - \frac{1}{AT_2}\right)(t-T)}}{1 + \frac{\left(1-2e^{-\frac{T}{BT_1}}\right)}{\left(1-2e^{-\frac{T}{AT_1}}\right)}e^{-\left(\frac{1}{BT_2} - \frac{1}{AT_2}\right)(t-T)}} \\ &= \frac{1 - \xi e^{-\frac{t-T}{\phi}}}{1 + \xi e^{-\frac{t-T}{\phi}}}.\end{aligned}$$

Here, ξ is the ratio of both proton densities (of the equilibrium magnetizations) $(\frac{{}_BM_0}{{}_AM_0})$,

$$\xi = \frac{\left(1 - 2e^{-\frac{T}{BT_1}}\right)}{\left(1 - 2e^{-\frac{T}{AT_1}}\right)}.$$

Additionally,

$$\phi^{-1} = \left(\frac{1}{{}_BT_2} - \frac{1}{{}_AT_2}\right).$$

ϕ^{-1} can be interpreted as the effective T_2-time.

3. If $T = 200\,\text{ms}$, ${}_AT_1 = 600\,\text{ms}$, ${}_AT_2 = 100\,\text{ms}$, ${}_BT_1 = 1155\,\text{ms}$, ${}_BT_2 = 145\,\text{ms}$ the parameters have the following values: $\xi = \frac{1-2\cdot1.2}{1-2\cdot1.4} = 0.78$ and $\phi = 59.2\,\text{ms}$. As such,

for contrast of 80%, we need

$$\begin{aligned}
0.8 &= \frac{1-\xi e^{-\frac{t-T}{\phi}}}{1+\xi e^{-\frac{t-T}{\phi}}},\\
0.8\left(1+\xi e^{-\frac{t-T}{\phi}}\right) &= 1-\xi e^{-\frac{t-T}{\phi}},\\
-0.2 &= -1.8\xi e^{-\frac{t-T}{\phi}},\\
\frac{0.2}{1.8} &= \xi e^{-\frac{t-T}{\phi}},\\
59.2\,\text{ms}\cdot\ln\left(\frac{0.2}{1.8\cdot 0.78}\right) &= t-T,\\
t-T &= 115.37\,\text{ms}.
\end{aligned}$$

After 115.37 ms the contrast exceeds 80% − 315.37 ms after inversion. A disadvantage of this method is the necessity of repeated measurements. Because each experiment must begin from equilibrium, a long total measurement time is required.

9.7 BOLD

? If activity has occurred in the brain, the body overcompensates by delivering oxygen-rich blood to the corresponding region. As oxygenated blood is diamagnetic, and deoxygenated blood is paramagnetic, T_2^* changes. How does T_2^* change through the **B**lood-**O**xygenation-**L**evel-**D**ependent-Signal (BOLD), and what influence does this have on a reconstructed T_2^*-weighted image?

! Diamagnetic blood has a susceptibility closer to that of tissue; the magnetic field of diamagnetic blood is less distorted than the magnetic field of paramagnetic blood. Due to the higher homogeneity of the magnetic field in the region of diamagnetic blood, T_2^* is longer. A T_2^*-weighted image therefore possesses greater intensities in regions with oxygenated blood. The time between cell activity and maximum BOLD signal is roughly 5 s, and the return to normal conditions takes around 30 s.

9.8 FOV and Resolution

? An object is given in k-space by $F(k_x, k_y)$.

1. What is the relation between the size of a pixel in position space, and the field of view (FOV) in k-space?
2. A gradient of $G = 1\,\text{mT/m}$ is applied for $t = 0.6\,\text{ms}$ in $N = 256$ steps. What is the smallest step width Δk, and the FOV in k-space? How big is a pixel in position

space? Assume that the gradient field $\vec{G}$ is point-symmetric around the center of the layer.

3. What must the gradient G_{new} be chosen to be so that at $t_{\text{new}} = 0.4\,\text{ms}$ acquisition time, the same resolution and the same FOV are obtained?

1. The FOV is given by the number of steps N and the step width Δk in the corresponding space $N\Delta k$: **!**

$$\Delta x = \frac{2\pi}{N\Delta k} = \frac{2\pi}{\text{FOV}_k}.$$

2. Considering the point symmetry of $\vec{G}$,

$$\text{FOV}_k = 2 \cdot 2\pi\, G\, t\, \gamma = 4\pi \cdot 1\,{}^{\text{mT}}/_{\text{m}} \cdot 0.6\,\text{ms} \cdot 2.675 \cdot 10^{8}\,{}^{\text{rad}}/_{\text{T s}} = 2{,}017\,\text{m}^{-1},$$

and the smallest unit in k-space is $\Delta k = \frac{\text{FOV}_k}{N} = \frac{2{,}017\,\text{m}^{-1}}{256} = 7.88\,\text{m}^{-1}$. A pixel in position space is therefore $\Delta x = \frac{2\pi}{\text{FOV}_k} = \frac{2\pi}{2.017}\,\text{mm} = 3.11\,\text{mm}$.

3. As the values are not dependent on one another, it is sufficient to require that one of them remains; for example, $\text{FOV}_k = 2{,}017\,\text{m}^{-1} \propto G\,t$, and therefore

$$G_{\text{new}} = \frac{G \cdot t}{t_{\text{new}}} = 1.5\,{}^{\text{mT}}/_{\text{m}}.$$

9.9 Slice Selection

To determine location in a 3 T MRI tomography, the static magnetic field $\vec{B}_0$ with gradient field $\vec{G}$ is applied ($|\vec{G}| = 2\,{}^{\text{mT}}/_{\text{m}}$). The following relationship for magnetic field strength applies: **?**

$$B = B_0 + \vec{r} \cdot \vec{G}.$$

The signals are received during measurement duration of $\tau_r = 10\,\text{ms}$.

1. What frequency resolution and what spatial resolution can be achieved using this device?
2. What is the bandwidth of the expected signal if the density of the layer in this system is 5 mm?
3. A squaring demodulator multiplies the incoming signal by $e^{-i\omega_0 t}$. What happens to the signal in frequency space – why would this demodulator be used, and what should ω_0 be chosen to be?
   [gyromagnetic ratio $\gamma = 8.5\pi \cdot 10^{7}\,{}^{1}/_{\text{sT}}$]

1. Temporal resolution: **!**
   For the sampling interval we have $t = \frac{\tau_r}{N}$, and therefore, sampling frequency is $f_{\max} = \frac{1}{t} = \frac{N}{\tau_r}$. The incident frequencies are therefore 0, $\frac{1}{\tau_r}$, $\frac{2}{\tau_r}$,$\frac{3}{\tau_r}$,…, $\frac{(N-1)}{\tau_r}$, with

resolution

$$\Delta f = \frac{1}{\tau_r} = 100\,\text{Hz}.$$

Spatial resolution:
Generally, between the resonant frequency and the applied magnetic field, we have

$$\omega = \gamma B \;\rightarrow\; \Delta\omega = \gamma \Delta B.$$

The value of the magnetic field changes in spatial dependency on the gradient G

$$B = B_0 + \vec{r}.\vec{G}.$$

This yields a difference for B between two points separated at Δr of

$$\Delta B = B(\vec{r} + \Delta\vec{r}) - B(\vec{r}) = \Delta\vec{r} \cdot \vec{G}.$$

leading to a relationship to frequency resolution

$$\Delta\omega = 2\pi\Delta f = \gamma\Delta\vec{r} \cdot \vec{G}.$$

If $\Delta\vec{r}$ is small enough that it connects two minimally resolvable points, we have

$$\Delta r_{\text{min}} = \frac{2\pi\Delta f}{\gamma G} = \frac{2\pi\ 100\,\text{Hz}}{8.5\pi\ \cdot\ 10^7 \frac{1}{\text{sT}}\ 2^{\text{mT}/\text{m}}} = 0.118\,\text{mm}.$$

2. The bandwidth can be calculated by substituting the maximum separation of points in the layer for Δr:

$$\Delta f_b = \frac{8.5\pi\ \cdot\ 10^7 \frac{1}{\text{sT}}\ 2\,^{\text{mT}}/_{\text{m}}\ 5\,\text{mm}}{2\pi} = 425\,\text{Hz}.$$

3. A shift in frequency space leads to modulation in the time domain, and vice versa: $F(\omega - \omega_0) \rightleftarrows e^{-i\omega_0 t} f(t)$. The modulator eliminates the contribution of B_0 components if frequency is set to $\omega_0 = \gamma B_0$.

9.10 Longitudinal Relaxation Time

? A 180°-RF pulse inverts the equilibrium magnetization M_0 of a sample of water (proton signal). Calculate, using the Bloch equation, the temporal behavior of the return to equilibrium, $M_z(t)$. How long does it take, with a longitudinal relaxation time of $T_1 = 1\,\text{s}$, until 90% of M_0 is restored? What is M_0 in a sample of water in a field of $B_0 = 2\,\text{T}$ and at temperature $T = 36{,}5\,^\circ\text{C}$?

The Bloch equation is

$$\frac{dM_z}{dt} = -\frac{M_z - M_0}{T_1} \; ; \; M_z(t=0) = -M_0.$$

Using it, we have the temporal behavior of the return to equilibrium

$$M_z = M_0\left(1 - 2 \cdot e^{-\frac{t}{T_1}}\right).$$

Until 90% of the equilibrium magnetization is restored, the time t_g that passes is

$$0.9M_0 = M_0\left(1 - 2 \cdot e^{-\frac{t_g}{T_1}}\right).$$
$$t_g = -T_1 \cdot \ln\, 0.05 = -1\,\text{s} \cdot \ln 0.05 \approx 3\,\text{s}.$$

For the calculation of the equilibrium magnetization, we need the number of spins per volume V (also designated n). As the proton signal is measured, and both protons of the water molecule contribute to the signal, we have

$$n = \frac{N_{\text{Spins}}}{V} = \frac{2N_{H_2O}}{V}.$$

The number of water molecules N_{H_2O} can be calculated from the density ρ of water and the molar mass $m_{\text{mol}}(H_2O)$ (m is the mass in kg, n_{mol} is the number of moles, N is the number of particles, and N_A is the Avogadro constant):

$$\rho = \frac{m}{V} = \frac{n_{\text{mol}} m_{\text{mol}}}{V} = \frac{N m_{\text{mol}}}{N_A V} \Rightarrow \frac{N_{H_2O}}{V} = \rho \frac{N_A}{m_{\text{mol}}}.$$
$$m_{\text{mol}}(H_2O) = 2 \cdot 1\,\text{g/mol} + 16\,\text{g/mol} = 18\,\text{g/mol}.$$

We have

$$n = \frac{2N_{H_2O}}{V} = 2\rho\frac{N_A}{m_{\text{mol}}} = 2 \cdot 1\,\text{g/cm}^3 \cdot \frac{6 \cdot 10^{23}\,\#/\text{mol}}{18\,\text{g/mol}} =$$
$$= 6.7 \cdot 10^{22}\,\#/\text{cm}^3 = 6.7 \cdot 10^{28}\,\#/\text{m}^3.$$

The equilibrium magnetization of the water sample is therefore

$$M_0 = n\frac{\gamma^2\hbar^2 I(I+1)}{3kT}B_0$$
$$= 6.7 \cdot 10^{28}\,\#/\text{m}^3 \cdot \frac{(2.675 \cdot 10^8\,1/\text{Ts})(6.626 \cdot 10^{-34}\,\text{Js})^2\,\frac{1}{2}\left(\frac{1}{2}+1\right)}{3 \cdot 1.38 \cdot 10^{-23}\,\text{J/K} \cdot 310\,\text{K} \cdot (2\pi)^2} 2\,\text{T}$$
$$= 6.2 \cdot 10^{-3}\,\text{A/m}.$$

9.11 Frequency and Phase Encoding

1. What is the frequency difference f of two point objects (protons) in a magnet with a separation in the direction of the gradient of $s = 10\,\text{cm}$ from one another? The readout gradient is $G_x = 2\,\text{mT/m}$.

2. A phase encoding gradient of $G_y = 0.1\ {}^{\mathrm{mT}}/_{\mathrm{m}}$ is switched on for 2 ms, with 0.5 ms of linear buildup time, and the same amount of fall-off time. What is the phase difference of the spins from the first part of the exercise?
[gyromagnetic ratio $\gamma = 2.675 \cdot 10^8 \cdot {}^{1}/_{\mathrm{Ts}}$]

! 1. For frequency encoding, we have

$$\Delta\omega = 2\pi\Delta f = \gamma G_x \Delta x.$$

Therefore, the frequency difference is

$$\Delta f = \frac{1}{2\pi}\gamma G_x \Delta x = \frac{1}{2\pi} \cdot 2.675 \cdot 10^8\, {}^{1}/_{\mathrm{Ts}} \cdot 2 \cdot 10^{-3}\, {}^{\mathrm{T}}/_{\mathrm{m}} \cdot 0.1\ \mathrm{m} = 8.515\ \mathrm{kHz}.$$

2. The phase gradient increases linearly from the beginning, remains constant, and falls off linearly. In total, for the phase difference, we have

$$\begin{aligned}
\Phi &= \gamma \int dt\, G_y \Delta y \\
&= \gamma \Delta y \left\{ \frac{1}{2} \cdot 0.5\ \mathrm{ms} \cdot G_y + 1\ \mathrm{ms} \cdot G_y + \frac{1}{2} \cdot 0.5\ \mathrm{ms} \cdot G_y \right\} \\
&= \frac{3}{2}\gamma G_y \Delta y \cdot 1\ \mathrm{ms} \\
&= \frac{3}{2} \cdot 2.675 \cdot 10^8\, {}^{1}/_{\mathrm{Ts}} \cdot 0.1 \cdot 10^{-3}\, {}^{\mathrm{T}}/_{\mathrm{m}} \cdot 0.1\ \mathrm{m} \cdot 10^{-3}\ \mathrm{s} \\
&= 4.01\ \mathrm{rad} = 230^{\circ}.
\end{aligned}$$

9.12 Gradient Strength and Field of View (FOV)

? The phase encoding gradient G_y is varied from $-G_{\max}$ to $+G_{\max}$ in an MRI reading; the gradient pulse has a total duration of 2 ms, with an increase and decrease time of 0.5 ms. What maximum gradient strength $G_{\max}$ is necessary if a measurement field (FOV) of 200 mm with resolution 256 points is to be phase coded?
[gyromagnetic ratio $\gamma = 2.675 \cdot 10^8\, {}^{1}/_{\mathrm{T \cdot s}}$]

! The phase change due to the gradient pulse is

$$\Phi = \gamma \int dt\, G_y y = \gamma \left\{ \frac{1}{2} \cdot 0.5\ \mathrm{ms} + 1\ \mathrm{ms} + \frac{1}{2} \cdot 0.5\ \mathrm{ms} \right\} G_y y = 1.5\ \mathrm{ms} \cdot \gamma G_y y.$$

In measuring, there should be no ambiguity. This means that a phase encoding step causes a phase of 2π over the entire FOV.

$$\Rightarrow 2\pi = 1.5\ \mathrm{ms} \cdot \gamma G_y \cdot \mathrm{FOV}.$$

As such, the required phase gradient is

$$G_y = \frac{2\pi}{\gamma \cdot 1.5\,\text{ms} \cdot \text{FOV}} = \frac{2\pi}{1.5\,\text{ms} \cdot 2.675 \cdot 10^8\,{}^1\!/_{\text{Ts}} \cdot 0.2\,\text{m}} = 7.83 \cdot 10^{-5}\,{}^{\text{T}}\!/_{\text{m}}.$$

The maximum gradient strength is therefore

$$G_{\max} = 128 \cdot G_y = 10\frac{\text{mT}}{\text{m}}.$$

9.13 Muscle Stimulation Using Pulsed Gradients

The lower limit for the simulation of a muscle is at induced current density $j = 1\,{}^{\text{A}}\!/_{\text{m}^2}$. Is this current density achieved in a muscle with conductivity $\sigma = 0.4\,{}^{\text{S}}\!/_{\text{m}}$ and an external radius of $R = 9\,\text{cm}$? Calculate the current density at the external surface of the muscle if the pulsed magnetic fields are applied parallel to the axis of the muscle at rate $\frac{dB}{dt} = 60\,{}^{\text{T}}\!/_{\text{s}}$. ?

The external surface of the muscle can be considered as a conductor loop in which the time-dependent magnetic field gives rise to a potential !

$$U = A \cdot \dot{B} = \pi R^2 \cdot \dot{B}$$

according to Faraday's law of induction. This corresponds to a field strength in the tangential direction of

$$E = \frac{U}{2\pi R} = \frac{\pi R^2 \cdot \dot{B}}{2\pi R} = \frac{R \cdot \dot{B}}{2}.$$

This leads to a current density

$$j = \sigma E = \sigma \frac{R \cdot \dot{B}}{2} = 0.4\,{}^{\text{Sv}}\!/_{\text{m}} \cdot \frac{0.09\,\text{m}}{2} \cdot 60\,{}^{\text{T}}\!/_{\text{s}} = 1.08\,{}^{\text{A}}\!/_{\text{m}}.$$

As this is somewhat above the boundary value, stimulation of the muscle is possible.

9.14 Multislice Technique In Spin-Echo Procedure

In a spin-echo experiment, with echo time chosen as $T_E = 15\,\text{ms}$, a cycle of data readouts concludes after 25 ms. The repetition time, however, is $T_R = 500\,\text{ms}$ due to the desired contrast. As the data readout is already complete at 25 ms, though, the repetition time can be used effectively; for example, during this time, other raw data from additional layers can be obtained. This technique is called multislice imaging. ?

1. How many layers in total can be measured during time T_R?
2. The desired resolution is 256 rows and 256 columns. What is the total measurement time?

! 1. The number of layers is, at most,

$$N = \frac{T_R}{T_D} = \frac{500\ \text{ms}}{25\ \text{ms}} = 20.$$

In reality, it is usually somewhat smaller.

2. The total time is

$$t_{\text{ges}} = N_{Ph} \cdot T_R = 256 \cdot 500\ \text{ms} = 128\ \text{s}.$$

9.15 Turbo Spin-Echo Sequences

? In a turbo-spin-echo sequence (TSE, also known as Fast Spin Echo – FSE), with T_2-weighting, multiple rows of raw data are taken from the same layer after excitation with a 90°-pulse. This occurs as multiple 180°-refocusing pulses are used to get an echo. These 180°-refocusing pulses, one after the other, are equidistant. So that more raw data can be obtained, each refocusing pulse has another phase coding gradient. More details are given in the Figure.

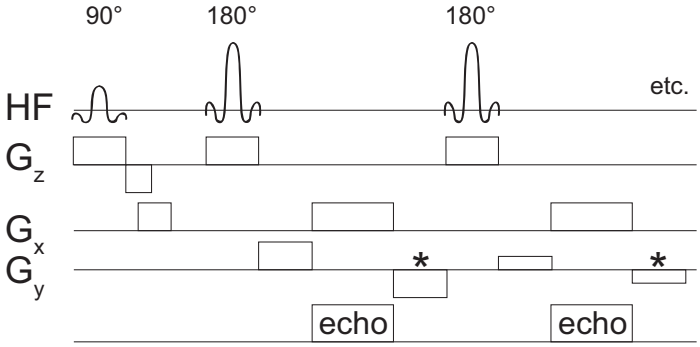

Fig. 9.3. Principles of a TSE sequence. *HF* is the high frequency stimulation, G_z is the layer selection gradient, G_x is the readout gradient, and G_y is the phase coding gradient. The first echo belongs to another raw data row as the second, as can be seen in the different phase coding gradients. After each readout of the echo, the phase coding gradient used must be reversed so that another row of raw data can be acquired. These additional gradients are marked with asterisks. (In the image, multislice technique is not considered.)

A TSE sequence for T_2-weighting delivers an echo every 15 ms, and the echo train is 150 ms long from the beginning of the first gradient to the end of the last. Ten layers are to be measured, at a resolution of 200 rows and 256 columns.

1. How many echoes occur in the echo train?
2. How many echo trains are necessary to achieve the desired resolution?

3. The TSE can be combined with the multislice technique described in Exercise 9.14. If all layers are to be measured in T_R, what is the minimum repetition time $T_{R,\min}$?
4. How long does the measurement last when using this minimum repetition time $T_{R,\min}$, if four accumulations are used to raise the signal-to-noise ratio?
5. How long would the same measurement last with accumulation with a conventional spin-echo with repetition time 2 s?
6. Does obtaining more rows of raw data using TSE sequencing lead to problems with T_2-weighting? If so, what are these problems?

1. In an echo train,
$$N_{\text{echoes}} = \frac{150\ \text{ms}}{15\ \text{ms}} = 10$$
echo trains pass. This corresponds to ten rows in the image.
2. To achieve the desired resolution,
$$N_{EZ} = \frac{N_{Ph}}{N_{\text{echoes}}} = \frac{200}{10} = 20$$
echo trains are required.
3. An echo train lasts for $t_{EZ} = 150$ ms. If all ten layers are to be observed during T_R the required minimum repetition time is
$$T_{R,\min} = 10 \cdot 150\ \text{ms} = 1.5\ \text{s}.$$
4. Under the boundary conditions given, the measurement lasts
$$t_{\text{measurement}} = 4 \cdot 20 \cdot T_{R,min} = 120\ \text{s}.$$
5. The conventional spin-echo would have lasted, for an accumulation with ten layers and 200 rows,
$$t_{\text{measurement,SE}} = 10 \cdot 200 \cdot 2\ \text{s} = 4{,}000\ \text{s}$$
6. As different rows of raw data are received at different times, they have different T_2-weightings.

Another effect of the TSE sequencing is that some tissues, in spite of equal echo time, resolve somewhat differently. For example, the fat signal is slightly increased with TSE. The origin of this effect is that multiple 180°-pulses suppress certain interactions (J-modulations). This leads to a longer decay for the signal.

9.16 Radiation Protection in MRI (HF Absorption)

1. Determine the specific absorption rate SAR (of absorbed HF power) in W/kg of a turbo-spin sequence with 11 echoes per pulse train. To simplify, assume that the

180 RF pulse lasts for 2.5 seconds, and has an median voltage amplitude of 150 V. The 90°-pulse has the same duration as the 180°-pulse. The sequence should be applied to 15 layers, with a repetition time of $TR = 4\,\mathrm{s}$. Furthermore, assume that half of the power is absorbed, and that the application of wave resistance is perfectly at $50\,\Omega$. The absorbed power is distributed evenly across a body of mass 60 kg.

2. By how many degrees would the body have warmed up after an hour under the HF power from (1) if the body was comprised of water only, and no cooling mechanism was available?

!

1. The power of a 180°-pulse is

$$P_{180} = \frac{U^2}{R} = \frac{(150\,\mathrm{V})^2}{50\,\Omega} = 450\,\mathrm{W},$$

and the energy is

$$E_{180} = P_{180}\, t_p = 450\,\mathrm{W} \cdot 2.5 \cdot 10^{-3}\mathrm{s} = 1.125\,\mathrm{J}.$$

For a 90°-pulse with the same length as the 180°-pulse, the HF field strength must be halved; therefore, the flip angle is

$$\Theta = \omega_1 t_p = \gamma B_1 t_p,$$

and the RF magnetic field strength is proportional to the applied voltage

$$B_1 \sim \sqrt{I} \propto \sqrt{P} \propto U.$$

This leads to the power of the excitation pulse

$$P_{90} = \frac{(U/2)^2}{R} = \frac{1}{4} P_{180} = 112.5\,\mathrm{W} \;\Rightarrow\; E_{90} = 0.2812\,\mathrm{J}.$$

The total energy of the TSE sequence is

$$E_{\mathrm{tot}} = 15 \cdot (1 \cdot E_{90} + 11 \cdot E_{180}) = 15 \cdot (0.2812\,\mathrm{J} + 11 \cdot 1.125\,\mathrm{J}) = 190\,\mathrm{J}.$$

The average power is

$$\bar{P} = \frac{E_{\mathrm{tot}}}{T_R} = \frac{190\,\mathrm{J}}{4\,\mathrm{s}} = 47.46\,\mathrm{W}.$$

Therefore, as only half of the power is absorbed by the body,

$$\mathrm{SAR} = \frac{1}{2} \cdot \frac{\bar{P}}{m} = \frac{47.46\,\mathrm{W}}{2 \cdot 60\,\mathrm{kg}} = 0.4\,{}^{\mathrm{W}}/_{\mathrm{kg}}.$$

2. For weight 60 kg, the energy absorption after an hour is

$$E = \mathrm{SAR} \cdot m \cdot t = 0.4\,{}^{\mathrm{W}}/_{\mathrm{kg}} \cdot 60\,\mathrm{kg} \cdot 3600\,\mathrm{s} = 86.4\,\mathrm{kJ},$$

and with the specific head of water $c_W = 4.187\,{}^{\mathrm{kJ}}/_{\mathrm{kg\,K}}$, the increase in temperature is

$$\Delta T = \frac{E}{m\, c_W} = \frac{86.4\,\mathrm{kJ}}{60\,\mathrm{kg}\, 4.187\,{}^{\mathrm{kJ}}/_{\mathrm{kg\,K}}} = 0.34\,{}^{\circ}\mathrm{C}.$$

10 Nuclear Diagnostics and Positron Emission Tomography

Nuclear diagnostics utilizes radioactive elements to make functional processes in the human body visible. To some extent, these techniques can show how these processes play out over time. Frequently, the introduction of radioactive isotopes offers a unique opportunity to follow how material is taken in by the body, processed, stored, and excreted. Morphological information (for example, the position and shape of the body's organs), though, is better obtained with other imaging techniques like ultrasound, X-rays, and magnetic resonance imagining (MRI).

Nuclear diagnostics is divided into two distinct areas: scintigraphy, and the investigation of kinetics. Scintigraphy involves the measurement of the spatial distribution of applied radioactivity in the body at a particular point in time. Kinetics is concerned with the changes in the distribution of this radioactivity in the body over time. It involves some procedures that are completed without any imaging. Kinetics is not determined using only radioactive decay, but also by the physiological processes of the body. For nuclear diagnostic investigations, a radioactive isotope is generally introduced into the patient's body; this can be achieved by injection into the bloodstream, by swallowing into the gastrointestinal tract, or by inhalation into the lungs. In order to track the radioactivity to be measured to the desired part of the body, tracers are introduced. These are radioactively marked molecules that reveal whether they are participating in the processes to be studied (for example, metabolism), or which diffuse into the target organs. The information desired from the nuclear diagnostic study determines what molecules can be introduced as tracers.

The decay of a radioactive nucleus is described by the law of decay:

$$N(t) = N_0 e^{-\lambda t}.$$

Here, $N(t)$ is the number of radioactive nuclei still present at time t, N_0 is the original number of radioactive nuclei at the moment of application $t = 0$, and λ is the rate of decay (decay constant). This is inversely proportional to the half-life $T_{1/2}$, after which exactly half of the radioactive nuclei originally present are still there: $T_{1/2} = \frac{\ln 2}{\lambda}$. The activity $A(t)$ of an amount of radioactive material is defined as the number of decays per unit time,

$$A(t) := -\frac{dN}{dt} = A_0 e^{-\lambda t},$$

and is measured in becquerels (Bq). Earlier, the unit curie (Ci) was used. It was defined as the activity of a gram of radium-226; later, though, $1\,\text{Ci} = 3.7 \cdot 10^{10}\,\text{Bq}$ was defined.

In nuclear diagnostics, the amount of activity introduced into the body is known, and can be calculated for subsequent points in time using the decay period from the law of decay. The goal of nuclear diagnostic measurement is to determine when and

where in the body this activity is distributed. As such, $A(x, y, z, t)$ is measured. Typical activities in nuclear medicine diagnostics are in the range of between 100 MBq and 1 GBq – that is, $10^8 - 10^9$ decays per second. Only nuclides with half-lives in the range from a few seconds to a few hours can be used. Shorter half-lives correspond to nuclides that decay too quickly to be used in a meaningful way; with longer half-lives, measurement times are very long, and the radiation exposure for the patient is too high.

The nuclides that occur in nature have half-lives much too long, are not nearly radio-chemically pure enough, are often radiotoxic, and do not emit only the desired kind of radiation. As such, the radionuclides that are used in nuclear medicine diagnostics are created artificially in a nuclear reactor or with a cyclotron. Technetium-99m performs a particularly significant role in nuclear medicine because it emits only gamma radiation (the m refers to a metastable state of the nucleus), and as such does not expose the patient to much radiation. Production of technetium-99m from molybdenum-99 is an example of the production of radionuclides; this process is accomplished in a nuclear reactor through neutron capture or nuclear fission. It is then brought into the clinic in lead containers, where the molybdenum-99 with a half-life of 66.7 seconds changes into metastable technetium-99m with half-life of 6 hours. The resulting pertechnetate is, unlike the molybdenum compound, soluble in water; as such, it can be washed out, drawn into a syringe, and injected. After around a week of daily "milking", the radionuclide generator is used up, and must be exchanged for a new one.

For image-producing measurements of gamma rays, scintillation counters have gained favor because they have high sensitivity, good energy resolution, and short cool-down periods. They are usually utilized in the range of 50–511 keV. A scintillation counter is principally comprised of a scintillation crystal (scintillator) with an adjacent photomultiplier. An incident gamma quantum is absorbed by the scintillator and creates optical photons, the number of which is proportion to the energy that the gamma quantum imparted to the crystal. With full absorption a flash of light occurs, and its quantity of photons is a direct measurement for the energy of the incident gamma quantum. These photons strike the photocathode of the photomultiplier, and photoelectrodes are created. These are amplified through a cascade of downstream dynodes by the "avalanche effect", until they finally strike the anode and are detected electrically. The scintillator must have the correct size for the measurement, be very homogeneous, and be as optically transparent as possible. Its size can vary from 1 cm^2 to $40 \cdot 60$ cm^2 for full-body scintigrams. So that the entire energy of the gamma quanta is detected, the scintillator must be thick enough, and its material must have a high effective atomic number. As such, thallium-doped sodium iodide crystals (NaI:Tl), or BGO ($Bi_4Ge_3O_{12}$), is used. While luminous efficiency is highest for NaI:Tl, the likelihood of absorption is higher for BGO.

In addition to the number of photons, their origin must also be determined for the measurement of activity distribution in the body. In order to obtain information on the

direction from which a detected photon comes, collimators are used. The dispersion direction of scattered gamma quanta no longer contains any information about their origin positions, and they only contribute to image noise. As these scattered gamma quanta lose energy at each scattering, a discriminator that only registers events in a predetermined range of momenta is used. This requires a compromise in determining the threshold so that noise is suppressed, while avoiding the elimination of too many primary gamma quanta of lower energies.

In order to simultaneously observe the distribution of activity in a large region of the body, the gamma camera was developed. In it, a fairly small number of photomultipliers (around 40 to 100) are connected over a resistance network so that despite their small number, a high spatial resolution can be achieved. As the quality of a gamma camera depends crucially on the uniform and stable sensitivity of the individual photoreceptors, regular calibration with a known source of distribution is necessary.

Planar scintigraphy corresponds to x-ray projection in that, as with the gamma camera, line integrals of activity are measured. SPECT, or Single Photon Emission Computer Tomography, is based on the same principle as planar scintigraphy – except it produces three-dimensional images. Analogously to x-ray computed tomography (CT), a computer reconstructs the three-dimensional distribution of activity using many different projections. There are multiple designs of SPECT devices; these have one or more measuring heads, which rotate around the patient in circular or elliptical fashion. Filtered rear projection is the most frequently utilized reconstruction technique. If it is possible to consider the absorption processes in the body along with a comparative model of the object, iterative reconstruction delivers better images.

In positron emission tomography (PET), the molecular marking of the tracers is done with a positron emitter. The average path length of a positron emitted in tissue is several millimeters, before the particle annihilates with an electron. At annihilation, two gamma quanta appear, each with an energy of 511 keV, that move away in essentially opposite directions. Due to the finite momentum of electrons and positrons, there is a change in angle of the relative directions of propagation of both photons of only around 0.3°. As opposed to SPECT, no collimators are necessary; yield is demonstrably greater, and the necessary activity applied is therefore significantly less. The decay of positrons is demonstrated by a coincidence measurement. To perform it, detectors are positioned around the patient. In order to achieve a high probability of proof, the detectors must be adjusted to the relatively high energy of 511 keV. The standard material for PET detectors is BGO. For image reconstruction, like when using SPECT, both rear projection and iterative processing can be used.

10.1 Decay Reaction

A sample contains 1.5 µg of pure nitrogen $^{13}_{7}\mathrm{N}$ with half-life $T_{1/2} = 10$ min.

1. How many nuclei N_0 are there at the beginning?

2. What is the activity at the beginning, and after 1 h?
3. How long is it until activity falls below $1\ \mathrm{s}^{-1}$?

!

1. As molar mass is $13\ \mathrm{g/mol}$, 13 g of the isotope contain ${}^{13}_{7}\mathrm{N} \rightarrow 6.02 \cdot 10^{23}$ nuclei (Avogadro constant N_A). There are $1.5\ \mathrm{mg} = 1.5 \cdot 10^{-6}\mathrm{g}$ available. Therefore,

$$\frac{N_0}{N_A} = \frac{1.5 \cdot 10^{-6}}{13}$$

and therefore, $N_0 = 6.94 \cdot 10^{16}$.

2. For $t_{1/2}$ the relationship is

$$T_{1/2} = \frac{\ln 2}{\lambda}.$$

The decay constant λ becomes

$$\lambda = \frac{0.693}{10\ \mathrm{min}} = \frac{0.693}{600\ \mathrm{s}} = 1.16 \cdot 10^{-3}\mathrm{s}^{-1}.$$

At time $t = 0$ we have

$$\frac{dN}{dt}|_{t=0} = \lambda N_0 = \left(1.16 \cdot 10^{-3}\ \mathrm{s}^{-1}\right)\left(6.94 \cdot 10^{16}\right) = 8.05 \cdot 10^{13}\ \mathrm{s}^{-1}.$$

After $t_1 = 1\ \mathrm{h} = 3{,}600\ \mathrm{s}$, activity is

$$\begin{aligned}\frac{dN}{dt}|_{t=1\,\mathrm{h}} &= \left(\frac{dN}{dt}|_{t=0}\right) e^{-\lambda t_1} = \left(8.05 \cdot 10^{13}\ \mathrm{s}^{-1}\right) \exp\left[\left(-1.16 \cdot 10^{-3}\ \mathrm{s}^{-1}\right)(3{,}600\ \mathrm{s})\right] \\ &= 1.23 \cdot 10^{12}\ \mathrm{s}^{-1}.\end{aligned}$$

3. The amount of time t_S after which $\frac{dN}{dt} \leq 1\ \mathrm{s}^{-1}$, can be calculated as

$$\exp\left(-\lambda t_S\right) = \frac{\frac{dN}{dt}|_{t=t_S}}{\frac{dN}{dt}|_{t=0}} = \frac{1\ \mathrm{s}^{-1}}{8.05 \cdot 10^{13}\ \mathrm{s}^{-1}} = 1.25 \cdot 10^{-14}.$$

Therefore,

$$t_S = \frac{\ln\left(-1.25 \cdot 10^{-14}\right)}{1.16 \cdot 10^{-3}\mathrm{s}^{-1}} = \frac{32}{1.16 \cdot 10^{-3}}\ \mathrm{s} = 7.67\ \mathrm{h}.$$

10.2 Age of a Mummy

? During a person's lifetime, the isotope ratio of ${}^{14}_{6}\mathrm{C}$ to ${}^{12}_{6}\mathrm{C}$ in the bones is constant at $1.3 \cdot 10^{-12}$. ${}^{14}_{6}\mathrm{C}$ is a radioactive isotope that decays with half-life $t_{1/2} = 5730\ \mathrm{a}$. After death, the ${}^{14}_{6}\mathrm{C}$ isotope decays. As such, the current activity of a bone can be used to determine the bone's age (as was done with Ötzi the Iceman). As an example, consider a bone

with carbon mass $m_K = 200\,\text{g}$. Activity is measured as $16\,\text{s}^{-1}$. How old is the bone (that is, how long ago t_A did the person die)?

The entire mass of carbon $m_K = 200\,\text{g}$ corresponds to $n_C = 200/12 = 16.7$ moles, and therefore to $n_C N_A = 16.7 \cdot 6 \cdot 10^{23} = 10^{25}$ atoms. Of these, there are $N_{C14} = 10^{25} \cdot 1.3 \cdot 10^{-12} = 1.3 \cdot 10^{13}$ ^{14}C nuclei. From $t_{1/2} = \frac{\ln 2}{\lambda}$ we have the decay rate

$$\lambda = \frac{0.693}{5{,}730\,\text{a}} = 3.83 \cdot 10^{-12}\,\text{s}^{-1}.$$

So, for the original activity of $^{14}_{6}$C, we have

$$\frac{dN}{dt}|_{t=0} = \lambda N_0 = \left(3.83 \cdot 10^{-12}\,\text{s}^{-1}\right)\left(1.3 \cdot 10^{13}\right) = 50\,\text{s}^{-1}$$

and for the activity dependent on the age t_A of the bone

$$\frac{dN}{dt}|_{t=t_A} = \left(\frac{dN}{dt}|_{t=0}\right)\exp\left(-\lambda t_A\right) = 16\,\text{s}^{-1}.$$

Solving for t_A we have

$$t_A = \frac{1}{\lambda}\ln\left(\frac{\frac{dN}{dt}|_{t=0}}{\frac{dN}{dt}|_{t=t_A}}\right) = \frac{1}{3.83 \cdot 10^{-12}\,\text{s}^{-1}}\ln\left(\frac{50}{16}\right) = 3.0 \cdot 10^{11}\,\text{s} = 9{,}506\,\text{a}.$$

10.3 Iodine

The iodine isotope $^{131}_{53}$I is used clinically to diagnose malfunctions of the thyroid gland. Calculate the activity

1. immediately after the patient is given 550 μg,
2. after 1, 2, and 10 hours,
3. after 6 months and 1 year. The half-life $T_{1/2}$ of $^{131}_{53}I$ is 8.02 days.

1. The original quantity N_0 of nuclei of $^{131}_{53}$I is

$$N_0 = \frac{m_J}{M_J}N_A = \frac{\left(5.5 \cdot 10^{-4}\,\text{g}\right)\left(6.02 \cdot 10^{23}\,\text{mol}^{-1}\right)}{131\,\text{g/mol}} = 2.53 \cdot 10^{18}.$$

2. From $T_{1/2} = 8.02\,\text{d} = 6.93 \cdot 10^5\,\text{s} = \frac{\ln 2}{\lambda}$ we have

$$\lambda = \frac{0.693}{6.93 \cdot 10^5\,\text{s}} = 10^{-6}\,\text{s}^{-1}$$

and

$$\frac{dN}{dt}|_{t=0} = \lambda\, N_0 = \left(1 \cdot 10^{-6}\right)\left(2.53 \cdot 10^{18}\,\text{s}^{-1}\right) = 2.53 \cdot 10^{12}\,\text{s}^{-1}.$$

$$\frac{dN}{dt}|_{t=t_j} = N_0 e^{-\lambda t_j} = 2.53 \cdot 10^{12}\exp\left[-\left(10^{-6}\,\text{s}^{-1}\right) \cdot (3{,}600\,\text{s/h})\; t_j\right]$$

$$= 2.53 \cdot 10^{12}\exp\left[-\left(0.0036\,\text{h}^{-1}\right)\, t_j\right].$$

For $t_j = 1\,\text{h}, 2\,\text{h}, 10\,\text{h}$, the activities are

t_j [h]	1	2	10
$\frac{dN}{dt}\vert_{t=t_j}\left[\text{s}^{-1}\right]$	$2.53 \cdot 10^{12}$	$2.52 \cdot 10^{12}$	$1.77 \cdot 10^{12}$

3. For 6 months with $t_j = 1/2\,\text{a} = \frac{8{,}766\,\text{h}}{2} = 4{,}383\,\text{h}$ and for a year with $t_j = 8{,}766\,\text{h}$ we find

	6 months	1 year
t_j [h]	4,383	8,766
$\frac{dN}{dt}\vert_{t=t_j}\left[\text{s}^{-1}\right]$	$3.54 \cdot 10^{5}$	$4.95 \cdot 10^{-2}$

10.4 Photomultiplier

? A photomultiplier is to be used for the detection of γ radiation. In front of the barium oxide cathode of the photomultiplier, there is a scintillator that changes the γ photons into visible light.

1. What maximum wavelength λ_0 should the photons emitted from the scintillator have if they are to be detected, if the work function for barium oxide is 1.3 eV?
2. Assume that such a photon strikes the barium oxide cathode and liberates an electron. At a minimum, how high must the electric potential of the first barium oxide dynode be if, when the original electron strikes, $Z = 5$ secondary electrons will be liberated?
3. The photomultiplier is made up of $N = 10$ dynodes in total. These are arranged such that the same number of secondary electrons is always liberated for each incident electron. How long does it take for the signal to reach the anode? The separation of the dynodes is $\delta = 1\,\text{cm}$.
4. In this case, how high is the measurable electron current I at the exit point if photons with power $P = 2.08 \cdot 10^{-16}\,\text{W}$ strike the cathode?

! 1. With h as Planck's constant, f as the frequency, and m_e as the electron mass,

$$hf = W_a + \frac{m_e v^2}{2}.$$

With velocity $v = 0$, we have $W_a = hf$ for the energy. Because $\frac{hc}{\lambda_0} = W_a$, for the wavelength, we have

$$\lambda_0 = \frac{hc}{W_a} = \frac{\left(6.63 \cdot 10^{-34}\,\text{Js}\right)\left(3 \cdot 10^{8}\,\text{m/s}\right)}{1.3\,\text{eV}\left(1.6 \cdot 10^{-19}\right)\text{J/eV}} = 9.52 \cdot 10^{-7}\,\text{m} = 952\,\text{nm}.$$

2. The original electron is absorbed. In order to be able to liberate Z electrons, its energy must be at least

$$E_{\text{sec}} = W_a Z.$$

With charge q, $E_{\text{sec}} = q\Delta V$. Therefore, $q\Delta V = W_a Z$ – that is,

$$\Delta V = \frac{W_a Z}{q} = \frac{1.3\,\text{V}\,5}{1.6 \cdot 10^{-19}\,\text{C}} = 6.5\,\text{V}.$$

3. Under the assumption that the dynode and anode have the same potential and the same separation δ, the acceleration of the electron is

$$a = \frac{q\Delta V}{\delta m_e}.$$

Set the original velocity = 0. Therefore, the electron travels $\delta = a\,\tau^2/2$ at constant acceleration. The time τ between two dynodes is therefore

$$\tau = \delta\sqrt{\frac{2\,m_e}{q\,\Delta V}}.$$

In total, there are $(N + 1)$ flight paths. The entire flight time is therefore

$$\tau_{\text{tot}} = (N + 1)\ \delta\ \sqrt{\frac{2\,m_e}{q\,\Delta V}} = 4.6 \cdot 10^{-7}\text{s} = 146\,\text{ns}.$$

4. For power P, we have

$$P = \frac{dE}{dt} = \frac{hc}{\lambda_0}\left(\frac{dN_\gamma}{dt}\right)$$

rearranged,

$$\frac{dN_\gamma}{dt} = \frac{P\,\lambda_0}{hc}.$$

With $N_e = Z^N N_\gamma$ we have

$$Z^{-N}\,\frac{dN_e}{dt} = \frac{P\,\lambda_0}{hc}.$$

As $\frac{dN_e}{dt}\,e^- = I$, we have

$$Z^{-N} \cdot I = \frac{P\,\lambda_0}{hc}$$

that is,

$$I = \frac{P\lambda_0 Z^N}{hc}e^- = P\,\frac{Z^N e^-}{E_0}.$$

Numerically, with $P = 2.08 \cdot 10^{-16}\,\text{W} = 1.3 \cdot 10^3\,\text{eV/s}$,

$$I = \left(1.3 \cdot 10^3\,\text{eV/s}\right)\left(\frac{5^{10}e^-}{1.3\,\text{eV}}\right) = 4.8\,\mu\text{A}.$$

10.5 Radionuclide Generator

? Assume that molybdenum ^{99}Mo will decay only to technetium ^{99m}Tc in a radionuclide generator. The technetium decays with a half-life of $T_{1/2} = 6.03\,\text{h}$. At time $t = 0$, all technetium is washed out, and as such only N_1 molybdenum atoms are available.

1. Determine the rate equation for ^{99m}Tc and integrate it under the assumption that the number N_1 does not change significantly due to decay.
2. After how many hours is the number of ^{99m}Tc constant up to 10^{-3}?

! 1. We have

$$\frac{dN_2}{dt} = \lambda_1 N_1(t) - \lambda_2 N_2(t) \approx \lambda_1 N_1 - \lambda_2 N_2(t).$$

Use $N_2(t) = C_1 + C_2 e^{-\lambda_2 t}$. From the original condition $N_2(0) = 0 = C_1 + C_2$ we have $C_1 = -C_2 = C$ and $N_2(t) = C(1 - e^{-\lambda_2 t})$. Substituting into the equation of motion yields

$$\frac{dN_2}{dt} = \lambda_2 C e^{-\lambda_2 t} = \lambda_1 N_1 - \lambda_2 C(1 - e^{-\lambda_2 t}).$$

Solving for C, we have

$$C = \lambda_2 C e^{-\lambda_2 t} = N_1 \frac{\lambda_1}{\lambda_2}.$$

Therefore, the number of ^{99m}Tc nuclei is

$$N_2(t) = N_1 \frac{\lambda_1}{\lambda_2}(1 - e^{-\lambda_2 t}).$$

2. The relative deviation from equilibrium is $e^{-\lambda_2 t}$. The value falls to $< 10^{-3}$ after time

$$t_g = \frac{3 \cdot \ln 10}{\lambda_2} = \frac{3 \cdot \ln 10}{\ln 2} \cdot T_{1/2} = 9.97 \cdot 6.03\,\text{h} = 60\,\text{h}.$$

10.6 Positron Emission Tomography

? In PET, a radiopharmaceutical is introduced into an organism. The annihilation of an emitted positron and an electron from surrounding tissue produces two photons that can be found by using a detector matrix.

1. If positrons and electrons create a quasi-atom with their spins directed opposite one another, this exotic structure is termed positronium. Show that in the decay of such a particle, two photons are emitted in opposite directions if the speeds of the electron and the positron are ignored. What energy E does such a photon have (in eV)?
2. What effects occur if (a) the positronium quasi-atom possesses kinetic energy, and (b) what relevance does this have for image production?

3. For ortho-positronium, the spins of the individual particles are aligned. What does this mean with respect to the emitted photons and their energy?
4. The organism is comprised of coaxial layers with absorption coefficients $\mu(r)$. Similarly, there is a coaxial, circular detector matrix around the organism with diameter 20 cm. What is the probability that both photons strike the detector matrix if a slow positronium quasi-atom decays 4 cm from the center?

$$\mu(r) = \begin{cases} \mu_{\text{blood}} = 0.18\,\text{cm}^{-1} & r \leq 3\,\text{cm} \\ \mu_{\text{tissue}} = 0.17\,\text{cm}^{-1} & 3\,\text{cm} < r < 7\,\text{cm} \\ 0 & 7\,\text{cm} \leq r \end{cases}$$

1. Energy balance for the positronium quasi-atom:

$$\begin{aligned} E = E_{p^+} + E_{e^-} &= \frac{1}{2} m_{p^+} v_{p^+}^2 + m_{p^+} c^2 + \frac{1}{2} m_{e^-} v_{e^-}^2 + m_{e^-} c^2 \\ &= \frac{1}{2} m_e \left(v_{p^+}^2 + v_{e^-}^2 \right) + 2 m_e c^2. \end{aligned}$$

For vanishing velocity, we then have

$$E = 2 m_e c^2.$$

For the energy of the photons, we have $E_\gamma = \frac{1}{2} E = m_e c^2 = 511\,\text{keV}$.
For the positronium quasi-atom, the total sum of the spins must add up to zero. Photon emission must also be limited to an even number; as the probability of emission of more than two photons is very small, however, it can be assumed that in this decay two photons are emitted.
The momentum balance is

$$\vec{P} = \vec{p}_{p^+} + \vec{p}_{e^-} = 0 = \vec{p}_{\gamma_1} + \vec{p}_{\gamma_2}$$

and therefore

$$\vec{p}_{\gamma_1} = -\vec{p}_{\gamma_2}$$

2. If the kinetic energy of the positronium quasi-atom is > 0, the following changes occur:
   (a) The Doppler effect causes a shift in the photon wavelength.
   (b) The angle between the two photons becomes $< 180^\circ$, and the photons do not move in opposite directions. This spoils the location coding.
3. Charge parity (charge conjugation operator $\hat{C}$, eigenvalue C) is a conserved quantity in electromagnetic interactions. The ortho-positronium quasi-atom has a total spin of $J = 1$ and $C = -1$. As the charge conjugation operator functions multiplicatively, for n photons, we have $C = (-1)^n$. If the ortho-positronium decays and in so doing emits photons, the charge parity of the photon system must correspond to that of the ortho-positronium; therefore, it decays to an odd number of photons. Due to the Lorentz invariance, though, cases of $n < 3$ are forbidden. The energy spectrum is continuous.

4. The probability W of detecting both photons is given by the product of the individual probabilities w_γ that a photon on path l from the point of decay to the detector will not be absorbed:

$$W = w_{\gamma_1} w_{\gamma_2}.$$

The individual probabilities are given as

$$w_{\gamma_1} \propto \exp\left[- \int_x^{x_1} \mu(l) dl \right]$$

and considering the opposite directions of propagation,

$$w_{\gamma_2} \propto \exp\left[\int_x^{x_2} \mu(l) dl \right].$$

Therefore, we have

$$W \propto \exp\left[- \int_x^{x_1} \mu(l) dl + \int_x^{x_2} \mu(l) dl \right] \exp\left[- \int_{x_2}^{x_1} \mu(l) dl \right].$$

This term is independent of the coordinate x, the position at which the positronium quasi-atom undergoes recombination.
Considering the corresponding symmetries, we have

$$\begin{aligned} W &\propto \exp\left[- 2\left(\int_{3\,\mathrm{cm}}^{7\,\mathrm{cm}} \mu_{\mathrm{tissue}} dl + \int_0^{3\,\mathrm{cm}} \mu_{\mathrm{blood}} dl \right) \right] \\ &\propto \exp\left[-2 \left(\mu_{\mathrm{tissue}} l \Big|_{3\,\mathrm{cm}}^{7\,\mathrm{cm}} + \mu_{\mathrm{blood}} l \Big|_0^{3\,\mathrm{cm}} \right) \right] \\ &\propto \exp\left[-2 \left(0.17 \cdot 4 + 0.18 \cdot 3 \right) \right] = 8.7\%. \end{aligned}$$

This value is normalized to the probability that both photons are detected in a vacuum.

11 Reconstruction Techniques

For all image-producing techniques, a picture of material properties or of a physical process is created. In order to accomplish this, subsequent processing of raw data, or the reconstruction of the objects from individual projections, is necessary in most cases. Especially important is the fact that measurement data are only available discretely, and are often cluttered with different artifacts. As such, analysis requires a detailed understanding of individual measurement techniques, and knowledge of the mathematical evaluation of measurement data.

In nuclear diagnostics, the most frequently utilized reconstruction technique is filtered back projection; it is used, for example, in single photon computed tomography (SPECT) and also serves as the basis of algorithms for computer tomography. This technique has the advantage of a relatively short image reconstruction time in comparison to iterative methods, as the computational cost is significantly lower. With SPECT the speed of quanta is relatively high, so analysis is limited to relatively small spatial frequencies. The resulting image resolution is in the range of 10 to 15mm. Better images can be obtained through iterative reconstruction techniques if absorption processes in the body are also taken into account. A direct reconstruction of the image produces a number of artifacts. The most important causes of these are:

- the collimators employed do not produce ideal beams of radiation, and the scattered radiation is not completely suppressed
- useful radiation is partially absorbed on its way to the detector

A possible correction to this problem is to compare two measurements in opposite directions. Without differences in absorption, both should yield identical line integrals. Considering absorption in the tissue and assuming first that the tissue is homogeneous with respect to absorption, the radiation that reaches a detector in the x-direction in this system has the value $S_A = k \cdot A \cdot \exp(-\mu x)$, where k is a calibration factor, A is the activity at position x, and μ represents the average attenuation coefficient of the tissue. A corresponding measurement in the opposite direction yields $S_P = k \cdot A \cdot \exp[-\mu(D-x)]$, with D as the diameter of the object. The undesired dependency on position x can as such be eliminated by taking the geometric average $S_{GM} = \sqrt{S_A \cdot S_P} = k \cdot A \cdot \exp(-\frac{\mu D}{2})$. An exact correction presupposes knowledge of the attenuation coefficients. These can be determined, for example, using a corresponding measurement of transmission. Within the scope of the iterative reconstruction technique, the attenuation coefficients can be adjusted to produce an optimal image. One possible application is the validation of the state of the cardiac musculature, for example after a heart attack. The cardiac muscle is still living if the tissue is still supplied with blood, and activity can be measured at this location.

Positron emission tomography, or PET for short, serves to portray metabolic processes and to answer various clinical questions. The method has taken on a significant

role in the field of oncology. It offers the possibility of determining absolute concentrations of activity, and the resulting quantitative metabolic parameters. As opposed to SPECT, with PET, positron-emitting substances are introduced into the body, and their bio-distribution as well as specific oncological information relating to the nourishment of tumors are acquired as raw data by detector systems. This method also requires subsequent image reconstruction using this data by different processes. Due to the development of computer systems with higher processing power, statistical and iterative processes are used more and more today for image reconstruction in PET. A constant repetition of calculation is common to all of them, in order to achieve the most mathematically exact image representation of the distribution of tracers possible. Powerful calculation systems are not only necessary due to the enormous quantity of incoming data that is processed into image reconstructions, but also for the correction of mistakes. Iterative methods calculate observed signals for an object by reference to a model. As such, for example, absorption in the tissue can also be considered. Parameters that describe the object are optimized until the best correspondence possible between calculated and measured signals is achieved. This method is significantly more complex than rear projection, but delivers sharper images. Imaging mistakes arise in ways similar to SPECT:

- absorption in the tissue;
- accidental coincidences during high counting rates;
- detection of scattered quanta.

Because with PET detection is always in two opposite directions, absorption correction is fundamentally simpler and more precise. The probability that a photon created at position x reaches Detector 1 at x_1 is $w_1 \propto \exp\left[-\int_x^{x_1} \mu(l)\, dl\right]$. The corresponding probability that the second photon reaches Detector 2 at x_2 is $w_2 \propto \exp[-\int_{x_2}^{x} \mu(l)\, dl]$. The probability of coincidence is $w = w_1 w_2 \propto \exp[-\int_{x_1}^{x_2} \mu(l)\, dl]$. As such, only the line integral $\int_{x_{21}}^{x_{12}} \mu(l)\, dl$ arises, and the dependency on position on this line disappears. It is exact if the integral $\int \mu(x)\, dx$ of a transmission measurement is calculated along the measurement path.

Reconstruction techniques are also necessary to produce images using MRI. The first MRI images were created, as with x-ray CT, by using back projection techniques. The Fourier technique, in which the image is created using a 2D Fourier transform, is both faster and leaves fewer artifacts. There is a relationship between the spatial resolution and the noise of an image. If, for a certain total measurement time, spatial resolution is increased, this also leads to greater noise. The use of more powerful magnetic fields is a possibility with otherwise equal parameters to improve the SNR (signal-to-noise) relationship; however, there are technical limits on the maximum usable field strengths. In addition to Fourier transforms, a range of digital filters are usually used in data reconstruction. The most important are the high-pass filter to bring out contrast edges, and the low-pass filter to suppress noise. In any case, in clini-

cal applications the use of filtering algorithms is frequently avoided in order to prevent mistakes in interpretation – for example, due to artifacts. Another concept in modern reconstruction techniques deals with joining often incomplete data with high-resolution, complete image data (reference images) that were previously recorded. Through reconstruction, artifacts can surface. Artifacts are pieces of the reconstructed image to which there is no correspondence in the real image. The most important of these with MRI include:

- movement artifacts;
- inhomogeneity artifacts;
- digital image artifacts.

Movement artifacts occur due to the involuntary or physiological movement of the patient. This leads to ghost signals along the phase coding direction. Countermeasures include certain triggers, or the use of extremely rapid sequences of pulses. Inhomogeneity artifacts have their origin, among other causes, in differences in susceptibility within the body. As a consequence, differences in intensity and image distortions can occur. According to the situation, these problems can be circumvented by using frequency coding, in which the sampling rate is chosen to be high enough, or by using phase coding. Digital image artifacts arise from the reconstruction of the image by using Fourier transforms, and can lead to a wide range of image flaws, like decreased contrast and phantom images. However, artifacts can also occur due to non-compensated spin evolution – for example, by diffusion or the movement of the organism within the pulse sequence. When using gradients, undesired dephasing must frequently be compensated for again; if this is ignored, characteristic artifacts can occur in the image even if the rest of the scan functions ideally.

As has been mentioned several times, the Fourier transform plays a significant role in the applicable reconstruction technique. The forward and back-transformations, which make the connection between the function $f(t)$ and its transform $F(\omega)$, are given by

$$F(\omega) = \mathcal{F}\{f(t)\} = \int_{-\infty}^{\infty} f(t)\, e^{-i\omega t} dt$$

$$f(t) = \mathcal{F}^{-1}\{F(\omega)\} = \frac{1}{2\pi} \int_{-\infty}^{\infty} F(\omega)\, e^{i\omega t} dt.$$

$F(\omega)$ is also known as the spectral density function $f(t)$. By targeted manipulation of the spectral density function of an image data set and subsequent back-transformation, filter algorithms can be implemented. In practice, measurement data exist in digital form. As such, the discrete Fourier transform (DFT) is used to process them; it is implemented numerically as the "fast Fourier transform" (FFT).

11.1 Discrete Fourier Transform

? Consider a function $f(t)$ that repeats with period T. Calculate the corresponding Fourier coefficients c_j in the Fourier series

$$f(t) = \sum_{j=-\infty}^{\infty} c_j e^{i\omega_j t} \quad \text{with } \omega_j = \frac{2\pi}{T} j$$

for a function $f(t)$, and discretize it to yield the smallest possible interval Δt that allows for division into N steps. What is the discrete Fourier transform of this $f(t)$:

$$f(t) = t \quad \text{for } 0 \le t < T \quad f(t) = f(t+T)? \tag{11.1}$$

! For a periodic function $f(t)$ with period T, the functional value $f(t) = f(t+T)$ is valid. The coefficients of the Fourier series are given by

$$c_j = \frac{1}{T} \int_0^T f(t)\, e^{-i\omega_j t}.$$

For a periodic function with period T, the functional value $f(t) = f(t+T)$ is valid. Through discretization, N steps (sampling points) in interval Δt are present, so $T = N\Delta t$ and $t = k\Delta t$. The Fourier coefficients are then

$$c_j = \frac{1}{\Delta t} \sum_{k=0}^{N-1} f(k\Delta t)\, \Delta t\, e^{-2\pi i j\, k\Delta t/n\Delta t} = \frac{1}{N} \sum_{k=0}^{n-1} f_k\, e^{-2\pi i j\, k/N}$$

with $f_k = f(k\Delta t)$. Therefore, the Fourier transform becomes $F_j = c_j$ and the back-transform is

$$f_k = \sum_{j=0}^{n-1} F_j e^{2\pi i j k/N}.$$

Here, in the interval $0 \le t < T$, the function $f(t) = t$ holds, and therefore f_k becomes $f_k = k\Delta t$. Therefore,

$$F_j = \frac{\Delta t}{N} \sum_{k=0}^{N-1} k\, e^{-2\pi i j k/N}.$$

11.2 Transfer Function

? Consider a signal $y(t)$ that is comprised of a linear combination of differential operations of sufficiently smooth entrance signals $f(t)$ in the following manner:

$$y(t) = \sum_{j=0}^{L-1} a_j \frac{d^j f(t)}{dt^j} \tag{11.2}$$

with $L > 1$.

1. Using a continuous Fourier transform, develop an expression of the transfer function $H(\omega)$ for which
$$Y(\omega) = H(\omega)F(\omega),$$
where $F(\omega) = \mathcal{F}(f(t))$ and $Y(\omega) = \mathcal{F}(y(t))$.
2. In using discrete (equidistant) data $y_k = y(k\,\delta t)$, the differential operators in (11.2) are only valid over finite intervals of duration δt. Show that y_k can be written as
$$y_k = \sum_{j=0}^{L-1} A_j\, f_{k+j}.$$
Use this form to derive the corresponding discrete transfer function H_j.
3. Using the smoothing algorithm $y_k = \frac{1}{3}\left(f_{k-1} + f_k + f_{k+1}\right)$, a diffuser is to be implemented. What is the corresponding transfer function H_j?

1. We have

$$y(t) = \sum_{j=0}^{L-1} a_j \frac{d^j f}{dt^j}$$

$$Y(\omega) = \int_{-\infty}^{\infty} \left(\sum_{j=0}^{L-1} a_j \frac{d^j f}{dt^j} \right) e^{i2\pi f t} dt = \left\{ \sum_{j=0}^{L-1} \left[a_j (i\omega)^j \right] \right\} F(\omega)$$
$$= H(\omega)\, F(\omega).$$

The transfer function $H(\omega)$ is
$$H(\omega) = \sum_{j=0}^{L-1} a_j\, (i\omega)^j .$$

2. First, consider the customary differential expression for a sufficiently smooth f (in the case that $j > 0$). According to the definition, this is, dependent on the $(j-1)$th derivative,
$$\frac{d^j}{dt^j} f = \lim_{\Delta t \to 0} \left[\frac{f^{(j-1)}(t + \Delta t) - f^{(j-1)}(t)}{\Delta t} \right],$$
or, as a function of the $(j-n)$-th derivative, with the binomial coefficient $\binom{j}{m} = \frac{j!}{m!(j-m)!}$,
$$\frac{d^j f}{dt^j} = \lim_{\Delta t \to 0} \left[\sum_{m=0}^{n} (-1)^{(m+n)} \binom{n}{m} \frac{f^{(j-n)}(t + m\Delta t)}{\Delta t^n} \right].$$
Substitution of $t \to k\delta t$, $dt \to dk\,\delta t$, and $\Delta t \to \Delta k \delta t$ yields
$$\frac{d^j f_k}{dk^j} = \delta t^j \frac{d^j f(t)}{dt^j}$$
$$= \delta t^j \lim_{\Delta k \to 0} \left[\sum_{m=0}^{n} (-1)^{(m+n)} \binom{n}{m} \frac{f^{(j-n)}(t + m\Delta t)}{\delta t^n \Delta k^n} \right].$$

In order to find an expression that depends on the values of the original function $f_k = f(k\,\delta t)$, we have, with $n = j$

$$\frac{d^j f_k}{dk^j} = \delta t^j \lim_{\Delta k \to 0} \left[\sum_{m=0}^{j} (-1)^{(m+j)} \binom{j}{m} \frac{f(t + m\Delta t)}{\delta t^j \Delta k^j} \right]$$

$$= \lim_{\Delta k \to 0} \left[\sum_{m=0}^{j} (-1)^{(m+j)} \binom{j}{m} \frac{f(t + m\Delta t)}{\Delta k^j} \right].$$

A discrete representation can be found if the limit is replaced with $\Delta k = 1$. The differential expression is then replaced with a forward difference.[1]

$$\frac{d^j f_k}{dk^j} \approx \sum_{m=0}^{j} (-1)^{(m+j)} \binom{j}{m} f(t + m\Delta t)$$

$$= \sum_{m=0}^{j} (-1)^{(m+j)} \binom{j}{m} f_{k+m}.$$

The case $k = 0$ must give the function value f_k, and must be checked specifically:

$$\frac{d^j f_k}{dk^j} \approx \begin{cases} \sum_{m=0}^{j} (-1)^{(m+j)} \binom{j}{m} f_{k+m} & j > 0 \\ f_k & j = 0 \end{cases}$$

With this result, the function y can be given in its discrete form

$$y_k = a_0 f_k + a_1 (f_{k+1} - f_k) + a_2 (f_{k+2} - f_{k+1} + f_k) + \ldots + a_{L-1} \left[f_{k+L-1} + ... + (-1)^{L-1} f_k \right].$$

This expression can only be simplified through the introduction of the coefficient A_l, for which

$$A_l = \begin{cases} -\sum_{j=l}^{L-1} (-1)^j \binom{j}{l} a_j & l > 0 \\ \sum_{j=0}^{L-1} (-1)^j a_j & l = 0, \end{cases}$$

so that

$$y_k = \sum_{l=0}^{L-1} A_l f_{k+l}.$$

If the discrete Fourier transform is applied to the sequence y_k , we have

$$Y_j = \mathcal{F} \sum_{l=0}^{L-1} A_l (f_{k+l})$$

$$= \frac{1}{N} \sum_{k=0}^{N-1} \sum_{l=0}^{L-1} A_l (f_{k+l})\, e^{-\frac{2\pi i k j}{N}}.$$

1 The use of a backwards-difference $(f_k - f_{k-j})$ or of a gradient $(f_{k+j} - f_{k-j})$ is possible in this situation as an alternative, but will not be considered here.

Now, substitute $k \to k' - l$, and exchange the sequence of the sums:

$$Y_j = \frac{1}{N} \sum_{l=0}^{L-1} A_l \frac{1}{N} \sum_{k'=l}^{N-1+l} f_{k'} e^{-\frac{2\pi i \left(k'-l\right) j}{N}}.$$

The phase factor, which is not dependent on k', can be written before the inner sum:

$$Y_j = \sum_{l=0}^{L-1} A_l e^{\frac{2\pi i l j}{N}} \left[\frac{1}{N} \sum_{k'=l}^{N-1+l} f_{k'} e^{-\frac{2\pi i k' j}{N}} \right].$$

Considering the periodicity of the Euler exponents, we can find the discrete Fourier transform F_j from the inner sum

$$\left(\sum_{l=0}^{L-1} A_l e^{\frac{2\pi i l j}{N}} \right) F_j = H_j F_j.$$

The discrete transfer function H_j becomes

$$H_j = \sum_{l=0}^{L-1} A_l e^{i\frac{2\pi j \Delta t\, l}{N\Delta t}} = \sum_{l=0}^{L-1} A_l e^{i\omega_j \Delta t\, l},$$

with discrete angular frequency $\omega_j = \frac{2\pi j}{N\Delta t}$.

3. To determine the transfer coefficients A_j from the function $y_k = \frac{1}{3}(f_{k-1} + f_k + f_{k+1})$, we must first consider the periodic exponent. We can use $A_{-1} = A_{N-1}$. Therefore $A_{N-1} = \frac{1}{3}$, $A_0 = \frac{1}{3}$, and $A_1 = \frac{1}{3}$; the transfer function is

$$H_j = \sum_{l=0}^{L-1} \frac{1}{3} \left(1 + e^{i\omega_j \Delta t} + e^{i(N-1)\omega_j \Delta t}\right) = \frac{1}{3} \left[1 + 2\, \cos\left(\omega_j \Delta t\right)\right].$$

11.3 Filtered Back Projection

In an image reconstruction technique, a high-pass filter $\{g_k\} = \{0, 1, 2, 3\}$ is used that repeats periodically. Carry out two projections along the x and y axes, and form the row and column sums ($f_i = \sum_j a_{il}$, f_l) to convolve these with the inverse Fourier transform of the filter. ?

a_{00}	a_{10}	a_{20}	a_{30}	$\Sigma \to_y f_0$
a_{01}	a_{11}	a_{21}	a_{31}	$\Sigma \to_y f_1$
a_{02}	a_{12}	a_{22}	a_{32}	$\Sigma \to_y f_2$
a_{03}	a_{13}	a_{23}	a_{33}	$\Sigma \to_y f_3$
$\Sigma \downarrow$	$\Sigma \downarrow$	$\Sigma \downarrow$	$\Sigma \downarrow$	
${}_x f_0$	${}_x f_1$	${}_x f_2$	${}_x f_3$	

Then, project the filtered data back to find the reconstructed image. The following objects should be used:

a) $\begin{matrix}1&0&0&0\\0&0&0&0\\0&0&0&0\\0&0&0&0\end{matrix}$ b) $\begin{matrix}1&1&1&1\\1&0&0&0\\1&0&0&0\\1&0&0&0\end{matrix}$ c) $\begin{matrix}1&0&0&0\\0&1&0&0\\0&0&1&0\\0&0&0&1\end{matrix}$ d) $\begin{matrix}1&1&1&1\\1&1&1&1\\1&1&1&1\\1&1&1&1\end{matrix}$.

discrete convolution: $h_k = (a \otimes b)_k = \sum_l A_l B_{k-l}$

! The Fourier transform of g is

$$\mathcal{F}^{-1}\{g_k\} = \sum_{k=0}^{N-1} g_k \exp\left(-\frac{2\pi}{N} ilk\right) = G_l.$$

With $N = 4$ and $g_k = k$, we have

$$G_l = 0 + 1 \cdot \exp\left(-\frac{\pi}{2} il\right) + 2 \cdot \exp(-\pi il) + 3 \cdot \exp\left(-\frac{3\pi}{2} il\right)$$

and therefore,

$$G_0 = 0 + 1\,e^0 + 2\,e^0 + 3\,e^0 = 6$$

that is,

$$\begin{aligned} G_1 &= 0 + 1 \cdot \exp\left(-\frac{\pi}{2} i\right) + 2 \cdot \exp(-\pi i) + 3 \cdot \exp\left(-\frac{3\pi}{2} i\right) \\ &= -2 + 2i \end{aligned}$$

and

$$\begin{aligned} G_2 &= -2 \\ G_3 &= -2 - 2i. \end{aligned}$$

These terms can be convoluted with the results of the projection by substitution into the equation $h_k = \sum_{l=0}^{3} f_l G_{k-l}$.

1.

$$\begin{array}{cccccc} & (y) & & & & \\ & \downarrow & \downarrow & \downarrow & \downarrow & \\ (x) \rightarrow & 1 & 0 & 0 & 0 & \rightarrow\ {}_yf_0 = 1 \\ \rightarrow & 0 & 0 & 0 & 0 & \rightarrow\ {}_yf_1 = 0 \\ \rightarrow & 0 & 0 & 0 & 0 & \rightarrow\ {}_yf_2 = 0 \\ \rightarrow & 0 & 0 & 0 & 0 & \rightarrow\ {}_yf_3 = 0 \\ & \downarrow & \downarrow & \downarrow & \downarrow & \\ & {}_xf_0 = 1 & {}_xf_1 = 0 & {}_xf_2 = 0 & {}_xf_3 = 0 & . \end{array}$$

For the projection along the y-direction, we have

$$
\begin{aligned}
{}_xh_0 &= {}_xf_0G_0 + {}_xf_1G_1 + {}_xf_2G_2 + {}_xf_3G_3 = 6\\
{}_xh_1 &= {}_xf_0G_1 + {}_xf_1G_0 + {}_xf_2G_3 + {}_xf_3G_2 = -2 + 2i\\
{}_xh_2 &= {}_xf_0G_2 + {}_xf_1G_1 + {}_xf_2G_0 + {}_xf_3G_3 = -2\\
{}_xh_3 &= {}_xf_0G_3 + {}_xf_1G_2 + {}_xf_2G_1 + {}_xf_3G_0 = -2 - 2i.
\end{aligned}
$$

Along the x-direction, due to symmetry, we have ${}_xh = {}_yh$. The back projection is

$$
\begin{array}{cccc}
{}_xh_0 + {}_yh_0 & {}_xh_1 + {}_yh_0 & {}_xh_2 + {}_yh_0 & {}_xh_3 + {}_yh_0\\
{}_xh_0 + {}_yh_1 & {}_xh_1 + {}_yh_1 & {}_xh_2 + {}_yh_1 & {}_xh_3 + {}_yh_1\\
{}_xh_0 + {}_yh_2 & {}_xh_1 + {}_yh_2 & {}_xh_2 + {}_yh_2 & {}_xh_3 + {}_yh_2\\
{}_xh_0 + {}_yh_3 & {}_xh_1 + {}_yh_3 & {}_xh_2 + {}_yh_3 & {}_xh_3 + {}_yh_3.
\end{array}
$$

Substituting in the numerical values,

$$
\begin{array}{cccc}
12 & 4 + 2i & 4 & 6 - 2i\\
4 + 2i & -4 + 4i & -4 + 2i & -4\\
4 & -4 + 2i & -4 & -4 - 2i\\
6 - 2i & -4 & -4 - 2i & -4 - 4i.
\end{array}
$$

Take note of the artifacts that occur. Use only the positive real portion; unnormalized, we have

$$
\begin{array}{cccc}
12 & 4 & 4 & 6\\
4 & 0 & 0 & 0\\
4 & 0 & 0 & 0\\
6 & 0 & 0 & 0
\end{array}.
$$

2.

$$
\begin{array}{ccccccc}
 & & (y) & & & & \\
 & & \downarrow & \downarrow & \downarrow & \downarrow & \\
(x) & \rightarrow & 1 & 1 & 1 & 1 & \rightarrow\ {}_yf_0 = 4\\
 & \rightarrow & 1 & 0 & 0 & 0 & \rightarrow\ {}_yf_1 = 1\\
 & \rightarrow & 1 & 0 & 0 & 0 & \rightarrow\ {}_yf_2 = 1\\
 & \rightarrow & 1 & 0 & 0 & 0 & \rightarrow\ {}_yf_3 = 1\\
 & & \downarrow & \downarrow & \downarrow & \downarrow & \\
 & & {}_xf_0 = 4 & {}_xf_1 = 1 & {}_xf_2 = 1 & {}_xf_3 = 1. &
\end{array}
$$

For the projection along the y-direction, we have

$$
\begin{aligned}
{}_xh_0 &= 4G_0 + G_1 + G_2 + G_3 = 21 + 3i \\
{}_xh_1 &= 4G_1 + G_0 + G_3 + G_2 = -5 + 9i \\
{}_xh_2 &= 4G_2 + G_1 + G_0 + G_3 = -5 + 3i \\
{}_xh_3 &= 4G_3 + G_2 + G_1 + G_0 = -1 + 6i.
\end{aligned}
$$

In this case, symmetry also allows ${}_xh = {}_yh$. As such, we have a symmetric matrix with the elements

$$
\begin{matrix}
42 + 6i & 16 + 15i & 16 + 6i & 20 + 9i \\
16 + 15i & -10 + 18i & -10 + 12i & -6 + 15i \\
16 + 6i & -10 + 12i & -10 + 6i & -6 + 15i \\
20 + 9i & -6 + 15i & -6 + 15i & -2 + 12i.
\end{matrix}
$$

The artifacts occur again. Ignoring the imaginary portions and the negative numbers, the upper left-hand value is still too large.

$$
\begin{matrix}
42 & 16 & 16 & 20 \\
16 & 0 & 0 & 0 \\
16 & 0 & 0 & 0 \\
20 & 0 & 0 & 0
\end{matrix}
.
$$

3.

$$
\begin{array}{cccccc}
 & & (y) & & & \\
 & & \downarrow & \downarrow & \downarrow & \downarrow & \\
(x) & \rightarrow & 1 & 0 & 0 & 0 & \rightarrow \; {}_yf_0 = 1 \\
 & \rightarrow & 0 & 1 & 0 & 0 & \rightarrow \; {}_yf_1 = 1 \\
 & \rightarrow & 0 & 0 & 1 & 0 & \rightarrow \; {}_yf_2 = 1 \\
 & \rightarrow & 0 & 0 & 0 & 1 & \rightarrow \; {}_yf_3 = 1 \\
 & & \downarrow & \downarrow & \downarrow & \downarrow & \\
 & & {}_xf_0 = 1 & {}_xf_1 = 1 & {}_xf_2 = 1 & {}_xf_3 = 1 & .
\end{array}
$$

For the y-projection, we have ${}_xh_0 = {}_xh_1 = {}_xh_2 = {}_xh_3 = 0$, and correspondingly for the x-direction. Here, through rear projection, we have

$$
\begin{matrix}
0 & 0 & 0 & 0 \\
0 & 0 & 0 & 0 \\
0 & 0 & 0 & 0 \\
0 & 0 & 0 & 0
\end{matrix}
.
$$

Obviously, the diagonal object cannot be found. We need another projection – for example along the diagonal!

4.

$$
\begin{array}{cccccccc}
 & & (y) & & & & & \\
 & & \downarrow & \downarrow & \downarrow & \downarrow & & \\
(x) & \rightarrow & 1 & 1 & 1 & 1 & \rightarrow & {}_yf_0 = 4 \\
 & \rightarrow & 1 & 1 & 1 & 1 & \rightarrow & {}_yf_1 = 4 \\
 & \rightarrow & 1 & 1 & 1 & 1 & \rightarrow & {}_yf_2 = 4 \\
 & \rightarrow & 1 & 1 & 1 & 1 & \rightarrow & {}_yf_3 = 4 \\
 & & \downarrow & \downarrow & \downarrow & \downarrow & & \\
 & & {}_xf_0 = 4 & {}_xf_1 = 4 & {}_xf_2 = 4 & {}_xf_3 = 4 & . &
\end{array}
$$

For the y-direction, we have ${}_xh_0 = {}_xh_1 = {}_xh_2 = {}_xh_3 = 0$, and correspondingly for the x-direction. Rear projection gives

$$
\begin{array}{cccc}
0 & 0 & 0 & 0 \\
0 & 0 & 0 & 0 \\
0 & 0 & 0 & 0 \\
0 & 0 & 0 & 0
\end{array} .
$$

Result: the object cannot be detected. It seems as if it is not there. This is a consequence of the fact that only the spatial frequency 0 is contained, which is suppressed by the high-pass filter.

12 Radiation Medicine and Protection

If the kinetic energy of photons or particles is high enough (in eV), they can create ions in material; as such, these photons or particles are known as ionizing radiation. In medicine, ionizing radiation is primarily used in two areas: for imaging using X-rays, and for radiation therapy with X-rays, gamma rays, or charged particles (like electrons or atomic nuclei). While with X-rays, the ionizing effects are kept to the minimum possible, radiation therapy is interested in delivering the maximum energy possible to a specific location in order to, for example, destroy malignant tissue.

All forms of radiation have primary and secondary effects. The primary effects involve the interaction of the incident radiation itself with the material. For photons, this interaction occurs primarily with electrons. In the case of heavy particles, interaction with nuclei also plays a role. Neutrons interact almost exclusively with the atomic nuclei of materials. If enough energy is delivered to the electrons by the primary processes, these can be liberated, and can themselves serve as a source of ionization for secondary processes.

For electromagnetic radiation it is true to a first approximation that transmitted intensity falls off exponentially with penetration depth x if the material is homogeneous: $I(x) = I_0 e^{-\mu x}$. The attenuation coefficient μ is the inverse of the average free path length $\bar{x}$, and is proportional to the particle density n and to the cross section σ: $\mu = n\sigma$. As the average free path length of 1 MeV photons in water is $\bar{x} = 14.4\,\text{cm}$, the cross section is $\sigma = 2.1 \cdot 10^{-24}\,\text{cm}^2$, or 2.1 barn.

The attenuation coefficient is comprised additively of the scattering coefficient Σ and the absorption coefficient τ: $\mu = \Sigma + \tau$. The scattering coefficient corresponds to the probability of a change in direction of a photon, and the absorption coefficient corresponds to the probability of the absorption of the radiation. Rayleigh scattering (coherent scattering by the entire atom) and Thomson scattering (elastic scattering by bound electrons) contribute to the scattering coefficient. The photoelectric effect, the Compton Effect, and pair production all contribute to the absorption coefficient.

A simple model for scattering uses an electron moving in the potential of a harmonic oscillator with a characteristic frequency ω_0 and damping $\Gamma < \omega_0$ The driving force comes from the electric field of an incident wave, with frequency ω. In the scope of this model, the typical resonance curve for the total cross section is:

$$\sigma_{\text{total}} = \sigma_T \cdot \frac{\omega^4}{(\omega_0^2 - \omega^2)^2 + \omega^2 \Gamma^2}.$$

For very high frequencies $\omega \gg \omega_0$, the boundary case of Thomson scattering is obtained: $\sigma_{\text{total}} \approx \sigma_T = \frac{8}{3}\pi r_e^2$ ($r_e = \frac{e^2}{4\pi\varepsilon_0 m_e c^2}$ is the classical electron radius), and for very small frequencies $\omega \ll \omega_0$, Rayleigh scattering with $\sigma_{\text{total}} \approx \sigma_R = \sigma_T \cdot \frac{\omega^4}{\omega_0^4}$.

In the photoelectric effect, the photon gives up its entire energy to a valence electron of the absorbing material. The cross section for photon absorption is at a maxi-

mum if the energy of the photon corresponds to the biding energy. There is, however, no simple analytical expression for the dependence of the penetration depth on energy and material. In the realm of biological tissues with atomic numbers $Z < 10$, photoabsorption (τ_{Ph}) rises roughly with the cube of Z; with heavy nuclei, roughly as Z^4. The photoelectric effect dominates for lower energies of the incident electromagnetic radiation. In the Compton Effect, the energy of the incident photon is only partially transmitted to a relatively weakly bound electron. This process dominates for middle energies, and its effect depends on the electron density of the absorbing material: $\tau_{\mathrm{C}} \propto \rho Z$. For quantum energy of greater than $2 \cdot 511\,\mathrm{keV}$, pair production becomes possible. Through the interaction of the photon with the strong electromagnetic field of the atomic nucleus, the incident photon can spontaneous convert into an electron-positron pair. The probability of occurrence of pair production increases with the square of the atomic number: $\tau_{\mathrm{P}} \propto \rho Z^2$. After pair production, the positron can move for several millimeters until it is annihilated by an electron. This leads to the emission of two photons in opposite directions, known as annihilation radiation.

For charged particles, the Coulomb interaction with the valence electrons of atoms dominates as the particles pass through material. For a mass m with $z \cdot e$ charged particles passes opposite the valence electrons, energy transfer per path length can be calculated by using the Bethe-Bloch formula:

$$-\frac{dE}{dx} = 4\pi z^2 r_e^2 \frac{mc}{(4\pi\varepsilon_0)^2\beta^2} \cdot n \cdot Z \cdot \left\{ \ln\left(\frac{2mc^2\beta^2}{I(1-\beta^2)} \right) - \beta^2 \right\}.$$

In the expression, r_e is the classical electron radius (see above), Z is the atomic number of the medium, and I is the average ion potential ($I \approx Z \cdot 13.5\,\mathrm{eV}$). $\beta := v/c$ is a measurement of the velocity of the particle, $n = \frac{N_A \rho}{m_{\mathrm{mol}}}$ is the number of atoms per unit volume in the medium (N_A: Avogadro constant, $\mathrm{m_{mol}}$: molar mass, ρ: density of the medium). $S(E) := -\frac{dE}{dx}$ is also called the linear stopping power (LSP), while in dosimetry, the concept of linear energy transfer (LET) is useful. Due to $-\frac{dE}{dx} \sim \frac{z^2}{v^2}$, energy transfer grows with the charge of the particle, and with falling velocity. As such, charged particles in a material have a finite penetration depth. The damage to material increases as this depth increases until a maximum is reached where the particles are slowed to zero. In this manner, for example, energy can be deposited in tumors in a targeted way; the tissue above the tumor experiences less damage, and the tissue beneath the tumor receives practically no dose.

In comparison to positively charged particles, the interaction of incident elections with the valence electrons of a material can lead to a change in direction. Furthermore, collision between identical particles occurs, so the Pauli principle must be considered. The Bethe-Bloch formula modified for electrons is:

$$-\frac{dE}{dx} = 2\pi r_e^2 \frac{mc^2}{\beta^2} \cdot n \cdot Z \cdot \left\{ \ln\left(\frac{\tau^2(\tau+2)}{2\left(\frac{I}{mc^2}\right)^2} \right) - F(\tau) \right\}.$$

$\tau := \frac{E_{\text{kin}}}{mc^2}$ is the ratio of kinetic energy to rest energy, and

$$F(\tau) := 1 - \beta^2 + \frac{\tau^2/8 - (2\tau + 1)\ln(z^2)}{(\tau + 1)^2}.$$

In addition to collisions, bremsstrahlung also contributes to the loss of energy from the electrons. This contribution can be described as

$$-\frac{dE}{dx} = 4Z^2 m r_e^2 E \cdot \ln\left(\frac{183}{Z^{\frac{1}{3}}}\right).$$

For small energies, the collision contribution dominates; for large energies, bremsstrahlung loss is predominant. The energy at which both contributions are equal is called the critical energy E_{crit}. It ranges from 9.5 MeV in lead up to around 100 MeV in water.

As uncharged particles, neutrons do not experience Coulomb interactions. As such, in addition to scattering, the capture of slow neutrons is possible. As the magnetic interaction of neutrons with atomic shells can be ignored, energy transfer occurs primarily through a collision process with nuclei. The transfer of energy at collision angle θ is:

$$\Delta E = \frac{4\frac{m_N}{M}}{\left(1 + \frac{m_N}{M}\right)} \cdot E_N \cos^2\theta.$$

This transfer is maximized if the mass of M of the atomic nucleus is comparable to the mass m_N of the neutron. Then, $\Delta E \approx E_N \cos^2\theta$, and in isotropic media around half of the neutron's energy is transferred in a single collision. As, in addition, the cross section of the neutron-proton collision is especially large, and that of other biologically significant nuclei like oxygen and carbon is especially small, around 90% of the loss in energy from neutrons is due to interaction with water. A second method of energy loss is the absorption of neutrons for the construction of a compound nucleus. This makes an effective local deposition of energy possible in treating tumors.

Through the primary interaction of charged particles in a material, additional charged particles, the secondary particles, can be created. These also interact with the material. The secondary electrons are also termed δ-particles. As many of the secondary particles are created with relatively little energy, they lose their energy close to the primary ionization. This generates primary ionization clusters.

Different processes contribute to tissue damage by ionizing radiation. Radiation injuries result from excitation, ionization, and dissociation of atoms and molecules, but the most serious damage in the long term is due to damage to the DNA. As such ionizing damage to DNA also occurs naturally (not only due to natural radioactivity), there are highly effective repair mechanisms in biological systems to combat it.

A description of the effect of ionizing radiation on biological tissue is not complete with the specification of the activity of a radioactive source. The specification of the energy dose $D := \frac{dE}{dm}$ (unit Gray, Gy) and energy dose power $\dot{D} := \frac{dD}{dt}$ is also not complete, as the method of delivery of the energy to the tissue must also be considered.

As such, an equivalent dose $H := Q \cdot D$ is introduced in which the dose is rated with a biological quality factor Q. Although the quality factor is unitless, the value of the equivalent dose is given its own unit, the Sievert (Sv).

In radiation protection, the effective dose E is calculated as the weighted sum over the individual organ dose H_T. For radiation R, organ dose is found according to $H_{T,R} = w_R \cdot D_{T,R}$. In this expression $D_{T,R}$ is the average energy dose across the tissue or organ (designated with T), and w_R is the beam-weighting factor (to differentiate from the quality factor Q). If the radiation affecting the tissue or organ is comprised of different types with different values of w_R, then the entire organ dose is $H_T = \sum_R w_R D_{T,R}$. For the effective dose, with the corresponding tissue weighting factors w_T, the expression is therefore:

$$E = \sum_T w_T H_T = \sum_T w_T \sum_R w_R D_{T,R}.$$

While the tissue weighting factors are in the range of between $w_T = 0.01$ for skin or bone surface and $w_T = 0.20$ for gonads, radiation weighting factors w_R have values of $w_R = 1$ for photons, electrons, and muons of all energies, and range up to $w_R = 20$ for neutrons in the energy region of $0.1 - 2\,\mathrm{MeV}$, alpha particles, fission fragments, and heavy nuclei. Details can be found in regulations dealing with radiation protection requirements.

12.1 Interactions of a High-Energy Primary Photon

? Complete the schematic of possible interactions of a high-energy primary photon.

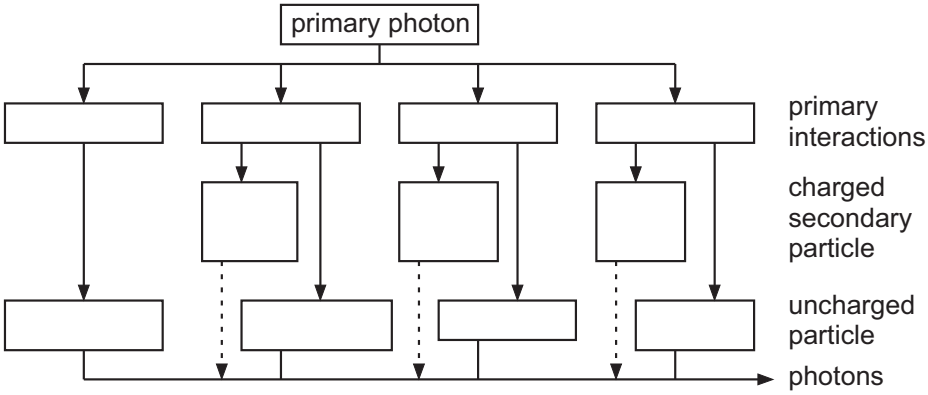

Fig. 12.1. Schema of possible interactions.

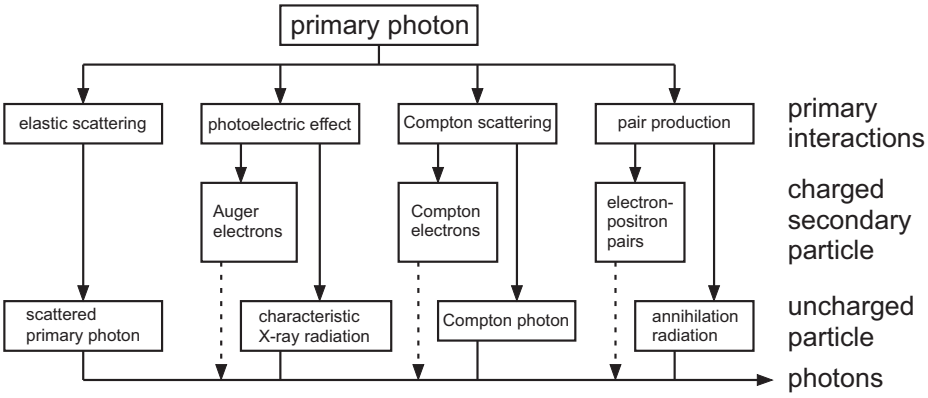

Fig. 12.2. Schema of possible interactions.

12.2 Pair Production in Radiation Therapy

1. Which effects are relevant for the transfer of energy from photons to material in radiation therapy? Which effect dominates at low ($\leq$ 0.1 MeV), middle, and high photon energies ($\geq$ 1 MeV)?
2. Why can't pair production occur in a vacuum?

1. The corresponding effects are
   (a) photoelectric effect (dominates at low energies)
   (b) Compton Effect (dominates at mid-range energies)
   (c) pair production (begins at higher energies)
2. The energy and momentum of a photon are proportional to each other according to the expression

$$E_\gamma = p_\gamma c.$$

Assuming that two particles that move with velocities v_1 and v_2 are created from the photon, the total energy of the particle can be written as

$$E = m_0 c^2 \left(\gamma\left(v_1\right) + \gamma\left(v_2\right)\right) \quad \text{with} \quad \gamma(v) = \frac{1}{\sqrt{1 - \left(\frac{v}{c}\right)^2}}$$

For the momentum of both particles,

$$\left|\vec{p}\right| = m_0 \left|\gamma\left(v_1\right)\vec{v}_1 + \gamma\left(v_2\right)\vec{v}_2\right|.$$

Therefore, its maximum value is

$$p_{\max} = m_0 \left(\gamma\left(v_1\right)v_1 + \gamma\left(v_2\right)v_2\right).$$

Substituting this expression into the conservation equations for energy $E_\gamma = E$ and momentum $p_\gamma = |\vec{p}|$,

$$(\gamma(v_1) + \gamma(v_2))\, m_0 c^2 = |\gamma(v_1)\,\vec{v}_1 + \gamma(v_2)\,\vec{v}_2|\, m_0 c.$$

This equation can only be solved for $v_1 = v_2 = c$; this is physically impossible, and would also violate the conservation of energy. As such, at some point in the process, energy and/or momentum must be exchanged with an additional partner – the process cannot take place in a vacuum.

12.3 Compton Scattering

? A photon of energy $h\nu = 1.173\,\text{MeV}$ is scattered by an electron at angle $\Theta = 55^\circ$. Calculate

1. the energy E of the scattered photon
2. the change $\Delta\lambda$ in the wavelength
3. the recoil energy T of the electron

! 1. The scattered photon has energy

$$E'_\gamma = \frac{E_\gamma}{1 + \frac{E_\gamma}{mc^2}(1 - \cos\Theta)} = \frac{1.173\,\text{MeV}}{1 + \frac{1.173\,\text{MeV}}{0.511\,\text{MeV}}(1 - \cos 55^\circ)} = 0.593\,\text{MeV}.$$

2. The wavelength changes by

$$\Delta\lambda := \lambda' - \lambda = \lambda \cdot \frac{E_\gamma}{mc^2}(1 - \cos\Theta) = \frac{h}{mc}(1 - \cos\Theta)$$
$$= \frac{6.626 \cdot 10^{-34}\,\text{Js}}{0.91 \cdot 10^{-30}\,\text{kg} \cdot 3 \cdot 10^{8}\,\text{m/s}}\left(1 - \cos 55^\circ\right) = 1.04 \cdot 10^{-12}\,\text{m}.$$

3. The recoil energy of the electron is

$$T = E_\gamma - E'_\gamma = 1.173\,\text{MeV} - 0.593\,\text{MeV} = 0.58\,\text{MeV}.$$

12.4 Radiation Damage from Potassium

? The percentage proportion of potassium in an adult human can be estimated as $\Phi = 0.35\%$. How many microcuries of ^{40}K are in the body of a person whose mass is $m = 70\,\text{kg}$? The natural occurrence of ^{40}K is $\Theta = 0.012\%$, and the half-life is $T_{1/2} = 1.8 \cdot 10^9\,\text{a}$.

For the activity we have

$$A = -\frac{dN}{dt} = \frac{\ln 2}{T_{1/2}} \cdot N,$$

with N as the number of atoms. We can calculate this from the mass m_K of potassium in the body:

$$m_K = \Phi \cdot m = 0.35\% \cdot 70\,\text{kg} = 0.0035 \cdot 70\,\text{kg} = 0.245\,\text{kg}$$

and from the isotopic proportion and molar mass $m_{mol} = 40$ g as

$$N = N_A \frac{m_{^{40}K}}{m_{\text{mol}}} = 6 \cdot 10^{23}\,\#_{\text{mol}} \frac{245}{40} 1.2 \cdot 10^{-4} = 4.4 \cdot 10^{20}.$$

The activity is

$$A = \frac{\ln 2}{T_{1/2}} \cdot N = \frac{0.693 \cdot 4.4 \cdot 10^{20}}{1.8 \cdot 10^9 \cdot 365 \cdot 24 \cdot 3{,}600\,\text{s}} = 5{,}100\,\#_{\text{s}} = 5.1\,\text{kBq} = 0.14\,\mu\text{Ci}.$$

12.5 Lethal Energy Dose

The fatal dose of energy D during the whole-body irradiation of a person of mass $m = 75$ kg is 500 rd. How many degrees of temperature ΔT can $m_W = 75$ kg of water be warmed if an amount of energy equivalent to the lethal dose is applied to the water in the form of heat energy?
[specific heat of water $c_W = 4.187 \cdot 10^3\,\text{J/kg K}$]

The conversion between the dated unit rad and the unit Gray is 1 Gy = 100 rd. For the energy E deposited in the body, then, we have

$$E = D\,m = 5\,\text{Gy} \cdot 75\,\text{kg} = 375\,\text{J}.$$

To warm the water by ΔT, we require energy

$$E = c_W m_W \Delta T.$$

Therefore,

$$\Delta T = \frac{E}{c_W m_W} = \frac{375\,\text{J}}{4.187 \cdot 10^3\,\text{J/kg K} \cdot 75\,\text{kg}} = 1.2 \cdot 10^{-3}\,\text{K}.$$

12.6 Fatal Dose Equivalents

1. What full-body dose does a 70 kg physics lab assistant exposed to a $^{60}_{27}$Co source with 40 mCi receive? On average over the day, he is 4 m away from the source. $^{60}_{27}$Co emits γ rays with energies 1.33 MeV and 1.17 MeV (one photon of each per decay). In the body, the γ radiation deposits half of its energy. The projection surface of the lab assistant is 1 m^2. Discuss the result while considering that, for γ rays, the relative biological efficiency as an assessment factor is equal to 1.

2. Assuming that the person contains around $2 \cdot 10^9$ nucleotide base pairs per strand of DNA, estimate the volume V of such a strand. To be destroyed in the biological sense, 1,000 ionizations are necessary in this volume. As such, what is the rough fatal dose equivalent for a person?

[the average relative molecular mass of a corresponding nucleotide is $M = 330\,\mathrm{g/mol}$; the ion charge is $q = 1.6{\cdot}10^{-19}\,\mathrm{C}$; the ionization potential of human tissue is $\varphi_G = 33.7\,\mathrm{V}$]

! 1. The total energy of the γ ray per decay is

$$E_{Co} = (1.33 + 1.17)\,\mathrm{MeV} = 2.50\,\mathrm{MeV}$$

and the total energy emitted by the source is

$$E = E_{Co}\frac{dN}{dt}.$$

As $1\,\mathrm{Ci} = 3.7 \cdot 10^{10}$ decays per second, we have

$$E = (2.5\,\mathrm{MeV})\,(0.04\,\mathrm{Ci})\left(3.7 \cdot 10^{10}\,\mathrm{Ci^{-1}s^{-1}}\right) = 3.7 \cdot 10^9\,\mathrm{MeVs^{-1}}.$$

The ray propagates spherically away from the source. A person 4 m away only receives a portion of it. This portion can be calculated using the ratio of the projection area of the person A_p on a spherical surface with radius $r = 4\,\mathrm{m}$:

$$\frac{A_P}{A_k} = \frac{A_p}{4\pi r^2} = \frac{1.0\,\mathrm{m^2}}{4\pi\,(4\mathrm{m})^2} = 6.33 \cdot 10^{-3}.$$

Because only half of the emitted energy interacts with the body, the active portion $E_a = \frac{1}{2}\frac{A_P}{A_k}E$ is

$$E_a = 0.5\left(6.33 \cdot 10^{-3}\right)\left(3.7 \cdot 10^9\,\mathrm{MeV/s}\right)\left(1.6 \cdot 10^{-13}\,\mathrm{J/MeV}\right) = 1.88 \cdot 10^{-6}\,\mathrm{J/s}.$$

The SI unit for absorbed radiation dose is the Gray [Gy]. $1\,\mathrm{Gy} = 1\,\mathrm{J/kg}$. Therefore, the rate of the whole-body dose of a 70 kg person is

$$\frac{dD}{dt} = \frac{1.88 \cdot 10^{-6}\,\mathrm{J/s}}{70\,\mathrm{kg}} = 2.69 \cdot 10^{-8}\,\mathrm{J/kg\,s} = 2.69 \cdot 10^{-8}\,\mathrm{Gy/s}.$$

Within 4 h hours, this dose is

$$D = (4\,\mathrm{h})\,(3{,}600\,\mathrm{s/h})\left(2.69 \cdot 10^{-8}\,\mathrm{Gy/s}\right) = 3.87 \cdot 10^{-4}\,\mathrm{Gy}.$$

This physical dose has, in biological material, dose equivalent

$$D_{\mathrm{eq}} = Q \cdot D$$

with Q as the relative biological effectiveness. D_{eq} is given in Sieverts [Sv] [1]. For γ rays, $Q = 1\ ^{\text{Sv}}/_{\text{Gy}}$. Therefore,

$$D_{\text{eq}} = 1\ ^{\text{Sv}}/_{\text{Gy}} \left(3.9 \cdot 10^{-4}\ \text{Gy}\right) = 0.39\ \text{mSv}.$$

The legal yearly dosage limit D^*_{leg} is

For a normal person,	$5\ ^{\text{mSv}}/_{\text{a}}$
For someone exposed to radiation,	$50\ ^{\text{mSv}}/_{\text{a}}$.

This means that the radiation-exposed lab assistant receives around ca. 1% of his yearly allowed dose each day. In order to reduce this number, the radiation source should be shielded. Without additional shielding, he should only work in the radiation laboratory for 128 d out of the year. The higher value of allowed radiation dose for those exposed is due to the medical check-ups that these people undergo frequently.

2. As the person has $n_p = 2 \cdot 10^9$ nucleotide base pairs per strand of DNA, and 1 nucleotide has an average relative molecular mass of $M_N = 330\ ^{\text{g}}/_{\text{mol}}$, the relative molecular mass of a strand is

$$M_{\text{St}} = n_p\, M_N = 2 \cdot 10^9 \cdot 330 = 6.6 \cdot 10^{11}\ ^{\text{g}}/_{\text{mol}}.$$

The mass of a strand of DNA is therefore

$$m_{\text{St}} = \frac{M_{\text{St}}}{N_A} = \frac{6.6 \cdot 10^{11}\ ^{\text{g}}/_{\text{mol}}}{6 \cdot 10^{23}\ ^{1}/_{\text{mol}}} = 10^{-12}\text{g} = 10^{-15}\text{kg}.$$

If we assume that $\rho_{\text{DNS}} = \rho_{\text{H}_2\text{O}}$, the volume of a DNA strand is then

$$V_{\text{St}} = \frac{m_{\text{St}}}{\rho_{\text{DNS}}} = \frac{10^{-15}\ \text{kg}}{10^3\ ^{\text{kg}}/_{\text{m}^3}} = 10^{-18}\ \text{m}^3.$$

With $n_{\text{ion}} = 1{,}000$ ionizations, the ionized volume per strand is

$$V_{\text{ion}} = \frac{V_{\text{St}}}{n_{\text{ion}}} = \frac{10^{-18}\ \text{m}^3}{10^3} = 10^{-21}\ \text{m}^3.$$

The number of ion pairs per volume j_2 is

$$j_2 = \frac{1}{\rho_{\text{DNS}}\, V_{\text{ion}}} = 10^{18}\ \frac{\text{ion pairs}}{\text{kg}}.$$

With ion charge $q_{\text{ion}} = 1.6 \cdot 10^{-19}\ ^{\text{C}}/_{\text{ion}}$ per ion, the fatal dose is

$$D_C = 2\, q_{\text{ion}}\, j_2 = 2 \cdot 1.6 \cdot 10^{-19}\ \frac{\text{C}}{\text{ion pairs}} \cdot 10^{18}\ \frac{\text{ion pairs}}{\text{kg}} = 0.32\ ^{\text{C}}/_{\text{kg}}.$$

---

1 The unit [rem] "*rad equivalent man*" is also sometimes used: 1 Sv = 100 rem

The corresponding dose of energy D_E can be found using the ionization potential of human tissue, $\varphi_G = 33.7\,\mathrm{V}$:

$$D_E = \varphi_G\, D_C = 33.7\,\mathrm{V} \cdot 0.32\,{}^{\mathrm{C}}/_{\mathrm{kg}} = 10.8\,{}^{\mathrm{J}}/_{\mathrm{kg}} = 10.8\,\mathrm{Gy}.$$

As the relative biological effectiveness is $Q = 1\,{}^{\mathrm{Sv}}/_{\mathrm{Gy}}$, the fatal dose equivalent is

$$D_M = Q \cdot D_E = 1\,{}^{\mathrm{Sv}}/_{\mathrm{Gy}} \cdot 10.8\,\mathrm{Gy} = 10.8\,\mathrm{Sv}.$$

12.7 Dose Burden from Milk Consumption

? What is the effective annual dose that an adult with mass $m_\mathrm{E} = 70\,\mathrm{kg}$ and a baby with mass $m_\mathrm{S} = 5\,\mathrm{kg}$ are exposed to if each of them drinks $V = {}^3/_4\,\mathrm{l}$ of milk each day? In cow's milk, the potassium isotope $^{40}_{19}\mathrm{K}$ occurs, and decays with a specific activity of $a = 2\,{}^{\mathrm{nCi}}/_{\mathrm{kg}}$. The retention time of milk in the body is $\tau = 12\,\mathrm{h}$, and $\kappa = 12\%$ of the energy $P = 1.5\,\mathrm{MeV}$ liberated in each decay is absorbed by the body. What percent of the permitted annual dose is absorbed in each case?
[density of milk $\rho_M = 0.95\,{}^{\mathrm{kg}}/_{\mathrm{l}}$]

! The daily dose absorbed D^* for a person j is

$$D_j^* = \frac{\kappa\tau\, a\, P \rho_M V}{m_j}$$

Numerically,

$$m_J\, D_j^* = 0.12\,(12\,\mathrm{h})\left(2 \cdot 10^{-9}\,{}^{\mathrm{Ci}}/_{\mathrm{kg}}\right)(1.5\,\mathrm{MeV})\,(0.95\,{}^{\mathrm{kg}}/_{\mathrm{l}})\,(0.75\,\mathrm{l}) \cdot$$
$$\cdot \left(1.6 \cdot 10^{-13}\,{}^{\mathrm{J}}/_{\mathrm{MeV}}\right)\left(3.7 \cdot 10^{10}\,{}^{1}/_{\mathrm{Cis}}\right)(3{,}600\,{}^{\mathrm{s}}/_{\mathrm{h}})\,.$$

With $m_j = m_\mathrm{E} = 70\,\mathrm{kg}$ for the adult, the annual dose is

$$D_\mathrm{E}^* = 5 \cdot 10^{-7}\,{}^{\mathrm{Gy}}/_{\mathrm{a}}$$

Under the assumption of a relative biological effectiveness of $Q = 1\,{}^{\mathrm{Sv}}/_{\mathrm{Gy}}$, the effective annual dose $D^*_{\mathrm{eff,E}}$ is

$$D^*_{\mathrm{eff,E}} = D^*_\mathrm{E} \cdot Q = \left(5 \cdot 10^{-7}\,{}^{\mathrm{Gy}}/_{\mathrm{a}}\right)(1\,{}^{\mathrm{Sv}}/_{\mathrm{Gy}}) = 0.5\,{}^{\mu\mathrm{Sv}}/_{\mathrm{a}}.$$

With $m_j = m_\mathrm{S} = 5\,\mathrm{kg}$ for the baby, we have a $\frac{m_\mathrm{E}}{m_\mathrm{S}} = \frac{70}{5} = 14$ times higher value for the effective annual dose:

$$D^*_{\mathrm{eff,S}} = 14 \cdot 0.5\,{}^{\mu\mathrm{Sv}}/_{\mathrm{a}} = 7\,{}^{\mu\mathrm{Sv}}/_{\mathrm{a}}.$$

In comparison to the permitted annual dose of $D^*_{\mathrm{leg}} = 1\,{}^{\mathrm{mSv}}/_{\mathrm{a}}$, we have, for

- adults: $\frac{D^*_\mathrm{E}}{D^*_{\mathrm{leg}}} = \frac{0.5}{1{,}000} = 0.5\,‰$
- babies: $\frac{D^*_\mathrm{S}}{D^*_{\mathrm{leg}}} = \frac{7}{1{,}000} = 7\,‰$

of the annual dose allowed.

13 Laser Therapy

Laser light, and light from conventional sources, differ in that a laser generates coherent light. In medicine, this spatial and temporal coherence is significant. The spatial coherence allows laser light to be focused in very small beam diameters in the range of a few optical wavelengths; this allows practitioners to achieve the high intensities that are important in therapy. The temporal coherence permits a high degree of time resolution, and is useful primarily in diagnostics. The creation of laser light is based on the principle of stimulated emission: when a photon strikes an electron in an excited state, it can cause this electron to return to its ground state. Energy is liberated in the process, and is emitted as a photon that has the same frequency and phase as the original photon. In order for this to occur efficiently there must be more electrons in the excited state than in the ground state, a condition termed inversion.

One of the first lasers was the ruby laser. The active amplifying material is comprised of ruby, which is excited by irradiation with light. The laser beam is emitted from the front surface of the ruby rod. In addition to the solid material category in which ruby is classified, gases and dyes are also used in laser as amplifiers. With solid materials, semiconductors have become more and more important in recent years. The first applications of coherent radiation were their use in ophthalmology. Applications in surgery and in other areas of medicine followed. Today, targeted lasers with a very short penetration depth in biological tissue are being developed. Lasers also play an important role in the diagnostic, physiological investigations of tissue, especially in the search for tumors. Lasers can excite fluorescent materials in a targeted manner. Florescent markers are attached, for example, to molecules, which are then preferentially stored in tumors. Lasers are also used to clarify molecular processes, as in "Förster Resonant Energy Transfer" (FRET), in which energy transport between molecules is investigated with the help of lasers.

A focused laser beam can produce very strong electric fields. As such, small transparent particles are brought into the focus of a laser beam. If the beam is moved, these particles move along with it. These mechanisms are called "optical tweezers"; they are not only used to move particles at higher spatial resolution within cells (even organelles) in a targeted way, but can simultaneously measure the resulting forces that occur. Through this use it is possible, for example, to determine the mechanical characteristics of body cells, like their elasticity and/or shear modulus, and to come up with a diagnosis of tissue condition through comparison of healthy and pathologically altered values. Generally, these moduli are significantly reduced in cancerous cells.

Although light is strongly scattered in human tissue, and it is therefore impossible to obtain optical images of the entire inner body, an image in the region of the body's surface can nonetheless be generated using "optical coherence tomography" (OCT). This technique is principally used in studying the eye, and works interferometrically. Three-dimensional images with very high spatial resolution can be generated by using

light sources with a wide range of wavelength spectra. An OCT image is comprised of a number of sectional images that are processed into a tomogram.

A laser beam can be absorbed, reflected, or scattered when it strikes some material. While reflected laser beams are of no use in medical applications, both absorption and scattering are important in therapy and diagnosis. The amount of absorption is substantively determined by the absorption coefficient of water, as human tissue is primarily comprised of this substance. Because biological tissue is inhomogeneous, in addition to absorption, simple and complex scattering can occur. The size of the particle with respect to the wavelength of the light beam determines which type of scattering, Rayleigh or Mie, will occur. For Rayleigh scattering, as wavelength decreases, scattering increases sharply; in the ultraviolet region, penetration depth and the free path length of the light in the tissue becomes shorter.

The therapeutic processes of laser application are photochemistry, photothermics, photomechanics, and photodisruption. Photochemical processes occur in tissues under low-intensity laser light (below $100\ \mathrm{W/cm^2}$) with long application times, as in wound repair and pain therapy. From an intensity of $100\ \mathrm{W/cm^2}$, the tissue is coagulated – photothermically altered. This process is used in managing tumors, to shrink tissues, and to control bleeding. At intensities of above $10^6\ \mathrm{W/cm^2}$ photoablation occurs, which is also known as photomechanics. A bounded volume of tissue is heated up and vaporized using pulses of light. Due to the short amount of time required for this vaporization, no heat is transferred by thermal conduction to the remaining tissue. In eye surgery, lasers with very short pulses (around 20 ns) are used. Even higher intensities can be achieved with special solid-state lasers. This leads to photodisruption, which creates plasma. This technique is used after cataract surgery. As all medical applications of lasers involve the creation of heat energy, the phenomenon of heat transfer must be considered with special attention. Above all, the effect of this energy on biological tissue must be taken into account. How far the energy introduced by a laser into tissue spreads depends on the parameters of the material, like water composition, density, heat conductivity, and heat capacity. The effects differ depending on the type of tissue. It must be remembered that in proteins, at temperatures over 40 °C, conformational changes occur; above 50 °C, different enzymes lose their ability to function. Above around 60 °C, denaturation occurs. In place of a scalpel, surgeons can use a CO_2-Laser laser with a wavelength of 10 μm in operations. At this wavelength, penetration depth in water is around 20 μm. As opposed to the scalpel, the laser offers the primary advantage that less bleeding occurs (due to coagulation by the laser beam).

13.1 Lasers in Ophthalmology

? A detached retina can be "welded" back into place by a pulse from an excimer laser focused on different spots. The laser generates pulses with a duration of $\tau = 20$ ms,

wavelength $\lambda = 600\,\text{nm}$, and pulse power $P = 60\,\text{mW}$. At the welding point (at the focus), the laser has a circular cross section with beam diameter $d = 125\,\mu\text{m}$. The energy is absorbed in a layer of thickness $l = 268\,\mu\text{m}$.

1. What is the pulse energy E_P?
2. What is the average number N_γ of photons in each pulse?
3. How much is the tissue in focus warmed?

[specific heat of the tissue $c_w = 4\,\text{kJ/kg K}$]

1. As the duration of the pulse is $\tau = 20\,\text{ms} = 20 \cdot 10^{-3}\,\text{s}$, with pulse power $P = 0.06\,\text{W}$, the pulse energy is

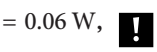

$$E_P = P\tau = (0.06\,\text{J/s})\left(20 \cdot 10^{-3}\,\text{s}\right) = 1.2 \cdot 10^{-3}\,\text{J}.$$

2. The energy of a photon is

$$E_\gamma = \frac{hc}{\lambda} = \frac{6.63 \cdot 10^{-34}\text{Js} \cdot 3 \cdot 10^{8}\text{m/s}}{600 \cdot 10^{-9}\text{m}} = 3.3 \cdot 10^{-19}\text{J}.$$

   The average number of photons N_γ is calculated as

$$N_\gamma = \frac{E_P}{E_\gamma} = \frac{1.2 \cdot 10^{-3}\,\text{J}}{3.3 \cdot 10^{-19}\text{J}} = 3.6 \cdot 10^{15}.$$

3. Assume that the beam in this region is roughly equivalent to a cylinder, and the corresponding volume with beam cross section $d = 125\,\mu\text{m}$ and penetration depth $l = 268\,\mu\text{m}$ is

$$V = \frac{\pi}{4} l d^2 = 3.3 \cdot 10^{-3}\,\text{mm}^3.$$

   The mass of the tissue m_N in volume V can be approximated using the density of water

$$m_N = \rho V = 10^3 \frac{\text{kg}}{\text{m}^3} \cdot 3.3 \cdot 10^{-3}\,\text{mm}^3 = 3.3 \cdot 10^{-9}\text{kg}.$$

   The pulse energy E_p leads to a warming of the tissue. We have $E_p = m_N c_W \Delta T$, and so after a pulse, the increase in temperature is

$$\Delta T = \frac{E_P}{m_N c_W} = \frac{1.2 \cdot 10^{-3}\,\text{J}}{3.3 \cdot 10^{-6}\text{g}\,4\,\text{J/g K}} = 91\,\text{K}.$$

13.2 Optical Sizing of Bacteria

On a glass plate are a number of spherical bacteria; a researcher wishes to determine their diameter d. A laser beam with wavelength $\lambda = 642\,\text{nm}$ strikes the glass plate,

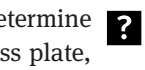

and creates a diffraction pattern on a screen $s = 3\,\text{m}$ behind the plate; the pattern is comprised of dark, circular rings in a light spot. The smallest ring has diameter $a = 20\,\text{cm}$. How can the desired diameter d of the bacteria be determined from a?

! The spherical bacteria create the same diffraction pattern as circular apertures with the same diameter. As such, the formulas necessary for evaluation will be derived from the circular aperture case. According to the Huygens principle, elementary waves proceed from all points within an aperture. Each element of area dA of the aperture contributes to the total amplitude of the elementary wave. If φ is the angle between the direction of the laser beam and the direction r of an elementary wave, for the total amplitude, we have

$$\Theta = \int_A \cos\, x\, dA \quad \text{with} \quad \mathrm{x} = \mathrm{x}(\varphi) = \frac{2\pi}{\lambda} r(\varphi).$$

Here, A is the surface of the circular aperture, and $r(\varphi)$ is the distance from the aperture to the point on the screen in question. The solution is[1]

$$\Theta(\varphi) \propto \frac{J_1[2\,z(\varphi)]}{z(\varphi)} \quad \text{with } z(\varphi) = \frac{\pi d}{2\lambda} \sin\varphi.$$

For the intensity $I(\varphi)$, squaring yields

$$I(\varphi) = I_0 \left\{ \frac{J_1[2\,z(\varphi)]}{z(\varphi)} \right\}^2.$$

The first root (corresponding to the smallest ring) has a Bessel function at $x = 3.84$, and therefore

$$2z|_{\min} = 3.84$$

or

$$\pi d\, \sin\varphi|_{\min} = 3.84 \quad \Rightarrow \sin\varphi|_{\min} = 1.22\, \frac{\lambda}{d}.$$

Considering the geometry of the array with s as the separation between the aperture and the screen, and a as the diameter of the smallest ring,

$$\sin\varphi|_{\min} = \frac{a/2}{s}$$

and finally,

$$d = 2.44\, \frac{\lambda\, s}{a}.$$

Because, as explained, the diffraction gratings of a circular aperture and of a sphere (and also of a circular disk) are equivalent, the final equation can be used to determine the diameter d of the bacteria. With $\lambda = 6.42 \cdot 10^{-7}\,\text{m}$, $s = 3\,\text{m}$, and $a = 0.2\,\text{m}$, we find

$$d = 2.44\, \frac{6.42 \cdot 10^{-7}\,\text{m}\ 3\,\text{m}}{0.2\,\text{m}} = 9.63 \cdot 10^{-6}\,\text{m} = 9.63\,\mu\text{m}.$$

---

1 as a first approximation of the Bessel function, use: $J_1(x) = \sqrt{\frac{2}{\pi x}} \sin\left(x - \frac{\pi}{4}\right)$

13.3 Small Particles in Optical Tweezers

1. Show, by solving the Heisenberg equation of motion, that the force that a laser beam exerts on a dielectric particle (small in comparison to the laser wavelength) with dipole moment $\vec{d}$ and linear polarizability α is directed opposite the intensity gradient of the laser beam. ?
2. An optical tweezer is used with a laser beam of wavelength λ, with a Gaussian intensity profile (TEM_{00}). The beam diameter is $w(z)$; at $z = 0$ the diameter has its minimum value w_0

$$w(z) = w_0 \sqrt{1 + \left(\frac{z}{z_R}\right)^2}$$

with $z_R = \frac{\pi}{\lambda} w_0^2$ for the Rayleigh length. The intensity profile is, in this case, given as

$$I(r, z) = I_0 \left(\frac{w_0}{w(z)}\right)^2 \exp\left(-\frac{2r^2}{w^2(z)}\right).$$

I_0 is the laser intensity in the center of the beam waist. The force field occurs in a plane along the direction of propagation. Calculate the maximum transverse force on a particle of polarizability α at position z along the propagation axis.

3. An optical tweezer with laser intensity $I_0 = 1.2 \cdot 10^9\ \mathrm{W/m^2}$ and wavelength $\lambda = 615\ \mathrm{nm}$ has a beam diameter of $w_0 = 10\ \mu\mathrm{m}$. What is the force of this optical tweezer on a particle of tissue that is primarily comprised of water? The polarizability α can be determined from the Clausius–Mosotti equation

$$\frac{\varepsilon_r - 1}{\varepsilon_r + 2} \frac{M_m}{\rho} = \frac{N_A}{3\varepsilon_0} \alpha$$

The molar mass of water is $M_m = 18\ \mathrm{g/mol}$, and the density is $\rho = 1{,}000\ \mathrm{kg/m^3}$. The relative permittivity constant ε_r is, in the optical frequency range, $\varepsilon_r = 1.7$ (for water), and $\varepsilon_0 = 8.85 \cdot 10^{-12}\ \mathrm{C^2/Nm^2}$.

1. The Hamiltonian operator that describes the interaction between the electric field $\vec{E}$ and a dipole $\vec{d}$ is !

$$\hat{H} = -\vec{d} \cdot \vec{E}.$$

Using the Heisenberg equation of motion

$$-i\hbar \frac{d\hat{p}}{dt} = \left[\hat{p},\ \hat{H}\right]$$

the interaction force can be written as

$$\begin{aligned} \vec{F} = \frac{d\hat{p}}{dt} &= \frac{i}{\hbar}\{(-i\hbar\vec{\nabla})(-\vec{d} \cdot \vec{E}) - (-\vec{d} \cdot \vec{E})(-i\hbar\vec{\nabla})\} \\ &= -\vec{\nabla}(\vec{d} \cdot \vec{E}) + (\vec{d} \cdot \vec{E})\vec{\nabla}. \end{aligned}$$

Using the equivalent of the chain rule for the gradients of a scalar product, and simplifying with the identities for the triple cross product, we have

$$\vec{\nabla}(\vec{d}\cdot\vec{E}) = (\vec{E}\cdot\vec{\nabla})\vec{d} + (\vec{d}\cdot\vec{\nabla})\vec{E} + \vec{d}\times(\vec{\nabla}\times\vec{E}) + \vec{E}\times(\vec{\nabla}\times\vec{d})$$

with

$$\vec{d}\times(\vec{\nabla}\times\vec{E}) = (\vec{d}\cdot\vec{E})\vec{\nabla} - (\vec{d}\cdot\vec{\nabla})\vec{E}$$
$$\vec{E}\times(\vec{\nabla}\times\vec{d}) = (\vec{d}\cdot\vec{E})\vec{\nabla} - (\vec{E}\cdot\vec{\nabla})\vec{d}$$

we have

$$\vec{E}\times(\vec{\nabla}\times\vec{d}) + \vec{d}\times(\vec{\nabla}\times\vec{E}) = 2(\vec{d}\cdot\vec{E})\vec{\nabla} - (\vec{d}\cdot\vec{\nabla})\vec{E} - (\vec{E}\cdot\vec{\nabla})\vec{d}$$
$$\vec{\nabla}(\vec{d}\cdot\vec{E}) = 2(\vec{d}\cdot\vec{E})\vec{\nabla}$$

and then,

$$\frac{d\hat{p}}{dt} = -\frac{1}{2}\vec{\nabla}(\vec{d}\cdot\vec{E}) + \vec{\nabla}\,(\vec{d}\cdot\vec{E})$$
$$= \frac{1}{2}\vec{\nabla}(\vec{d}\cdot\vec{E}).$$

For a linear dipole moment with polarizability α, the dipole moment is

$$\vec{d} = \alpha\vec{E}$$

and therefore, the force applies in the direction of the intensity gradient of the laser beam, with c as the speed of light and ε as the permittivity constant:

$$\vec{F} = \frac{1}{2}\alpha\vec{\nabla}(\vec{E}\cdot\vec{E})$$
$$= \frac{\alpha}{\varepsilon_r\varepsilon_0 c}\vec{\nabla}I.$$

2. The intensity profile of a Gaussian beam is

$$I(r,z) = I_0\left(\frac{w_0}{w(z)}\right)^2 \exp\left(-\frac{2r^2}{w^2(z)}\right)$$
$$= I_0\frac{1}{1+\left(\frac{z}{z_R}\right)^2}\exp\left(-\frac{2r^2}{w_0^2\left(1+\left(\frac{z}{z_R}\right)^2\right)}\right).$$

This leads to an intensity gradient

$$\vec{\nabla}I(r,z) = \frac{\partial I}{\partial r}\hat{r} + \frac{1}{r}\frac{\partial I}{\partial\theta}\hat{\theta} + \frac{\partial I}{\partial z}\hat{z}.$$

Due to the rotational symmetry of the intensity profile, the gradient $\frac{\partial}{\partial\theta}$ disappears, so that

$$\frac{\partial I}{\partial\theta} = 0.$$

The radial and axial components are calculated as

$$\frac{\partial I}{\partial r} = -\frac{4w_0^2 r}{w^4(z)} I_0 \exp\left[-\frac{2r^2}{w^2(z)}\right],$$
$$\frac{\partial I}{\partial z} = 2w_0^4 \frac{z}{z_R^2}\left\{\frac{2r^2}{w^6(z)} - \frac{1}{w^4(z)}\right\} I_0 \exp\left[-\frac{2r^2}{w^2(z)}\right].$$

Therefore, the force that acts on a particle is

$$\vec{F} = \begin{pmatrix} F_r \\ 0 \\ F_z \end{pmatrix} = -\frac{\alpha}{\varepsilon_r \varepsilon_0 c} \begin{pmatrix} \frac{4r}{w^2(z)} \\ 0 \\ 2w_0^4 \frac{z}{z_R^2}\left\{\frac{2r^2}{w^6(z)} - \frac{1}{w^4(z)}\right\} \end{pmatrix}_{r,\theta,z} I_0 \exp\left[-\frac{2r^2}{w^2(z)}\right].$$

In order to find the maximum of the force in the radial direction, we differentiate the corresponding components of the force vector. A laser tweezer with laser intensity $I_0 = 1.2 \cdot 10^9\ \mathrm{W/m^2}$ and wavelength $\lambda = 615\ \mathrm{nm}$ has a beam diameter $w_0 = 10\ \mu\mathrm{m}$.

$$F_r = -\frac{\alpha}{\varepsilon_r \varepsilon_0 c} \frac{4r}{w^2(z)} I_0 \exp\left[-\frac{2r^2}{w^2(z)}\right],$$
$$\frac{\partial F_r}{\partial r} = -\frac{\alpha}{\varepsilon_r \varepsilon_0 c} \frac{4}{w^2(z)}\left\{1 - \frac{4r^2}{w^2(z)}\right\} I_0 \exp\left[-\frac{2r^2}{w^2(z)}\right]$$

leading to the maximum force that acts at half the beam diameter $r = \pm\frac{1}{2}w(z)$ of

$$F_{r,\max} = -\frac{2\alpha I_0}{\varepsilon_r \varepsilon_0 c w_0} \exp\left[-\frac{1}{2}\right] = -1.2\,\frac{2\alpha I_0}{\varepsilon_r \varepsilon_0 c w_0}.$$

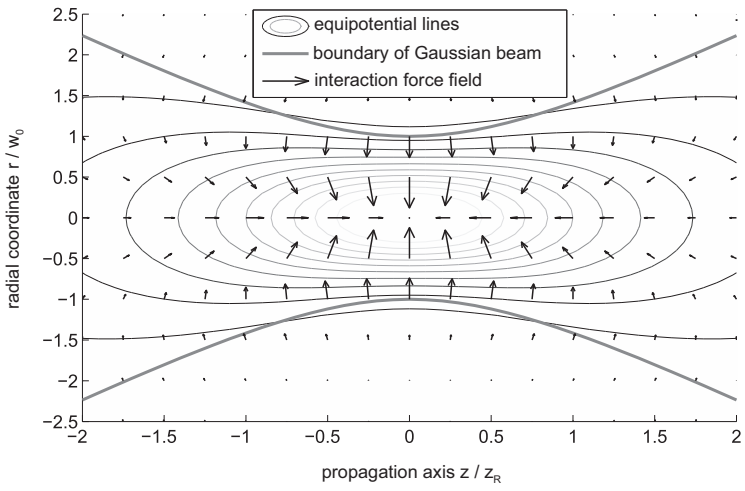

Fig. 13.1. Equipotential lines and forces in the region of the beam waist.

The force in the axial direction is

$$F_Z = -\frac{\alpha}{\varepsilon_r \varepsilon_0 c} 2 w_0^4 \frac{z}{z_R^2} \left\{ \frac{2\,r^2}{w^6\,(z)} - \frac{1}{w^4\,(z)} \right\} I_0 \, \exp\left[-\frac{2r^2}{w^2\,(z)} \right].$$

For the middle of the beam $r = 0$, we have

$$F_z = \frac{2\alpha I_0 z_R^2}{\varepsilon_r \varepsilon_0 c} \cdot \frac{z}{\left(z^2 + z_R^2\right)^2},$$

$$\frac{\partial F_z}{\partial z} = C \frac{\left(z^2 + z_R^2\right)^2 - 4z^2\left(z^2 + z_R^2\right)}{\left(z^2 + z_R^2\right)^4}.$$

F_z is maximized at position $z = z_0$,, at which $\frac{\partial F_z}{\partial z} = 0$. Therefore,

$$\left(z_0^2 + z_R^2\right)^2 - 4z_0^2\left(z_0^2 + z_R^2\right) = 0$$
$$\left(z_0^2 + z_R^2\right) - 4z_0^2 = 0$$
$$3z_0 = z_R$$
$$z_0 = \frac{1}{\sqrt{3}} z_R.$$

And therefore,

$$F_{z,\,\max} = \frac{3\sqrt{3}\,\alpha I_0}{16\,\varepsilon_r \varepsilon_0 c\, z_R} = \frac{3\sqrt{3}\,\alpha I_0 \lambda}{16\,\pi \varepsilon_r \varepsilon_0 c\, w_0^2} = 0.1\,\frac{\alpha \lambda I_0}{\varepsilon_r \varepsilon_0 c w_0^2}.$$

The value of $F_{\max}$ is

$$F_{\max} = \sqrt{F_{r,\,\max}^2 + F_{z,\,\max}^2}$$
$$= \frac{1.2\,\alpha I_0}{\varepsilon_r \varepsilon_0 c w_0} \sqrt{1 + \left(\frac{0.1\,\lambda}{1.2\,w_0}\right)^2}.$$

3. For the numerical calculation, the polarizability α must first be calculated. According to the Clausius–Mosotti equation we have

$$\frac{\varepsilon_r - 1}{\varepsilon_r + 2} \cdot \frac{M_m}{\rho} = \frac{N_A}{3\varepsilon_0} \cdot \alpha$$

and, solving for α,

$$\alpha = \frac{3\varepsilon_0}{N_A} \cdot \frac{\varepsilon_r - 1}{\varepsilon_r + 2} \cdot \frac{M_m}{\rho}.$$

For water, the values are $\varepsilon_r = 1.7$, $M_m = 18 \cdot 10^{-3}\ \mathrm{kg/mol}$, and $\rho = 1{,}000\ \mathrm{kg/m^3}$. With Avogadro constant $N_A = 6.03 \cdot 10^{23}\,\mathrm{1/mol}$ and permittivity in a vacuum $\varepsilon_0 = 8.85 \cdot 10^{-12}\,\mathrm{C^2/N\,m^2}$, the polarizability is

$$\alpha = \frac{3 \cdot 8.85 \cdot 10^{-12}\,\mathrm{C^2/Nm^2}}{6.03 \cdot 10^{23}\,\mathrm{1/mol}} \cdot \left(\frac{1.7 - 1}{1.7 + 2}\right) \cdot \frac{18 \cdot 10^{-3}\ \mathrm{kg/mol}}{1.000\ \mathrm{kg/m^3}} = 1.5 \cdot 10^{-40}\,\mathrm{m\,C^2/N}.$$

Using this, we can find with the values given – $I_0 = 1/2 \cdot 10^9 \mathrm{W/m^2}$; $w_0 = 10\,\mu\mathrm{m}$, and $\lambda = 615\,\mathrm{nm}$ – the maximum force

$$F_{\max} = \frac{1.2\,\alpha I_0}{\varepsilon_r \varepsilon_0 c w_0} \sqrt{1 + \left(\frac{0.1\,\lambda}{1.2\,w_0}\right)^2}$$

$$= \frac{1.2 \cdot 1.5 \cdot 10^{-40} 1.2 \cdot 10^9}{1.7 \cdot 8.85 \cdot 10^{-12} 3 \cdot 10^8} \sqrt{1 + \left(\frac{0.1 \cdot 6.15 \cdot 10^{-7}}{1.2 \cdot 1 \cdot 10^{-5}}\right)^2}\,\mathrm{N} = 4.62 \cdot 10^{-29}\mathrm{N}.$$

A Constants, Material Parameters, and Values

A.1 Table of Values

Table A.1. Constants of Nature

Constant	Symbol	Value	Unit
Avogadro constant	N_A	$6.02 \cdot 10^{23}$	mol^{-1}
Boltzmann constant	k_B	$1.38 \cdot 10^{-23}$	$\mathrm{J} \cdot \mathrm{K}^{-1}$
universal gas constant	R	8.314	$\mathrm{J} \cdot \mathrm{mol}^{-1} \cdot \mathrm{K}^{-1}$
Planck constant	h	$6.626 \cdot 10^{-34}$	$\mathrm{J} \cdot \mathrm{s}$
reduced Planck constant	$\hbar = \frac{h}{2\pi}$	$1.055 \cdot 10^{-34}$	$\mathrm{J} \cdot \mathrm{s}$
speed of light in a vacuum	c	$2.998 \cdot 10^{8}$	$\mathrm{m} \cdot \mathrm{s}^{-1}$
atomic mass unit	$u = \frac{1}{12} m(^{12}C)$	$1.66 \cdot 10^{-27}$	kg
proton magnetic moment	μ_p	$1.41 \cdot 10^{-26}$	$\mathrm{J} \cdot \mathrm{T}^{-1}$
proton gyromagnetic ratio	γ_p	$2.675 \cdot 10^{8}$	$\mathrm{rad} \cdot \mathrm{T}^{-1} \cdot \mathrm{s}^{-1}$

Table A.2. Material Properties of Air and Water

Property	Symbol	Value	Unit
density of air	ρ_L	1.3	$\mathrm{kg} \cdot \mathrm{m}^{-3}$
speed of sound in air	c_L	330	$\mathrm{m} \cdot \mathrm{s}^{-1}$
acoustic impedance of air	Z_L	430	$\mathrm{N} \cdot \mathrm{s} \cdot \mathrm{m}^{-3}$
density of water	ρ_L	1.0	$\mathrm{kg} \cdot \mathrm{m}^{-3}$
speed of sound in water	c_W	1,480	$\mathrm{m} \cdot \mathrm{s}^{-1}$
acoustic impedance in water	Z_W	$1.48 \cdot 10^{6}$	$\mathrm{N} \cdot \mathrm{s} \cdot \mathrm{m}^{-3}$

B Relevant Literature

B.1 Physics

[1] L. Bergmann and C. Schaefer. *Lehrbuch der Experimentalphysik*, Volume 2 (Elektrizität und Magnetismus). de Gruyter, Berlin, 1986.

[2] L. Bergmann and C. Schaefer. *Lehrbuch der Experimentalphysik*, Volume 3 (Optik). de Gruyter, Berlin, 2004.

[3] L. Bergmann and C. Schaefer. *Lehrbuch der Experimentalphysik*, Volume 5 (Vielteilchen-Systeme). de Gruyter, Berlin, 1992.

[4] B. R. Bird, W. E. Steward, and E. N. Lightfoot. *Transport Phenomena*. Wiley, New York, 1960.

[5] M. J. Crocker. *Handbook of Acoustics*. Wiley, New York, 1998.

[6] A. Das and T. Ferbel. *Kern- und Teilchenphysik*. Spektrum Akademischer Verlag, Heidelberg, 1995.

[7] R. P. Feynman. *The Feynman Lectures on Physics*. Addison-Wesley, London, 2006.

[8] H. Gerthsen and C. Vogel. *Physik*. Springer, Berlin, 1993.

[9] D. C. Giancoli. *Physics for Scientists and Engineers with Modern Physics*. Pearson Education, Upper Saddle River, New Jersey, 2000.

[10] F. Kneubühl and M. W. Sigrist. *Laser*. Teubner, Wiesbaden, 1999.

[11] D. Meschede. *Optik, Licht und Laser*. Vieweg-Teubner, Wiesbaden, 2008.

[12] J. R. Meyer-Arendt. *Introduction to Classical and Modern Optics*. Prentice Hall, Englewood Cliffs, New Jersey, 1995.

[13] J. Orear. *Physik*. Hanser, München, 1991.

[14] H. J. Paus. *Physik in Experimenten und Beispielen*. Hanser, München, 2002.

[15] F. L. Pedrotti and L. S. Pedrotti. *Introduction to Optics*. Prentice Hall, Englewood Cliffs, New Jersey, 1993.

[16] H. Stöcker. *Taschenbuch der Physik*. Harri Deutsch, Frankfurt am Main, 2000.

[17] H. Stroppe, P. Streitenberger, and E. Specht. *Physik: Beispiele und Aufgaben*, Volume 1 (Mechanik und Wärmelehre). Fachbuchverlag Leipzig, Leipzig, 2003.

[18] C. W. Turtur. *Prüfungstrainer Physik*. Teubner, Wiesbaden, 2007.

[19] M. Warren. *Handbook of Heat Transfer*. McGraw-Hill, New York, 1998.

[20] E. Hecht and A. Zajac. *Optics*. Addison-Wesley, Amsterdam, 2002.

[21] R. A. Serway and J. W. Jewett. *Physics for Scientists and Engineers*. Cengage Learning, Belmont, 2000.

B.2 Medical Physics

[22] J. Bille and W. Schlegel. *Medizinische Physik*, Volume 1 (Grundlagen). Springer, Berlin, 1999.

[23] J. Bille and W. Schlegel. *Medizinische Physik*, Volume 2 (Medizinische Strahlenphysik). Springer, Berlin, 2002.

[24] J. Bille and W. Schlegel. *Medizinische Physik*, Volume 3 (Medizinische Laserphysik). Springer, Berlin, 2005.

[25] P. P. Dendy and B. Heaton. *Physics for Diagnostic Radiology*. Institute of Physics Publishing, Bristol, Philadelphia, 1999.

[26] O. Dössel. *Bildgebende Verfahren in der Medizin*. Springer, Heidelberg, 2000.

[27] E. Ernst. *Hämorheologie für den Praktiker*. Zuckschwerdt, München, 1986.
[28] R. Freeman. *Magnetic Resonance in Chemistry and Medicine*. Oxford University Press, Oxford, 2002.
[29] R. Glaser. *Biophysics*. Springer, Berlin, 2001.
[30] W. Hoppe, W. Lohmann, H. Markl, and H. Ziegler. *Biophysik*. Springer, Berlin, 1982.
[31] H. Krieger. *Grundlagen der Strahlungsphysik und des Strahlenschutzes*. Teubner, Wiesbaden, 2007.
[32] D. W. McRobbie, E. A. Moore, M. J. Graves, and M. R. Prince. *MRI from Picture to Proton*. Cambridge University Press, Cambridge, 2003.
[33] D. L. Leger and N. Özkaya. *Fundamentals of Biomechanics*. Springer, Berlin, 1998.
[34] P. Thurn. *Einführung in die Röntgendiagnostik*. Thieme, Stuttgart, 1982.
[35] M. A. Bernstein, K. F. King, and X. J. Zhou. *Handbook of MRI pulse sequences*. Elsevier Academic Press, London, 2004.

B.3 Mathematics

[36] M. L. Boas. *Mathematical Methods in the Physical Sciences*. Wiley, New York, 1983.
[37] I. N. Bronstein and K. A. Semendjajew. *Taschenbuch der Mathematik*. Harry Deutsch, Frankfurt am Main, 1971.
[38] P. Hartmann. *Mathematik für Informatiker* Vieweg, Wiesbaden, 2004.
[39] K. F. Riley, M. P Hobson, and S. J. Bence. *Mathematical Methods for Physics and Engineering*. Cambridge University Press, Cambridge, 2002.
[40] T. Butz. *Fouriertransformation für Fußgänger*. Teubner, Wiesbaden, 2007.

B.4 Medicine, Biology, and Chemistry

[41] E. Budecke. *Grundriss der Biochemie*. de Gruyter, Berlin, 1982.
[42] P. Deetjen and E. J. Speckmann. *Physiologie*. Urban & Fischer, München, 2004.
[43] A. Faller and M. Schönke. *Der Körper des Menschen*. Thieme, Stuttgart, 2004.
[44] P. Karlson. *Kurzes Lehrbuch der Biochemie*. Thieme, Stuttgart, 1972.
[45] K. Kunsch. *Der Mensch in Zahlen*. Spektrum Akademischer Verlag, Heidelberg, 2000.
[46] R. F. Schmidt. *Physiologie kompakt*. Springer, Berlin, 2001.
[47] W. Schröter, K.-H. Lautenschläger, and H. Bibrack. *Taschenbuch der Chemie*. Harri Deutsch, Frankfurt am Main, 1995.
[48] W. F. Ganong and W. Auerswald. *Lehrbuch der Medizinischen Physiologie: Die Physiologie Des Menschen für Studierende der Medizin und Ärzte*. Springer, Berlin, 1979.
[49] J. Sobotta, R. Putz, R. Pabst, and S. Bedoui. *Sobotta Atlas of Human Anatomy: Trunk, Viscera, Lower Limb*. Atlas of Human Anatomy (Sobotta) Series. Urban & Fischer, München, 2006.
[50] R. L. Drake, W. Vogl, and A. W. M. Mitchell. *Anatomie für Studenten*. Urban & Fischer, München, 2007.

B.5 Manuscripts and Additional References

[51] *BGBl Nr. 51: Atomgesetz mit Verordnungen*. Nomos Gesetze, Baden-Baden, 2005.
[52] F. Bloch. *Nuclear Induction*. *Phys. Rev*., 70:460–474, 1946.
[53] E. Konecny. *Studienbrief MPT0005: Medizintechnik*. Technische Universität Kaiserslautern: Zentrum für Fernstudien und Universitäre Weiterbildung, Kaiserslautern, 2003.
[54] H. Meier and B. Schröder. *Studienbrief MPT0007: Einführung in den Strahlenschutz*. Technische Universität Kaiserslautern: Zentrum für Fernstudien und Universitäre Weiterbildung, Kaiserslautern, 2004. R. Millner. *Studienbrief MPT0015: Physik und Technik der Ultraschallanwendung in der Medizin*. Technische Universität Kaiserslautern: Zentrum für Fernstudien und Universitäre Weiterbildung, Kaiserslautern, 2002.
[55] H. Kolem. *Studienbrief MPT0018: Kernspintomografie und Kernspinspektroskopie*. Technische Universität Kaiserslautern: Zentrum für Fernstudien und Universitäre Weiterbildung, Kaiserslautern, 2005.
[56] D. Gosch, S. Lieberenz, J. Petzold, B. Sattler, and A. Seese. *Studienbrief MPT0019: Bilderzeugung und Bildbewertung in der Strahlenphysik*. Technische Universität Kaiserslautern: Zentrum für Fernstudien und Universitäre Weiterbildung, Kaiserslautern, 2003.
[57] D. Schlegel et al. *Schleichende Strömung einer newtonschen Flüssigkeit durch eine hyberbolische Verengung*. *Rheol. Acta*, 14:963–967, 1975.
[58] P. Schümmer et al. *An Elementary Method for the Evaluation of a Flow Curve*. *Chemical Engineering Science*, 33:759–763, 1978.